ORTA DOĞU TEKNİK ÜNİVERSİTESİ
FEN BİLİMLERİ ENSTİTÜSÜ MÜDÜRLÜĞÜ

TEZ ŞABLONU ONAY FORMU
THESIS TEMPLATE CONFIRMATION FORM

1. Şablonda verilen yerleşim ve boşluklar değiştirilmemelidir.
2. **Jüri tarihi** Başlık Sayfası, İmza Sayfası, Abstract ve Öz'de ilgili yerlere yazılmalıdır.
3. İmza sayfasında jüri üyelerinin unvanları doğru olarak yazılmalıdır. Tüm imzalar **mavi pilot kalemle** atılmalıdır.
4. **Disiplinlerarası** programlarda görevlendirilen öğretim üyeleri için jüri üyeleri kısmında tam zamanlı olarak çalıştıkları anabilim dalı başkanlığının ismi yazılmalıdır. Örneğin: bir öğretim üyesi Biyoteknoloji programında görev yapıyor ve biyoloji bölümünde tam zamanlı çalışıyorsa, İmza sayfasına biyoloji bölümü yazılmalıdır. İstisnai olarak, disiplinler arası program başkanı ve tez danışmanı için disiplinlerarası program adı yazılmalıdır.
5. Tezin **son sayfasının sayfa** numarası Abstract ve Öz'de ilgili yerlere yazılmalıdır.
6. Bütün chapterlar, referanslar, ekler ve CV sağ sayfada başlamalıdır. Bunun için **kesmeler** kullanılmıştır. **Kesmelerin kayması** fazladan boş sayfaların oluşmasına sebep olabilir. Bu gibi durumlarda paragraf (¶) işaretine tıklayarak kesmeleri görünür hale getirin ve yerlerini **kontrol edin**.
7. Figürler ve tablolar kenar boşluklarına taşmamalıdır.
8. Şablonda yorum olarak eklenen uyarılar dikkatle okunmalı ve uygulanmalıdır.
9. Tez yazdırılmadan önce PDF olarak kaydedilmelidir. Şablonda yorum olarak eklenen uyarılar PDF dokümanında yer almamalıdır.
10. Tez taslaklarının kontrol işlemleri tamamlandığında, bu durum öğrencilere METU uzantılı öğrenci e-posta adresleri aracılığıyla duyurulacaktır.
11. Tez yazım süreci ile ilgili herhangi bir sıkıntı yaşarsanız, **Sıkça Sorulan Sorular (SSS)** sayfamızı ziyaret ederek yaşadığınız sıkıntıyla ilgili bir çözüm bulabilirsiniz.

1. Do not change the spacing and placement in the template.
2. Write **defense date** to the related places given on Title page, Approval page, Abstract and Öz.
3. Write the titles of the examining committee members correctly on Approval Page. **Blue ink** must be used for all signatures.
4. For faculty members working in **interdisciplinary programs**, the name of the department that they work full-time should be written on the Approval page. For example, if a faculty member staffs in the biotechnology program and works full-time in the biology department, the department of biology should be written on the approval page. Exceptionally, for the interdisciplinary program chair and your thesis supervisor, the interdisciplinary program name should be written.
5. Write **the page number of the last page** in the related places given on Abstract and Öz pages.
6. All chapters, references, appendices and CV must be started on the right page. **Section Breaks** were used for this. **Change in the placement** of section breaks can result in extra blank pages. In such cases, make the section breaks visible by clicking paragraph (¶) mark and **check their position.**
7. All figures and tables must be given inside the page. Nothing must appear in the margins.
8. All the warnings given on the comments section through the thesis template must be read and applied.
9. Save your thesis as pdf and Disable all the comments before taking the printout.
10. This will be announced to the students via their METU students e-mail addresses when the control of the thesis drafts has been completed.
11. If you have any problems with the thesis writing process, you may visit our **Frequently Asked Questions (FAQ)** page and find a solution to your problem.

☒ **Yukarıda bulunan tüm maddeleri okudum, anladım ve kabul ediyorum. / I have read, understand and accept all of the items above.**

Name : Mustafa
Surname : Güzel
E-Mail : mustafaguzel@hitit.edu.tr
Date : 03.06.2022
Signature : _____

AN ALTERNATIVE WAY FOR REDUCTION OF SALMONELLA IN
POULTRY PRODUCTS: BACTERIOPHAGES

A THESIS SUBMITTED TO
THE GRADUATE SCHOOL OF NATURAL AND APPLIED SCIENCES
OF
MIDDLE EAST TECHNICAL UNIVERSITY

BY

MUSTAFA GÜZEL

IN PARTIAL FULFILLMENT OF THE REQUIREMENTS
FOR
THE DEGREE OF DOCTOR OF PHILOSOPHY
IN
BIOTECHNOLOGY

JUNE 2022

Approval of the thesis:

AN ALTERNATIVE WAY FOR REDUCTION OF SALMONELLA IN POULTRY PRODUCTS: BACTERIOPHAGES

submitted by **MUSTAFA GÜZEL** in partial fulfillment of the requirements for the degree of **Doctor of Philosophy** in **Biotechnology, Middle East Technical University** by,

Prof. Dr. Halil Kalıpçılar
Dean, Graduate School of **Natural and Applied Sciences**   _____

Assoc. Prof. Dr. Yeşim Soyer
Head of the Department, **Biotechnology**   _____

Assoc. Prof. Dr. Yeşim Soyer
Supervisor, **Biotechnology, METU**   _____

Prof. Dr. Mustafa Akçelik
Co-Supervisor, **Biology, Ankara University**   _____

Examining Committee Members:

Prof. Dr. Candan Gürakan Gültekin
Food Engineering, METU   _____

Assoc. Prof. Dr. Yeşim Soyer
Supervisor, Biotechnology, METU   _____

Prof. Dr. Zeliha Yıldırım
Food Engineering, Niğde Ömer Halisdemir University   _____

Prof. Dr. Bülent Kabak
Food Engineering, Hitit University   _____

Assoc. Prof. Dr. Halil Mecit Öztop
Food Engineering, METU   _____

Date: 03.06.2022

I hereby declare that all information in this document has been obtained and presented in accordance with academic rules and ethical conduct. I also declare that, as required by these rules and conduct, I have fully cited and referenced all material and results that are not original to this work.

Name Last name : Mustafa Güzel

Signature :

ABSTRACT

AN ALTERNATIVE WAY FOR REDUCTION OF SALMONELLA IN POULTRY PRODUCTS: BACTERIOPHAGES

Güzel, Mustafa
Doctor of Philosophy, Biotechnology
Supervisor: Assoc. Prof. Dr. Yeşim Soyer
Co-Supervisor: Prof. Dr. Mustafa Akçelik

June 2022, 234 pages

Antibiotic resistance of pathogenic microorganisms is a severe public health problem. One of the main reasons of the resistance is the overuse of antibiotics in veterinary and food animals. Non-typhoidal *Salmonella* is a major foodborne pathogen that causes millions of cases each year, worldwide. Although *Salmonella* causes outbreaks in almost all food commodities, it is mostly associated with poultry. In addition to high prevalence in poultry, *Salmonella* isolates recovered from poultry have shown multi drug resistance. Use of bacteriophages (phages) has been emerged as a viable alternative for biocontrol of *Salmonella*. Phages are bacterial viruses that have narrow host range, and are unable to infect eukaryotic cells. They could be utilized for different applications from medicine to food safety. In this study, the main purpose was to isolate and characterize bacteriophages that can be used against multidrug resistant *Salmonella* serotypes in cattle and poultry farms. 57 samples were collected from poultry farms, cattle farms, and wastewater facility, in 11-month span. From the samples, 12 *Salmonella* and 68 phages were isolated. Antibiotic resistance profiles of *Salmonella* isolates were characterized. 66% of Salmonella

isolates were multidrug resistant. Genomic clustering and serotypes were determined by pulsed field gen electrophoresis (PFGE). Most abundant phages were Enteritidis phages. Isolated phages purified and stored. Lytic profiles of phages against various hosts were determined. Most of the phages showed broad host range. Based on the host range most potent phages were determined, and phenotypic (host-range, one-step growth, latent period, burst size, adsorption rate, transmission electron microscopy (TEM)) and genomic (PFGE, genome sequencing) features were characterized. Dynamic interaction between phages and hosts were investigated with bacterial reduction curves and virulence index. Enteritidis phages inhibited bacterial growth even at low concentrations. Effectiveness of several phages were tested against their hosts in *in vitro* feed model. Enteritidis phage significantly reduced host population in feed. In conclusion, a fundamental basis was prepared for a potential phage product.

Keywords: *Salmonella*, Bacteriophage, Genomics, Food Safety

ÖZ

KANATLI ÇİFTLİKLERİNDE SALMONELLANIN AZALTILMASI İÇİN ALTERNATİF BİR YOL: BAKTERİYOFAJLAR

Güzel, Mustafa
Doktora, Biyoteknoloji
Tez Yöneticisi: Doç. Dr.Yeşim Soyer
Ortak Tez Yöneticisi: Prof. Dr. Mustafa Akçelik

Haziran 2022, 234 sayfa

Patojenik mikroorganizmaların antibiyotik direnci çok ciddi bir halk sağlığı sorunudur. Gelişen direncin temel sebeplerinden biri antibiyotiklerin veteriner ve Çiftlik hayvanlarındaki aşırı kullanımıdır. Tifo etmeni olmayan *Salmonella* her yıl milyonlarca vakaya sebep olan gıda kaynaklı bir patojendir. *Salmonella* hemen her türlü gıdada salgınlara yol açsa da temel olarak kanatlılarla ilişkilendirilir. Kanatlılardaki yüksek görünme oranına ek olarak kanatlılardan izole edilen *Salmonella* çoklu ilaç direnci göstermektedir. Bakteriyofajlar, kısaca fajlar, *Salmonella*'nın biyokontrolünde başarılı bir alternatif olarak ilgi görmektedir. Fajlar dar konakçı aralığına sahip bakteri virüsleridir ve ökaryotik hücreleri enfekte edemezler. Fajlar tıptan gıdaya kadar birçok farklı alanda değerlendirilebilir. Bu çalışmanın temel amacı büyükbaş ve kanatlı çiftliklerinde çoklu ilaç direnci gösteren *Salmonella* serotiplerine karşı etkili fajların izolasyonu ve karakterizasyonudur. 11 aylık bir dönemde, kanatlı çiftlikleri, büyükbaş çiftlikleri ve atık su tesisinden toplam 57 örnek toplanmıştır. Bu örneklerden 12 *Salmonella* ve 68 faj izole edilmiştir. *Salmonella* izolatlarının antibiyotik direnci profili karakterize edilmiştir. *Salmonella* izolatlarının %66'sı çoklu ilaç direnci göstermiştir. Genomik kümeler ve serotipler

vuruşlu alan jel elektroforezi (PFGE) ile analiz edilmiştir. Enteritidis fajları en sık karşılaşılan fajlar olmuştur. İzole edilen fajlar saflaştırılıp dondurulmuştur. Fajların farklı konakçılara karşı litik profilleri belirlenmiştir. Fajların çoğunluğu geniş konakçı aralığına sahiptir. Konakçı aralığı temel alınarak en etkili fajlar belirlenmiş ve fenotipik (tek adımlı büyüme eğrisi, latent periyodu, patlama büyüklüğü, adsorpsiyon oranı ve geçirimli elektron mikroskobu (TEM)) ile genomik (PFGE, tüm genom sekansları) özellikleri karakterize edilmiştir. Fajlar ve konakçıları arasındaki dinamik ilişki bakteriyel azalma eğrisi ve virülans endeks ile analiz edilmiştir. Enteritidis fajları, düşük konsantasyonlarda bile bakteriyel büyümeyi engellemişlerdir. Çeşitli fajların yem ortamında konakçılarına karşı etkisi *in vitro* olarak test edilmiştir. Enteritidis fajı yem ortamında konakçı popülasyonunu önemli ölçüde azalttığı görülmüştür. Sonuç olarak, çalışmamızla birlikte potansiyel bir faj ürünü için gerekli olan temel altyapı sağlanmıştır.

Anahtar Kelimeler: *Salmonella*, Bakteriyofaj, Genomik, Gıda Güvenliği

To my spouse and daughter

and

To my parents

ACKNOWLEDGEMENTS

TABLE OF CONTENTS

LIST OF TABLES

LIST OF FIGURES

FIGURES

CHAPTER 1

INTRODUCTION

Foodborne diseases have been a global health problem. World Health Organization (WHO) estimated that 600 million people suffered from foodborne illnesses, and 420000 deaths were associated with foodborne diseases. Furthermore, most impacted group from deaths were the infants. Although children under 5 years old were represented 9% of the world population, 40% foodborne mortalities linked with children (Havelaar et al., 2015). Among the most prevalent causative agents, top 5 organisms were; Norovirus, *Escherichia coli*, *Campylobacter* spp., Non-Typhoidal *Salmonella* spp, (*Salmonella*), and *Shigella* spp.

As one the major foodborne pathogens, *Salmonella* causes both diarrheal and invasive diseases. *Salmonella* was associated with nearly 80 million cases, and 60000 deaths (Havelaar et al., 2015). In addition to health related issues, *Salmonella* related annual economic loss was estimated as 2.7 billion Dollars in the United States (US), and 3 billion Euros for the European Union (EU) (Mather et al., 2013).

The main source of *Salmonella* is the poultry, pork and egg products (Antunes et al., 2016). Indeed, highest number of *Salmonella*-positive samples were spotted in poultry samples. Furthermore, poultry meat were the most *Salmonella* outbreak associated food commodities in 2020 in the EU (EFSA & ECDC, 2021). However, all of the food commodities have been linked with *Salmonella* outbreaks worldwide.

Prevention of salmonellosis requires careful implementation of intervention strategies throughout food production chain, from farm to fork (Ehuwa et al., 2021). Pathogenic microorganisms that are already present in animal before slaughter might cause contamination. In addition, cross contamination might occur during processing from contaminated carcasses or surfaces (Milho et al., 2019). Therefore, intervention strategies should start pre-slaughter by both reducing the prevalence of *Salmonella*

contaminated flocks, and reducing the pathogen concentration in contaminated flocks (Pessoa et al., 2021). Moreover, interventions possess a critical importance in terms of elimination of this foodborne pathogen at every step of production.

A number of intervention strategies are readily used in poultry production from chemical decontaminants to physical treatments. However, each strategy has a downside. For example, chlorine based chemicals are not generally recognized as safe (GRAS), organic acids cause undesirable changes in organoleptic properties, and physical treatments (e.g. ionizing radiation, UV) have negative effect on texture and color (Han et al., 2022). Antibiotics have widely been used in farm animals in order to fight against *Salmonella*. However, misuse and overuse of these substances leads spreading of antibiotic resistant bacteria (WHO, 2021). More than 700000 mortality is associated with antibiotic resistance infections annually (El-Shibiny & El-Sahhar, 2017). In addition to health and sociological consequences, each year antibiotic resistant infections cause more than 200 million Dollars economic loss in the EU alone (OECD, 2016). Due to the downsides of conventional intervention methods, implementing new strategies to control *Salmonella* in foods and production facilities gained importance (Barroug et al., 2021).

Bacteriophages, phages, are the prokaryotic viruses. Phages, the most abundant entities on the planet, their number is 8 to 10 fold higher than bacteria (Dion et al., 2020). They are abundant in variety of environments and non-pathogenic to humans. Phages have two possible life cycles depending on their interactions with the target host; lysis and lysogeny. Lytic phages lyse the cell after an infection cycle. A phage that replicates only with lytic cycle is called virulent. On the other hand, phages undergo lysogeny are called temperate (Gao et al., 2020). Virulent phages have been emerged as viable biocontrol agents against pathogenic bacteria due to several advantages. First of all phages are natural and the most environmentally friendly intervention method available (Moye et al., 2018). There are commercial phage products on the market with generally regarded as safe (GRAS), Halal and Kosher certificates. Phages do not require additives or adjuvants; they often come with a low

2

level saline solution. Furthermore, cost of phage application is typically much less than most other intervention methods (Moye et al., 2018). On the other hand, phages are required to be well characterized phenotypically and genotypically before applications (Chan et al., 2013). Phages must satisfy a number of genomic and phenotypic features to avoid complications. Their interactions with their hosts must be fully uncovered before application (Żbikowska et al., 2020).

In this study, bacteriophages infecting *Salmonella* were isolated from cattle-poultry feces and wastewater in order to offer an alternative method to antibiotics since antibiotic resistance became an important concern. The samples were supplied from several locations in Turkey. Since the distribution of *Salmonella* serovars is different in distinct regions, bacteriophages isolated in Turkey have a significant importance because they can be effective against local *Salmonella* serovars prevalent in Turkey. Besides that, *Salmonella* isolation and their genomic characterization was performed to provide a better understanding of *Salmonella* strains in these samples.

Moreover, the efficacy of isolated bacteriophages was evaluated on various *Salmonella* strains and some of their characteristics were determined to identify them so that they can be employed as biocontrol agents to reduce the risk of *Salmonella* contamination in foods and food processing facilities. The identified bacteriophages will make a major contribution to the phage database.

The main purpose of this study was to isolate and characterize phages that effective against the most prevalent *Salmonella* serotypes in cattle and poultry farms. It was aimed to create a fundamental basis for a phage product that could be used feed additive and/or surface decontaminant in the short term, and to reduce the *Salmonella* population in poultry and cattle products in the long term. To reach these goals:

- Determination of *Salmonella* load and serotypes in poultry and cattle farms and sewage – *Salmonella* isolation and count in poultry farms and sewage was done and serotypes were determined via molecular identification

methods. Antimicrobial resistance of *Salmonella* isolates was also determined.

- Isolation and characterization of bacteriophages from poultry and cattle farms and sewage – Isolated bacteriophages characterized phenotypically and genotypically. Depending on the host range, most effective phages were whole genome sequenced.

- Reducing *Salmonella* load in feed– Bacteriophages were selected based on their target host, and were tested as potential feed additive.

CHAPTER 2

LITERATURE REVIEW

2.1   *Salmonella*

Salmonella is a Gram negative, rod shaped, facultative anaerobic bacteria. *Salmonella* cells are motile with peritrichous flagellae. *Salmonella* is able to grow between 5-46 °C and 3.8-9.5 pH range (Vandeplas, 2017). Salmonella has two species; *Salmonella bongori* and *Salmonella enterica*. *S. enterica* is mainly associated with warm-blooded animals, and has six subspecies. These subspecies are further divided into "serotypes" based on their flagellar and somatic antigen structures. Among those subspecies, *S. enterica* subsp. *enterica* (*Salmonella*) is the main zoonotic pathogen that causes diseases humans and animals (Chan et al., 2003). Currently, there are 1585 serotypes under *S. enterica* subsp. *enterica*, most of which were named after a geographical location. These locations are including but not limited to cities, countries, rivers, and lakes. Some earlier serotype names such as Enteritidis and Typhi were associated to clinical syndromes (Gossner et al., 2016). Some of the serotpyes are host specific, such as *S.* Gallinarum and *S.* Pullorum are specific to poultry, and *S.* Dublin in cattle. On the other hand, some serotypes are not host specific, and may infect multiple species, including humans (Revolledo & Ferreira, 2012; Wigley, 2014).

As one of the most prevalent foodborne pathogens, *Salmonella* cause millions of cases worldwide (Hendriksen et al., 2011). Although *Salmonella* is abundant in environment major source of it is poultry. EFSA report confirms that most of the *Salmonella* cases in Europe is linked to zoonoses. In addition to humans, *Salmonella* impose a constant threat to farm animals. For example, *Salmonella* infection in cattle often result with diarrhea and fever. In uncommon cases, *Salmonella* infection resulted in death (Hoelzer et al., 2011). *Salmonella* infection in dairy herds are

associated with reduced milk production that resulted in increased production costs and antibiotic residue in milk. In asymptomatic cases, animals become carriers of *Salmonella* and might transmit the pathogen to humans (Cobbold et al., 2006). Antibiotics have been used in veterinary for the treatment of diseases (Landers et al., 2012).

Antibiotics inhibit or eliminate bacteria with five main mechanisms. These are, protein synthesis inhibition, nucleic acid synthesis disruption, metabolic pathway interference, and cell wall synthesis inhibition, and disruption of cell wall (Tenover, 2006). Different antibiotic classes affect the target with a different mechanism. For example, fluoroquinolones inhibit DNA synthesis, while cephalosporins inhibits cell wall synthesis. However, overuse of antibiotics in chicken farms to prevent pathogen contamination was linked to rapid increase in antibiotic resistant bacteria (Landers et al., 2012).

Antibiotic resistance is a natural phenomenon. Antibiotic resistance occurs when a drug is ineffective for the treatment of the given pathogen (Alcaine et al., 2007). It is caused by plasticity and adaptability of bacterial genome (McDermott et al., 2018). The resistance occurs with a number of mechanisms. For example, bacteria might alter the configuration or cleave the antibiotic with the enzymes such as β-lactamases, or modify the target of antibiotic such as mutations in DNA gyrase for quinolone resistance (Peterson & Kaur, 2018). Antibiotic resistance might be intrinsic, meaning that pathogen might be less susceptible innately to antibiotic class due to surface characteristics or genomic features (Tenover, 2006). However, a more serious public health threat is the acquired resistance. Acquired resistance is the acquisition of resistance factor (e.g. efflux pump) via horizontal gene transfer (HGT) (Baquero et al., 2009). HGT occurs via three mechanisms; transformation of free DNA from environment, conjugation by mobile genetic elements, and transduction by bacteriophages (Hu et al., 2017). Horizontal gene transfer enables the spread of resistance genes presented on mobile genetic elements such as plasmids and transposons. With horizontal gene transfer, resistance may spread globally in a very short span (Ochman et al., 2000). For example, colistin resistance, which previously

6

known to occur only through chromosomal mutations, has disseminated worldwide in 10 years through *mcr* gene family (Hussein et al., 2021). In addition, chromosomal genes might also be mobilized and disseminated by plasmids. For example, *ampC* gene, a chromosomal β-lactamase gene which confers cephalosporin resistance in *Enterobacteriaceae*, has been found on plasmids, and spread globally (Jacoby, 2009).

Starting with the early 90s, antimicrobial resistance has been observed in *Salmonella* (WHO, 2013). However, over and misuse in medicine and veterinary practices, as well as using antibiotics as growth promoters in food animals accelerated the spread of antibiotic resistance greatly (CDC, 2013). Antimicrobial resistance is one of the most severe health problems. Ineffective antibiotics leads longer treatment durations, and even life threatening situations in surgeries, cancer treatment, and organ transplants and dialysis. EU parliament banned the growth promoter of antibiotic in 2006, and banned prophylactic use of antibiotics by 2022 (Patel et al., 2020).

Fluoroquinolones, third generation cephalosporins, and azithromycin are clinically important antibiotics for the treatment of *Salmonella*. Moreover, carbapenems are used as last resort antibiotics as most *Salmonella* strains are susceptible to carbapenems. Therefore, emerging resistance against these antibiotics are considered as a serious public health issue (WHO, 2017). Antibiotic resistance of *Salmonella* from various sources have been monitored in different parts of the World for over 20 years. For example, in the US, antimicrobial resistance data is collected and published by National Antimicrobial Resistance Monitoring System (NARMS). The results are available publicly in an interactive interface (Karp et al., 2017). In general resistance rates were higher in animal isolates than human isolates. In animals, resistance of *Salmonella* from poultry sources was higher than cattle (Bjork et al., 2015). Antibiotic resistance patterns also show geographical variations. For example, ciprofloxacin resistance rates in broilers in the EU were 53%, whereas in the US nearly all *Salmonella* strains isolated from broilers were susceptible to ciprofloxacin. Furthermore, resistance rates fluctuated between the European

countries. For example, ciprofloxacin resistance rates in Denmark were zero, while in Hungary resistance rates reached 91% (McDermott et al., 2018).

Salmonella serotypes show geographical clustering. For example, while *S*. Sofia is a rare serotype in rest of the world, it is the most prevalent serotype in poultry products in Australia. In addition to regional differences, *Salmonella* serotypes show matrix based differences as well. For example, in Europe Typhimurium is the most prevalent serovar in pigs, whereas Enteritidis is the most prevalent in poultry. In general, Typhimurium and Enteritidis are the two serotypes that show global presence, despite the regional differences are observed for the rest of the serovars (Ferrari et al., 2019). In fact, spread of Enteritidis is considered as an ongoing pandemic which was emerged in 80s. It was believed that dispersal of this serotype was associated to globalization of poultry supply chain. In addition, feed contamination was another likely source for the spread of Enteritidis (Li et al., 2021). Similarly, spread of multidrug resistant strain Typhimurium (DT4) was considered as global epidemic during the 90s. main driver of dissemination of that strain was thought be animals and foods (Mather et al., 2013a). Infantis, Kentucky, Derby, and Agona serovars also distributed globally. (Singer et al., 2009) showed that some serotypes show more competitiveness than others, and cultivation media and method also affects the bias.

One of the main sources of *Salmonella* is poultry and poultry products (Rajan et al., 2017). *Salmonella* contamination may occur in all steps of poultry production, from farm to process, storage, and distribution, and preparation (Abhisingha et al., 2020). One of the main contamination routes of *Salmonella* is through contaminated feed (Nair & Kollanoor Johny, 2019). Contamination might occur through a number of ways, and *Salmonella* might survive in dry feed for months (Jones, 2011). Although contamination route is complicated and hard to associate with, contamination in feed may introduce *Salmonella* into supply chain (Harrison et al., 2022). Several feed additives have been proposed to tackle *Salmonella* in feed, including prebiotics and probiotics (Maciorowski et al., 2006). Before their ban due to resistance concerns, antibiotics had been used for over 50 years as feed additive (Dibner & Richards,

2005). Bacteriophages have also been emerged as a viable feed additive (Nair & Kollanoor Johny, 2019).

In a comprehensive study in Turkey, 35.9% of the 417 broiler was found to be contaminated with *Salmonella*. In addition, *Salmonella* isolation rate was 24.5% and 12.5% for the mats and feed, respectively. *Salmonella* isolates were grouped under 22 serotypes. Infantis was the most prevalent serotype, 76.5% of the isolates were Infantis. Kentucky, Enteritidis, Senftenberg, Mbandaka, Hadar, and Typhimurium serotypes were also found. Almost all of isolates were found resistant against at least one antibiotic. Furthermore, 460 of 652 Infantis isolates, and 104 of 121 Kentucky strains were multidrug resistant (Gida ve Kontrol Genel Mudurlugu, 2018). In another study antimicrobial resistance of 99 *Salmonella* that were isolated from chicken carcasses was investigated. More than half of the isolates were found to be resistant two or more antibiotics (Zafer et al., 2015).

Salmonella contamination in poultry products in Turkey was reported to be high (Acar et al., 2017; Gida ve Kontrol Genel Mudurlugu, 2018). Studies also showed that isolated *Salmonella* serovars showed multi drug resistance. In our previous studies, prevalent serovars in Turkey were Infantis, Typhimurium, Montevideo, Kentucky, Enteritidis, and Telaviv (Acar et al., 2017). In another study, Infantis, Kentucky, Enteritidis, Senftenberg, Mbandaka, Hadar, and Typhimurium were reported as the most prevalent serotypes (Gida ve Kontrol Genel Mudurlugu, 2018). In our latest study, we found that Liverpool was a prevalent serovar in food and environmental samples in Ankara region (Tok et al., 2022). In that study, 66% of the *Salmonella* isolates showed multidrug resistance. Successful previous examples of Denmark and the Netherlands showed that fighting with foodborne diseases should be localized. A national burden of foodborne disease estimate should be conducted by authorities based on the scientific data (Pires et al., 2021). For *Salmonella*, all of these studies showed that serotype distribution of *Salmonella* was dynamic and needs to be monitored regularly. Furthermore, antibiotic resistance of *Salmonella* strains isolated from poultry in Turkey was high and needs to be reduced.

2.2   Bacteriophages

Bacteriophages were discovered by Felix d'Herelle in 1917 (Summers, 2016). Phages are the most abundant and diverse organisms on earth (Dion et al., 2020). It is estimated that total phage number is nearly 10 times more than bacteria (Żbikowska et al., 2020). They have major roles in every environment, from biochemical cycling in oceans, to modulating human metabolism through lysogeny in human gut microbiota (Kim & Bae, 2018). *Salmonella* and *E. coli* phages have recovered from human stool (Fortier & Sekulovic, 2013; McGrath & Sinderen, 2007).

Phages are the main driver of evolution of pathogenic bacteria (Fortier & Sekulovic, 2013). Lysogenic phages provide many benefits to its host; such as toxin production in *Corynebacterium dipteriae*, *Clostridium botulinum*, *Vibrio cholera,* and *E. coli* O157:H7 (Brüssow et al., 2004), sporulation in *Clostridium* (Postollec et al., 2012) and *Bacillus cereus* (Boudreaux & Srinivasan, 1981), virulence in *Salmonella enterica, Staphylococcus aureus,* and *Streptococcus pyogenes* (Aziz et al., 2005; Cooke et al., 2007). In addition to these well-known examples, prophages are also involved in biofilm formation, viral resistance, and antibiotic resistance of host (Fortier & Sekulovic, 2013; Wang et al., 2010).

Phages had been used as an antimicrobial agent until the discovery of antibiotics. Recently, phages have started gaining popularity due to high prevalence of antimicrobial resistance. One of the most important features of phages is the limited host range. It was shown in different applications that phages do not harm natural microflora, animal or human cells. Moreover, Food and Drug Administration (FDA) declared the status of several commercial phage cocktails GRAS (Hagens & Loessner, 2010). In addition, a number of phage products were Halal and Kosher certified (Moye et al., 2018).

2.2.1   Bacteriophage classification

Classification of phages, or viruses in general, has always been complicated. Initially, tailed phages (*Caudovirales*) were grouped under 3 morphologies; contractile tail, long non contractile tail, and short non contractile tail (Turner et al., 2021). Later, the main three family of tailed phages were named as *Myoviridae*, *Siphoviridae*, and *Podoviridae*. Classification of phages took a big leap with the introduction of electron microscopy (Ackermann, 2011). This allowed the morphology based classification. In 1970s, David Baltimore introduced another classification method based on genome type and relation to mRNA synthesis. According to that scheme, phages were classified under seven groups; double stranded (ds)DNA, single stranded (ss)DNA, double stranded (ds)RNA, single stranded (ss)RNA, positive sense RNA, negative sense RNA, and reverse transcribing DNA. This system is very useful as it still is used today, but it is missing evolutionary relationship of viruses (ICTV, 2020).

With the rapid emergence of genomics, phage sequences provided magnitudes of more resolution compared to previous techniques. Therefore, instead of host range or physical features based classification, a genome based taxonomy was proposed (Rohwer & Edwards, 2002). More than 96% of known phages are tailed ds DNA phages (Żbikowska et al., 2020). Bacterial and Archaeal Viruses Subcommittee of ICTV adopted a new genome based taxonomy approach. In the 1999 ICTV reported consisted of three families and 30 species. On the other hand, 2018 report had 5 families and 1320 species (Dion et al., 2020). Very recently, new families have been derived from *Myoviridae*, *Siphoviridae*, and *Podoviridae* (Turner et al., 2021). ICTV accepts proposals, and with the rapid increase in the number of phage genomes on databases, new families and subfamilies are expected in near future (Aiewsakun & Simmonds, 2018).

2.2.2 Bacteriophage structure

Based on their morphology phages are investigated under 3 families; *Myoviridae*, *Siphoviridae*, and *Podoviridae*. Although their enormous diversity, phages have a basic structure design; a head, consisting of a capsid, a protective protein coat, which is containing genetic material, and a tail which is essential for infection (Figure 2.1). Bacteriophage structure has been studied for decades with different visualization techniques from X-ray crystallography to nuclear magnetic resonance, and most importantly, electron microscopy (White & Orlova, 2019). The resolution has been vastly increased, and protein structures of capsids of well-known phages like T4 (Chen et al., 2017) , T5 (Vernhes et al., 2017), and P22 (Parent et al., 2010) has been explained in detail. Vast majority of phage heads have an icosahedral shape. Ackerman recorded the diameter of the head of more than 100 *Salmonella* phages in electron microscope, and measurements were in range between 44 to 104 nm (Ackermann, 2007).
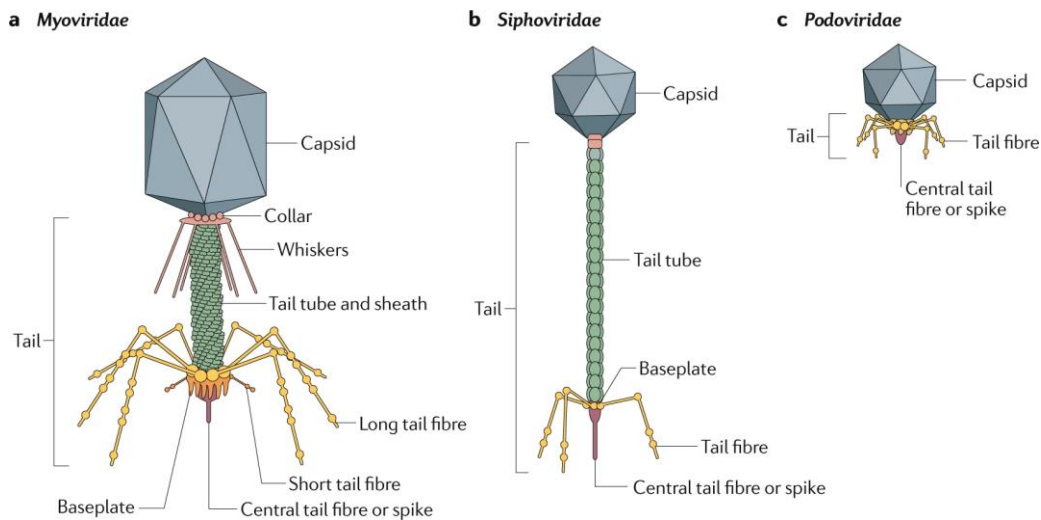
Figure 2.1 Morphology and structure of phages. Image was taken from Nobrega et al. (2018) with permission.

Phage tail structure differ between the families. *Myoviridae* has a contractile tail, *Siphoviridae* have long, elastic, and non-contractile tail, and *Podoviridae* have short

non contractile tail (Turner et al., 2021). At the distal end of the tail, there are tail fibers and tail spikes. These tail fibers and spikes are attached to a base plate in *Myoviridae* and *Siphoviridae*. However, since tail is short in *Podoviridae*, tail fibers and spike is directly attached to tail (Nobrega et al., 2018). The tail of *Salmonella* phages belong to *Podoviridae* were less than 20 nm, whereas *Siphoviridae* family might reach up to 280 nm length (Ackermann, 2007).

2.2.3   Bacteriophage infection mechanism

Phage infection always starts with physical interaction between phage and host. Initial contact occurs by diffusion or Brownian motion (Harada et al., 2018). The receptor binding proteins presented at the tail fibers of phages, recognize the receptors on the bacterial surface and two step binding is initiated. First stage is reversible binding, in which the adsorption is not complete and phage could desorb (Dowah & Clokie, 2018). The surface receptors on bacteria are including, glycoproteins, lipopolysaccharides, amino acids, teichoic acids, or flagella and pili (Harada et al., 2018). Since cell structures of Gram-positive and Gram-negative bacteria are different, phage binding receptors differ. For example, main binding receptor of Gram-negative bacteria is the lipopolysaccharide (LPS) layer. Tail fibers of phage recognize O-antigen on LPS, and hydrolyze it for the penetration of tail (Golomidova et al., 2016). On Gram-positive bacteria, phages mainly attach teichoic acid. However, Xia et al. (2011) showed that phages from different families prefer different binding sites. For example, *Siphoviridae* prefer substituent groups, while *Myoviridae* binds the backbone. Phages are also reported to bind flagella (Choi et al., 2013), pili (Chibeu et al., 2009), and capsule (Pickard et al., 2010). In addition to infection, host range of phage is determined by the attachment of receptor binding proteins on tail fibers (Abdelsattar et al., 2021). In general, phages are monovalent, they can infect only a narrow strain range. Polyvalent phages that can infect multiple strains are rare in nature.

In the second stage, irreversible binding occurs as a result of adsorption of the receptor. Multiple tail fibers bind to receptors, and baseplate conformation of phage changes. Then, tail spike binds the host receptor irreversibly. In case of *Myoviridae*, binding and baseplate configuration change occur, tail contracts for the ejection of genetic material. (Nobrega et al., 2018). After irreversible binding, phage inject its DNA into the host cell by cleaving host membrane with it enzymes (Bertozzi Silva et al., 2016). A number of proteins have role in DNA injection into host cell. These proteins are called membrane penetrating proteins, and structurally different than tail fiber. Although main function of membrane penetrating proteins, they might be associated with host range (Nobrega et al., 2018). In addition to membrane penetration proteins, phages also consist of lytic enzymes for local degradation of bacterial membrane. These enzymes are grouped under 5 classes based on their specificity; lytic transglycosylases, endopeptidases, N-acetyl-muramoylamidases, lysozymes, and N-acetyl-β-δ-muramidases.

After injection, phage genome must be protected from bacterial exonuclease degradation. For that, phage has a small specific site named cos region. This region helps DNA circularization. Host enzyme, DNA ligase seals the cos site at the either hand to produce circular DNA. Another host enzyme, DNA gyrase supercoils the phage DNA (Trun & Trempy, 2009).

2.2.4   Bacteriophage lifecycle

Bacteriophages are called lytic or temperate (lysogenic) based on path the followed after infection. Lytic phages lyse the host after an infection cycle, while temperate phages integrate their genetic material into the host DNA. Temperate phages can initiate lytic cycle based on some environmental responses. However, due to the unpredicted nature temperate phages are not preferred in phage applications (Chan et al., 2013). Lytic phages lyse the bacteria with a mechanism called as "lytic cycle". Lytic cycle is consisted of mainly 4 stages. Attachment of the phage is the first stage of infection in which phages recognize specific binding sites (e.g. outer membrane

proteins, teichoic acid) on the host membrane with the specialized proteins in tail fibers. In the second stage of infection, penetration, phage inject its genetic material into the cell by either mechanical force or with lysozyme activity. Third stage is called as biosynthesis or redirection. At this stage, phage viral components are produced by hosts synthesis mechanisms. In the next stage, maturation, newly formed viral components are assembled to form virions. At the final stage, release, host cell is lysed by lytic enzymes such as lysin, holin and murein, and virions are released into environment (Drulis-Kawa et al., 2012).

Lysogenic relationship between phage and host is very complex, and may result in different outcomes. Lysogenic pathway of phage λ is used as model. According to Brady et al. (2021), phage decides lytic or lysogenic pathway based on the environmental responses. There are two main regulators that control lytic lysogenic switch; Cro and CI. Lysogenic pathway is regulated by CI, which repress lytic operators, while Cro controls lytic pathway (Brady et al., 2021). For instance, phages might enter pseudolysogenic life cycle. In this state, phage genome stays unintegrated to host, and transferred to only one daughter cell. This lifecycle often associated with stress conditions like, starvation. Phage might turn lytic or lysogenic when the stress conditions disappear (Monteiro et al., 2019). Lysogenic phages might turn in cryptic prophage due to gradual decay or genome rearrangements during the evolution. The cryptic prophages are unable to initiate lysis contrary to active prophages, and became a permanent part of host genome (Wang et al., 2010). For example, one of the most studied bacteria, *E. coli* K-12, has 9 cryptic phages which constitutes 3.6% of the total genome (Canchaya et al., 2003).

Phenotypically, one-step growth is a convenient and descriptive characteristic to describe the virus lytic life cycle. A cycle starts when the virus bind and penetrate the cell. This initial phase is called as latent period, and no viral particles are found in media at this stage. After the latent period, the burst occurs and newly formed virions are bursted out of cell. In this period, the number of viruses in the media is increased sharply, and is called as the one-step growth (Kropinski, 2018).

2.2.5   Bacteriophage application

An important feature of phages is the ability to be used in very diverse applications. There are a wide variety of reports of phage applications in medicine in the literature (Pirnay et al., 2019), environment (Ye et al., 2019), veterinary (Atterbury et al., 2007). In the recent years, pre-clinical and clinical studies involving phage or phage combinations have been widely popular due to potential of phages. For example, Altamirano et al. (2022) combined a phage and an antibiotic for treatment of *Acinetobacter baumannii* in vivo. Although *A. baumannii* was resistance to given antibiotic, bacteria become susceptible again. In foods, phages can be used as antimicrobial agents. In addition, phage enzymes, endolysins can also be utilized as agents (Lee et al., 2022). Phage applications can be evaluated in 4 main groups; therapy, sanitation, control and prevention. Sanitation is the application of phages on food contact surfaces. Phage applications in pre-harvest or pre-slaughter is called as therapy, in process named as control, and after process (e.g.) storage is called as prevention (Greer, 2005).

Phages can be used as biocontrol agents in farm animals for therapeutic purposes. In a study, phages were applied to poultry orally as a feed additive, and 1.3 log reduction in *Salmonella* population was observed (Sklar & Joerger, 2001). In a similar study, phages reduced *Salmonella* population by 3.5 log in broiler, when applied orally as an additive (Fiorentin et al., 2005). Borie et al. (2008) reported that *Salmonella* colonization in digestive track was completely prevented with phage application. Landers et al. (2014) showed that phages could be used as growth promoter in farm animals as an alternative to antibiotics.

Phages can also be used in processing stage for biocontrol of foodborne pathogens. Bacteriophage addition to milk during cheese production prevented *Salmonella* growth for 89 days (Modi et al., 2001). Abdelsattar, Safwat, et al. (2021) used a monophage to reduce *Salmonella* Enteritidis contamination in milk. After 3-hour incubation at 37 °C, phage reduced *Salmonella* population by 10^3.

Bacteriophages are also viable sanitation agents, as they are reported effective against biofilms in various foodborne pathogens including *Salmonella* (Islam et al., 2019), *E. coli* (Lee & Park, 2015), and *Vibrio* (Sasikala & Srinivasan, 2016). In another study, a phage cocktail containing 6 phages was applied to reduce *Salmonella* population on glass and steel surfaces. Phage cocktail reduced the *Salmonella* population by 2-4 logs on surfaces (Woolston et al., 2013). In the same study, researchers used *S.* Paratyphi B as the target on surface. Phage cocktail was ineffective against Paratyphi B in initial experiments. However, when two of the phages were replaced with Paratyphi targeting phages, phage cocktail significantly reduced the Paratyphi B on the surfaces. Authors stated that the results showed the flexibility of phage application (Woolston et al., 2013).

There are a number of FDA approved phage based biocontrol agent that targets *Salmonella*, including but not limited to SalmoFresh^{TM} by Intralytix (US), PhageGuard-S by PhageGuard (Netherlands), Armament by Omnilytics (US), and Biotector by Cheiljedang (South Korea). These products are sprayable to food and food contact surfaces. These products are included in the USDA Food Safety and Inspection Service (FSIS) list for safe products for chicken and meat process. Moreover, some of those products (e.g. SalmoFresh) has halal certification. However, due to the nature of phages, these products were prepared for specific serotypes, and may not affect others. For example, SalmoFresh targeted Typhimurium, Enteritidis, Heidelberg, Newport, Hadar, Kentucky, Thompson, Georgia, Agona, Grampian, Senftenberg, Alachua, Infantis, Reading, and Schwarzengrund. On the other hand, Biotector targets poultry pathogens, Gallinarum and Pullorum. Host ranges of commercial phages indicates the need of more local targeted phage products. For instance, in our previous studies we discovered Telaviv and Liverpool were two emerging serotypes in Turkey. As a result, current commercial products may not be effective in Turkey. For a successful phage product, first most prevalent and most infectious serotypes in that region must be determined, and a target based product must be developed. A similar observation was made by Moreno Switt et al. (2013). Host range of 108 phages isolated from 10 different farms

were investigated. While 51% of phages showed narrow host range, remaining phages infected a broad range of hosts. In the same study, it was determined that there is a correlation between the isolated phage and their hosts. For instance, if the dominant serotype was Enteritidis in a farm, isolated phages from that farm was generally effective against Enteritidis (Moreno Switt et al., 2013).

Timing, delivery method, and titer are the key factors in phage application (Atterbury et al., 2007). Phages are generally applied in solution in food and farm applications (Han et al., 2022). Phages might be developed in powdered or tablet form. Vandenheuvel et al. (2013) dried phages in a spray dryer with lactose, dextrose, and trehalose. In that study, phage titer was significantly dropped when dried with lactose and dextrose. However, trehalose addition was found successful in phage drying. Even with the successful drying application with trehalose, phages powder had to be kept under a certain temperature and relative humidity (Landers et al., 2014). Lyophilization is another drying application that shows promising results. Merabishvili et al. (2013) lyophilized phages with sucrose and trehalose addition, successfully stored for more than 2 years with a stable titer. Chan et al. (2013) described several aspects for a successful phage therapy experiment; First of all, phage must be strictly lytic. Secondly, phage must successfully lyse the representative strains of host. Moreover, models should represent the real life scenarios. Authors stated that purification through filtration would be sufficient for in vitro models (Chan et al., 2013). Furthermore, rapid development in synthetic biology created a lot of promising therapy options. For example, Monteiro et al. (2019) reviewed the phage therapy methods involving temperate phages. Advances in bioengineering enabled the development of lytic phages from temperate phages.

2.2.6 Bacteriophage application on poultry production

Ability of phages to reduce *Salmonella* in all stages of poultry chain has been studied extensively. Atterbury et al. (2007) tested the ability 3 phages to reduce cecal colonization *Salmonella* in broiler. Phages were administered orally with an antacid

suspension. After 24 hours, when treated with their phages, *Salmonella* Enteritidis and *Salmonella* Typhimurium loads were reduced by 4.2 and 2.19 log CFU, respectively. However, Hadar phage was unable to reduce Hadar population. Authors explained the ineffectiveness of Hadar phage might be due to the phage resistance developed during the treatment (Atterbury et al., 2007). In a similar study, Bardina et al. (2012), tested a phage cocktail against *S*. Tyhpimurium in mouse and chicken models in vivo. In mouse models, authors reported 50% survival was achieved when cocktail was given with infection. In chicken models, significant reductions were obtained when phage cocktail applied pre-infection. In a comprehensive study, Clavijo et al. (2019) tested a commercial phage cocktail (SalmoFREE®) in two field trials with nearly 35000 broilers each. In each trials there were a control farm as well. Researchers added the phage cocktail and control suspension to drinking water of broilers for trial and control groups, respectively. After a production cycle (33 days) *Salmonella* prevalence in cloacal swabs was 0%, whereas *Salmonella* positive samples were observed in control farm. Researchers also reported that phage cocktail didn't affect broiler production parameters, or broiler behavior. The results showed that phages might be used against *Salmonella* in poultry production without affecting the production quality (Clavijo et al., 2019).

Phages also tested as a post slaughter control tool against *Salmonella*. Higgins et al. (2005) designed two experiments to test the efficacy of phages against *S*. Enteritidis. In the first experiment, authors treated carcass rinse waters with a single phage. Secondly, they artificially contaminate the carcass with *S*. Enteritidis, and sprayed the phage in different concentrations. Authors reported significant reductions in *S*. Enteritidis populations in all experiments (Higgins et al., 2005). Phage biocontrol of *Salmonella* on chicken carcasses was also studied by a different study design (Atterbury et al., 2020). Broiler chickens were infected with *S*. Enteritidis and *S*. Typhimurium. Animals were euthanized 7 days later, and 25 cm^2 area of skins were recovered. Respective phage suspensions were sprayed onto samples, and SM buffer were sprayed to control samples. After incubation period *Salmonella* colonies counted with most probable number (MPN) method. While Enteritidis phage

reduced Enteritidis counts by 1.38 log MPN, Typhimurium phage reduced Typhimurium population by 1.83 log. Both of the reductions were found significant compared to control (Atterbury et al., 2020).

Phages were found effective during the various processing steps of poultry. In a study, trimmed poultry were inoculated with *Salmonella* to a final concentration of 7 log CFU/g in ground product. A commercial phage suspension was added during the tumbling process at levels 10^8 plaque forming unit per mL (PFU/mL). After samples held at 4 °C for 6 hours, phage reduced *Salmonella* population by 1.1 and 0.9 log in chicken and turkey, respectively (Yeh et al., 2017). Sukumaran et al. (2015) evaluated the effectiveness of a commercial phage (SalmoFresh) when applied combined sequentially or combined with various antimicrobials in poultry cuts. The authors reported that combination phage and lauric arginate reduced *Salmonella* by 1.3 log. When the phage and peracetic acid was applied in sequence, the reduction reached 2.5 log (Sukumaran et al., 2015).

Phage application during storage at various temperatures was studied by different groups. Bao et al. (2015) tested phages against *Salmonella* on chicken breast at 4 °C and 25 °C. Phage suspension reduced *Salmonella* population significantly (1.65 log) after 5-hour storage at both temperatures. Authors reported that a bigger reduction in *Salmonella* numbers was observed at 4 °C (Bao et al., 2015). Contrarily, Duc et al. (2018) reported bigger reduction was observed in 25 °C. In that study, chicken pieces were artificially contaminated with *S*. Enteritidis and *S*. Typhimurium, and treated with a phage cocktail at 8 °C and 25 °C. 1.41 log and 1.86 log reduction was observed for Enteritidis and Typhimurium, respectively at 8 °C. However, reduction was 3.06 log and 2.21 log for Enteritidis and Typhimurium at 25 °C (Duc et al., 2018). Abhisingha et al. (2020) used a phage cocktail to reduce *Salmonella* Typhimurium on chicken. Artificially contaminated chicken meat was treated with phage cocktail, and stored at 4 °C and -20 °C for 24 hours. Significant reductions in *Salmonella* population were observed in both storage conditions. Combination of a commercial phage cocktail and packaging conditions on *Salmonella* during storage was studied. *S*. Typhimurium, Heidelberg, and Enteritidis were treated with phages

$(10^9$ PFU/mL), and stored up to 7 days in two different packaging conditions; aerobic and modified atmosphere (95 CO_2 and 5% O_2). Phages reduced the *Salmonella* counts significantly in both packaging. Highest reduction was observed when MAP and phage cocktail combined (Sukumaran et al., 2016).

CHAPTER 3

MATERIALS AND METHODS

3.1 Chemicals and materials

A list of chemicals, materials and the commercial manufacturers of those materials are presented in the Appendix J. All of the substances used in the study were analytical grade.

3.2 Sample collection

In the study, samples from farms in different cities were collected. Cities in the study were Adıyaman, Şanlıurfa, Ankara, Bolu, and Denizli. Cities were selected from different regions to provide phage and *Salmonella* diversity. Adıyaman and Şanlıurfa samples were kindly provided by Prof. Dr. Yasar Osman Tel. 100 g samples were collected in sterile cups with sterile spoons from each farm. From wastewater facility, 100 mL sample was collected in sterile 50 mL tubes. Samples were brought to lab as soon as possible without breaking the cold chain. Samples were taken in 11-month span to observe the effect of seasonal changes and shifts on *Salmonella* and bacteriophages.

A total of 57 sample was collected in 11 months (Table 3.1). 25 samples were collected from Adıyaman. 5 different farms were visited in 5 different months. Similarly, 5 farms in Şanlıurfa were visited in 4 different months. In Denizli, 3 different farms were visited in June, while 5 farms were visited in Bolu, in August. METU wastewater facility was visited in 4 different months in order to increase sample diversity.

Table 3.1 Sampling dates and locations

Month	Sampling Sites		
February	Adıyaman (n=5) (2P, 3C)	Şanlıurfa (n=5) (2P, 3C)	
June	Adıyaman (n=5) (2P, 3C)	Şanlıurfa (n=5) (2P, 3C)	Denizli (n=3) (3P)
August	Adıyaman (n=5) (5P)	Bolu (n=5) (5P)	Wastewater (n=1)
September	Şanlıurfa (n=5) (2P, 3C)		
October	Adıyaman (n=5) (2P, 3C)		Wastewater (n=1)
November	Adıyaman (n=5) (2P, 3C)	Şanlıurfa (n=5) (2P, 3C)	Wastewater (n=1)
December			Wastewater (n=1)

n: Total number of samples P: samples collected from poultry farms, C samples collected from cattle farms

3.3   *Salmonella* isolation

Samples collected for phage isolation, was also used for *Salmonella* isolation, synchronously. Isolation of *Salmonella* was carried out as described by ISO 6579:2002 protocol. Briefly, 25 g farm sample or 25 mL wastewater sample was added into 225 mL buffered peptone water (BPW) and homogenized for 1 minute. Samples were incubated 20±4 hours at 37 ◦C for pre enrichment. Then, 100 µL mixture was taken from stomacher bag, and added onto rappaport vassiliadis soy (RVS) broth. Broths were incubated for overnight, and 10 µL sample were plated onto xylose lysine desoxcholate (XLD) agar plates by spread plate. After another incubation for 24 hours at 37 ◦C, suspected colonies (black with transparent halo) from plates were transferred onto brain heart infusion (BHI) agar. For each sample 3 different colonies were picked and transferred separately. When too many colonies grew on plates, serial dilutions were prepared from RVS broth, and spread plate was performed for each dilution.

3.4   Molecular confirmation of *Salmonella* isolates

Salmonella confirmation was done via polymerase chain reaction (PCR) screening of *invA* gene (Rahn et al., 1992). Single colonies from suspected isolates were streaked onto BHI agar and incubated for 18 hours. After incubation, single colonies from BHI agar were taken with a sterile stick and transferred into a 0.2 mL PCR tube containing 95 µL sterile distilled water. Cells were ruptured with microwave treatment for 30 seconds. 1 µL of lysed cell solution were added to master mix tube. PCR master mix and *invA* primer sequences are given in Table 3.2.

Table 3.2 PCR Master Mix and *invA* primer sequence

PCR Reaction Solution [Concentration]	Primer sequence 5' –3'	Volume (µl)
dH2O	- - -	17.5
5X Go Taq Flexi buff	- - -	5
invA-F [12.5 µM]	GAATCCTCAGATTTTCAACGTTTC	0.5
invA-R [12.5 µM]	TAGCCGTAACAACCAATACAAATG	0.5
Taq DNA polymerase	- - -	0.5
TOTAL		24

For each isolate, 24 µL master mix and 1 µL lysed cell was added into PCR tubes. Then, *invA* gene region (678 base pairs) was amplified by T100™ Thermal Cycler (Bio-Rad) with the conditions given in Table 3.3.

Table 3.3 Amplification conditions of *invA* gene

Temperature (°C)	Time	Cycles
94	8 min	1
94	30 sec	
60	30 sec	35
72	30 sec	
72	5 min	1
4	∞	1

5 µL PCR products was run at 110 V for 50 min in a 1.5% agarose gel in gel electrophoresis. A ladder with known molecular weight and a positive control (MET S1-001, *Salmonella* Enteritidis) was added. Bands were displayed after staining in ethidium bromide (Et-Br) solution for 5 minutes, following by a 30 minutes destaining in ddH$_2$O. Gels were visualized under UV light (Biorad-Gel Doc XR Documentation System, USA). Lanes with a band at 678 bp was confirmed as *Salmonella*. A single colony from confirmed isolates was put into 5 mL BHI broth, and was incubated for 16 hours. 850 µL of isolate was mixed with 150 µL glycerol solution, and frozen -80 °C for further experiments. All the isolates were labeled, and frozen in triplicate.

3.5   Genomic characterization of *Salmonella* isolates

Genomic relatedness of analysis was done by PFGE (Acar et al., 2017). For this experiments, isolates were streaked onto BHI agar and incubated for 20±4 hours at 37 °C. Colonies were collected with a sterile cotton swab and transferred cell suspension buffer (CSB). Concentrations were adjusted by spectrophotometer (OD$_{610}$:1.3-1.4). Adjusted suspensions were immediately taken on ice until the experiment. From each suspension 400 µL were transferred into 1.5 mL centrifuge tubes and incubated at 37 °C for 10 minutes. After incubation, 20 µL Proteinase K solution (20 mg/L) was added into each tube. Samples then mixed with 400 µL 1%

SKG agarose with %1 SDS solution in plug molds. Mixture was held in room temperature for 15 minutes to solidify. For each sample, 5 mL cell lysis buffer (CLB) and 25 μL Proteinase K solution (20 mg/L) were put into 50 mL falcon tubes. Solidified plugs were transferred into labeled falcon tubes, and tubes were incubated for 2 hours at 54 °C in shaking incubator (170 rpm). After incubation, plaques were washed with sterile ddH₂O two times and tris-EDTA (TE) buffer four times. TE and ddH₂O was held in water bath (55 °C) prior to washing. In each washing step, a filter was attached to tubes, then all liquid content was discarded, and replaced with ddH₂0 and TE according to washing step. After fresh ddH₂O or buffer addition, tubes were incubated in a shaking incubator at 55 °C. After washing, plaques stored in TE solution at 4 °C. Next day, plaques were cut in 2mm sizes and placed in the agarose gel.

Plaques of samples and reference strain were cut in 2 mm size, and placed into 1.5 mL centrifuge tubes. 200 μL H buffer (175 μL ddH₂O; 20 μL H buffer; 5 μL Xba1) was added, and the tubes were incubated for 10 minutes at 37 °C. After 10 minutes, H buffer was replaced with XbaI solution (175 μL ddH₂O; 20 μL H buffer; 5 μL Xba1) and incubated for 4 hours at 37 °C. 2.2 L running buffer (0.5% TBE) was loaded into PFGE tank and, the system was started in order to cool the buffer to 15 °C. After the incubation, plaques were loaded into 1.5% SKG agarose gel. Wells on the gel was sealed with sealing agarose. Before the run, approximately, 1.5 mL thiourea solution was added to running buffer. The gel run in DNA-Chef DR III Biorad electrophoresis system with the conditions in Table 3.5. After running for 19 hours, the gel stained in Et-Br solution for 45 minutes, and distained in ddH₂O for 30 minutes. The gels than visualized under UV light in Biorad-Gel Doc XR Documentation System. The gel pictures were loaded into Bionumerics software (Applied Maths, Belgium) for clustering analysis. Dice coefficient was used similarity analysis, and clustering was performed by using unweighted pair group method by arithmetic mean (UPGMA).

3.6 Antibiotic resistance characterization of *Salmonella* isolates

Antimicrobial resistance of *Salmonella* isolates was characterized by using disc diffusion method suggested by European Union Committee on Antimicrobial Susceptibility Testing (EUCAST, 2015). 18 different antibiotics from different classes were screened (Table 3.4). Briefly, *Salmonella* isolates were inoculated into MHB and incubated for 20±2 hours at 37 °C. After incubation, concentration of isolates was adjusted with a densitometer (Biosan Den 1B) to 0.5 McFarland which is equal to 1×10^8 by using 0.9% NaCl solution. After that, bacteria were taken with cotton swab from NaCl solution and carefully streaked onto MHA plates. Antibiotic disks (Oxoid) were placed onto plates with the help of an antibiotic disk dispenser.

Plates were incubated for 18 hours at 37 °C, and zone diameters were recorded for each antibiotic. Data was processed in Excel, and a heatmap was created based on susceptibly data.

Table 3.4 Antibiotic agents, disk contents and diameter zones used in phenotypic characterization (EUCAST, 2015).

Antimicrobial agent	Disc Content	Diameter zone (mm)	
	(µg)	S≥	R <
Amikacin	30	18	18
Gentamicin	10	17	17
Kanamycin	30	18	13
Streptomycin	10	15	11
Ampicillin	10	14	14
Ceftiofur	30	21	17
Cefoxitin	30	19	19
Ceftriaxone	30	25	22
Cephalothin	30	18	14
Amoxicillin-clavulanic acid	20/10	19	19
Ertapenem	10	25	25
Imipenem	10	22	22
Chloramphenicol	30	18	12
Nalidixic acid	30	19	13
Pefloxacin	5	24	24
Tetracycline	30	15	11
Trimethoprim-sulfamethoxazole	1.25/23.75	16	10
Sulfisoxazole	300	12	12

3.7 Bacteriophage isolation

Phage isolation was carried out as soon as the samples were transferred to lab. Isolation was carried out according to Moreno Switt et al. (2013) and Bonilla et al. (2016), with small modifications that were explained below for wastewater and farm samples.

3.7.1 Bacterial strains

Since phages are obligatory parasites and requires a host to replicate, various *Salmonella* strains were used in phage isolation. For phage isolation, 8 different isolates representing most prevalent *Salmonella* serotypes were selected from our culture collection (Table 3.5). The serovars were selected according to (I) their prevalence in human, animal, and food samples in Turkey and the EU (WHO, 2021), (ii) their relation to previous foodborne outbreaks (iii) their prevalence in poultry (Gıda ve Kontrol Genel Müdürlügü, 2018; EFSA, 2021). All strains were isolated from food sources previously and were kept at -80 ∘C. Two days before the experiment isolates were revived by streaking onto BHI agar. Isolates were incubated at 37 ∘C for overnight. Next day, a single colony from BHI agar was taken with a sterile loop and transferred into 10 mL Luria Bertani (LB) broth (Madrid, Spain). Isolates were incubated in LB broth at 37 ∘C for 18-20 hours, before used as host organism in isolation.

Table 3.5 *Salmonella* isolates that are used as target strains in phage isolation

METUID	Genus	Species	Serotype	Resistance Profile	Source	Date	City
MET S1-001	*Salmonella*	*enterica*	Enteritidis	Susceptible	Chicken meat	11/9/2005	Ankara
MET S1-002	*Salmonella*	*enterica*	Typhimurium	CipAzm	Chicken meat	11/11/2005	Ankara
MET S1-006	*Salmonella*	*enterica*	Infantis	KKfSxtSfN Cip	Chicken meat	11/7/2005	Ankara
MET S1-015	*Salmonella*	*enterica*	Montevideo	KSTSfN	Ground meat	12/14/2005	Ankara
MET S1-063	*Salmonella*	*enterica*	Telaviv	Susceptible	Offal	11.04.2012	Şanlıurfa
MET S1-007	*Salmonella*	*enterica*	Kentucky	Susceptible	Chicken meat	10/10/2005	Ankara
MET S1-248	*Salmonella*	*enterica*	Anatum	Susceptible	Sheep ground meat	7/18/2012	Şanlıurfa
MET S1-163	*Salmonella*	*enterica*	Hadar	KfAmpN	Cheese	12/24/2012	Şanlıurfa

3.7.2   Phage isolation from manure samples

For farm samples, 10 g sample was weighted with sterile spoon and cup, and was transferred into a filtered stomacher bag. Sample was diluted with salt magnesium (SM) buffer (5.8 g NaCl, 2.0 g MgSO$_4$·7H2O, 50 mL 1 M Tris-HCl pH 7.4, in 1 liter dH$_2$O). by 1:10 in stomacher bags for 2 minutes, and the put into shaker for two hours in room temperature. Then, samples were taken centrifuge tubes, and centrifuged for 10 minutes 9000 × g. After centrifugation, supernatant was taken, and the pellet was discarded. Samples were filtrated through 0.45 and 0.22 µm cellulose acetate filters, respectively. In farm samples, MET S1-001, MET S1-002 and MET S1-006 were used as host organisms (Table 3.5). For pre-enrichment, 5 mL filtrate and 100 µL of each target host strain (*S.* Enteritidis, *S.* Typhimurium, and

S. Infantis) were added to 5 mL 2 X tryptic soy broth (TSB), and were incubated in a shaking incubator at 37 °C overnight. Next day, samples were centrifuged for 10 minutes at 9000 × g and filtered through 0.22 μm filter to get rid of host bacteria and other contamination. Resulting solution was presumed as phage solution. The solution was labeled accordingly, and kept at 4 °C.

3.7.3 Phage isolation from wastewater samples

Wastewater samples were centrifuged directly without dilution at 9000 x g for 10 minutes. Supernatant was filtered through 0.22 μm cellulose acetate filter. For the pre-enrichment step, wastewater filtrates were separated into 3 aliquots with 5 mL each. Each aliquot was mixed with 5 mL 2 × TSB. All hosts are used in wastewater samples. For pre-enrichment, hosts were divided into 3 different groups according to their genetic relatedness and added to phage-TSB mixture, 100 μL each (Table 3.6).

Table 3.6 Host cocktails for pre-enrichment for phage isolation for wastewater

Groups	Serotype
1	100 μL- S1-001
	100 μL - S1-002
2	100 μL - S1-006
	100 μL - S1-007
	100 μL - S1-015
3	100 μL - S1-063
	100 μL - S1-163
	100 μL-S1-248

Pre-enrichment mixtures were incubated at 37 °C overnight. Next day, mixtures were centrifuged for 10 minutes 9000 × g, and filtrated through 0.22 μm cellulose acetate filter. Like in farm samples, resulting 3 solutions were labeled accordingly and were kept at 4 °C.

3.7.4   Double plaque assay

For both farm and wastewater samples, existence of phages in phage solutions was tested by double plaque assay. For this, 100 μL phage solution from isolation steps and 100 μL host were added into 4 mL semi solid (0.6% agar) LB agar. After shaking gently, semi solid agar was poured onto solid LB agar on plate. Plates were incubated for 20 ± 4 hours at 37 °C, and plaque formation was observed. Serial dilutions from phage solutions were prepared when the resulting petri contained too many phage plaques. For serial dilutions 900 μL 0.9% NaCl solutions were used. In that case, a double plaque assay by using NaCl solution instead of phage solution was also included as control. In this step, hosts were selected according to isolation type. For example, phage solutions from farm samples were tested against MET S1-001, MET S1-002, and MET S1-006 as these isolates were used as hosts. On the other hand, phage solutions from wastewater samples were tested against all hosts from Table 3.5.

3.8   Bacteriophage purification

Petri plates from double plaque assay were examined carefully to spot morphologically different phage plaque formations. Each morphologically different plaque was subjected to purification step. For purification, single and isolated plaques with different morphologies were selected and marked. After that, by using a pipet tip plaque was gently touched without disrupting the agar or rest of the plate. Pipet tip than dipped into 100 μL 0.9% NaCl solution to transfer plaques. A serial dilution was prepared with 900 μL 0.9% NaCl solutions up to 10^{-8} and double plaque

assay was conducted from 10^{-3} to 10^{-8} in order to obtain separated phage plaques in petri plates. The purification step was conducted at least 3 times or until a uniform plaque formation was observed. When the uniform plaque formation was reached, a single, well separated plaque was taken with a pipet tip into 100 μL 0.9% NaCl solution, and double plaque assay was conducted directly from that solution in order to obtain fully lysed petri plate.

The series of dilutions were done up to 10^{-8}, in order to determine phage titer. Phage titer was calculated as follows;

Equation 3.1 $\qquad Phage\ Titer\ (\frac{PFU}{mL}) = \frac{Number\ of\ plaques}{d*V}$

Where d is dilution, and V is the inoculation volume.

3.9 Bacteriophage storage

Bacteriophage storage was performed as suggested by Fortier & Moineau (2009). Petri plate from the last step of purification was examined after overnight incubation. If fully lysed profile was observed, 10 mL SM Buffer poured onto the plate. Petri plate with SM buffer was incubated at room temperature for 30 minutes, and gently shaken in every 3-5 minutes. After incubation, SM buffer was transferred into a centrifuge tube, and centrifuged at 9000 × g for 10 minutes. Supernatant was collected with a sterile syringe and filtered through 0.22 μm filter. Titers of phages were determined before storage. To determine the titers, series of dilutions were done up to 10^{-11}, and double plaque assay was conducted from 10^{-6} and below dilutions. After overnight incubation, phage titer was calculated as formulated in Equation 3.1.

If the phage titer was above 10^8 PFU/mL, portions were prepared from purified phage lysate for different storage conditions (Figure 3.1). From the filtrate, 1 mL was transferred into 1.5 mL Eppendorf tubes. These lysates are labeled as working

solution, and stored at 4 °C. Another 1 mL was transferred into Eppendorf tubes and these tubes were stored at -20 °C. From the remaining lysate, 850 µL was mixed with 150 µL glycerol in the cyrotubes and stored at -80 °C. All the portions were prepared in triplicates. In one of the triplicates, chloroform solution was added 1:100 ratios (10 µL for 1 mL tubes) to prevent contamination.
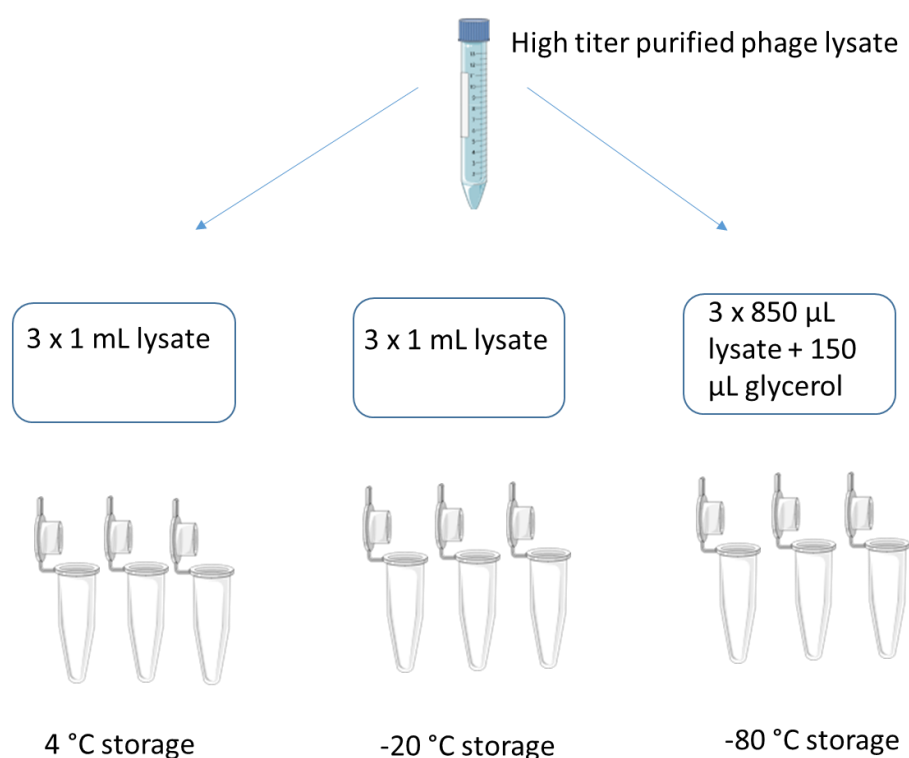
Figure 3.1 Storage scheme of phages

All the stocks were labeled; a unique ID code was assigned (METU ID), and a database, which contains all relevant information regarding the phages was created.

3.10 Bacteriophage lysis profiles on different hosts

Lysis profiles of all phages were tested on various *Salmonella* isolates in order to determine the host range. Hosts were chosen from our culture collection based on these selection criteria; (i) Serotype is listed by EFSA as the most common disease

causing serotypes, (ii) Serotype is commonly isolated in studies conducted in Turkey, (iii) Serotype caused an outbreak in the last 10 years. Based on these criteria 36 isolates representing 19 different serotypes were selected as hosts (Table 3.7). For eligible serotypes, isolates from different sources, and isolates with different PFGE types were chosen. For example, 5 different Enteritidis isolates were tested as hosts. 2 of those were clinical, 2 were food, and the other was environmental isolate. 2 clinical isolates and 2 food isolates had different PFGE types.

Table 3.7 Information of *Salmonella* isolates used in host range determination

METUID	Serotype	Antibiotic Resistance	Isolate Source	PFGE Type
MET S1-742	Enteritidis	Susceptible	Food	PT06
MET S1-217	Enteritidis	Susceptible	Human	PT04
MET S1-221	Enteritidis	Susceptible	Human	PT05
MET S1-411	Enteritidis	Susceptible	Food	PT51
MET A2-012	Enteritidis	Susceptible	Sludge	PT55
MET S1-223	Typhimurium	TAmp	Human	PT23
MET S1-185	Typhimurium	Sf	Human	PT15
MET S1-663	Typhimurium	TAmpKf	Animal	PT13
MET A2-003	Typhimurium	Susceptible	Sludge	PT59
MET A2-088	Typhimurium	NI	DT104	NI
MET S1-657	Typhimurium	STAmpAmcSfCn	Animal	PT14
MET S1-050	Infantis	KSTAmpSfN	Food	PT08

Table 3.7 Continued

METUID	Serotype	Antibiotic Resistance	Isolate Source	PFGE Type
MET S1-807	Infantis	CroEftSfSxtCKSAmp AmcTeFoxKf	Human	NI
MET S1-240	Kentucky	Susceptible	Human	PT10

MET S1-542	Kentucky	Sf	Animal	PT03
MET A2-072	Kentucky	KfSfAmpNAzmPef	Sludge	PT72
MET S1-065	Montevideo	SfSxtNT	Food	PT25
MET S1-170	Montevideo	Susceptible	Animal	PT44
MET S1-172	Montevideo	Sf	Animal	PT31
MET S1-548	Anatum	Susceptible	Food	PT42
MET S1-579	Anatum	Susceptible	Food	PT42
MET S1-163	Hadar	AmpKfN	Food	PT41
MET S1-074	Telaviv	SfSxtNT	Food	PT33
MET S1-530	Telaviv	Susceptible	Food	PT34
MET S1-008	Thompson	KSTAmpKfSfSxtCn	Food	NA
MET S1-010	Senftenberg	STSfN	Food	NA
MET S1-087	Othmarschen	Susceptible	Food	PT27
MET S1-166	Newport	Sf	Animal	PT39
MET S1-713	Braenderup	NI	NI	PFGE Ref.
MET S1-864	Mbandaka	SxtSfAmpAzmPef	Sludge	PT65
MET A2-099	Liverpool	Susceptible	Food	PT54
MET S1-003	Virchow	Susceptible	Food	NA
MET S1-011	Agona	KSTSfN	Food	NA
MET S1-220	Typhi	Sf	Human	PT23
MET S1-184	Paratyphi B	Susceptible	Human	PT15

Host range of phages was determined as described by Moreno Switt et al. (2013) and Fong et al. (2017). Briefly, 100 μL host were put into molten (50 °C) semi solid (0.6% agar) LB agar. Agar mixed gently and poured onto solid LB plate slowly. After soft LB agar was solidified (15 to 30 min), petri plates were divided 8 parts, and labeled with the ID codes of phages. In each part 5 μL of corresponding phage was spotted. Plates were left in room temperature to let the droplet dry for 30 min,

then incubated overnight at 37 °C. The next day, formations were observed and spots were graded based on the scale below:

(+) complete clearing

(T+) clearing throughout but with faintly hazy background

(T) substantial turbidities throughout the cleared zone

(P) a few individual plaques

(-) no clearing

Results were recoded as an Excel table right after the analysis. To identify phages with similar lysis profiles, a cluster analysis performed. For this, Ward's method of binary distance for hierarchical clustering was deployed in R software (RStudio version 2022.02); (R Development Core Team, Vienna, Austria [http://www.R-project.org]).

3.11 One-step growth curves, tatent periods and burst sizes

One step growth curves were determined as described by (Clokie et al., 2018). From the Table 3.9, representative phages were selected for Enteritidis and Typhimurium (MET P1-001), Kentucky (MET P1-137), Infantis (MET P1-091 and MET P1-179). In addition, MET P1-088 and MET P1-197 were also selected as representatives for Hadar and Anatum, respectively. Host bacteria was cultured into LB broth a day before the analysis. Also, 8 hours prior to analysis host cultured into another LB broth to obtain a mid-exponential log culture. Phage titer in this study was adjusted to 1×10^6 a day before the analysis. Before the analysis, concentration of mid-exponential log culture was adjusted to 10^8 by spectrometer ($OD_{600} = 0.1$) by using 0.9% NaCl solution. From that culture, 9.9 mL was transferred into a flask (Adsorption flask), and incubated for 5 min at 37 °C. 100 μL of 10^6 phage solution was added into the Adsorption flask, and the flask was swirled gently and incubated

for another 5 minutes. From the adsorption flask, 1 mL of the mixture was transferred into a test tube containing 100 μL chloroform. Tube was vortexed and put into an ice bath. Another 1 mL mixture was transferred into 9 mL pre-warmed LB broth (Flask B). After a mixing, 1 mL content from Flask B was transferred to 9 mL pre-warmed LB broth (Flask C). Then, in every 6 minute for 90 minutes, 100 μL content from each of the flasks were plated with the overnight host culture using double plaque assay. At the end of the 90 minutes, 100 μL control sample was used inoculated from the test tube with chloroform. After overnight incubation plaques were counted, and data was plotted in SigmaPlot 14 software. By analyzing the plot, latent period and burst size were also characterized (Figure 3.2). Latent period was determined from plot as the intersect between the initial count and the slope (end of Average 1 in Figure 3.2). Burst size were determined as average of final count (Average 2) divided by average of the initial count (Average 1).
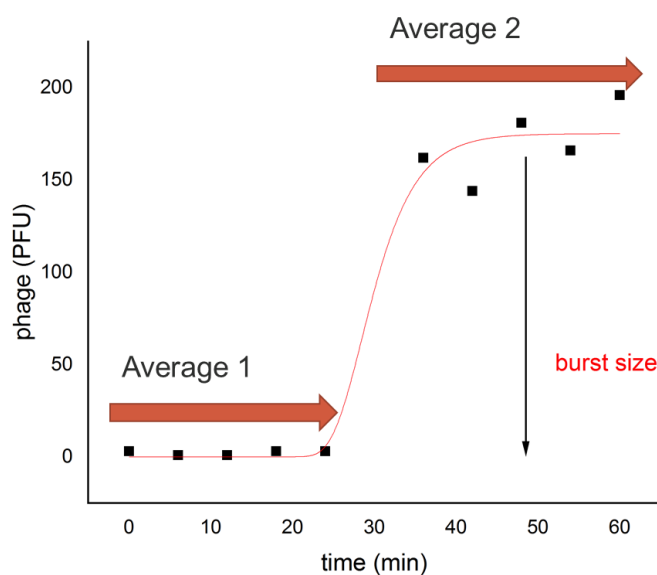
Figure 3.2 One-step growth curve, latent period estimation, and burst size determination

3.12   Adsorption rates

Attachment rate of bacteriophage to target cells were determined as described by Kropinski (2009). Similar to one step growth analysis, representative phages were selected for Enteritidis and Typhimurium (MET P1-001), Kentucky (MET P1-137), Infantis (MET P1-091 and MET P1-179). In addition, MET P1-088 and MET P1-197 were also selected as representatives for Hadar and Anatum, respectively. Host bacteria was cultured into LB broth a day before the analysis. Also, 8 hours prior to analysis host cultured into another LB broth to obtain a mid-exponential log culture. Phage titer in this study was adjusted to 1×10^5 a day before the analysis. Before the analysis, concentration of mid-exponential log culture was adjusted to 1×10^8 by spectrometer ($OD_{600} = 0.1$) by using 0.9% NaCl solution. 12 eppendorf tubes containing 950 µL sterile LB broth was prepared, and labeled as A1-A10 and C1-C2. The tubes were ordered numerically, and chilled prior to experiment. 9 mL host culture with adjusted concentration was transferred into a sterile flask, and labeled as flask A. 9 mL sterile LB broth was transferred into sterile flask, and labeled as flask C for control. Both flasks were incubated at 37 ◦C for 5 minutes for temperature equilibrium, and after that 1 mL 1×10^5 phage suspension was added to flask A and flask C, and the timer was started. For 10 minutes, 50 µL aliquot was transferred into eppendorf tubes starting with A1. Each eppendorf tube was vortexed and put back on ice. Similarly, after 10 minutes, 2 50 µL aliquots were transferred into the tubes C1 and C2, vortexed, and put on the ice. After that 100 µL from each tube was mixed with 100 µL host in 4 mL soft LB agar poured onto LB agar. Plates were incubated for 24 hours at 37 ◦C, and plaques were counted. Plate counts were processed in Excel and a plaque vs time graph was drawn. Adsorption rate constant k was then calculated according to the equation;

Equation 3.2
$$k = \frac{2.3}{\text{Bt}} \log \frac{P0}{P}$$

Where k is the adsorption rate constant, in mL/min; B is the concentration of bacterial cells; t is the time interval in which the titer falls from P_0 (original) to P (final).

3.13   Genome size estimation

Genome size of bacteriophages were determined by Pulsed Field Gel Electrophoresis (PFGE) as described by Lingohr et al. (2009) and Acar et al. (2017). *Salmonella* Braenderup (MET S1-713) was used as reference. Fresh high titer phages ($>1 \times 10^8$ PFU/mL) were prepared for the analysis. To remove any bacterial contamination, phage lysates were centrifuged at $6250 \times$ g for 15 minutes and filtered through 0.22 μm filter. 400 μL 1% Seakem Gold (SKG) Agarose were mixed with equal amount of phages filtrate, and mixture was loaded in to gel cast to create plaques. After the gel was solidified, plaques were put in to 50 mL tubes containing phage lysis buffer (50 mM tris; 50 mM EDTA; 1% SDS) and 20 mg/L Proteinase K solution. Plaques were incubated at 55 °C in shaking incubator for 1.5 hours. After incubation, plaques were washed with sterile ddH_2O two times and tris-EDTA (TE) buffer four times. TE and ddH_2O was held in water bath (55 °C) prior to washing. In each washing step, a filter was attached to tubes, then all liquid content was discarded, and replaced with ddH_2O and TE according to washing step. After fresh ddH_2O or buffer addition, tubes were incubated in a shaking incubator at 55 °C. After washing, plaques stored in TE solution at 4 °C. Next day, plaques were cut in 2mm sizes and placed in the agarose gel.

Plaques of reference strain were cut in 2 mm size, and placed into 1.5 mL centrifuge tubes. 200 μL H buffer (175 μL ddH_2O; 20 μL H buffer; 5 μL Xba1) was added, and the tubes were incubated for 10 minutes at 37 °C. After 10 minutes, H buffer was replaced with XbaI solution (175 μL ddH_2O; 20 μL H buffer; 5 μL Xba1) and incubated for 4 hours at 37 °C. 2.2 L running buffer (0.5% TBE) was loaded into PFGE tank and, the system was started in order to cool the buffer to 15 °C. After the incubation, plaques were loaded into 1.5% SKG agarose gel. Wells on the gel was

sealed with sealing agarose. Before the run, approximately, 1.5 mL thiourea solution was added to running buffer. The gel run in DNA-Chef DR III Biorad electrophoresis system with the conditions below (Table 3.8):

Table 3.8 Electrophoresis Conditions

DNA Size	30 kb – 700 kb
% Agarose	%1
Voltage	6.0 v/cm
Electrophoresis duration	19 h
Angle	120°
Initial Switch Time	2.16s
Final Switch Time	1.03 min 80 s
Pump Speed	70 (0.75 L/minutes)

After electrophoresis gels were stained with 10 mg/mL ethidium bromide solution for 45 minutes, and destained in distilled water for 30 minutes. Gel images were taken with Molecular Imager-Gel Doc-XR System Universal Hood II, and the software (PDQuest) provided by manufacturer. Band images were transferred to Bionumerics software. A dendogram showing genotypic clustering was drawn in Bionumerics, and band sizes of phages were estimated by using software tools.

3.14   Morphological analysis

Morphology of phages were determined in METU Central Laboratory by using high contrast transmission electron microscopy (CTEM). 10 phages were selected from our collection for TEM analysis (Table 3.9).

Table 3.9 Isolation data of selected phages for TEM analysis

METUID	Genus	Serotype	Isolate Source	Month	Date	City
MET P1-001	*Salmonella*	Enteritidis, Typhimurium	Cattle Farm	February	10.02.2020	Adiyaman
MET P1-082	*Salmonella*	Typhimurium	Poultry Farm	August	14.08.2020	Bolu
MET P1-103	*Salmonella*	Enteritidis	Cattle Farm	October	08.10.2020	Adiyaman
MET P1-122	*Salmonella*	Enteritidis	Cattle Farm	October	08.10.2020	Adiyaman
MET P1-164	*Salmonella*	Enteritidis	Cattle Farm	November	19.11.2020	Adiyaman
MET P1-091	*Salmonella*	Infantis	Cattle Farm	October	08.10.2020	Adiyaman
MET P1-100	*Salmonella*	Infantis	Wastewater Facility	August	17.08.2020	Ankara
MET P1-116	*Salmonella*	Infantis	Wastewater Facility	October	01.10.2020	Ankara
MET P1-137	*Salmonella*	Kentucky	Wastewater Facility	October	11.11.2020	Ankara
MET P1-179	*Salmonella*	Infantis	Wastewater Facility	December	09.12.2020	Ankara

Samples were prepared just before the analysis as described by Ackermann (2009). 1 mL of fresh and high titer phage stocks ($> 1 \times 10^8$) were transferred into centrifuge tubes, and centrifuged for 90 minutes at $21000 \times g$. Then supernatant was discarded, and replaced with 1 mL 0.1 M ammonium acetate solution. This step was repeated two more times. After that, 10 µL sample was deposited on the TEM grid for phage adsorption. After 2 minutes, the droplet was taken carefully with a filter paper, and 10 µL dye was added immediately. 2% sodium phosphotungstate was adjusted to pH 7.2 with 1 M NaOH, and was used as dye. After 2 minutes, remaining dye on the grid was removed with filter paper. Grids then allowed to air dry for 10 minutes, and then sent to METU Central laboratory immediately for examination. In Central Lab, images were taken with Tecnai T20 G^2 electron microscope operating at the accelerating voltage of 120 keV.

Phage morphologies were investigated in ImageJ image processor (Abràmoff et al., 2004). Head diameter for capsid size and tail size of each phage were measured at

least 30 times (Kuźmińska-Bajor et al., 2021). Averages and standard deviations (±SD) were calculated. Measurements were compared statistically by using student t-test. Shape and measurement of phages were compared to Ackermann's guide. This guide contains TEM images, measurements, and explanations of 177 *Salmonella* phages (Ackermann, 2007).

3.15   Bacterial reduction and virulence index

Effectiveness of phages against target bacteria was characterized by planktonic killing assay and virulence index (Haines et al., 2021; Storms et al., 2020). For this, mid-log culture was adjusted to 1×10^8 CFU/mL by using spectrophotometer (OD_{600} = 0.1). Also, fresh phage titers were prepared and titers were adjusted to 1×10^9. 96 well plate was used for this analysis. In the first 4 wells of first column 180 µL phage free bacteria added as control. In the last 4 columns, 180 µL LB broth with colistin (512 mg/L) were added as blank. As a result, first column had control and blank only. 180 µL bacteria was added to rest of the wells (Figure 3.3). Phage stock were diluted from 10^9 to 10^2 PFU/mL in eppendorf tubes, so that MOI of the wells ranged from 1 to 10^{-7}. Experiments were conducted with all the phage samples in triplicate. MULTISKAN SKY plate reader was used. Incubation temperature was set to 37 ℃. For 24 hours OD (600nm) was measured for every 5 minutes. Plate was shaken for 5 seconds before each reading.
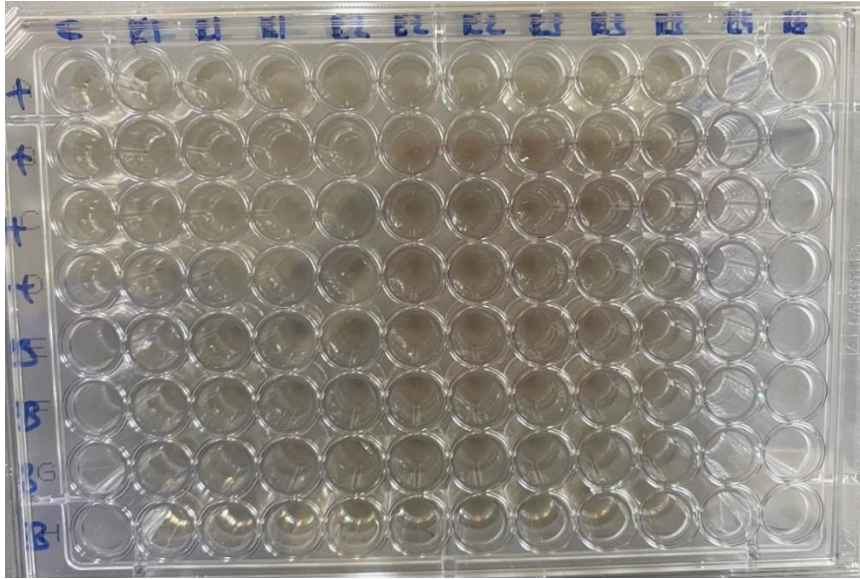
Figure 3.3 Plate setup for bacterial reduction curve. First 4 wells in the first column contains phage free DNA. Antibiotic added media was put in the last 4 wells as blank. Remaining wells contains bacteria plus phage solutions in decreasing MOI order (from 1 to 10^{-7}). Second, third and fourth wells belongs to cocktail 1, fifth, sixth and seventh wells belongs to cocktail 2, and eighth, ninth, and tenth wells belongs to cocktail 3.

Data was kept in the manufacturer software during the analysis, then were exported into Excel. Killing assay curves for each MOI were modeled with standard deviations based on the data. Virulence index was calculated from the area difference between the control (phage free bacteria) and each reduction curves by using the formula;

Equation 3.3
$$v_i = 1 - \frac{A_i}{A_0}$$

In the equation; V_i is the virulence index, A_i is the area of phage/ phage cocktail killing curve, and A_0 is the area of bacterial growth curve (Figure 3.4). Areas were calculated according to trapezoid rule.
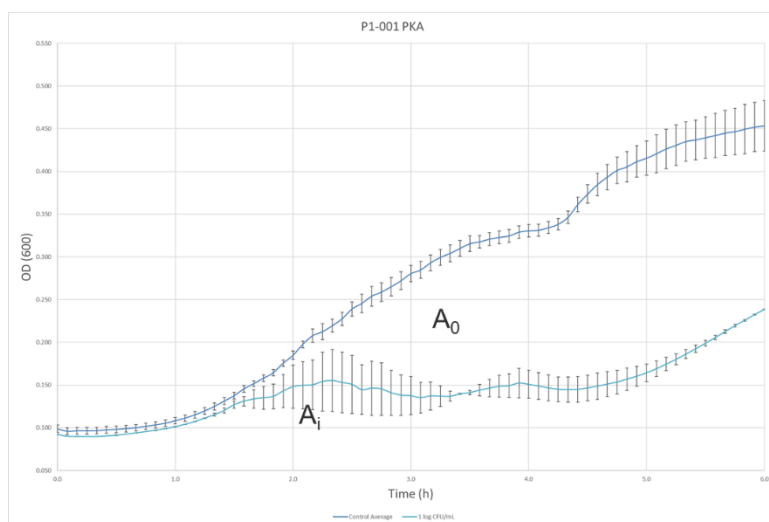
Figure 3.4 Bacterial growth curves of control (A_0) and phage added bacteria (A_i)

3.16 Whole genome sequencing and bioinformatics

Whole genome sequencing was done commercially. Bacteriophages were analyzed in TEM were selected for whole genome sequencing (Table 3.9). DNA of the phages were extracted by Norgen Phage DNA isolation kit according to protocol provided by the manufacturer. Briefly, 10 mL fresh phage lysate with more than 1×10^8 PFU/mL titer was prepared for this analysis. 1 mL of the lysate were transferred into 15 mL falcon tube. Than DNase, lysis buffer, Proteinase K, and isopropanol were added, respectively. 650 µL samples then were taken into spin columns that are attached to collection tubes. Tubes centrifuged for 1 min at 6000 × g. Flowthrough were discarded, and columns were washed with wash solution thrice with centrifugation in each step. After that columns were centrifuged at 14000 g for 2 minutes in order to dry the spin column thoroughly. Spin columns were attached to elution tubes, 75 µL elution buffer was added to columns, and columns were spinned for 1 minutes at 6000 × g. A second elution step was performed in order to increase the yield. Purified DNA samples were stored at -20 °C, and sent to service provider a day after. Samples were analyzed by Illumina NovaSeq platform.

46

Bioinformatics analyses of the samples were done in our lab. For the general pipeline, methods and software were mainly used as described in Shen & Millard, (2021) (Figure 3.5). Sequence files were obtained as raw reads (fq files). Quality check of raw reads were carried out by using FastQC (Storms et al., 2010). Trimmomatic (v 0.39) software was used to remove the Illumina adapters (Bolger et al., 2014). Since the phage genomes were short (e.g. 100kbp) a data reduction and subsampling were done in applied.
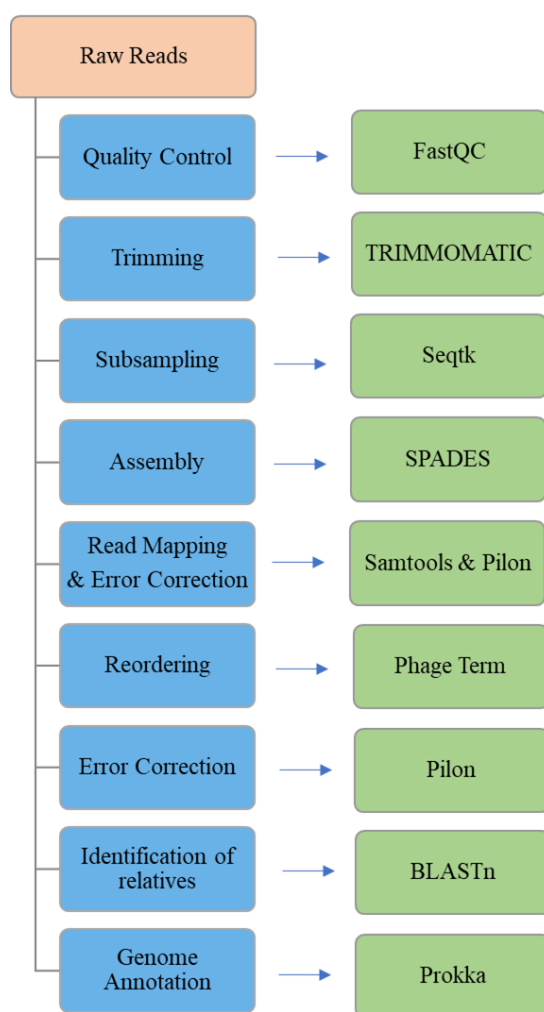
Figure 3.5 Workflow of analysis of phages from raw reads to annotation. Left column shows the analysis, and right column shows the tool. Pipeline was adapted from (Turner et al., 2021).

Phage genome assembly was done with SPAdes version 3.9.0 (Bankevich et al., 2012) by using default options, and assemblers were compared. Quality of assemblies, genome sizes and GC% contents was evaluated with QUAST (Gurevich et al., 2013). Assemblies graphs were first visualized by Bandage to ensure that there was no DNA contamination (Wick et al., 2015). After assembly, reads were mapped with bbmap.sh, as it gives the read coverage as default (Bushnell et al., 2019). Ideally, phage genome coverage should be between 20X and 200X (Shen & Millard, 2021). Based on the coverage scores, subsampling and assembly process were repeated. Assembly polishing and error correction was made by pilon (Walker et al., 2014). A preliminary check for closest relatives of assembled genomes were identified by BLASTn against Caudovirales database. Since the assemblers built genomes not in the correct order, a reordering step was applied to phage genome assemblies. Genomes from assemblies were reordered in two ways. First, all assemblies were assessed with PhageTerm (Garneau et al., 2017). PhageTerm is a software which predicts the genome packaging strategy and genome termini, and reorders the genome accordingly. For the assemblies that could be assessed by PhageTerm, reordered assembly produced by the software was used. For the phages that termini sites cannot be identified by PhageTerm, closest relative was identified (ANI > 90%). First 500 base pair of that relative was extracted with a python script, and aligned with the assembly in BLAST to determine the starting site. New assemblies then reordered (reversed, if necessary) with a python script according to alignment result. After reordering, all assemblies were assessed with pilon once again to ensure there were no errors.

Structural and functional annotations were done by Prokka (Seemann, 2014). Multiple genome alignments of phages were done in progressive Mauve (Darling et al., 2010). Taxonomic features (e.g. family, subfamily) were determined based on alignment scores the BLASTn. In addition, GRAViTy online tool was used to create a proteome based clustering by using DB-B: Baltimore Group lb-Prokaryotic and archaeal dsDNA virus database (VMRv34) (Aiewsakun & Simmonds, 2018; Turner, Adriaenssens, et al., 2021). The dendogram was visualized by using ITOL (Letunic

& Bork, 2019). Phylogenomic distance between the sequenced phages was evaluated by VICTOR (Meier-Kolthoff & Göker, 2017). Amino acid sequences were compared by pairwise comparisons using the Genome-BLAST Distance Phylogeny (GBDP) method (Meier-Kolthoff et al., 2014) with the settings proposed by Meier-Kolthoff & Göker (2017).

The resulting intergenomic distances were used to infer a balanced minimum evolution tree with branch support via FASTME including SPR postprocessing (Lefort et al., 2015) for each of the formulas D0, D4 and D6, respectively. Branch support was inferred from 100 pseudo-bootstrap replicates each. Trees were rooted at the midpoint (Farris, 1972) and visualized with FigTree (Rambaut, 2006).

Virulence genes were assessed by VFDB, the database provided by Liu et al. (2019). Antibiotic genes determinants in phage sequences were analyzed in ResFinder 4.1 with the default settings (Bortolaia et al., 2020).

3.17 *In vitro* phage application on feed

A crop assay was designed to test the ability of phages to reduce *Salmonella* Enteritidis and *Salmonella* Infantis in vitro as described by Andreatti Filho et al. (2007). In this assay MET P1-001, MET P1-100, MET P1-137, and MET P1-179 was tested. 500 g commercial poultry feed ration was obtained from retailer. Feed was autoclaved before the crop assay. Then 2 g of feed was weighted into sterile falcon tubes (50 mL). Concentrations of overnight *Salmonella* Enteritidis (MET S1-001) and Infantis (MET S1-006) cultures were adjusted to 1 x 10^8 by using a spectrophotometer (OD:0.1 at 600 nm). From that culture, two different concentrations, 8×10^6 and 8×10^3, was prepared into 10 mL 0.9% NaCl solutions. 10 tubes containing 2g feed were prepared for each assay. In each tube, 5 mL 0.9% NaCl, 500 μL adjusted *Salmonella* culture, and 1 mL 10^8 phage solution was added. 3 replicate tubes were prepared for each treatment. In addition, a control tube containing 1 mL 0.9% NaCl instead of phage solution was added for each test. All

of the tubes was vortexed 5 seconds in the beginning of the experiment, and incubated at room temperature (25 °C) at shaking incubator (150 rpm). Tubes were taken from incubator at 2. and 6. hour of experiment and vortexed for 5 seconds again. 100 µL of each tube was taken and plated onto XLD agar. Plates were incubated at 37 C for 24 hours, and colonies were counted. The data was processed in Excel. *Salmonella* levels for each treatment was plotted against control. In addition, means of treatment and control for each experiment was compared by student's t-test to determine if the difference between the means were significant.

CHAPTER 4

RESULTS AND DISCUSSION

4.1   Sample collection

In our study, 57 manure or wastewater sample were collected from various locations (Table 3.1). 53 of these samples were collected from farms, while 4 were taken from wastewater. Farm samples distribution was 55% poultry (29/53) to 45% cattle (24/53). 45 samples were collected in South Eastern Anatolia; 25 samples collected from Adıyaman, 20 samples were collected from Şanlıurfa (Figure 4.1). 5 Samples were collected from Bolu, 3 were collected from Denizli, and 4 collected in Ankara (Figure 4.2).
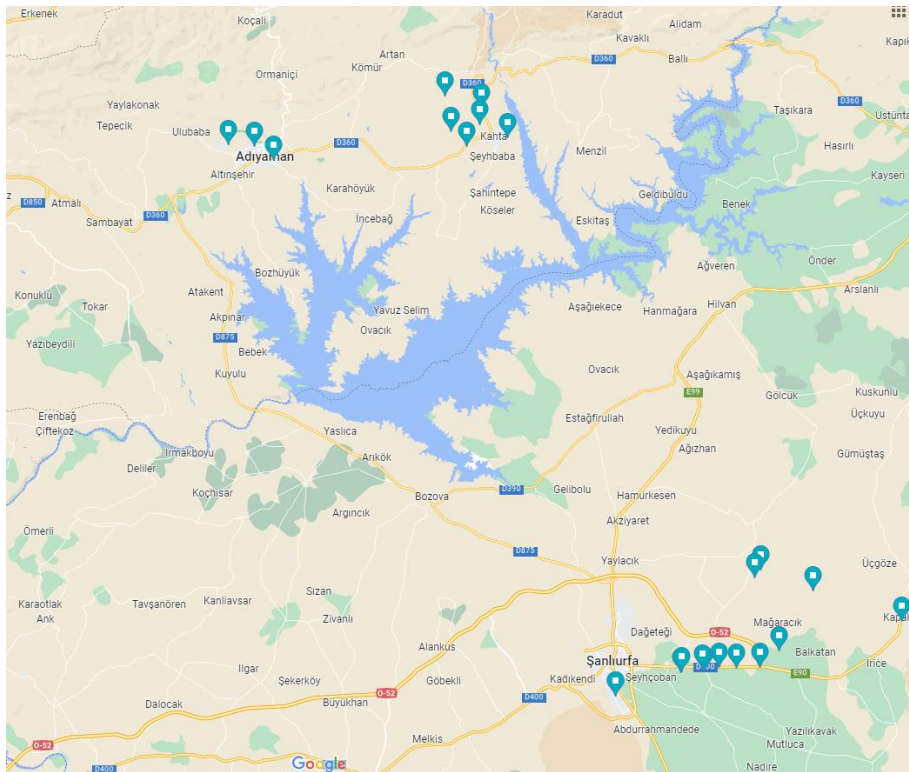
Figure 4.1 Location of farms in Adıyaman and Şanlıurfa.
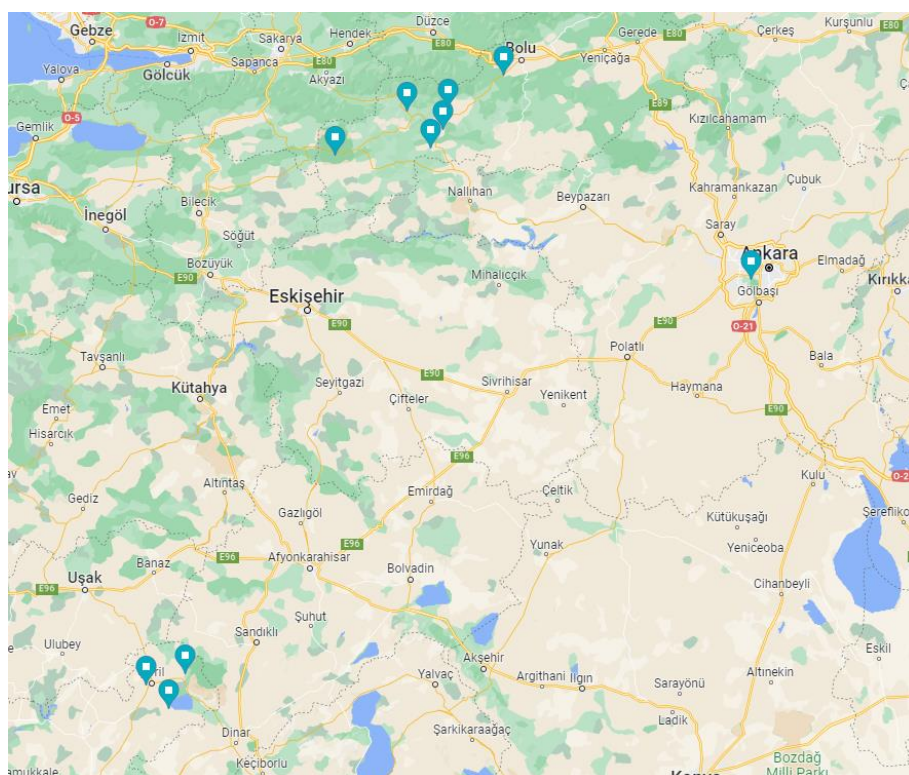
Figure 4.2 Location of farms in Bolu and Denizli, location of wastewater facility in Ankara

24 of the samples were collected in summer, 22 were obtained in autumn, and 11 samples were collected in winter. Due to COVID precautions no sampling made in spring season. *Salmonella* and bacteriophage isolation were conducted synchronously from the samples.

4.2   Isolation of *Salmonella*

In our study, 12 *Salmonella* were isolated from a total of 57 samples (Table 4.1). Isolated colonies were confirmed by PCR amplification of *invA* gene (Figure 4.3). Isolation of *Salmonella* were not distributed homogenously between isolation dates and locations. For example, all 3 farm samples from Denizli were *Salmonella* positive, whereas *Salmonella* couldn't be isolated from Bolu samples. Moreover, more than half of the *Salmonella* isolation (7/12) was conducted from November samples. On the other hand, prevalence in February, August, and October samples were 0. Similarly, all isolation was made from farm samples, whereas all wastewater samples were

52

Salmonella free. Even the farm samples showed non-homogenous distribution. While 55 % of samples were collected from poultry farms, 75 % (9/12) of isolated *Salmonella* came from poultry farms. On the other hand, only 3 *Salmonella* were able to be isolated from 24 cattle samples.

Table 4.1 *Salmonella* isolation from farm samples

METUID	Genus	Serotype	Source	Isolation Date	City
MET A2-188	*Salmonella*	Anatum	Poultry Farm	29/06/2020	Şanlıurfa
MET A2-191	*Salmonella*	Infantis	Poultry Farm	29/06/2020	Denizli
MET A2-194	*Salmonella*	Infantis	Poultry Farm	29/06/2020	Denizli
MET A2-197	*Salmonella*	-	Poultry Farm	29/06/2020	Denizli
MET A2-200	*Salmonella*	Kentucky	Poultry Farm	25/09/2020	Şanlıurfa
MET A2-209	*Salmonella*	Montevideo	Cattle Farm	19/11/2020	Şanlıurfa
MET A2-212	*Salmonella*	Kentucky	Poultry Farm	19/11/2020	Şanlıurfa
MET A2-215	*Salmonella*	Typhimurium	Poultry Farm	19/11/2020	Şanlıurfa
MET A2-218	*Salmonella*	Mikawasima	Poultry Farm	19/11/2020	Şanlıurfa
MET A2-221	*Salmonella*	Kentucky	Cattle Farm	19/11/2020	Adiyaman
MET A2-224	*Salmonella*	-	Cattle Farm	19/11/2020	Adiyaman
MET A2-227	*Salmonella*	-	Poultry Farm	19/11/2020	Şanlıurfa

All in all, *Salmonella* prevalence 31% and 12.5% in poultry manure and cattle manure, respectively. Our findings were comparable with Gıda ve Kontrol Genel Müdürlüğü's report. In that report *Salmonella* prevalence was found 24% in broiler chicken, and 47% in chicken carcasses (Gıda ve Kontrol Genel Müdürlüğü, 2018). However, our results indicate that *Salmonella* prevalence in poultry was much higher than the EU average, which was 3.9% in 2020 and 3.6% in 2019 (EFSA, 2021).

Figure 4.3 PCR gel image for invA (389 bp) gene. L: Ladder (100 bp), +:positive control (MET S1-001), -: negative control, 1-12: samples collected in June.

In literature, there are contradictory reports regarding the prevalence of *Salmonella* in poultry and poultry products. In a study, *Salmonella* prevalence in broiler flocks from Southeastern Anatolia, Marmara and Black Sea regions was reported as 15.6% (Yapicier & Sareyyupoglu, 2022). In another study conducted in Eastern Anatolia region, *Salmonella* prevalence in poultry was higher than 80% (Arkali & Çetinkaya, 2020). Siriken et al. (2015) reported prevalence of *Salmonella* in chicken meat was 42.6%. In another study, *Salmonella* prevalence in samples from ground meat and meatballs were 20% (Siriken et al., 2020). All these results show that a more comprehensive and regular monitoring should be conducted in each region.

4.3   Genomic characterization of *Salmonella* isolates

Genomic characterization of isolates was done by PFGE, which was the gold standard for bacterial subtyping until the emergence of whole genome sequence analysis, due to its discriminatory power (Neoh et al., 2019). PFGE gel pictures were presented in Appendix I.

PFGE patterns are also useful for serotype estimation of *Salmonella* isolates. After clustering analysis, patterns can be compared with an existing database of PFGE patterns for serotyping (Gaul et al., 2007). In addition to accurate estimation of serotype,

PFGE also offers less labor intensive, rapid, and cheaper way compared to traditional methods (Zou et al., 2010). Therefore, *Salmonella* serotypes were determined based on their PFGE patterns. For this, our PFGE database was used for comparison. 9 of the samples were able to be serotyped with PFGE (Figure 4.4). 3 isolates were serotyped as Kentucky, and 2 isolates were determined as Infantis, both of which were amongst the most prevalent serovars in Turkey. From the other serotypes, we found a Typhimurium, Anatum, Montevideo, and a Mikawasima, while the former 3 serotypes are also common, Mikawasima is a relatively rare serotype. Clustering analysis showed that Infantis isolates showed the same band pattern. Those isolated also showed same antibiotic resistance profile. Considering the fact that those isolates recovered from different farms in Denizli, there might be a clonal dissemination of multidrug resistant Infantis strain in Denizli region.

Key	Genus	Species	Serovar	Source	Location	Year
MET A2-212	Salmonella	enterica	Kentucky	Poultry farm	Sanliurfa	2020
MET A2-221	Salmonella	enterica	Kentucky	Cattle farm	Adiyaman	2020
MET A2-201	Salmonella	enterica	Kentucky	Poultry farm	Sanliurfa	2020
MET A2-209	Salmonella	enterica	Montevideo	Cattle farm	Sanliurfa	2020
MET A2-215	Salmonella	enterica	Typhimurium	Poultry farm	Sanliurfa	2020
MET A2-218	Salmonella	enterica	Mikawasima	Poultry farm	Sanliurfa	2020
MET A2-192	Salmonella	enterica	Infantis	Poultry farm	Denizli	2020
MET A2-195	Salmonella	enterica	Infantis	Poultry farm	Denizli	2020
MET A2-189	Salmonella	enterica	Anatum	Poultry farm	Sanliurfa	2020
MET A2-224	Salmonella	enterica		Cattle farm	Adiyaman	2020
MET A2-227	Salmonella	enterica		Poultry farm	Sanliurfa	2020

Figure 4.4 Cluster analysis of *Salmonella* isolates

Clustering analysis also revealed serotype based clustering (Figure 4.4). Date, source, and location was not found relevant in clustering. However, this might be due to the small sample size.

4.4 Antibiotic resistance characterization of *Salmonella* isolates

All isolates were tested with disk diffusion method (Table 4.2). Disk diameters (mm) were given in Appendix A. Only 2 isolates (MET A2-188 and MET A2-209) were found susceptible to antibiotics. In addition, 2 isolates (MET A2-197 and MET A2-218) were resistant to streptomycin. Remaining isolates (8/12) showed multidrug resistance. Among those, 5 isolates showed resistance to fluoroquinolone class (ciprofloxacin and

pefloxacin). Fluoroquinolones are clinically important drugs for the treatment of Gram negative infections including *Salmonella*, which are considered as first line of treatment with third generation cephalosporins (WHO, 2020). In addition, 6 isolates showed resistance against ampicillin, another important drug from penicillin class that was used against salmonellosis, previously.

Table 4.2 Antibiotic resistance profiles and antibiotic genes of *Salmonella* isolates

Serotype	Source	METUID	City	Resistance Profile	AR Genes
Anatum	Poultry Farm	MET A2-188	Şanlıurfa	Susceptible	-
Infantis	Poultry Farm	MET A2-191	Denizli	SPefNTeSxtSf	*parC tetA sul1*
Infantis	Poultry Farm	MET A2-194	Denizli	SPefNTeSxtSf	*parC tetA aadA1 sul1*
-	Poultry Farm	MET A2-197	Denizli	S	*parC aadA1*
Kentucky	Poultry Farm	MET A2-200	Şanlıurfa	CnSAmpKfAmcPefNTeSfCip	*parC tetA strB sul1*
Montevideo	Cattle Farm	MET A2-209	Şanlıurfa	Susceptible	
Kentucky	Poultry Farm	MET A2-212	Şanlıurfa	CnSAmpPefNTeSfCip	*tetA sul1*
Typhimurium	Poultry Farm	MET A2-215	Şanlıurfa	AmpCPefNTe	*qnrB qnrS*
Mikawasima	Poultry Farm	MET A2-218	Şanlıurfa	S	-
Kentucky	Cattle Farm	MET A2-221	Adiyaman	AmpFoxKfAmc	-
-	Cattle Farm	MET A2-224	Adiyaman	AmpFoxKfAmc	-
-	Poultry Farm	MET A2-227	Şanlıurfa	SAmpFoxKfAmcTeSf	*tetA sul1*

Sf: Sulfisoxazole, Sxt: sulfamethoxazole-trimethoprim, Ak: Amikacin, Cn: Gentamicin, K: Kanamycin, S: Streptomycin, Cip: Ciprofloxacin, N: Nalidixic Acid, Amp: Ampicillin, Amc: Amoxicillin-clavulanic acid, T: Tetracycline, Fox: Cefoxitin, Kf: Cephalotin , Pef: Pefloxacin

Comparison of resistance profiles revealed that 2 Infantis isolates showed identical resistance. A similar pattern was observed for MET A2-221 and MET A2-224 both of which were isolated from a cattle farm in Adiyaman. Two Kentucky isolates from poultry farms showed resistance against 8 and 10 drugs. This might explain the high prevalence of Kentucky serotype in poultry. Although Kentucky is rarely associated with human salmonellosis cases spread of antibiotic resistance is still a threatening

issue. Resistance genes might spread interspecies on mobile genetic elements through horizontal gene transfer (Arnold et al., 2021).

Screening of AR genes revealed *qnrB* and *qnrS* genes in Typhimurium (MET A2-215). These genes are responsible from plasmid mediated quinolone resistance, and linked with the rapid spread of quinolone resistance globally (Lin et al., 2015). In addition, 4 isolates had chromosomal mutations in topoisomerase IV *parC* region, which is often associated with elevated resistance levels against fluoroquinolones (Pribul et al., 2016). In some instances, mechanism of phenotypic resistance couldn't be determined genotypically. This was due to the fact that there are multiple mechanisms that might confer resistance. For example, there are over 1100 β-lactamase genes known to confer resistance against β-lactam class antibiotics (McDermott et al., 2018). Similarly, many different aminoglycoside and fluoroquinolone resistance mechanisms were reported. Screening all of these mechanisms would not be feasible. With the rapid advances in technology, *in silico* determination of the mechanisms through whole genome sequencing is available. Combining sequencing data with lab screening would be the most reliable determination of resistance (Carroll et al., 2017). However, the cost of whole genome sequencing is still high for routine screening.

Our findings were also in agreement with our previous studies. Durul et al. (2015) reported high resistance rates among the *Salmonella* isolated from various foods in Şanlıurfa region. Similarly, Acar et al. (2017) reported very high resistance rates among *S.* Infantis isolates.

4.5   Isolation and titer determination of bacteriophages

In this study, 68 phages targeting different *Salmonella* serotypes were isolated from 53 farm and 4 wastewater samples. While some hosts (Kentucky, Anatum, Montevideo, Telaviv, Hadar) were used only in wastewater samples, Enteritidis, Typhimurium, and Infantis were used in all 57 samples, as they are determined as the most clinically relevant serotypes. According to Gıda ve Kontrol Genel Müdürlüğü's report, more than 80% of clinical *Salmonella* isolates were belong to those 3 serotypes (Gida ve Kontrol Genel Müdürlüğü, 2018). This was also the case in the EU. Most isolated clinical

isolates in the EU were Enteritidis, Typhimurium and its monophasic variant, and Infantis (EFSA, 2021). In addition, using all 8 hosts in farm samples would not be feasible as farm samples were obtained in batches (5 samples per location, per month).

Phage isolation rates in summer, autumn and winter were 62%, 131%, and 114%, respectively (Figure 4.5, Figure 4.6, Figure 4.7). After our study, Deniz (2022) collected samples in Spring season, reported phage isolate 90%. There was no relationship between the seasons and isolation rates. In our study, wastewater samples were collected in August, October, November, and December. Using more hosts for wastewater samples, caused an apparent increase in isolation rates.
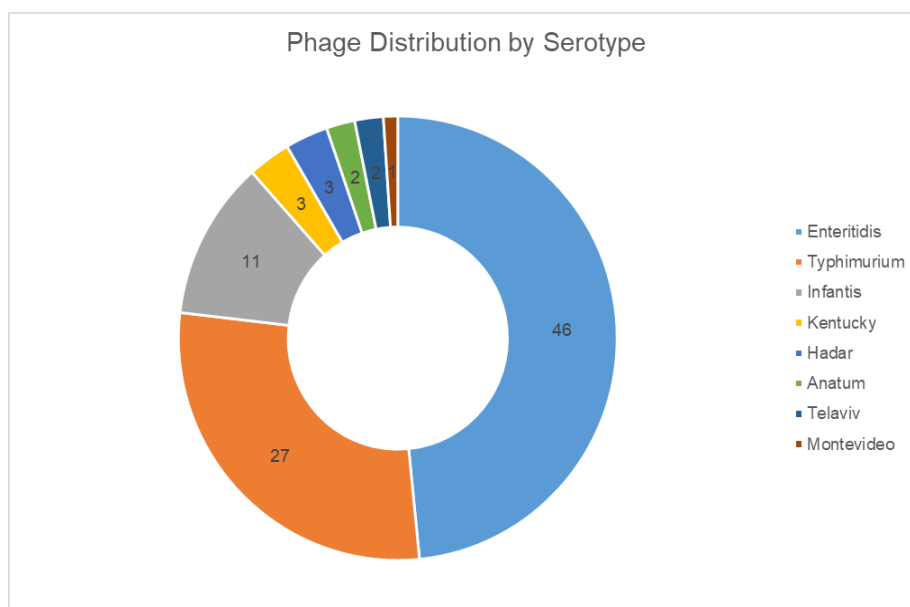
Figure 4.5 Pie chart of isolated phage distribution by serotype.

Enteritidis, Typhimurium, and Infantis were used as host in all 57 sample. Therefore, comparing the phages that belong to those 3 hosts might be a better idea. In that case, overall Enteritidis phage isolation rate was 80% (46/57), and isolation rate from farms only was 83% (44/53). A similar, small increase were observed for Typhimurium as well; isolation rate was 47% and 49%, for overall and farm only isolation rates. However, isolation rate of Infantis phages in farms (13%) were lower than overall

isolation rate (19%). This is due to the fact that in Infantis phages were abundant in wastewater, and unlike Enteritidis and Typhimurium, at least one Infantis phage were isolated from wastewater samples. However, Infantis phage prevalence were significantly lower than Enteritidis and Typhimurium. This was particularly interesting because in separate studies prevalence of Infantis in poultry were reported higher than Enteritidis and Typhimurium (Durul et al., 2015; Gida ve Kontrol Genel Mudurlugu, 2018). During the isolation a notable month was December in which we collected sample from METU wastewater facility. From that sample we were able to isolate one phage for each host; Enteritidis, Typhimurium, Infantis, Kentucky, Montevideo, Telaviv, Hadar, and Anatum. However, during the isolation it is impossible to decide if all the phages were unique, or the same phage that were able to infect all the hosts.
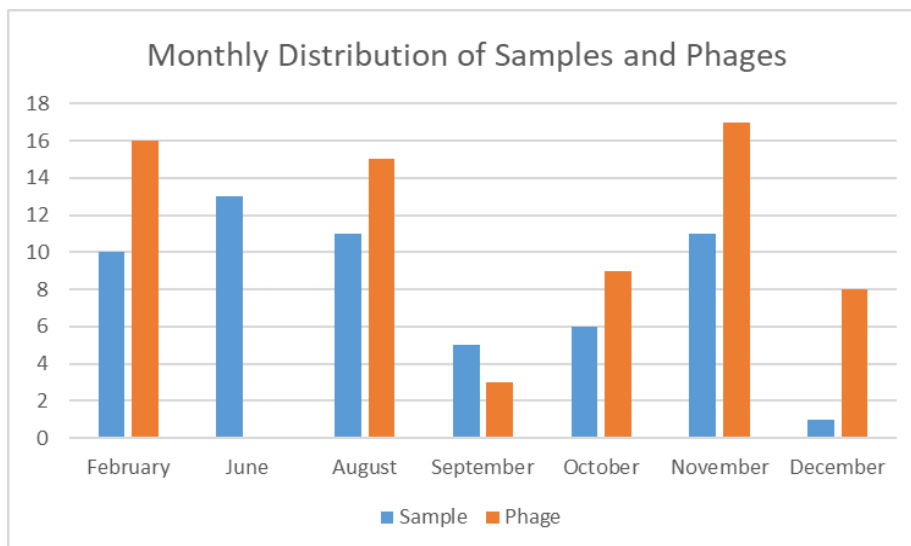
Figure 4.6 Bar chart shows how many samples were taken, and how many phages were isolated monthly

In a similar study, Yildirim et al. (2018) isolated 33 Typhimurium and 56 Enteritidis phages from 92 wastewater samples. Their isolation rates were 35% and 60% for Typhimurium and Enteritidis, and were comparable to ours.
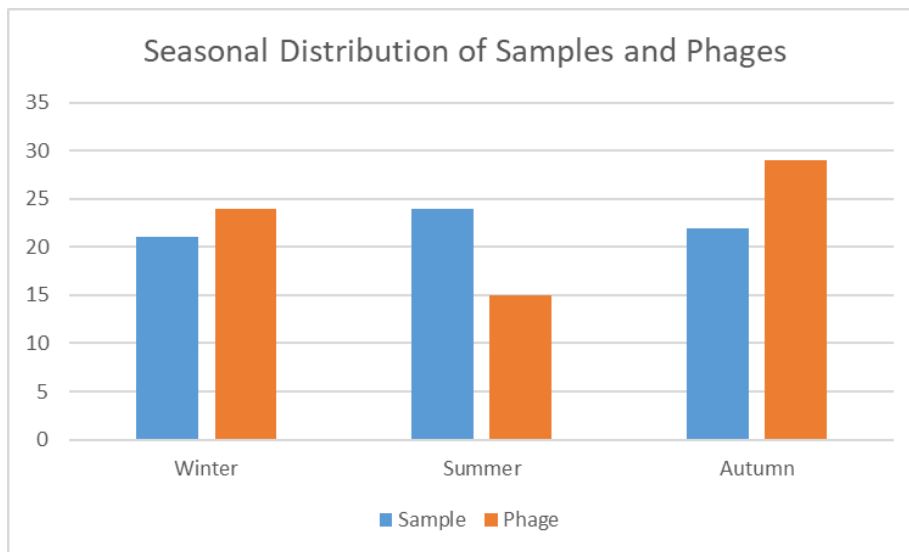
Figure 4.7 Seasonal changes in phage isolation. Bar chart shows how many samples were taken, and how many phages were isolated in that season.

After isolation, phages purified with a 3 step purification process because in some samples there were several different phage plaques (Figure 4.8). These steps were necessary to obtain single phages.
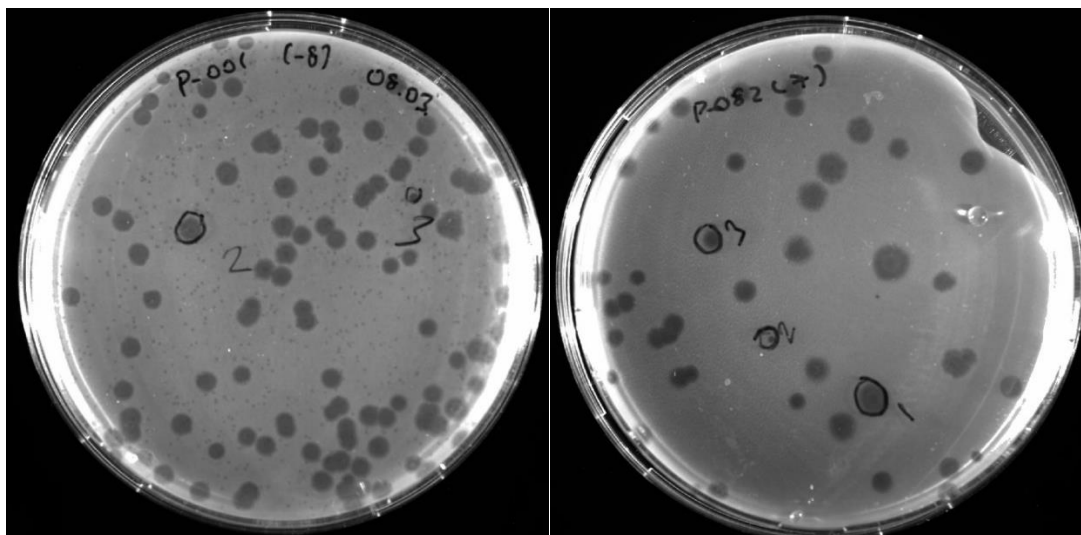
Figure 4.8 Different plaque formations observed in petri plates.

After purification, phages were stored according to the scheme (Figure 3.1). Before storage, a unique identifier (METU ID) was assigned each phage (Table 4.3). Since

each phage were stored in triplicate, a phage databank was created containing 204 entries (68 x 3). Whole table was given in Appendix B.
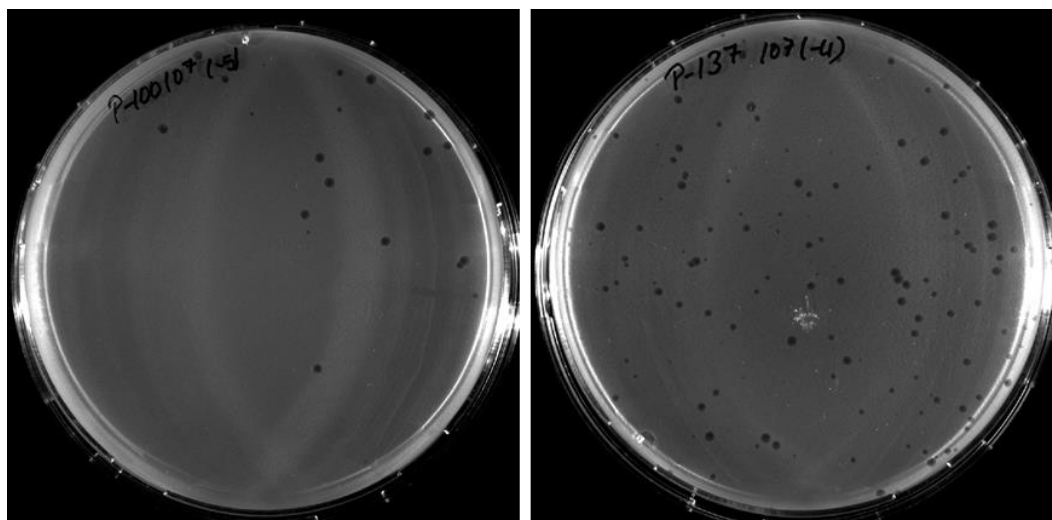
Figure 4.9 Sample phage photos; left: MET P1-100 (Infantis), right: MET P1-137 (Kentucky)

In general, Enteritidis and Typhimurium phages produced bigger plaques than the rest Figure 4.9 and Figure 4.10. Phage plaque size is dependent of phage intrinsic characteristics and environmental determinants (i.e. agar density, time, and host concentration) (Abedon & Yin, 2009). Since extrinsic factors such as agar density and time were equal, intrinsic factors might determine the plaque size. Gallet et al. (2011) found that phage concentration and lysis time relationship, virion morphology and adsorption rate affects the plaque size. In addition, phage diffusivity, latent period and burst size were also found effective on plaque size (Abedon & Yin, 2009).

Several phages showed depolymerase activity (Figure 4.10). These phage plaques had an outer zone that more faint than actual plaque zone. This zone is called as translucent halo, and means that phage produces a depolymerase enzyme (Lai et al., 2016). Phage tail proteins, tail spike and tail fiber, were reportedly show depolymerase activity (Yan et al., 2014). The depolymerase enzyme might diffuse further than phage itself due to its smaller size, and might degrade exopolysaccharides of host. This enzyme had a lot

of potential in a number of biomedical applications such as biofilm removal and antibiotic adjuvant (Pires et al., 2016). The polymerase activity was specifically observed in Enteritidis phages.
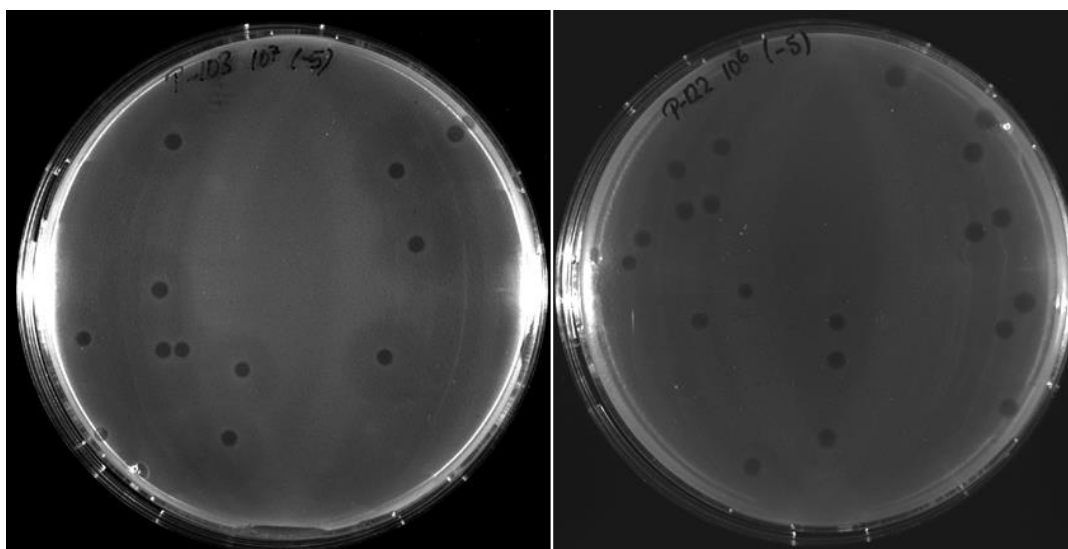
Figure 4.10 Phage depolymerase activity. Phage on the left (P1-103) showed polymerase activity (outer halo) whereas phage on the right (P1-122) did not.

Characterization of phages has started in January 2021 with titer determination of phage stocks. Phage titers are indicators of stock efficiency. Since some of the phages were frozen more than a year ago, titers had to be determined to check if there was a drop in phage titers. Also, phage titers need to be adjusted for further characterization steps. For example, in host-range determination analysis, phage titers should be at least 1×10^8. As a result, titers of all phages were determined before further characterization (Appendix C). All of the phages titers were higher than $1*10^8$. Furthermore, more than half of the phages had titers above 10^{11}. Significant drops in phage titers were not observed. The results showed that concentration of phages was not affected by storage at 4 ˚C.

Table 4.3 Sample phage databank entry which contains general phage isolation information

METUID	PreviousID	Genus	Serotype	Titer (PFU/mL)	Verified By	Source General	Source Specific	Keywords	Month	Year	Exact Date	City	Country
MET P1-100	Aug_MW1p2	*Salmonella*	Infantis	8.50E+10	Mustafa Guzel	Wastewater Facility	Wastewater	True	August	2020	17.08.2020	Ankara	Turkey
MET P1-101	Aug_MW1p2	*Salmonella*	Infantis	8.50E+10	Mustafa Guzel	Wastewater Facility	Wastewater	Representative	August	2020	17.08.2020	Ankara	Turkey
MET P1-102	Aug_MW1p2	*Salmonella*	Infantis	8.50E+10	Mustafa Guzel	Wastewater Facility	Wastewater	Representative	August	2020	17.08.2020	Ankara	Turkey

4.6   Bacteriophage lysis profiles on different hosts

Host range determination of bacteriophages were determined 36 isolates representing 18 serotypes given in Table 3.7. Complete table of interactions were given in Appendix D. A sample figure was presented in Figure 4.11. 66 of 68 phages were able to partly or completely lysed 10 or more hosts. Furthermore, 19 phages lysed 20 or more hosts. Most efficient phages based on the host range were P1-091, P1-094 and P1-125; these phages lysed 27, 28, and 27 different hosts respectively. P1-091 and 094 were isolated in October from Adiyaman samples by using Infantis as target host. P1-091 was isolated from cattle farm sample while P1-094 was isolated from poultry farm sample. P1-125 was isolated same month from wastewater sample by using Kentucky as target host.
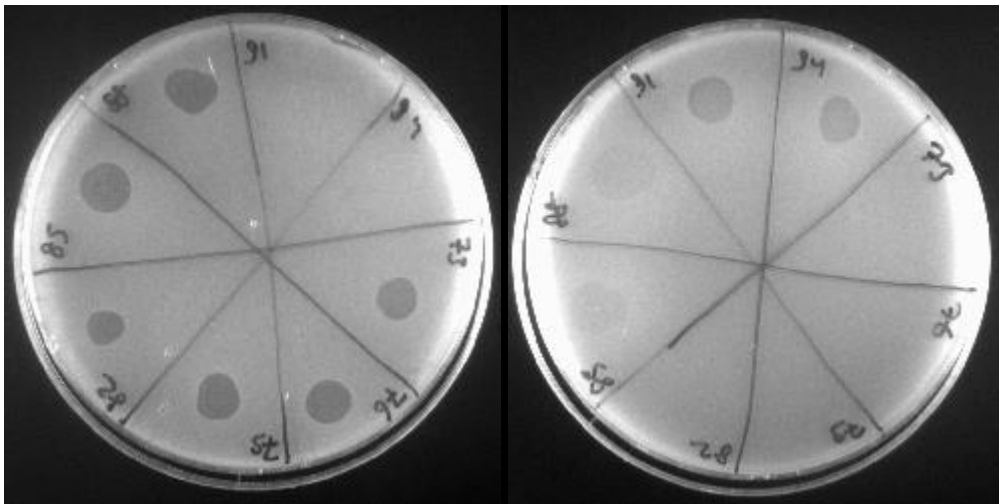
Figure 4.11 Host ranges of phages P1-073 to P1-094 against the A2-012 (Enteritidis) and A2-072 (Kentucky)

On average, phages were lysed 16 different hosts (Figure 4.12). While a phage completely lysed 7 of 36 hosts, partly lysed 9. On average, phages were ineffective against 19 hosts. There was no apparent relationship between host-range and isolation date or location. Isolation location was found effective on phage host range on a larger scale. Wongsuntornpoj et al. (2014), reported that phages isolated in Thailand shoed broader host range than isolated in the US.
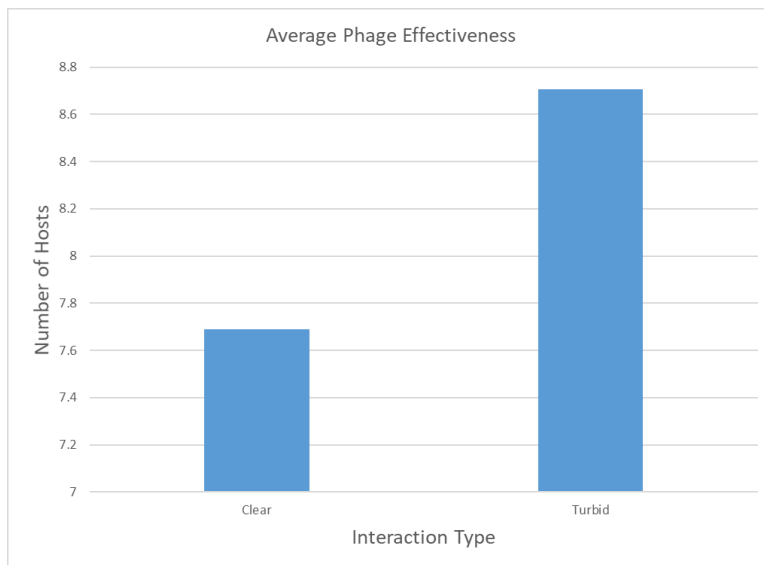
Figure 4.12 Bar graph of phage effectiveness.

While phages isolated from farms lysed 15 hosts in average, wastewater phages lysed 19 hosts (Figure 4.13). The results suggested that the host-range of wastewater phages are more diverse and broader than the farm phages. This result might be due to the fact that wastewater consist a vast variety of sources such as human, animal, and environmental, the phages in wastewater were evolved to infect more serotypes than the farm counterparts. Indeed, broader host range of wastewater phages compared to manure was reported (Akhtar et al., 2014). In another study, Parmar et al. (2018) suggested that since wastewater microflora is more distinct and changes frequently, host range of phages from wastewaters were expected to be broader. On the other hand, since farms have predominant serotypes, phages from farms were not able to diverse set of bacteria.
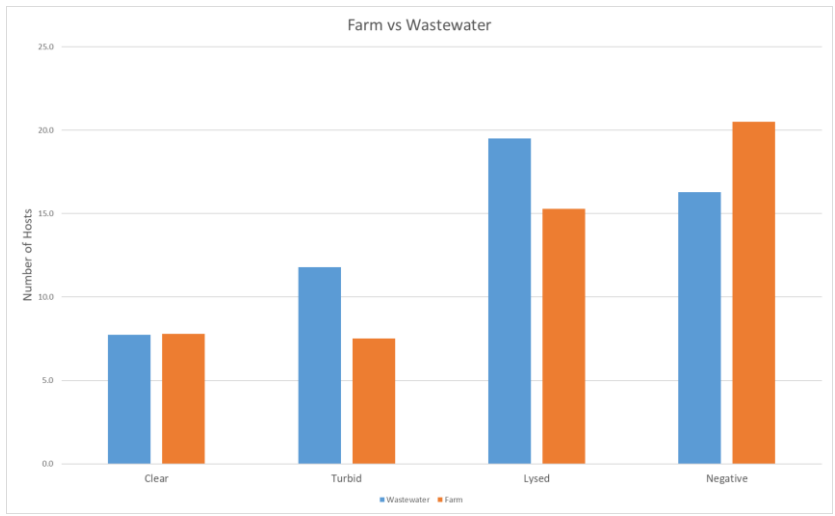
Figure 4.13 Comparison of the effectiveness of phages isolated from farm and wastewater.

In addition to most prevalent non-typhodial serotypes, we also tested 2 human pathogens *Salmonella* Typhi and *Salmonella* Paratyphi B. Only 2 phages were not able to lyse Paratyphi B, 66 phages lysed the target partly or completely. Conversely, Typhi was much less effected from the phages. 8 phages lysed Typhi, while only 3 of those completely lysed the bacteria. All in all, the results showed the therapeutic potential of phages.
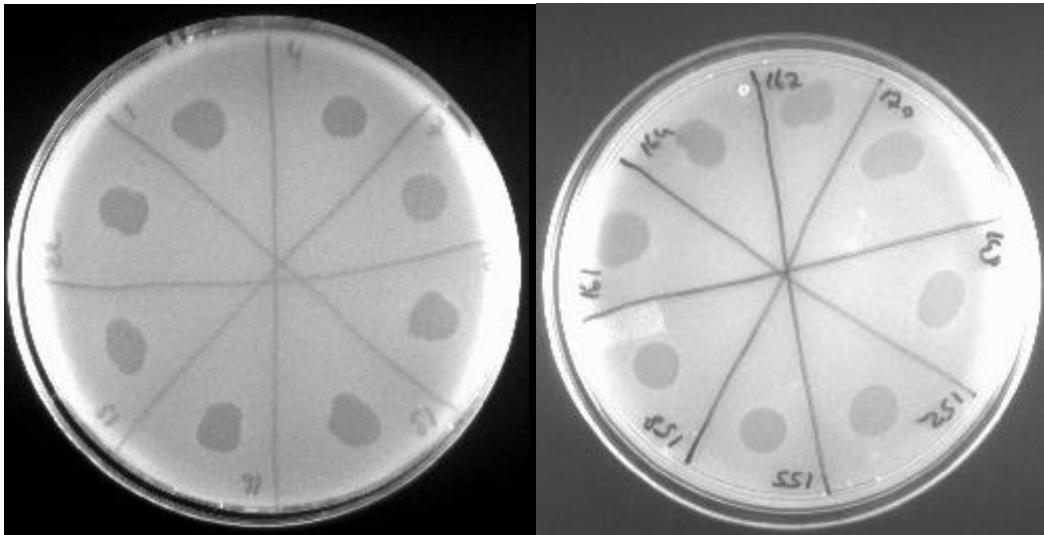
Figure 4.14 Effect of different phages on Salmonella Paratyphi B. 61 phages were able to lyse Paratyphi B.

As stated in 3.6, phage-host interactions were graded based on the interaction type, from complete clearing to no interaction. Based on those interactions, a heat map was built in R software (Figure 4.15). In the heatmap, darker colors indicated strong interaction. In general, isolates from Typhimurium and Enteritidis serotypes were affected from same set of phages. Phages that were isolated using Enteritidis and Typhimurium affected both serotypes. However, other phages were not very effective against these serotypes. Similarly, while Enteritidis and Typhimurium phages were generally ineffective against Infantis, other phages successfully interacted with Infantis.
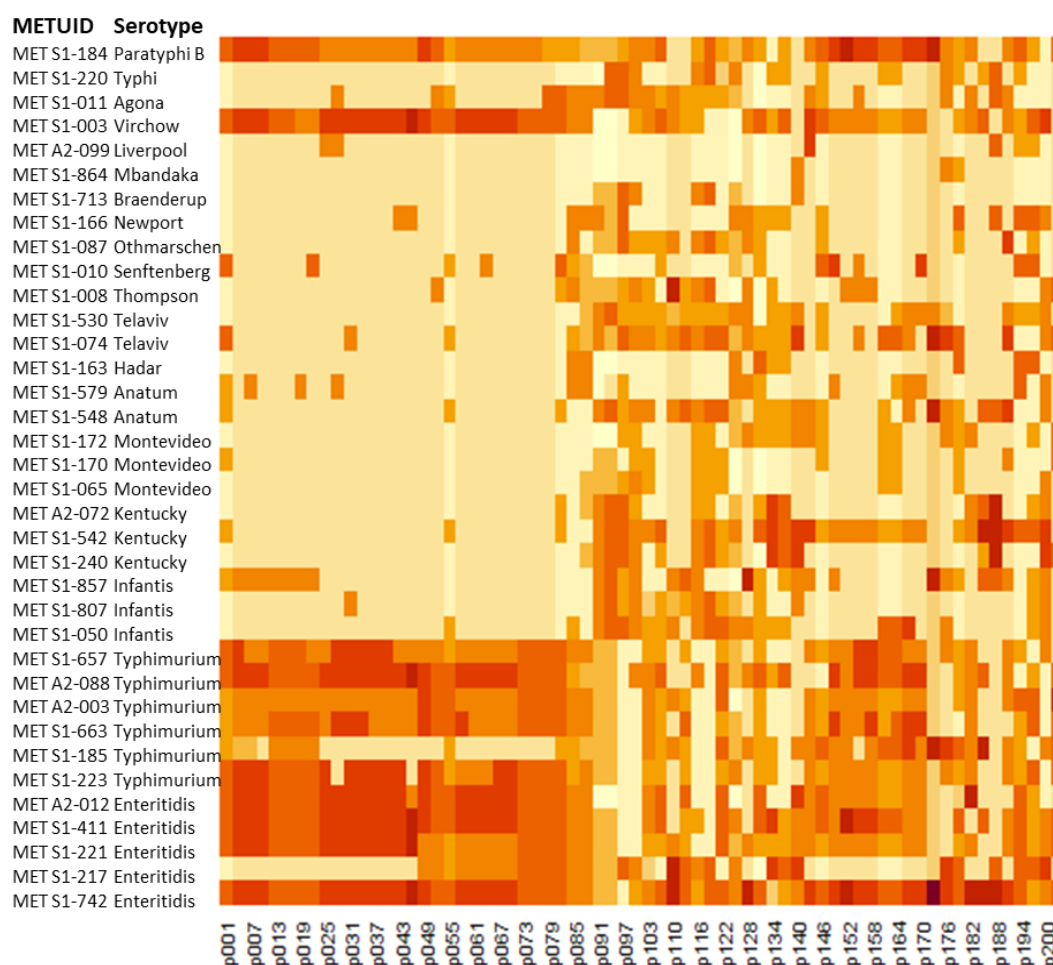
Figure 4.15 Heatmap showing phage-host interactions. Darker colors (red) indicate a strong lytic activity whereas light colors mean no interaction.

Based on their interactions with their hosts phages were clustered in R by using Ward's method (Figure 4.16). This hierarchal clustering method classified phages in 2 large branches, both of which divided into further subgroups. Also, a cluster plot was drawn based on Ward's method. As expected, phages were clustered according to their hosts. For example, almost all of the Enteritidis and Typhimurium phages were presented in two neighbor branches, while the others were in the other major branch, with several exceptions. For example, MET P1-131, an Enteritidis phage, was clustered with Hadar and Anatum phages. More intriguingly, 2 Typhimurium, 2 Infantis, 1 Enteritidis, Anatum and Kentucky phages were clustered together. More interestingly, there were no apparent relation among these phages. For instance, one of the Typhimurium phages was isolated from wastewater in December, while the other was isolated from cattle farm in November. Moreover, one of the two phages were isolated from samples from Sanliurfa in September, while the other was recovered from Adiyaman samples in November. However, other than that branch, other phages were clustered expectedly. In fact, several phages showed exact same profile, namely MET P1-013 and MET P1-016, MET P1-037 and MET P1-040, and MET P1-073 and MET P1-076. All of these same profile showing phages came from same farms in same month. They were either isolated by different hosts (Enteritidis and Typhimurium) or showed different morphologies. However, based on their host range analysis, they were most likely same phages.
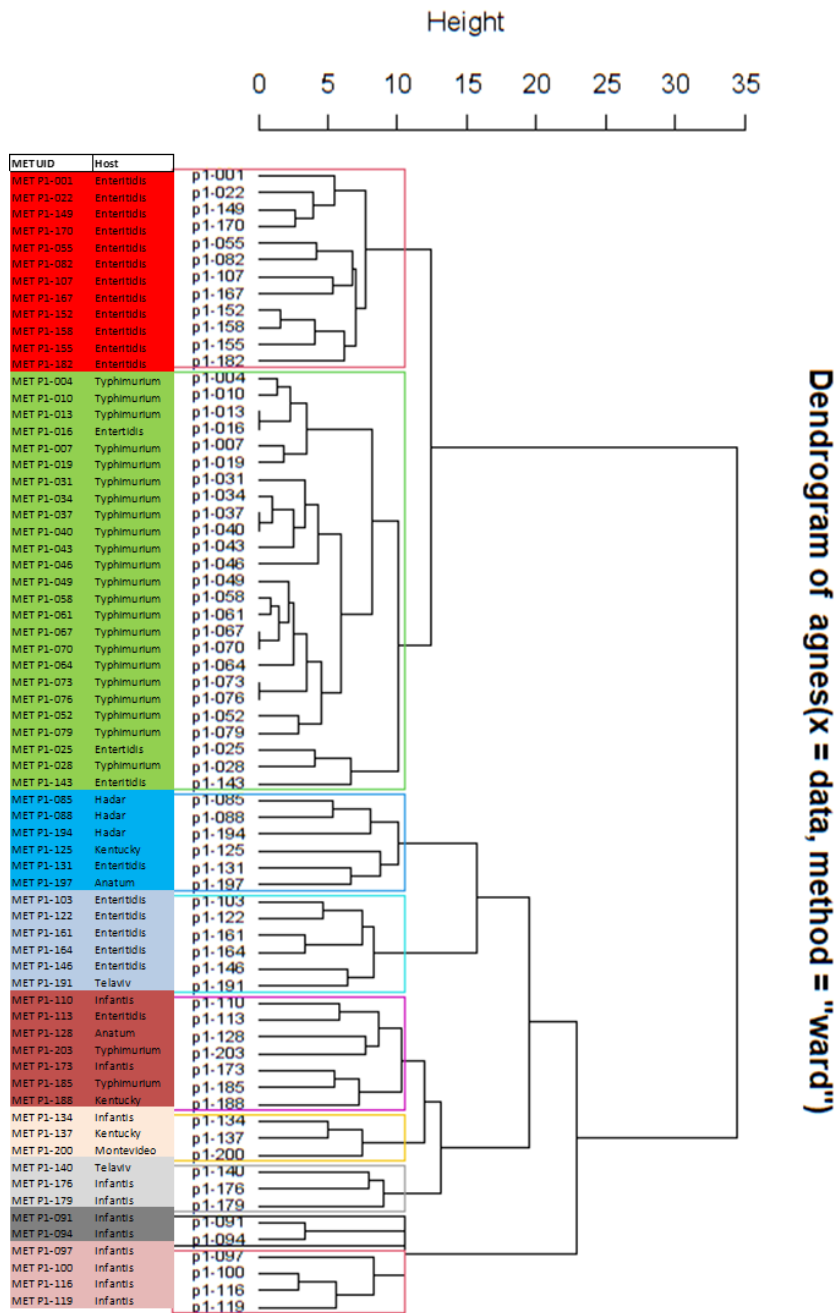
Figure 4.16 Phage clustering by Ward's method.

Host range analysis is a good method for clustering the *Salmonella* isolates as well. Historically, phage typing is an important phenotypic sub typing method for *Salmonella* (Callow, 1959; Ward et al., 1987). Phage typing lost a lot of interest with the emergence of molecular subtyping methods with much more resolution (Crabb et al., 2019).

However, it might be still useful in epidemiological studies with a well-defined set of phages (Baggesen et al., 2010). In our study, hosts were clustered with Ward's method like phages (Figure 4.17).

METUID	Serotype
MET S1-742	Enteritidis
MET S1-221	Enteritidis
MET S1-411	Enteritidis
MET S1-003	Virchow
MET A2-088	Typhimurium
MET S1-184	Paratyphi B
MET A2-012	Enteritidis
MET S1-223	Typhimurium
MET S1-657	Typhimurium
MET S1-663	Typhimurium
MET A2-003	Typhimurium
MET S1-217	Enteritidis
MET S1-807	Infantis
MET S1-713	Braenderup
MET S1-010	Othmarschen
MET S1-065	Montevideo
MET S1-170	Montevideo
MET S1-172	Montevideo
MET S1-220	Typhi
MET S1-240	Kentucky
MET A2-072	Kentucky
MET S1-008	Thompson
MET S1-011	Agona
MET S1-579	Anatum
MET S1-010	Senftenberg
MET S1-163	Hadar
MET S1-166	Newport
MET S1-864	Mbandaka
MET A2-099	Liverpool
MET S1-185	Typhimurium
MET S1-542	Kentucky
MET S1-050	Infantis
MET S1-530	Telaviv
MET S1-548	Anatum
MET S1-074	Telaviv
MET S1-857	Infantis

Figure 4.17 Clustering of 36 *Salmonella* isolates based on their phage interactions.

Isolates were grouped under 2 major branches. While the upper branch mostly consisting the Enteritidis and Typhimurium isolates, lower branches were more heterogeneous. Similar to phages, isolates were clustered expectedly and consistent

with their serotypes, with a few exceptions. For example, 3 Infantis isolates were presented in different nodes. This might be a feature of Infantis serotype. Pardo-Este et al. (2021) reported that very diverse Infantis strains might present in poultry farms. Isolates in the upper branch were mostly susceptible to phage infections. For example, Paratyphi B were infected by 61 phages, and Virchow were infected by 57.

Another different response to phages was observed in Anatum isolates (Figure 4.18). Although both isolates were isolated in same day from food sources, and they had same PFGE profiles, their phage susceptibility were different. As shown in Figure 4.18, while S1-548 was infected by Infantis phages (P1-091 and P1-094), S1-579 lysed by Hadar phages (P1-085 and P1-088). All in all, S1-579 showed resistance against 51 phages while S1-548 was unaffected by 39. Another different isolate was MET S1-217, a clinical Enteritidis isolate. That Enteritidis isolate were resisted nearly all Enteritidis phages, while lysed by Infantis, Hadar, and Anatum phages. That was not observed in any other isolate.
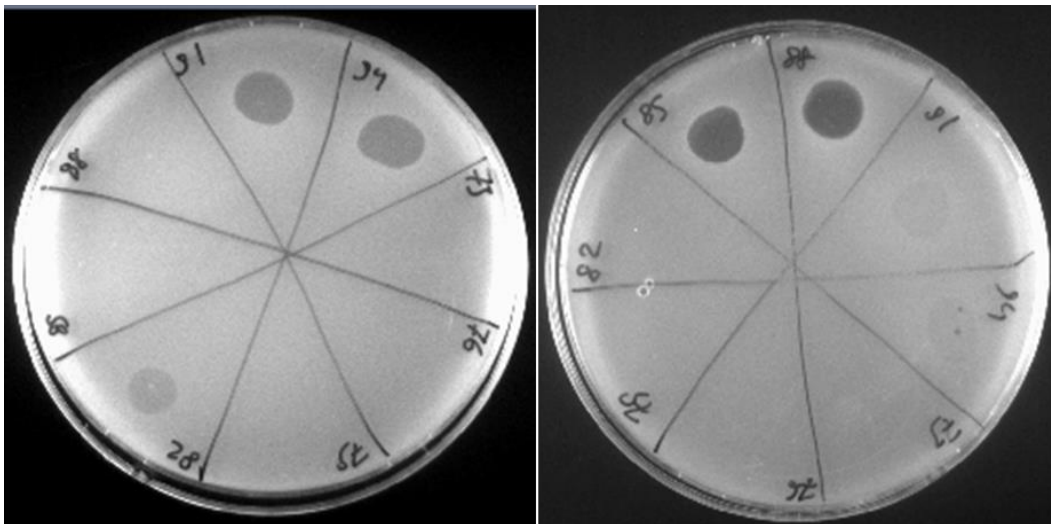
Figure 4.18 Host ranges of phages P1-073 to P1-094 against the S1-548 (Anatum) and S1-579 (Anatum).

In four isolates, namely Hadar, Braenderup, Mbandaka, and Liverpool, unusually high phage resistance observed (Figure 4.19). Braenderup resisted 60 phages, Liverpool resisted 62, and Mbandaka resisted 65 phages. Furthermore, Mbandaka isolate couldn't

be fully lysed by any of the phages. Also, Hadar isolate resisted 59 phages. In addition, 3 of the 7 phages that infected Hadar, were Hadar phages. Apart from Braenderup, all 3 serotypes were among the most prevalent serotypes in poultry (Gida ve Kontrol Genel Mudurlugu, 2018). In addition, Braenderup recently caused outbreaks, one associated with eggs in the US (Garcia et al., 2022) and another one associated with melons in the EU (EFSA, 2021).
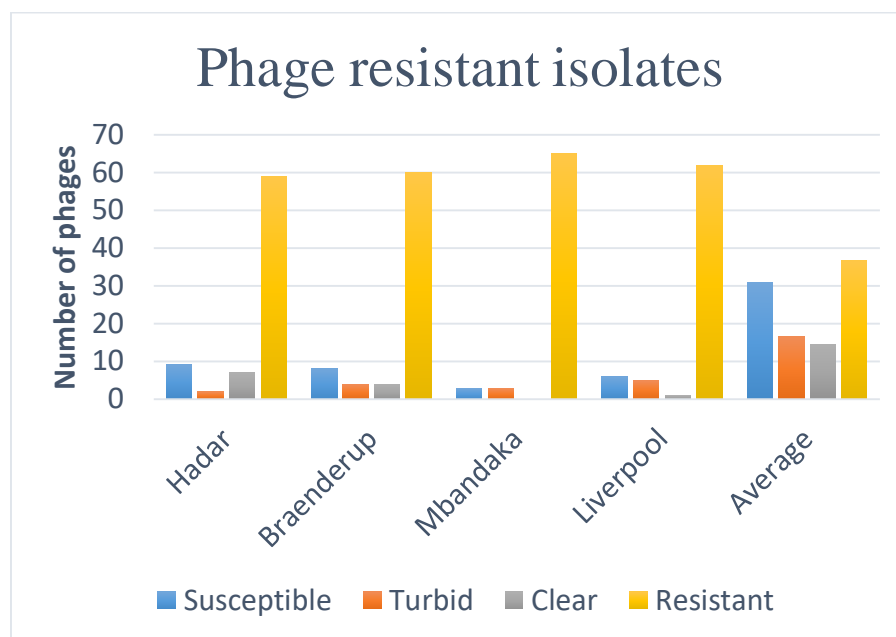
Figure 4.19 Phage resistant isolates, and average resistance rates of all isolates.

Based on the host interactions, 10 phages were chosen for further characterization experiments (Table 3.9). These phages were also tested against *E. coli* O104:H4 and *E. coli* O157:H7. While none of the phages was effective against O104:H4, one phage (MET P1-179) was able to produce a clear plaque by lysing O157:H7 (Figure 4.20).

Figure 4.20 Host range analysis of selected phages against *E. coli* O157:H7 (MET K1-30).

4.7 One-step growth curves, latent periods and burst sizes

One-step growth curve, latent period, and burst size of selected phages were determined for selected phages (Figure 4.21, Figure 4.22, Figure 4.23, Figure 4.24, Figure 4.25, Figure 4.26, Figure 4.27). 2 different Infantis phages (P1-116 and P1-179) were characterized due to genomic differences. P1-179 had a different genome than rest of the Infantis phages, and closer to Kentucky phage (P1-137). Although sigmoidal growth curves are used to describe bacterial growth, Gompertz model was fitted into model with a high R^2 value (R^2: > 0.92 for all phages). This model was found useful for latent period and burst size determinations as well. Latent period of the phage was determined as from the graphs, and burst sizes were calculated (Table 4.4).

73
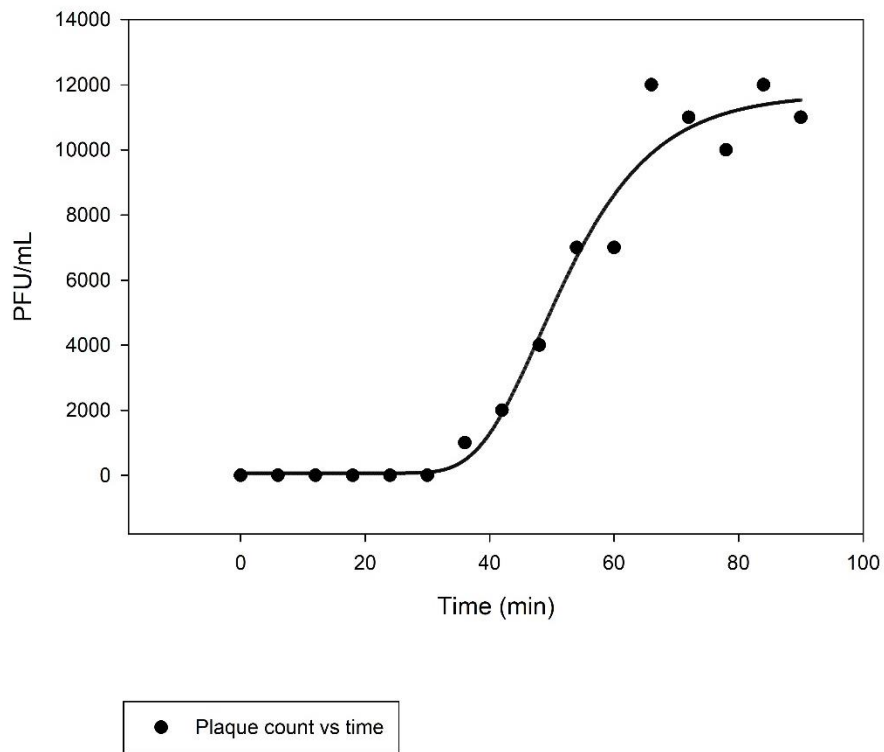
Figure 4.21 One step growth graph of MET P1-001. This phage was the representative of Enteritidis and Typhimurium phages.

MET P1-164
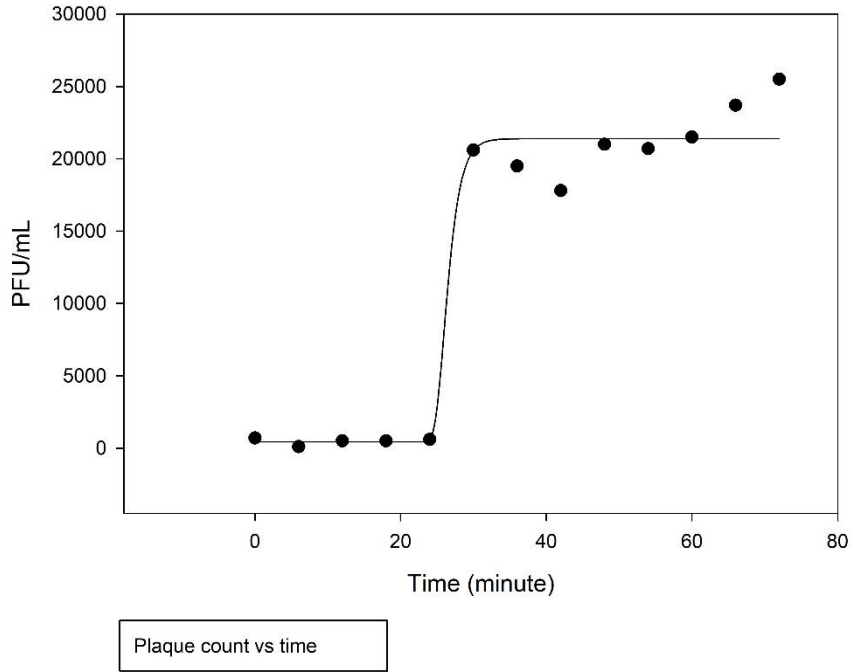
Figure 4.22 One step growth graph of MET P1-164. This phage was the representative of Enteritidis and Typhimurium phages.

MET P1-088
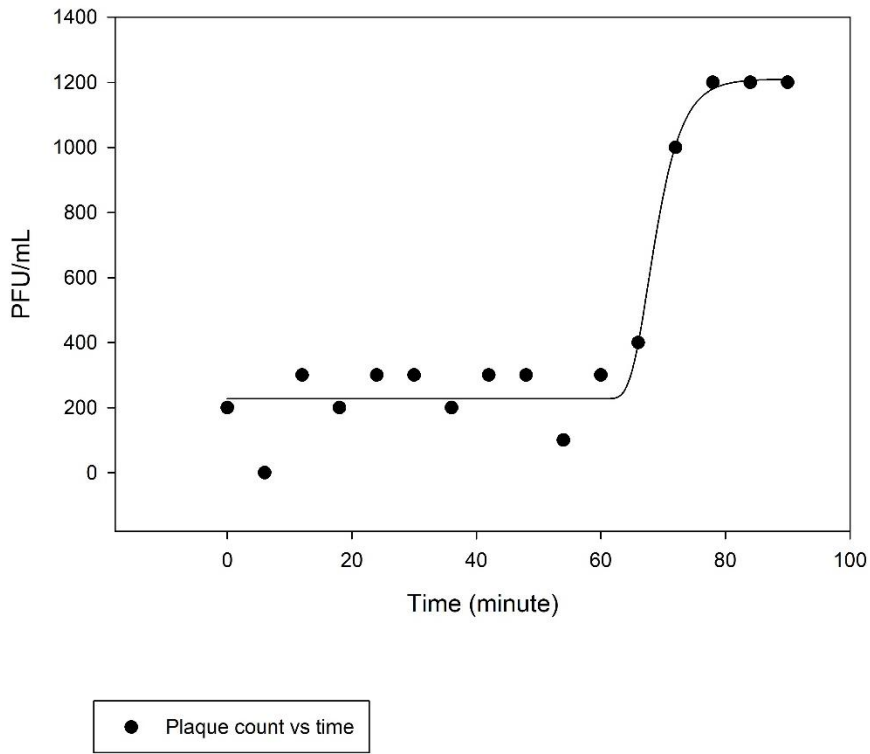
Figure 4.23 One step growth graph of MET P1-088. This phage was the representative of Hadar phages.
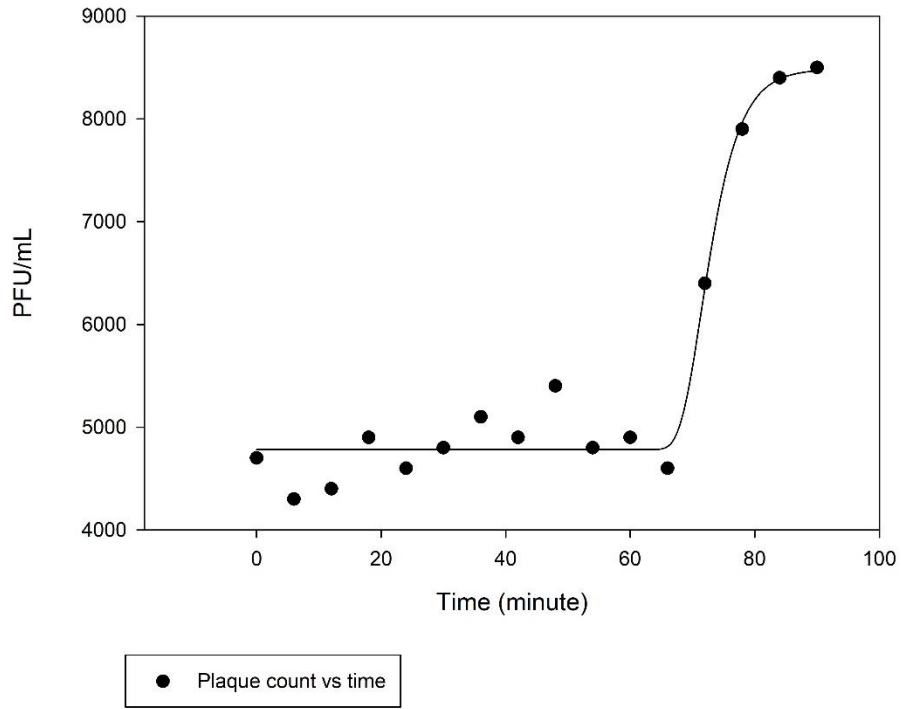
Figure 4.24 One step growth graph of MET P1-137. This phage was the representative of Kentucky phages.
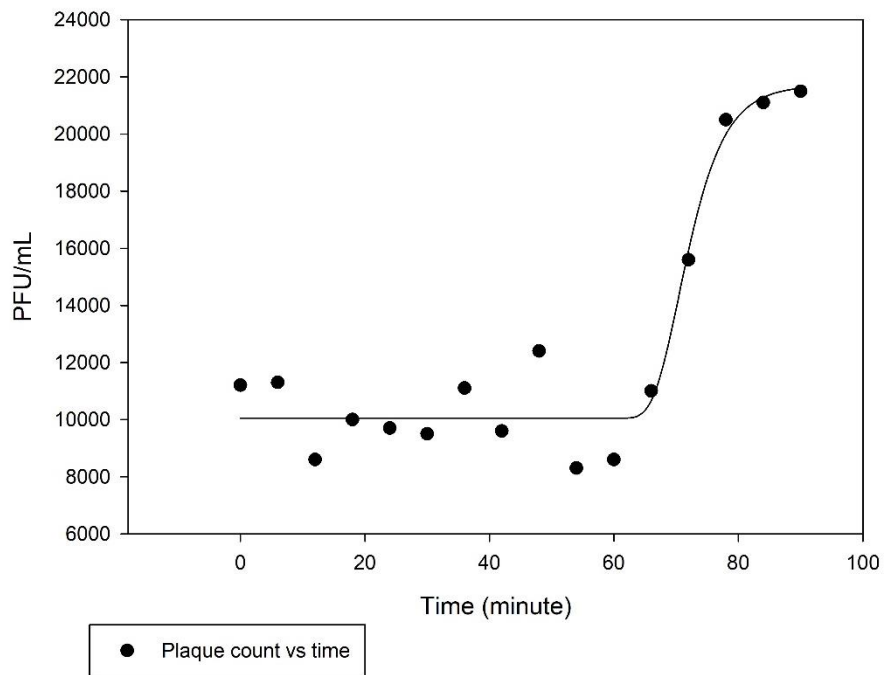
Figure 4.25 One step growth graph of MET P1-116. This phage was the representative of Infantis phages.

MET P1-179
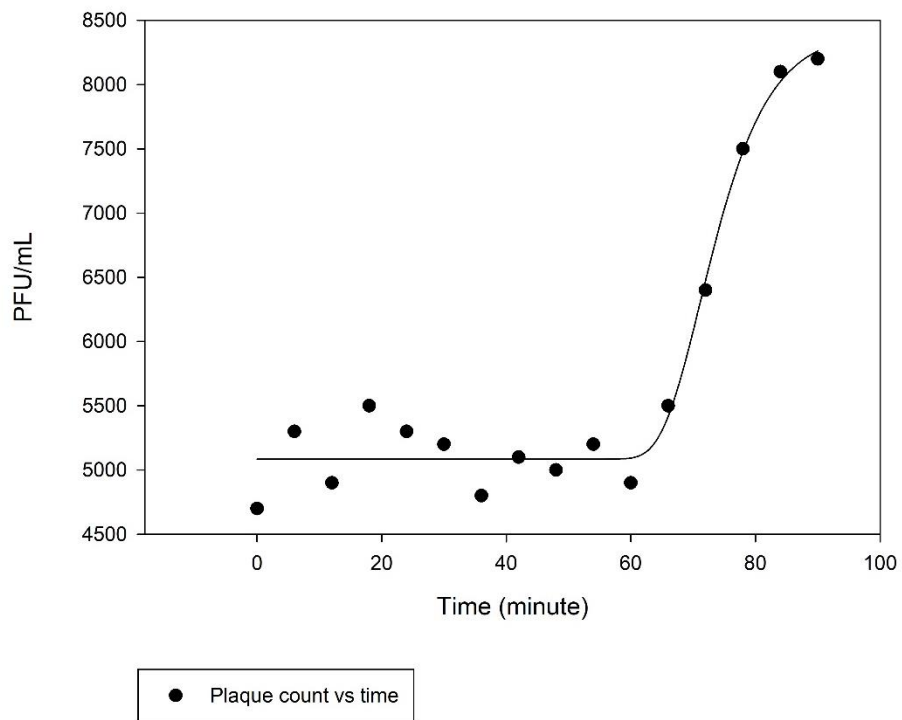
Figure 4.26 One step growth graph of MET P1-179. This phage was the representative of Infantis phages.

MET P1-197
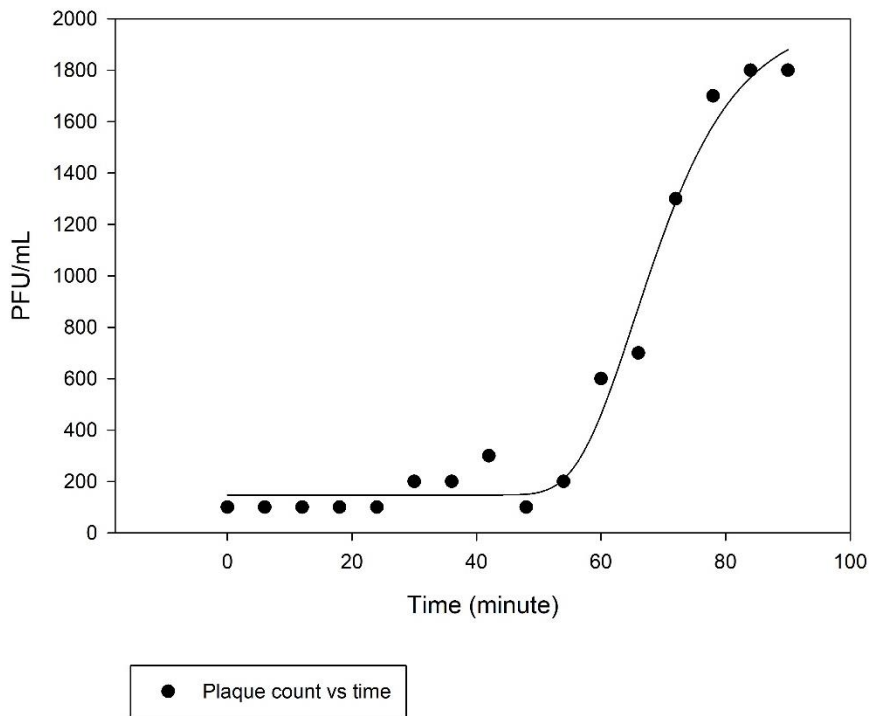
Figure 4.27 One strep growth graph of MET P1-197. This phage was the representative of Anatum phages.

Table 4.4 Latent period and burst sizes of selected phages

Phage ID	Host	Latent Period (min)	Burst Size (PFU/cell)
MET P1-001	Enteritidis, Typhimurium	36	120
MET P1-164	Enteritidis, Typhimurium	30	42
MET P1-088	Hadar	66	47
MET P1-137	Kentucky	66	18
MET P1-197	Anatum	54	110
MET P1-116	Infantis	72	21
MET P1-179	Infantis	60	16

Phages that affecting different hosts showed different characteristics with some exceptions. Kentucky and Infantis phages were exhibited very similar burst sizes and latent periods. Considering the fact that these phages were very closely related genomes, the results were found consistent with whole genome analysis. In fact, one of the Infantis phages (P1-179) were had a closer phylogeny to Kentucky phage (P1-137). Their phenotypic characteristics were also almost identical, while showing a small variation to other Infantis phage (P1-116). Based on the results, MET P1-001 showed the best burst size – latent period combination. Anatum phage P1-197 had a similar burst size, but a longer latent period than P1-001. After these two phages, Hadar phage P1-088 had a considerably longer latent time and smaller burst size. However, burst sizes Infantis and Kentucky were about 6 times less than P1-001, while latent period was nearly 2 times longer.

In literature, there are a wide variety of reports present. For example, latent period and burst size of a Chi-like phage was determined by Choi et al. (2013). Latent period of that phage was 30 minutes, and burst size was 100 PFU/infected cell, both of which were close to our findings for P1-001. However, in another study with Chi like phages, latent period was found 60 minutes and burst size was 48 PFU/infected cell (Phothaworn et al., 2019). In a study, phenotypic characteristics of 5 Jerseyvirus were determined (Kuźmińska-Bajor et al., 2021). Although the phages had very similar genomes, burst sizes varied from 23 PFU/cell to 201 PFU/cell. In addition, latent periods of phages were in between 9 and 24 minutes. The results indicated that the functional characteristics are not directly associated with genomic features (Kuźmińska-Bajor et al., 2021).

The relationship between latent period and burst size was reported inconclusive and weak (Ranasinghe, 2019). As a rule of thumb, shorter latent periods and higher burst sizes are favorable in phage applications. In a study, Li et al. (2021) reported a *Salmonella* phage with 10-minute latent period and 163 PFU/infected cell, and describe that phage as a viable candidate for phage application. However, in another study, Zhang described their *Salmonella* phages latent period as 20 minutes and burst size 34 PFU/infected cell. In that study, authors also speculated that the phage was a promising

biocontrol agent due to short latent period (Zhang et al., 2021). Although these characteristics might be useful to evaluate the phage effectiveness, candidate phages should be tested in designated application conditions such as food or feed matrix.

4.8 Adsorption rates

Adsorption rates of selected phages were determined (Figure 4.28, Figure 4.29 Figure 4.30, Figure 4.31, Figure 4.32, Figure 4.33, and Figure 4.34). All the graphs were drawn in Sigmaplot.
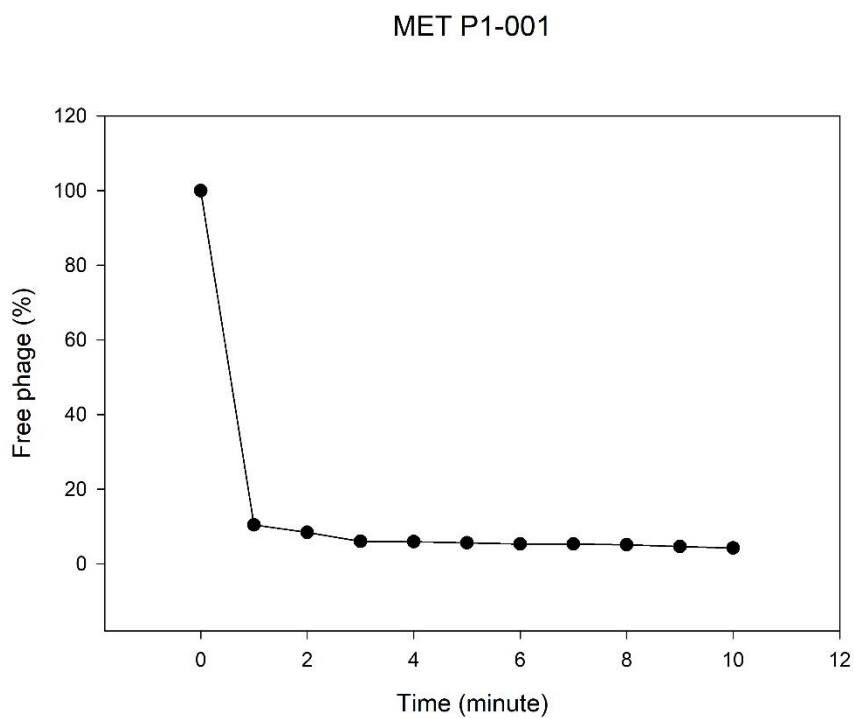
MET P1-001

Figure 4.28 Adsorption rate of MET P1-001 (Enteritidis, Typhimurium)

MET P1-164
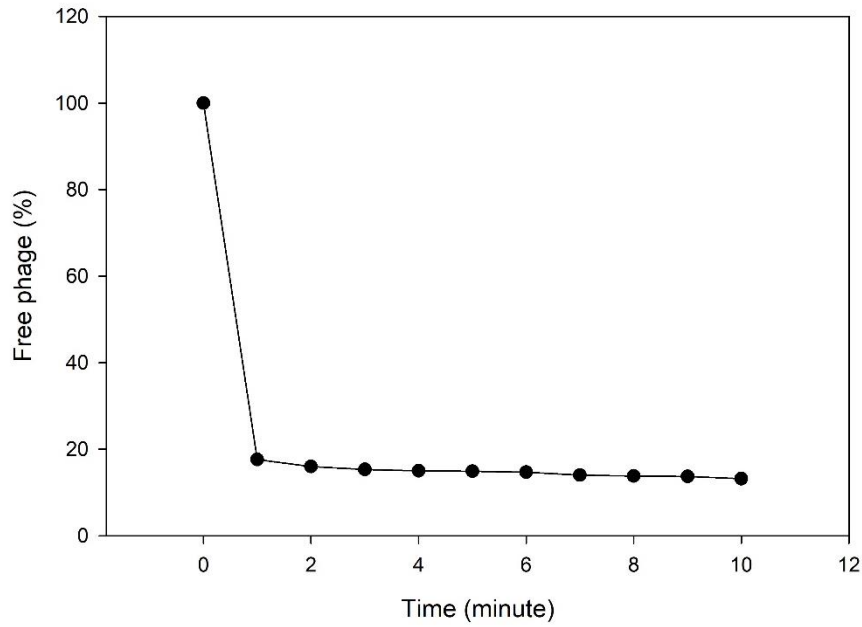
Figure 4.29 Adsorption rate of MET P1-164 (Enteritidis, Typhimurium)

MET P1-088
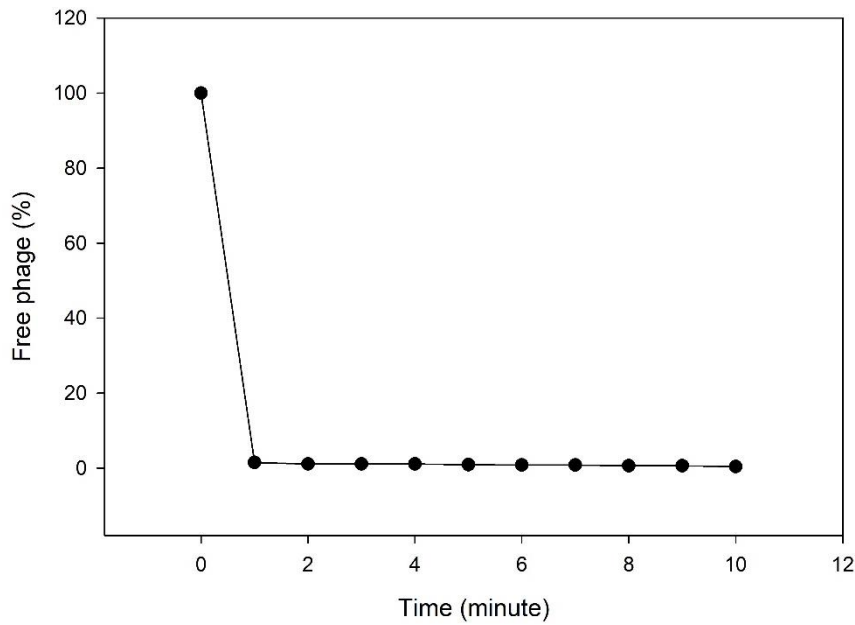
Figure 4.30 Adsorption rate of MET P1-088 (Hadar)

MET P1-116
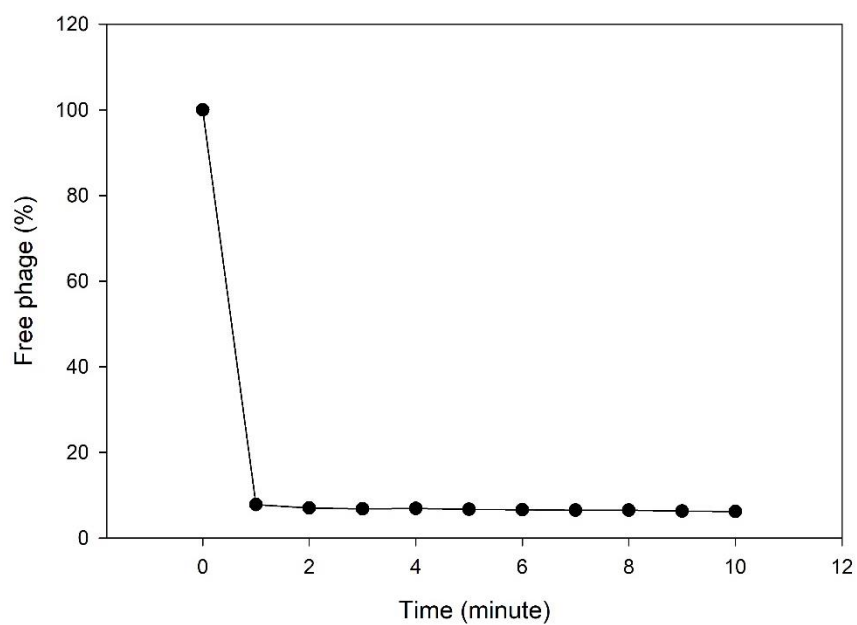
Figure 4.31 Adsorption rate of MET P1-116 (Infantis)

MET P1-179
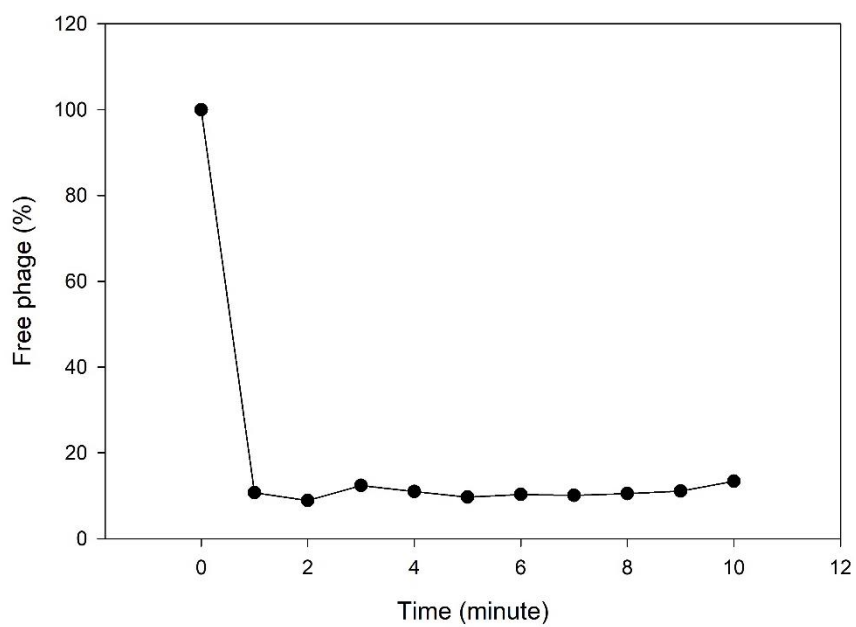
Figure 4.32 Adsorption rate of MET P1-179 (Infantis)

MET P1-137
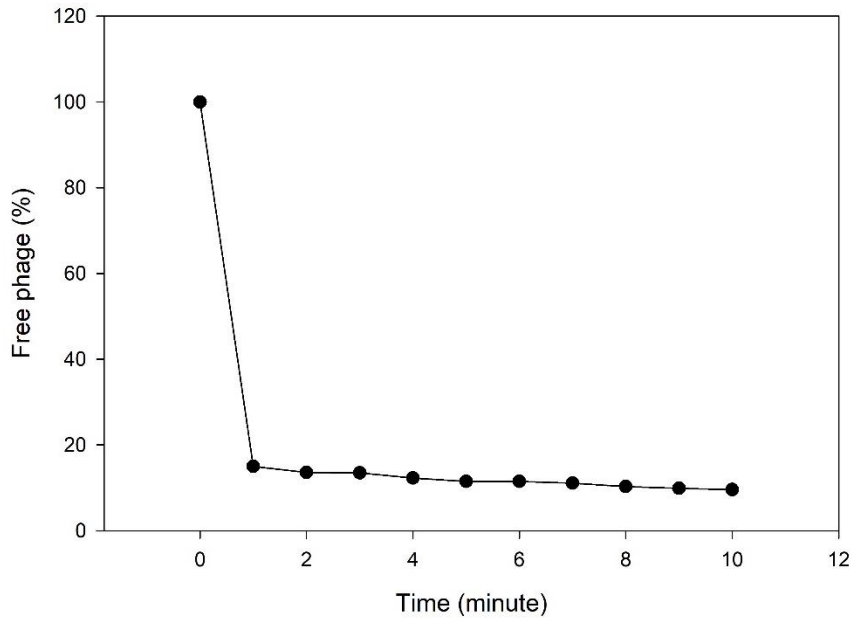
Figure 4.33 Adsorption rate of MET P1-137 (Kentucky)

MET P1-197
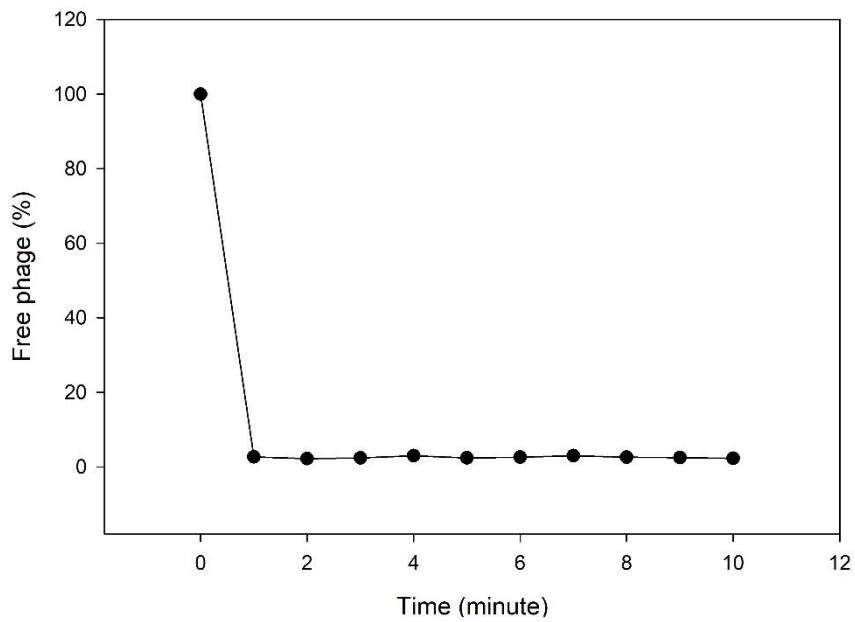
Figure 4.34 Adsorption rate of MET P1-197 (Anatum)

Adsorption rate is an important feature for phage applications for food protection (Kosznik-Kwaśnicka et al., 2020). In our study, Hadar phage showed the best adsorption rate among the tested phages with 0.4% free phage at 10 minute (Table 4.5). Indeed, free phage % were dropped below 1 % at 5 minute. Anatum and Enteritidis phages had 2.3 and 4.2 free phage % at 10 minutes, respectively. However, adsorption rate of the other Enteritidis phage (P1-164) were less than 87%. In general, Infantis and Kentucky phages showed similar performances. Moreover, similar to one step growth analysis, results of P1-179 and P1-137 were closer than P1-179 and P1-116. In a study, adsorption rates of 5 closely related phages were determined. Although genomes of those phages showed 99% similarity, adsorption rates varied from 1 % free phage to 20 % free phage (Kuźmińska-Bajor et al., 2021).

Table 4.5 Adsorption constants and free phage % at 10 minute

Phage ID	Host	Free phage (%)	Adsorption Constant (k)
MET P1-001	Enteritidis, Typhimurium	4.2	8.46×10^{-7}
MET P1-164	Enteritidis, Typhimurium	13.2	7.31×10^{-7}
MET P1-088	Hadar	0.4	1.08×10^{-7}
MET P1-137	Kentucky	9.6	7.63×10^{-7}
MET P1-197	Anatum	2.3	9.06×10^{-7}
MET P1-116	Infantis	6.2	8.07×10^{-7}
MET P1-179	Infantis	11.1	7.5×10^{-7}

4.9   Genome size estimation

Fresh high titer phages were entrapped into SKG agarose gels and their genome size were investigated. All PFGE gel pictures were presented in Appendix I. Most of the phage genomes couldn't be visualized on gels (Figure 4.35). Analysis were repeated with high titer phage lysates, and also different phages. However, the problem persisted, especially for Enteritidis phages. All in all, bands were observed for 5 different phages.

In some cases, multiple bands (one bright and one faded) were observed (Figure 4.35). These bands were considered as ghost bands due to phage DNA degradation during the plaque preparation. However, these bands might as well be resulted from a contamination of another phage. (Gao et al., 2020). investigated the comparative genomics of *Salmonella* prophages. In that study, majority of the prophages had between 30 to 50 kb genomes. The faint bands in our study were also found in that size range. Therefore, some of those phages (P1-001, P1-122) were further investigated with whole genome sequencing.
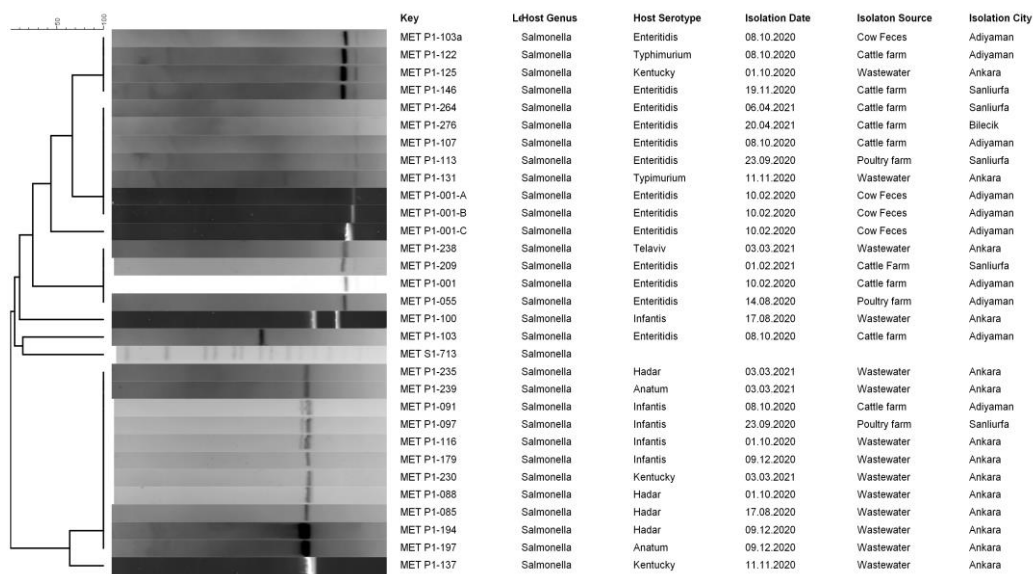
Figure 4.35 Cluster analysis of phages.

In one phage (P1-100), two sharp bands were observed. Later in genome analysis, it was seen that there were actually two different phages in P1-100. For another phage, P1-103, we initially observed two bands, one bright and one faded. In another PFGE run, this phage exhibited a band at 240 kb region. This phage was also selected for sequencing as well.

Phage gels were investigated in Bionumerics for band size (Figure 4.36). In our phage PFGE database, we have a total of 26 phage genomes (19 from this study). A dendogram created based on the genome size. However, it should be noted that dendogram was

based on a single band. As a result, it was inconclusive in terms of genetic relationships of phages. For instance, if two phages produced bands in different sizes, they could be appointed as different phages. However, same conclusion couldn't be made for phages with similar band sizes.

Key	Host Genus	Host Serotype	Isolation Date	Isolaton Source	Isolation City	Band size (kb)
MET P1-122	Salmonella	Typhimurium	08.10.2020	Cattle farm	Adiyaman	53.55
MET P1-125	Salmonella	Kentucky	01.10.2020	Wastewater	Ankara	56.54
MET P1-146	Salmonella	Enteritidis	19.11.2020	Cattle farm	Sanliurfa	57.19
MET P1-264	Salmonella	Enteritidis	06.04.2021	Cattle farm	Sanliurfa	34.40
MET P1-276	Salmonella	Enteritidis	20.04.2021	Cattle farm	Bilecik	33.62
MET P1-107	Salmonella	Enteritidis	08.10.2020	Cattle farm	Adiyaman	34.84
MET P1-113	Salmonella	Enteritidis	23.09.2020	Poultry farm	Sanliurfa	35.32
MET P1-131	Salmonella	Typimurium	11.11.2020	Wastewater	Ankara	36.65
MET P1-238	Salmonella	Telaviv	03.03.2021	Wastewater	Ankara	49.80
MET P1-209	Salmonella	Enteritidis	01.02.2021	Cattle Farm	Sanliurfa	56.41
MET P1-001	Salmonella	Enteritidis	10.02.2020	Cattle farm	Adiyaman	51.00
MET P1-055	Salmonella	Enteritidis	14.08.2020	Poultry farm	Adiyaman	53.13
MET P1-235	Salmonella	Hadar	03.03.2021	Wastewater	Ankara	123.54
MET P1-239	Salmonella	Anatum	03.03.2021	Wastewater	Ankara	120.37
MET P1-091	Salmonella	Infantis	08.10.2020	Cattle farm	Adiyaman	117.59
MET P1-097	Salmonella	Infantis	23.09.2020	Poultry farm	Sanliurfa	119.47
MET P1-116	Salmonella	Infantis	01.10.2020	Wastewater	Ankara	121.93
MET P1-179	Salmonella	Infantis	09.12.2020	Wastewater	Ankara	119.79
MET P1-230	Salmonella	Kentucky	03.03.2021	Wastewater	Ankara	117.27
MET P1-088	Salmonella	Hadar	01.10.2020	Wastewater	Ankara	119.64
MET P1-085	Salmonella	Hadar	17.08.2020	Wastewater	Ankara	123.30
MET P1-194	Salmonella	Hadar	09.12.2020	Wastewater	Ankara	130.01
MET P1-197	Salmonella	Anatum	09.12.2020	Wastewater	Ankara	126.05
MET P1-103	Salmonella	Enteritidis	08.10.2020	Cattle farm	Adiyaman	238.92

Figure 4.36 Band size estimation of phages by Bionumerics. Phages P1-209, P1-230, P1-235, P1-238, P1-239, P1-264, and P1-276 belongs to another study.

In general, phages that target same serovar produced bands in similar sizes with a few exceptions (Table 4.6). Bands sizes of 8 Enteritidis phages clustered in 3 groups; 5 phages had bands around 55 kb, 2 phages had 35 kb bands, and 1 phage with 240 kb band. There was no apparent relationship between the band size and isolation date or region. 3 Hadar phages had bands around 120 kb. Similar size region was also observed in Infantis and Anatum phages. Kentucky phage was similar to one of the Enteritidis clusters with 55 kb size. Typhimurium phage was also similar to one of the Enteritidis clusters with 35 kb.

Table 4.6 Band sizes of typed phages

Phage	Host Serotype	Isolation Date	Band Size (kb)
P1-001	Enteritidis	10.02.2020	51
P1-055	Enteritidis	14.08.2020	53.1
P1-085	Hadar	17.08.2020	123.3
P1-088	Hadar	01.10.2020	119.6
P1-091	Infantis	08.10.2020	117.5
P1-097	Infantis	23.09.2020	119.4
P1-100a	Infantis	17.08.2020	117.9
P1-100b	Infantis	17.08.2020	57.2
P1-103a	Enteritidis	08.10.2020	53.5
P1-103b	Enteritidis	08.10.2020	238.9
P1-107	Enteritidis	08.10.2020	34.8
P1-113	Enteritidis	23.09.2020	35.3
P1-116	Infantis	01.10.2020	121.9
P1-122	Enteritidis	08.10.2020	53.5
P1-125	Kentucky	01.10.2020	56.5
P1-131	Typhimurium	11.11.2020	36.6
P1-137	Kentucky	01.11.2020	121.4
P1-146	Enteritidis	19.11.2020	57.2
P1-179	Infantis	09.12.2020	119.8
P1-194	Hadar	09.12.2020	130
P1-197	Anatum	09.12.2020	126

Although PFGE provided only genome sizes, we could associate the data with literature to make assumptions on phage families. For this, Infrastructure for a Phage Reference Database (INPHARED) was used (Cook et al., 2021). This database contains 556 *Salmonella* phage genome uploaded to NCBI database. Although *Salmonella* phage genomes varies from 11 kbp to 350 kbp, there were some distinguishable clusters. For example, all 30 phage genomes with 240 kbp size were identified as *Myoviridae* family. In addition, all 30 phages were lytic. Most of our phages were in between 110 to 120 kbp range. There were 104 phages in INPHARED in that genome size range. All of those phages were from *Demerecviridae* family. While majority of those phages were identified as Epseptimavirus, a small portion were from Tequintavirus family. Similarly, all 104 phages in that range were lytic phages (Cook et al., 2021). For other ranges, genome sizes of database entries were highly diverse, thus linking our phages to families based on genome size were impossible.

4.10   Morphological analysis

Phage morphology was investigated by CTEM images. 10 phages were prepared and stained for TEM and images were taken by Central Laboratory (Figure 4.37, Figure 4.38, Figure 4.39, Figure 4.40, Figure 4.41). Images of a phage (MET P1-091) was unsatisfactory. Rest of the images were processed with ImageJ software, and head and tail measurements were recorded (Table 4.7). Means of measurements were analyzed by student's t-test, to determine if the difference between the measurements were significant. In total, 18 different phages with different measurements were identified in 10 phage lysate image ($p<0.05$). In terms of measurements, in 5 of the images, there were two distinct phages, and images belong to P1-164 and P1-179 had single phage. In two images, 3 phages with significantly different head and tail measurements were observed. However, different measurements are not necessarily mean that phages are different (H.-W. Ackermann, 2007). Without a morphological difference, making a conclusion just based on measurements would be misleading. TEM images revealed

phages with different morphologies co-exist in phage lysates. two phages with different morphologies were observed in phage lysate MET P1-100.
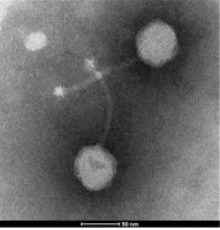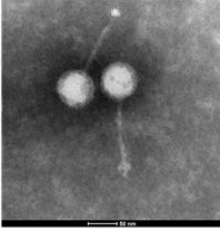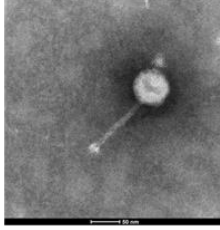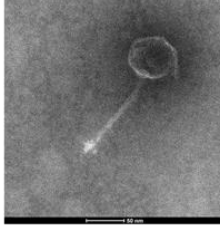
P1-001_1	P1-001_2	P1-082_1	P1-082_2
Head: 62.05±4.46 nm	Head: 80.46±5.81 nm	Head: 63.80±4.67 nm	Head: 98.54±14.87 nm
Tail: 116.53±9.94 nm	Tail: 150.88±5.35 nm	Tail: 113.71±4.29 nm	Tail: 153.16±5.50 nm

Figure 4.37 TEM analysis of phages P1-001 (left) and P1-082 (right). Two different phages were determined in both images.

Morphological differences were observed between Enteritidis phages. While 3 Enteritidis phages (P1-001, P1-082, and P1-103) had shorter tails with distinguishable base plates, P1-122 and P1-164 had considerably longer tails with an attached base plate.
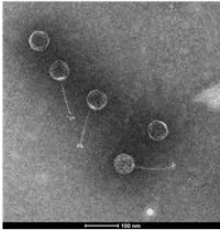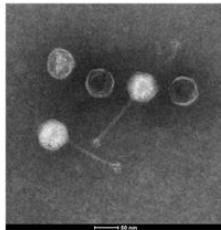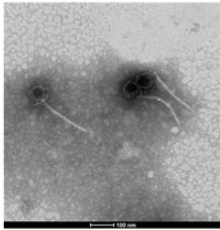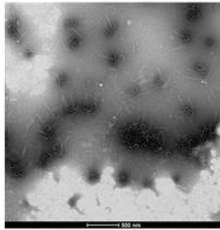
P1-103_1	P1-103_2	P1-122_1	P1-122_2
Head: 69.57±9.87 nm	Head: 54.62±6.19 nm	Head: 70.21±12.97 nm	Head: 73.11±4.94 nm
Tail: 130.88±11.06 nm	Tail: 103.05±4.69 nm	Tail: 199.76±8.78 nm	Tail: 246.36±12.67 nm

Figure 4.38 TEM analysis of phages P1-103 (left) and P1-122 (right). Two different phages were determined in both images.
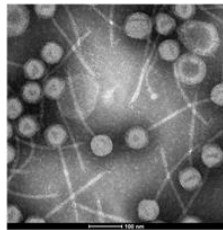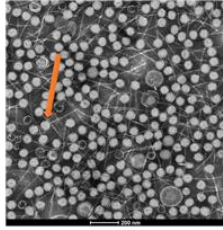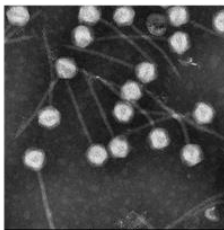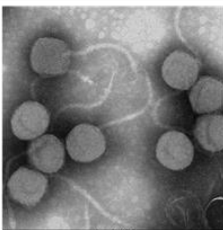
P1-116_1	P1-116_2	P1-164_1	P1-179_1
Head: 79.86±2.44 nm	Head: 67.08±3.63 nm	Head: 60.76±6.60 nm	Head: 69.13±3.84 nm
Tail: 265.53±9.41 nm	Tail: 221.07±9.55 nm	Tail: 220.66±17.46 nm	Tail: 165.66±28.24 nm

Figure 4.39 TEM analysis of phages P1-116 (left 2), P1-164 (middle) and P1-179 (right). Two different phages were determined in P1-116, while single phage morphology was observed in P1-164 and P1-179.

Phages were attempted to be define based on Ackermann's guide (Ackermann, 2007). Principal classification of phages was carried out based on the morphological features. Beside the shape, tail and head sizes were also considered. All phages were determined as in *Caudovirales* (tailed phages) order. Majority of the phages (14/18) were assigned as a member of *Siphoviridae*, while the rest of the phages were grouped under *Myoviridae*. Typically, *Siphoviridae* has long non-contractible tail while *Myoviridae* has a contractile tail. Phages from both family had icosahedral heads (Martino et al., 2021). Classifications were determined according to ICTV Virus Taxonomy report (King et al., 2011).
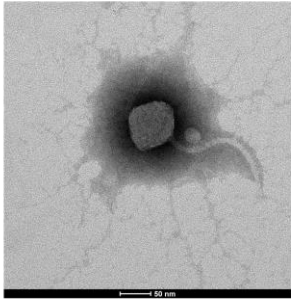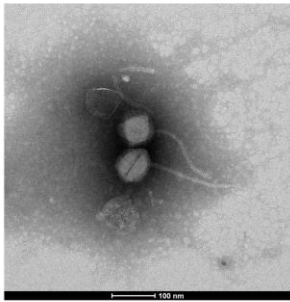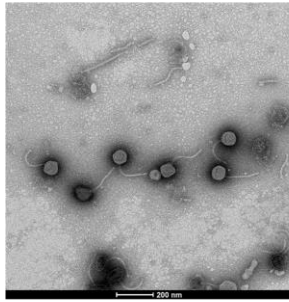
P1-137_1	P1-137_2	P1-137_3
Head: 67.70±3.70 nm	Head: 91.57±8.28 nm	Head: 79.31±4.50 nm
Tail: 160.96±14.77 nm	Tail: 251.07±12.09 nm	Tail: 181.55±6.35 nm

Figure 4.40 TEM analysis of phages P1-137. Three distinct measures were taken from the images belong to P1-137.
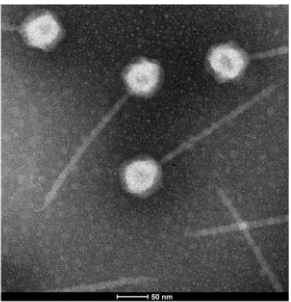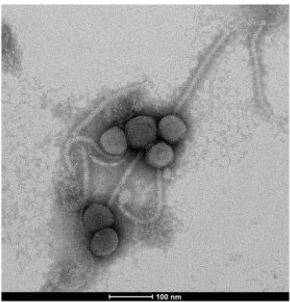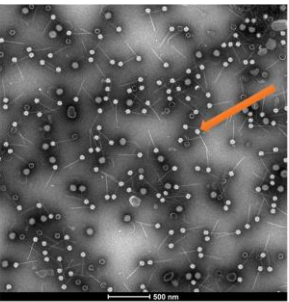
P1-100_1	P1-100_2	P1-100_3
Head: 50.64±3.43 nm	Head: 72.38±6.68 nm	Head: 68.06±7.15 nm
Tail: 201.63±4.91 nm	Tail: 200.12±20.53 nm	Tail: 252.89±8.54 nm

Figure 4.41 TEM analysis of phages P1-100. Three distinct measures were taken from the images belong to P1-137.

Table 4.7 Summary of measurements from TEM analysis of 9 phages.

	Phages	Head Average	Head Std.Dev	Tail Average	Tail Std.Dev	Family
P1-001	**Phage 1**	62.05	4.5	116.53	9.9	*Myoviridae*
	Phage 2	80.46	5.8	150.88	5.3	*Myoviridae*
P1-082	**Phage 1**	63.80	4.7	113.71	4.3	*Myoviridae*
	Phage 2	98.54	14.9	153.16	5.5	*Myoviridae*
P1-103	**Phage 1**	69.57	9.9	130.88	11.1	*Myoviridae*
	Phage 2	54.62	6.2	103.05	4.7	*Myoviridae*
P1-122	**Phage 1**	70.21	13.0	199.76	8.8	*Siphoviridae*
	Phage 2	73.11	4.9	246.36	12.7	*Siphoviridae*
P1-116	**Phage 1**	79.86	2.4	265.53	9.4	*Siphoviridae*
	Phage 2	67.08	3.6	221.07	9.6	*Siphoviridae*
P1-164	**Phage 1**	60.76	6.6	220.66	17.5	*Siphoviridae*
P1-179	**Phage 1**	69.13	3.8	165.66	28.2	*Siphoviridae*
P1-137	**Phage 1**	67.70	3.7	160.96	14.8	*Siphoviridae*
	Phage 2	91.57	8.3	251.07	12.1	*Siphoviridae*
	Phage 3	79.31	4.5	181.55	6.4	*Siphoviridae*
P1-100	**Phage 1**	50.64	3.4	201.63	4.9	*Siphoviridae*
	Phage 2	72.38	6.7	200.12	20.5	*Siphoviridae*
	Phage 3	68.06	7.1	252.89	8.5	*Siphoviridae*

Siphoviridae are the most common family in *Caudovirales*. 61% of *Caudovirales* order belongs to *Siphoviridae*, whereas 25% of the order are grouped under *Myoviridae* (Ackermann, 2009). TEM analysis showed that almost all lysates have more than one phage. Contrarily, very similar phage plaques were observed in double plaque assay. Our results indicated that new methods should be employed to distinguish and purify the plaques.

4.11   Bacterial reduction and virulence index

Bacterial reduction experiments were done in liquid media in 96 well plates. Planktonic killing assay (PKA) were conducted in the same group of phages used in characterization by using their hosts in order to determine the kinetic relationship between the phage and the host.

Bacterial reduction curves showed the effect of phage titers on bacterial growth (Figure 4.42, Figure 4.43, Figure 4.44, Figure 4.45, Figure 4.46). Phages inhibits bacterial growth when the titer was higher than 6 log PFU/mL for at least 4 hours. After 4 to 6 hours, host developed resistance, and started to grow in all experiments (Figure 4.42). Consistently, inhibition efficacy of phages was increased with increasing titer in all experiments. Enteritidis phages inhibited bacterial growth even in low titers, (Figure 4.45, Figure 4.46). However, this was not observed for Infantis and Kentucky phages. At low levels, Infantis phages failed to inhibit bacterial growth (Figure 4.43, Figure 4.44). When phages were 8 log PFU/mL, bacterial growth was completely inhibited for hours, in all instances. Rest of the graphs were given in Appendix G. For Enteritidis phages, there was no apparent relationship with the host resistance and phage titer. The results showed that there is no linear correlation between the phage titer and host resistance. Host started to grow around same time for all titers. Since Infantis and Kentucky phages were ineffective at low titers, it might be hosts gained resistance rapidly.
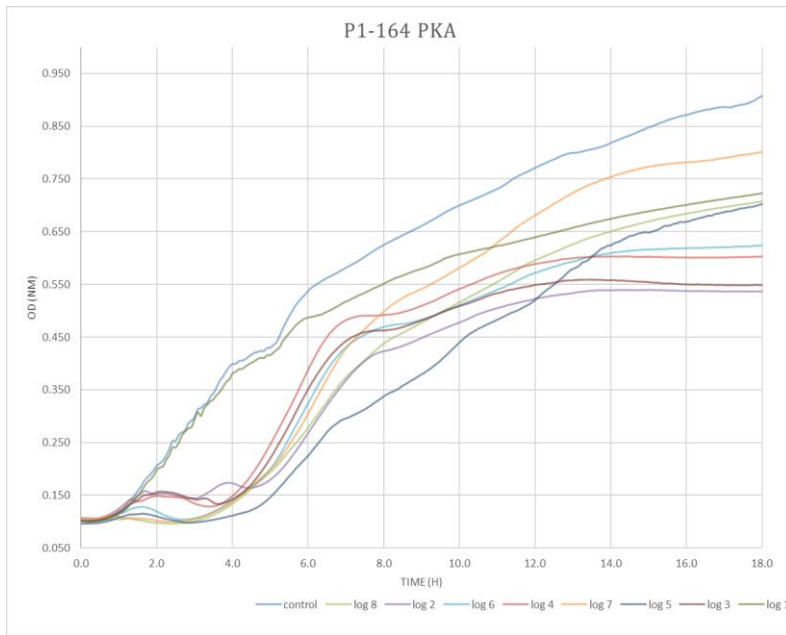
Figure 4.42 Bacterial reduction curve of P1-164 (Enteritidis). This graph shows the growth of control and phage added bacterial cultures for 18 hours.
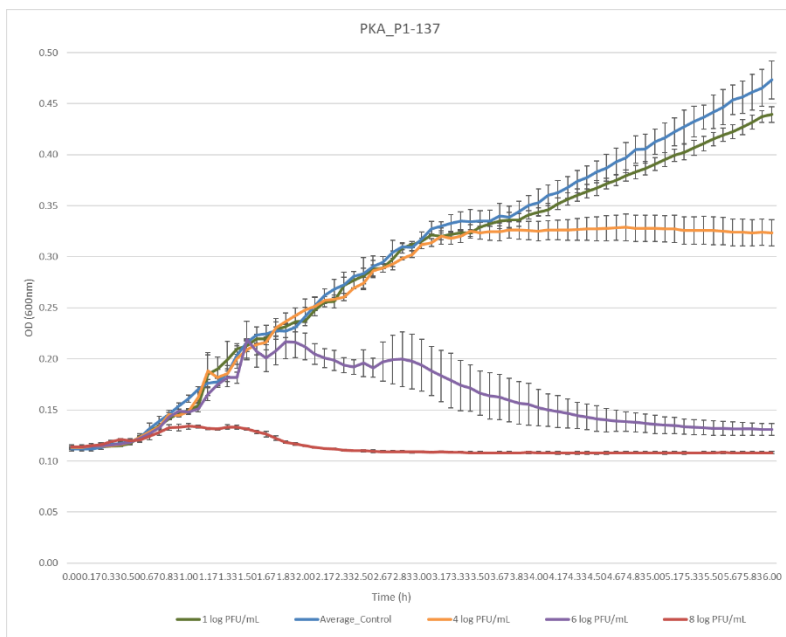
Figure 4.43 Bacterial reduction curve of P1-0137 (Kentucky). In the graph, blue line is control (phage-free bacteria), green 10^{-7} MOI, orange: 10^{-4} MOI, violet: 10^{-2} MOI, and red: 1 MOI
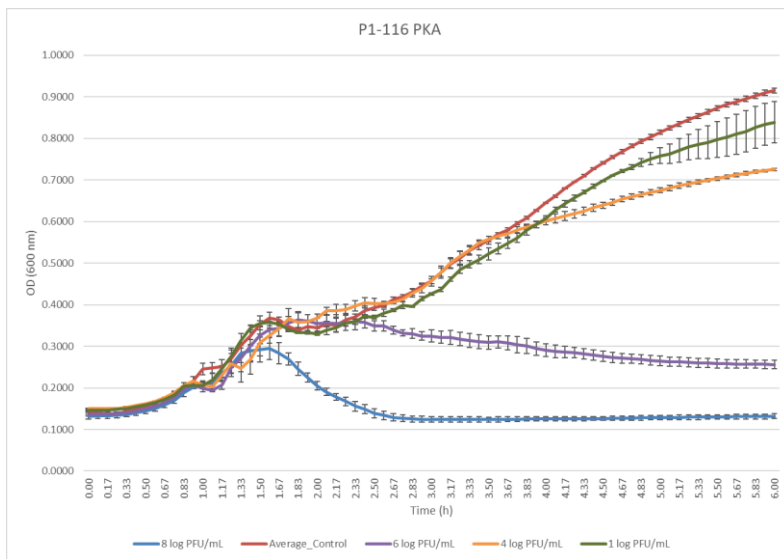
Figure 4.44 Bacterial reduction curve of P1-116 (Infantis). In the graph, red line is control (phage-free bacteria), green 10^{-7} MOI, orange: 10^{-4} MOI, violet: 10^{-2} MOI, and blue: 1 MOI
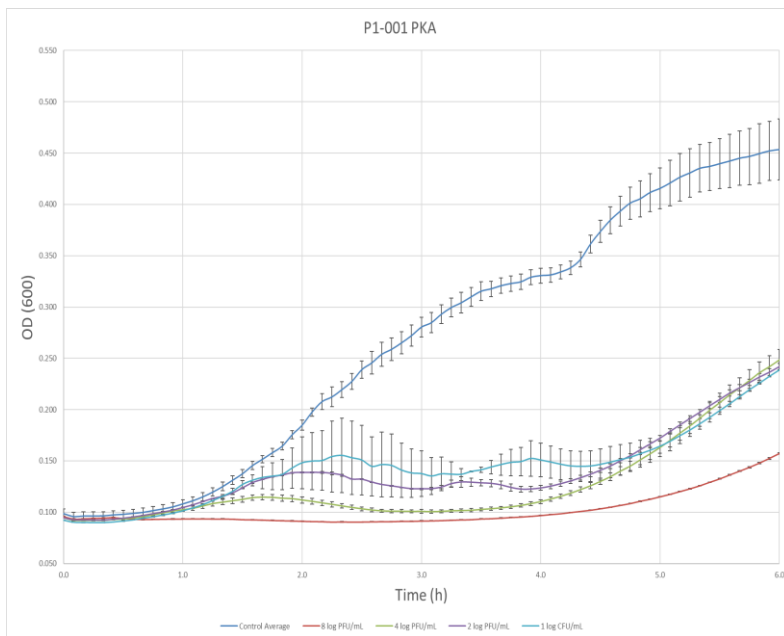
Figure 4.45 Bacterial reduction curve of P1-001 (Enteritidis). In the graph, blue line is control (phage-free bacteria), cyan: 10^{-7} MOI, violet: 10^{-6} MOI, green 10^{-4} MOI, and red: 1 MOI
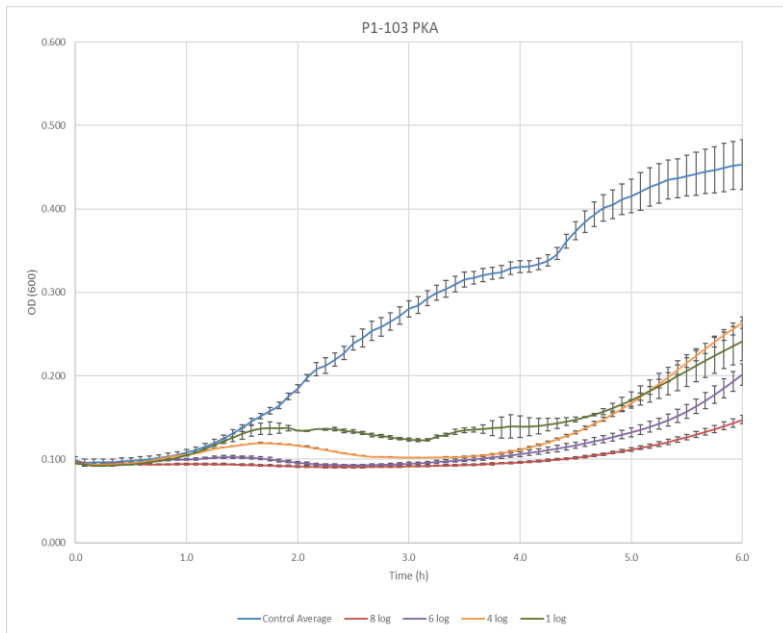
Figure 4.46 Bacterial reduction curve of P1-103 (Enteritidis). In the graph, blue line is control (phage-free bacteria), green 10^{-7} MOI, orange: 10^{-4} MOI, violet: 10^{-6} MOI, and red: 1 MOI

Virulence index is the area between host growth curve and phage and host growth curve, and shows the effectiveness of phage. Area difference for all phage titers from 1 log to 8 log PFU/mL was calculated, and virulence index for each titer was found Figure 4.47, Figure 4.48). Expectedly, virulence index was increased with the increased titer in all phages. For Enteritidis phages, P1-001, P1-103, and P1-082 had similar final virulence index results, whereas P1-122 and P1-164 were similar to each other and lower than the rest.
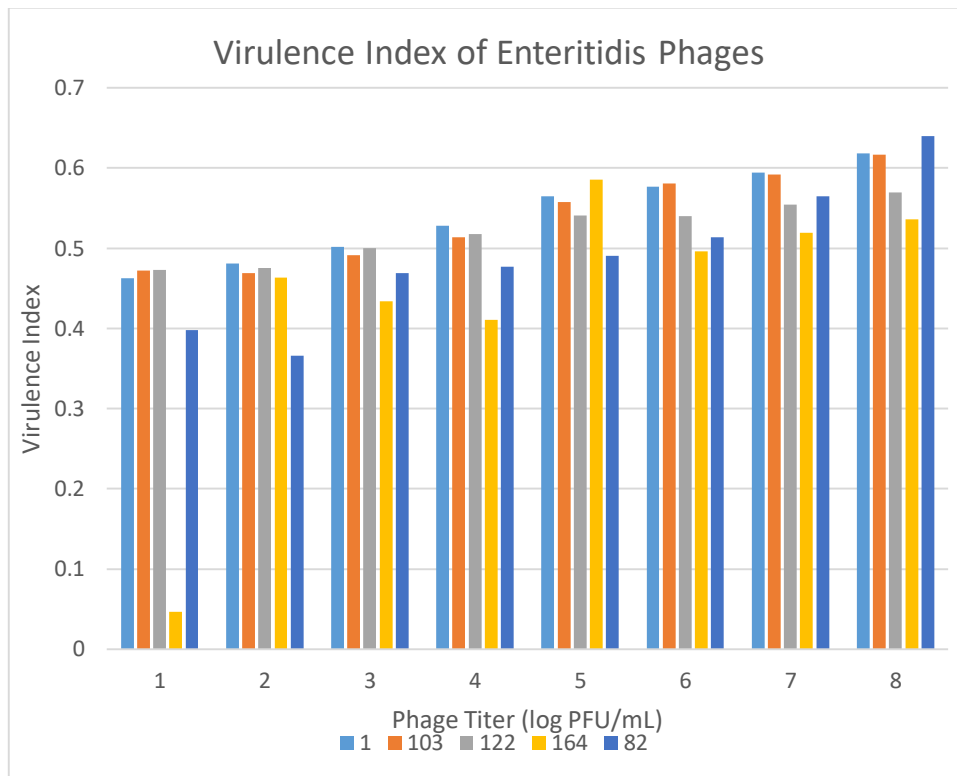
Figure 4.47 Virulence index score of Enteritidis phages with respect to titers

Virulence of phages is affected by a number of extrinsic and intrinsic factors. Extrinsic conditions are environmental conditions like pH, application matrix, temperature. Intrinsic conditions are phenotypic characteristics of phage such as latent period, adsorption rate and burst size (Storms et al., 2020).

For Infantis phages, a similar trend was observed. While P1-091 and P1-116 had lower virulence index than the rest of the phages, all phages showed satisfactory results at 8 log PFU/mL level.
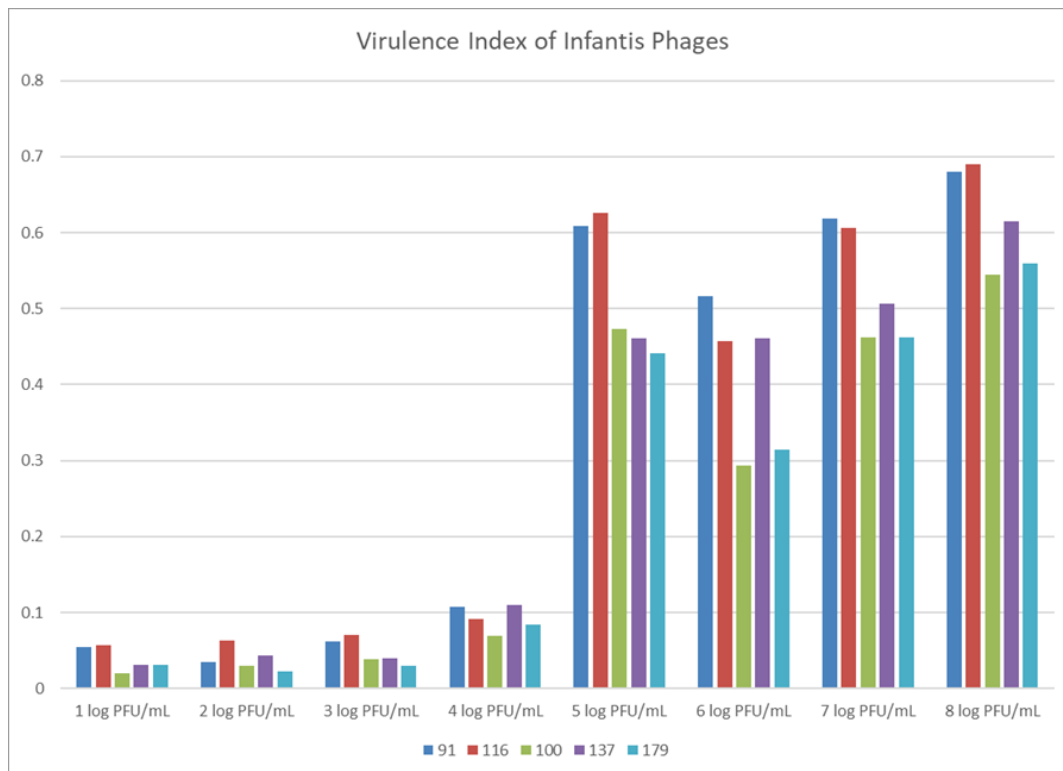
Figure 4.48 Virulence index score of Infantis phages with respect to titers

Virulence index is a fairly new analysis to test the efficacy of phages. This experiment was introduced by Storms et al. (2020). This analysis was more reliable than spot test, as it allows phage and host grow simultaneously. In spot tests, phages might kill bacteria with lysis from without mechanism. With his mechanism, phages kill bacteria on initial contact, instead of infecting the host. In addition, it is more convenient than efficacy of plating test, which requires a lot of dilution and double plaque testing. Also, this analysis helps standardization of phage selection (Haines et al., 2021) However, it should be noted that this analysis is directly related to host. For instance, within our results, we could compare the phages affecting same hosts. Nevertheless, this analysis is particularly useful for cocktail development, as it allows the identification of phage – host combinations (Steffan et al., 2022). In their study Haines et al. (2021) compared the efficacy of plating and virulence index scores of phages. There was a direct correlation between the methods, and the authors stated that phages with a virulence

index score higher than 0.2 could be considered as efficient for a given host. In our analysis, majority of phages had Vi above 0.4 even in low levels.

4.12   Whole genome sequencing and bioinformatics

In total, 10 phages were selected for whole genome sequencing. Files of raw reads were obtained in fq format. For the bioinformatics, first, files were checked with FASTQC for read quality. All of the reads had good (>20) per base sequence quality. Adapters trimmed with TRIMMOMATIC by using default settings and quality of reads were checked once more with FASTQC. Reads had around 4.5 Mbp sequence content. Preliminary assemblies of reads were by SPAdes, and contigs were visualized with Bandage (Figure 4.49).
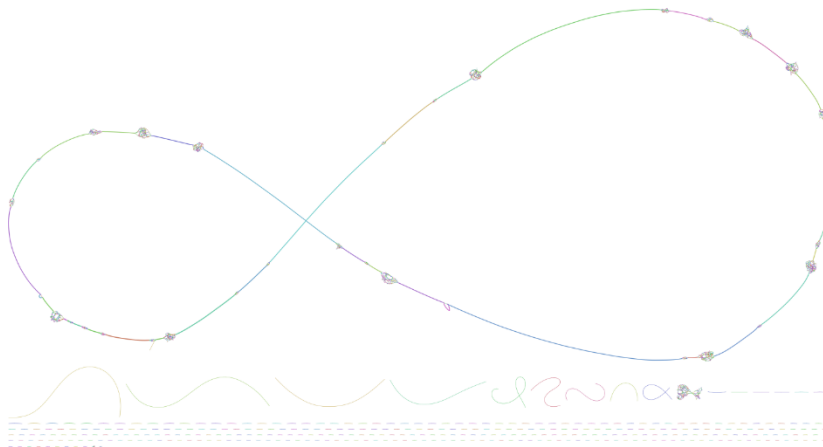
Figure 4.49 Bandage plot of MET P1-179 initial assembly. In the initial assembly more than 1000 contigs were produced.

However, since the coverage was too high, assemblies had very high number of contigs containing small sequences. These sequences were mostly coming from bacterial contamination (Shen & Millard, 2021). For the shorter genomes like phages it is advised to adjust coverage around 25 to100 X (Turner, et al., 2021). Approximate coverage of reads was adjusted with the assumption that each phage genome was 100 kbp long, and coverage was calculated with the formula below;

Equation 4.1 $$Coverage = \frac{number\ of\ reads\ x\ read\ lenght}{genome\ size}$$

In the equation, read length was pre-determined by the sequence technology, (Illumina NextSeq) as 150 bp, and genome size was assumed as 100 kbp, and the coverage was 100. Therefore, number of reads was adjusted to 66666 by using Seqtk toolkit. After random subsampling with Seqtk, reads were assembled again with SPAdes and visualized with Bandage. This time, a single contig with two small repeat contigs was observed (Figure 4.50).
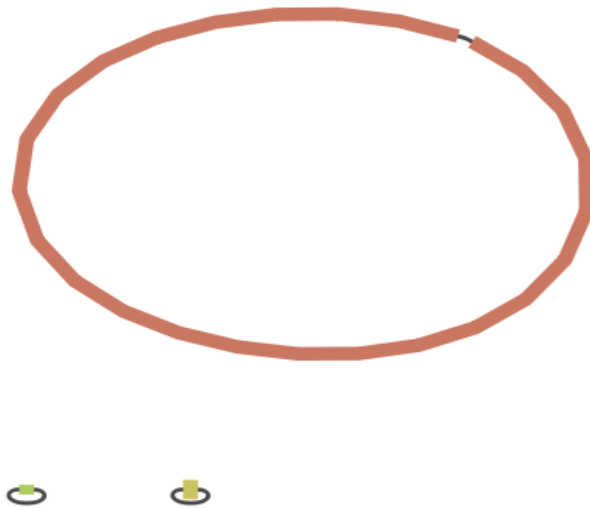
Figure 4.50 Bandage plot of MET P1-179 assembly after subsampling. Phage genome was clearly presented in a single contig.

Contigs were examined based on their length and coverage, and optimum subsampling size was calculated accordingly for each phage genome. For example, initial assumption produced a single contig with 112 X for MET P1-179. For smaller phage genomes (e.g. 59 kbp) subsampling were adjusted to 40000 according to formula above. In most of the samples, phage genomes with acceptable coverage were assembled.

In 8 of the assemblies, more than one phage genome was observed (Table 4.8). Six of the assemblies had 2 phage genomes with acceptable coverages (25X-200X). Assemblies of MET P1-082 and MET P1-103 had 3 phages. However, for both

assembly, one of the phage contigs had lower than 25 X coverage. Those contigs were analyzed as well, but since the coverage was too low, they were considered as contamination of other phages. In two assemblies (MET P1-137 and MET P1-179) there were only one phage genome.

Presence of two phage genomes in some of the assemblies were investigated further. None of those phages produced different shaped plaque morphologies. In addition, phenotypic features such as one-step and adsorption also didn't indicate the presence of two viruses. The case of two phages might be explained with co-infection phenomenon (Diaz-Munoz, 2017). Co-infection is the simultaneous infection of two phages to same host. These phages could either be lysogenic or lytic. Co-infection is common in nature In fact, nearly 38% of the infected bacteria contained multiple phages (Roux et al., 2015). When two phages co-infect the same host, they compete for the host resources (Chevallereau et al., 2022). In that case, only dominant phages morphology could be observed.

Assembled phage genomes were clustered according to their genome sizes. Based on the genome size, 4 different group of phages were identified. Group 1 phages were found in 8 sequences, had the highest coverage, and around 59 kbp genome size. This genome size was also observed in PFGE experiments. Group 2 phages were presented in all 5 Enteritidis sequences. These phages were around 43 kbp long, were again very similar to each other in terms of genome size. Group 3 phages were presented in three Infantis sequences, and was around (117k kbp). Group 4 had 2 phages, one Kentucky and one Infantis and had 123 kbp long genome. We also had two outlier phages (Group 5) with small coverage, one of which had more than 200 kbp genome size, and found in P1-082 which was isolated from a poultry farm in Bolu. This phage was also observed in PFGE gel pictures. The other one had 31 kbp, and found in one of the Enteritidis phages. A total of 7 phages were deposited into NCBI database. These phages were; MET P1-001_43k, P1-001_59k, P1-082_240k P1-103_31k, P1-116_117k, P1-137, and P1-179. All in all, each unique phage from our culture collection was represented. Rest of the phages will be deposited as well.

All assemblies were visualized with Bandage to check the assembly errors. Although there were small contamination sequences around 100 bp (Figure 4.50), phage contigs could be extracted by a python script. After phage genomes were cleaned from contamination, contigs were checked with Pilon for assembly errors. All assemblies were mapped with reads by using bbmap.sh tool. Resulting BAM file was sorted and indexed with Samtools (http://www.htslib.org/doc/samtools-sort.html). Assemblies than detected and corrected by Pilon automatically. In all assemblies, Pilon reported that confirmed bases were higher than 99.5%, and there were no corrections made.

Although assemblers produce assemblies correctly, a reordering is necessary for the phage genomes. For reorientation of genomes, all assemblies were checked by PhageTerm software. PhageTerm automatically detects the phage packaging strategy, and reorders genome accordingly. Group 1 (59 kbp), Group 3 (117 kbp), Group 4 (123 kbp) assemblies were evaluated by PhageTerm, and genomes of these phages were reoriented by the software. Packaging strategy of Group 3 and 4 phages were Direct Terminal Repeats, while Group 1 phages had clearly defined ends similar. Group 2 phages, and the outlier phages were circularly permuted with no clear, physical ends, and couldn't be evaluated by PhageTerm. PhageTerm reports were given in Appendix E. Closest relatives of these phages were identified by BLASTn. Phages were queried against Caudovirales database. Closest relatives of phages were determined, and genomes were reordered by python scripts based on the closest relative. After reordering process, all assemblies were checked for errors again by Pilon. No error was found in genome assemblies.

Table 4.8 Metadata table of Phage sequences

METUID	Host	Group	Source	Month	Date	City	Genome Size	GC %
MET P1-001_43k	Enteritidis	Group 2	Cattle Farm	February	10.02.2020	Adiyaman	43282	50.0
MET P1-001_59k	Enteritidis	Group 1	Cattle Farm	February	10.02.2020	Adiyaman	59899	56.3
MET P1-103_31k	Enteritidis	Group 5	Cattle Farm	October	08.10.2020	Adiyaman	31582	52.1

Table 4.8 continued

MET P1-103_43k	Enteritidis	Group 2	Cattle Farm	October	08.10.2020	Adiyaman	43300	50.0
MET P1-103_59k	Enteritidis	Group 1	Cattle Farm	October	08.10.2020	Adiyaman	59942	56.3
MET P1-122_43k	Enteritidis	Group 2	Cattle Farm	October	08.10.2020	Adiyaman	43282	50.0
MET P1-122_59k	Enteritidis	Group 1	Cattle Farm	October	08.10.2020	Adiyaman	59843	56.3
MET P1-164_43k	Enteritidis	Group 2	Cattle Farm	November	19.11.2020	Adiyaman	43282	50.0
MET P1-164_59k	Enteritidis	Group 1	Cattle Farm	November	19.11.2020	Adiyaman	59899	56.3
MET P1-082_43k	Typhimurium	Group 2	Poultry Farm	August	14.08.2020	Bolu	43217	50.0
MET P1-082_59k	Typhimurium	Group 1	Poultry Farm	August	14.08.2020	Bolu	59899	56.3
MET P1-082_240k	Typhimurium	Group 5	Poultry Farm	August	14.08.2020	Bolu	243301	48.4
MET P1-091_59k	Infantis	Group 1	Cattle Farm	October	08.10.2020	Adiyaman	59899	56.3
MET P1-091_117k	Infantis	Group 3	Cattle Farm	October	08.10.2020	Adiyaman	117817	39.3
MET P1-100_58k	Infantis	Group 1	Wastewater	August	17.08.2020	Ankara	60108	56.5
MET P1-100_117k	Infantis	Group 3	Wastewater	August	17.08.2020	Ankara	117826	39.3
MET P1-116_59k	Infantis	Group 1	Wastewater	October	01.10.2020	Ankara	59835	56.3
MET P1-116_117k	Infantis	Group 3	Wastewater	October	01.10.2020	Ankara	117827	39.3
MET P1-137	Kentucky	Group 4	Wastewater	November	11.11.2020	Ankara	122742	39.8
MET P1-179	Infantis	Group 4	Wastewater	December	09.12.2020	Ankara	123768	39.0

All phage assemblies were annotated by Prokka in two ways. First, genomes were annotated by using default settings (--genus Caudovirales --kingdom viruses). Secondly, phages were annotated by using a closely related and well defined phage genome. For this, related phages were identified by BLASTn, and complete entry of the phages were downloaded as Genbank file from NCBI database (Table 4.9).

Table 4.9 Phage information that were used as template in annotation

Phages used	Scientific Name	Max Score	Total Score	Query Cover	Per. ident	Acc. Len
Group 1	*Salmonella* virus Chi	50752	82919	95%	94.2	59578
Group 2	*Salmonella* phage celemicas	15302	59526	90%	92.08	43193
Group 3	*Salmonella* phage SE8	39515	1.54E+05	89%	95.74	107763
MET P1-137	Escherichia virus VEc33	49046	1.70E+05	89%	94.8	108640
MET P1-179	*Salmonella* phage bux	41142	1.78E+05	88%	97.66	112486
MET P1-82_240k	*Salmonella* phage SPN3US	1.21E+05	3.96E+05	97%	97.19	240413
MET P1-103_31k	Escherichia virus P2	21545	45047	86%	97.34	31200

When the results from both methods compared, annotation by using a closely related genome as template produced a more detailed annotation (Table 4.10). In default annotation most of the coding sequences (CDS) could not be defined, and annotated as hypothetical protein, whereas in close relative annotation functional annotation of proteins were done. All annotations tables were given in Appendix F.

Table 4.10 Annotation of Group 2 phage by using Caudovirales database and close relative

Annotations from different databases			
Gene	length_bp	Close Relative (celemicas)	Caudovirales Database
locus_tag		product	product
BICAFKDG_00001	411	amidase	hypothetical protein
BICAFKDG_00002	282	amidase	hypothetical protein
BICAFKDG_00003	1860	head morphogenesis	hypothetical protein
BICAFKDG_00004	79	tRNA-Ser(tga)	tRNA-Ser(tga)

Table 4.10 continued

BICAFKDG_00005	387	Rz-like spanin	hypothetical protein
BICAFKDG_00006	702	head scaffolding protein	hypothetical protein
BICAFKDG_00007	1050	major head protein	Major capsid protein
BICAFKDG_00008	288	head fiber protein	hypothetical protein
BICAFKDG_00009	351	Hoc-like head decoration	hypothetical protein
BICAFKDG_00010	189	hypothetical protein	hypothetical protein
BICAFKDG_00011	510	head-tail adaptor Ad1	hypothetical protein
BICAFKDG_00012	606	hypothetical protein	hypothetical protein
BICAFKDG_00013	360	tail completion or Neck1 protein	hypothetical protein
BICAFKDG_00014	396	tail completion or Neck1 protein	hypothetical protein
BICAFKDG_00015	420	tail terminator	hypothetical protein
BICAFKDG_00016	1170	minor tail protein	hypothetical protein
BICAFKDG_00017	672	anti-repressor Ant	hypothetical protein
BICAFKDG_00018	231	hypothetical protein	hypothetical protein
BICAFKDG_00019	1155	DNA repair exonuclease	hypothetical protein
BICAFKDG_00020	180	immunity to superinfection	hypothetical protein
BICAFKDG_00021	417	tail assembly chaperone	hypothetical protein
BICAFKDG_00022	360	hypothetical protein	hypothetical protein
BICAFKDG_00023	2334	tail length tape measure protein	hypothetical protein
BICAFKDG_00024	501	virion structural protein	hypothetical protein
BICAFKDG_00025	516	minor tail protein	hypothetical protein
BICAFKDG_00026	366	minor tail protein	hypothetical protein
BICAFKDG_00027	2559	tail protein	hypothetical protein
BICAFKDG_00028	2031	tail spike protein	hypothetical protein
BICAFKDG_00029	162	hypothetical protein	hypothetical protein
BICAFKDG_00030	1389	DNA helicase	hypothetical protein

Table 4.10 continued

BICAFKDG_00031	1023	DNA methyltransferase	hypothetical protein
BICAFKDG_00032	192	hypothetical protein	hypothetical protein
BICAFKDG_00033	288	endonuclease	hypothetical protein
BICAFKDG_00034	132	hypothetical protein	hypothetical protein
BICAFKDG_00035	2202	DNA polymerase	hypothetical protein
BICAFKDG_00036	627	Gp2.5-like ssDNA binding protein and ssDNA annealing protein	hypothetical protein
BICAFKDG_00037	1437	exonuclease	hypothetical protein
BICAFKDG_00038	522	HNH endonuclease	hypothetical protein
BICAFKDG_00039	531	hypothetical protein	hypothetical protein
BICAFKDG_00040	258	hypothetical protein	hypothetical protein
BICAFKDG_00041	219	hypothetical protein	Regulatory protein cro
BICAFKDG_00042	2187	replicative helicase-primase	hypothetical protein
BICAFKDG_00043	234	hypothetical protein	hypothetical protein
BICAFKDG_00044	171	hypothetical protein	hypothetical protein
BICAFKDG_00045	204	hypothetical protein	hypothetical protein
BICAFKDG_00046	114	hypothetical protein	hypothetical protein
BICAFKDG_00047	315	hypothetical protein	hypothetical protein
BICAFKDG_00048	228	hypothetical protein	hypothetical protein
BICAFKDG_00049	372	hypothetical protein	hypothetical protein
BICAFKDG_00050	435	peptidase HslV family protein	hypothetical protein
BICAFKDG_00051	282	holin	hypothetical protein
BICAFKDG_00052	291	holin	hypothetical protein
BICAFKDG_00053	489	endolysin	Endolysin
BICAFKDG_00054	186	hypothetical protein	hypothetical protein
BICAFKDG_00055	156	hypothetical protein	hypothetical protein
BICAFKDG_00056	234	hypothetical protein	hypothetical protein

Table 4.10 continued

BICAFKDG_00057	150	hypothetical protein	hypothetical protein
BICAFKDG_00058	225	hypothetical protein	hypothetical protein
BICAFKDG_00059	300	hypothetical protein	hypothetical protein
BICAFKDG_00060	108	hypothetical protein	hypothetical protein
BICAFKDG_00061	546	terminase	hypothetical protein
BICAFKDG_00062	1272	hypothetical protein	hypothetical protein
BICAFKDG_00063	165	hypothetical protein	hypothetical protein

Annotation results revealed that phage genomes highly dense with CDS (Table 4.11). There were very small gaps between the genes. For example, 38 kbp of 43 kbp phages were annotated. Sixty-three proteins were identified with average product size 603 bp. Similarly, 28 kbp of 31 kbp phage was annotated. There were nearly no gaps between the genes. This was consistent with the literature. Phage genomes were reportedly had small gaps, even small overlaps between the genes. Furthermore, apart from some exceptions, large gaps often mean faulty annotation (Turner et al., 2021). Group 4 phages (MET P1-137 and MET P1-179) had the densest genomes. These genomes had 1.7 genes per 1 kbp on average. Both genomes had over 200 annotated proteins with 500 bp average product length.

Another feature of phage genomes is the presence of tRNA. tRNAs in phage genomes are relatively common. For example, Fong et al. (2019) reported that 36% of the sequenced *Salmonella* phages had at least one tRNA. In another study, Delesalle et al. (2016) investigated *Mycobacterium* phages and found tRNA in 41% of the genomes. In our study, only Group 1 phages lacked tRNA. Group 2 phages had 1 tRNA, and 240 k phage had 2 tRNAs. On the other hand, Group 3 phages had 24 tRNAs, whereas P-137 and P1-179 genomes had 25 and 26 tRNAs, respectively. High number of tRNAs were in agreement with literature for T5 like phages. For example, phage T5 had 24 tRNAs (J. Wang et al., 2005). There is hesitation that presence of tRNAs in the phage genomes might potentially be advantageous to host infection or replication. Therefore, phages

containing tRNAs might not be desirable in biocontrol applications (Fong et al., 2019). However, according to Bailly-Bechet et al. (2007), tRNAs increases phage virulence. In general, number of tRNAs were found in virulent phages were higher than temperate ones. tRNAs in phages allows high translation speed. Although phages rely on host cell for assembly, using their own tRNA might increase their fitness (Bailly-Bechet et al., 2007). In another view, multiple tRNAs in phage genomes might be associated with increased host range. tRNAs might be acquired by phage by recombination events involving more than one bacterial host (Delesalle et al., 2016).

Table 4.11 Basic Structural annotation results

METUID	Host	Groups	Genome Size	CDS	tRNA	Gene Density
MET P1-001_43k	Enteritidis	Group 2	43282	63	1	1.45
MET P1-001_59k	Enteritidis	Group 1	58899	72	-	1.22
MET P1-103_31k	Enteritidis	Group 5	31582	42	-	1.32
MET P1-103_43k	Enteritidis	Group 2	43300	63	1	1.45
MET P1-103_59k	Enteritidis	Group 1	58942	72	-	1.22
MET P1-122_43k	Enteritidis	Group 2	43282	63	1	1.45
MET P1-122_59k	Enteritidis	Group 1	58843	72	-	1.22
MET P1-164_43k	Enteritidis	Group 2	43282	62	1	1.43
MET P1-164_59k	Enteritidis	Group 1	58899	72	-	1.22
MET P1-082_43k	Typhimurium	Group 2	43217	64	1	1.48
MET P1-082_59k	Typhimurium	Group 1	58899	73	-	1.23
MET P1-082_240k	Typhimurium	Group 5	243301	262	2	1.07
MET P1-091_59k	Infantis	Group 1	58899	73	-	1.23
MET P1-091_116k	Infantis	Group 3	116817	172	24	1.47
MET P1-100_59k	Infantis	Group 1	59108	72	-	1.21
MET P1-100_116k	Infantis	Group 3	116826	178	24	1.52
MET P1-116_59k	Infantis	Group 1	58834	72	-	1.22
MET P1-116_116k	Infantis	Group 3	116827	171	24	1.46

Table 4.11 continued

| MET P1-137 | Kentucky | Group 4 | 122746 | 203 | 25 | 1.65 |
| MET P1-179 | Infantis | Group 4 | 122768 | 209 | 26 | 1.70 |

Molecular taxonomy of phages was determined based on BLASTn results (Table 4.12). Phages were compared with the reference phages in NCBI database, and were considered in same genus when they share high DNA identity score (>90%) and protein identities (90%) (Moreno-Switt et al., 2015). As expected, all of the phages were in *Caudovirales* order which includes 96% of all phages (Zinke et al., 2022).

Table 4.12 Molecular Taxonomy of phages

METUID	Host	Group	Order	Family	Subfamily	Genus
MET P1-001_ 43k	Enteritidis	Group 2	*Caudovirales*	*Siphoviridae*	*Guernseyvirinae*	*Jerseyvirus*
MET P1-001_ 59k	Enteritidis	Group 1	*Caudoviricetes*	*Casjensviridae*	-	*Chivirus*
MET P1-103_31k	Enteritidis	Group 5	*Caudovirales*	*Myoviridae*	*Peduovirinae*	*Peduovirus*
MET P1-082_240k	Typhimurium	Group 5	*Caudovirales*	*Myoviridae*	*Myoviridae*	*Seoulvirus*
MET P1-091_116k	Infantis	Group 3	*Caudovirales*	*Demerecviridae*	*Markadamsvirinae*	*Tequintavirus*
MET P1-179	Infantis	Group 4	*Caudovirales*	*Demerecviridae*	*Markadamsvirinae*	*Tequintavirus*
MET P1-137	Kentucky	Group 4	*Caudovirales*	*Demerecviridae*	*Markadamsvirinae*	*Epseptimavirus*

Taxonomic classification further confirmed the host based differences in phages. While Enteritidis and Typhimurium phages were classified under the same subfamilies,

Infantis and Kentucky phages were grouped under same subfamilies. *Siphoviridae* are the most prevalent family of *Caudovirales*, more than half of the phage genomes in NCBI database were belong to *Siphoviridae* family. In our study, Group 1 phages were belonging to *Chivirus* genus from *Casjensviridae* family. This family was created by ICTV in 2021. *Chivirus* was previously classified under *Caudovirales* order and *Siphoviridae* family. Group 2 phages were in *Siphoviridae* family and *Jerseyvirus* genus. Both of these subfamilies were abundant in the environment, shows global presence, and targets Enteritidis and Typhimurium (Ge et al., 2022; Moreno Swith et al., 2013; Phothaworn et al., 2019, 2020). Chi like viruses are identified in 60s, and they have been reported to infect a number of genus including *Salmonella*, *Escherichia* and *Serratia* (Schade et al., 1967). The genome of Chi was sequenced in 2015 (Hendrix et al., 2015). Phage Chi is a flagellotropic phage. Infection starts with binding of phage to flagellar filament, and uses rotation of flagella to reach to cell (Esteves et al., 2021). In addition, two outlier phages from Group 5 were belong to *Myoviridae* family. One the outlier phages (31 kbp) were belong to *Peduovirinae* subfamily, and classified as P2 like virus due to close genomic relatedness. Coliphage P2 is a temperate phage that has been identified in *Escherichia*, *Pseudomonas*, and *Salmonella* (Moreno-Swith et al., 2015). 240 kbp phage was a jumbophage (>200 kbp). Jumbophages are so rare that Yuan and Gao reported less than 100 jumbophages were managed to isolated and classified by 2016 (Yuan & Gao, 2017). Although the number of known jumbo phages has been increased in the last 5 years, they are still very rare compared to other phages. Closest relative of the jumbophage was sequenced by (Lee et al., 2011). Genomic features of that jumbophage (SPN3US) were very similar to ours. It had a genome around 240 kbp with a %48,5 GC content, had two tRNAs and had similar gene density.

Group 3 and 4 phages were identified as *Demerecviridae*. *Demerecviridae* was appointed as a new family by International Committee on Taxonomy of Viruses (ICTV) (Adriaenssens et al., 2020). The members of this family were formerly belong to Siphoviridae (Turner et al., 2021). Three subfamilies were presented in this family, including Markadamsvirinae. The most well-known phage of this group is coliphage T5. T5 has a very similar genomic features to Group 3 and 4 phages. It has 121kb

genome, 24 tRNAs and 39.3% GC content (Adriaenssens et al., 2020). Similar to our phages, T5 has long DTR.

Taxonomy of our phages were also investigated by using Genetic Relationship Applied to Virus Taxonomy (GRAViTy) tool (Turner et al., 2021). A dendogram that contains all dsDNA prokaryotic viruses plus our phages was created (Figure 4.51). In addition, another dendogram, built by orthologous genes of lytic *Salmonella* phages were visualized to see the distribution of our phages (Figure 4.52). Phylogenetic relationship of our phages were given in Appendix G.
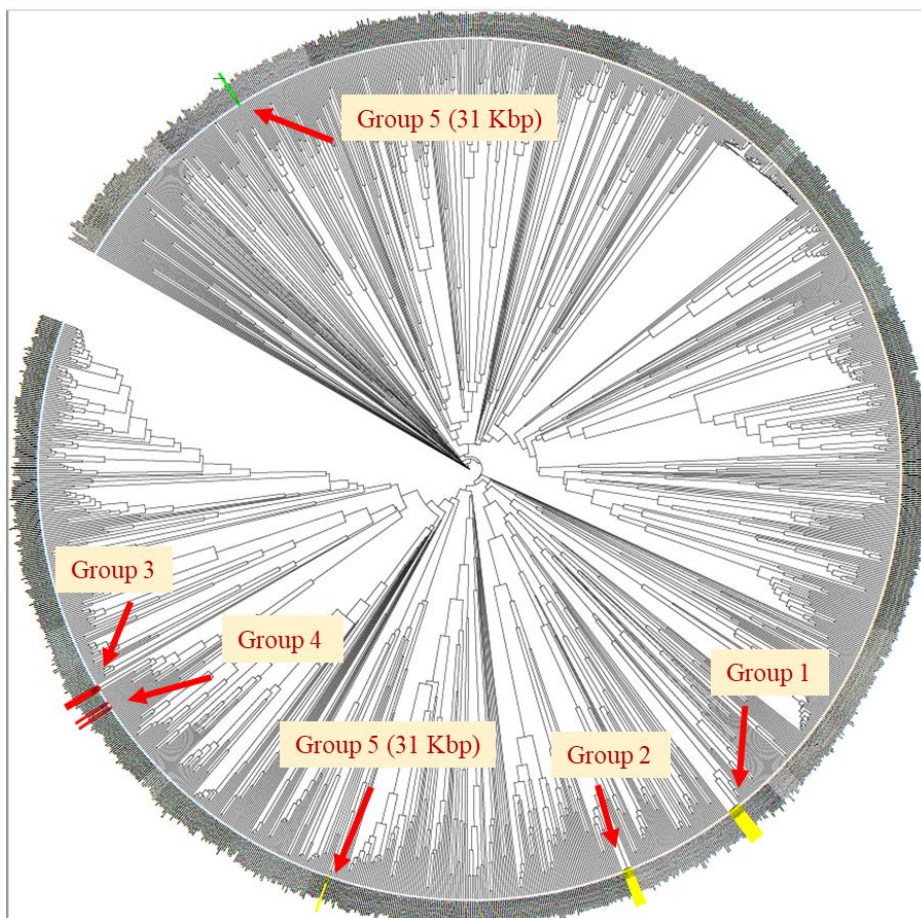
Figure 4.51 Dendogram of all dsDNA bacterial viruses. Dendogram generated by Gravity, and visualized using ITOL.
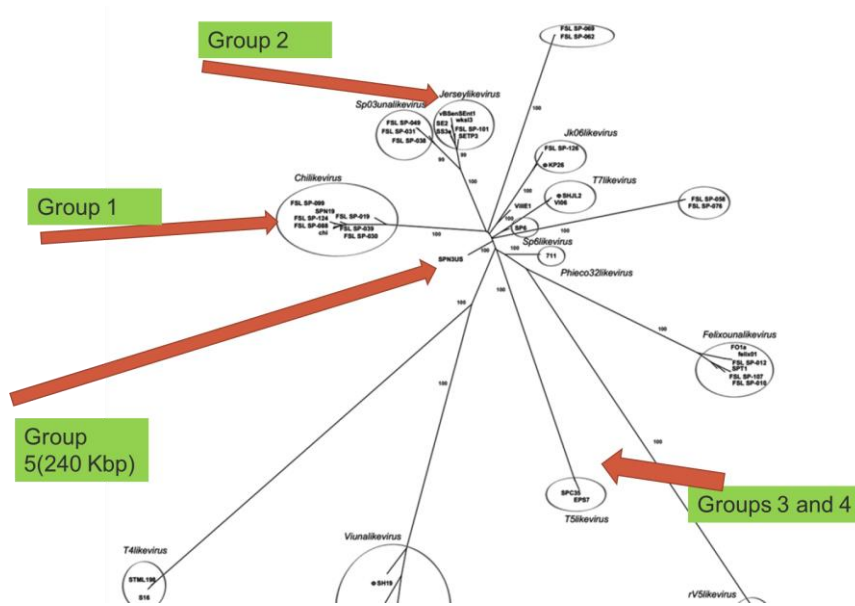
Figure 4.52 Neighbor joining tree based on orthologues genes of lytic *Salmonella* phages. Adapted from (Moreno-Switt et al., 2015).

Horizontal gene transfer is the one of the major drivers of bacterial evolution. Bacteria may acquire genetic materials from environment, other prokaryotes, and even eukaryotes. Transduction is a horizontal gene transfer mechanism, in which genetic material is acquired by bacteria through phage infection (Soucy et al., 2015). Brown-Jaque et al. (2015) stated that up to 20% of bacterial phage has viral origins, which shows the effect of transduction on bacterial evolution. Transduction is also a significant mechanism in the recent spread of antibiotic resistance genes (Hassan et al., 2021). Recent studies showed that *Salmonella* might acquire resistance genes via transduction (Bearson & Brunelle, 2015; Gabashvili et al., 2020). These studies showed the importance of phage genome analysis before biocontrol applications. Therefore, all phages were screened for the presence of AR genes with ResFinder database. None of the phages had AR genes.

In addition to resistance, virulence genes might also be transferred by transduction (Kondo et al., 2020). A striking example was the outbreak strain of *E. coli* O104:H4 which caused more than 3800 cases across the EU. That strain gained stx2a Shiga-toxin encoding gene via transduction (Beutin & Martin, 2012). Similar to antibiotic genes,

virulence factors genes had to be screened. Virulence genes were screened by BLAST. Virulence Factors of Pathogenic Bacteria (VFDB) database was downloaded to our local computer, and genes were queried in BLAST against the phages. There was no virulence gene in our phages. However, there were a number of hypothetical proteins with unknown function in phage annotations. As a result, these hypothetical genes should be evaluated to ensure they are not harmful (Ge et al., 2022).

Lysogenic phages are significantly more associated with transduction compared to lytic phages (L.-C. Fortier & Sekulovic, 2013). For example, a monophasic *S.* Typhimurium strain that is associated with an epidemic had acquired virulence gene *sopE* from a lysogenic phage (Tassinari et al., 2020). As a result, lysogenic phages cannot be used in pathogen biocontrol. Therefore, integrase gene, which is found in temperate phages, was screened in phages. Group 5 31 kbp phage had 2 integrase genes. That phage was most probably existed in host Enteritidis strain (MET S1-001) as a prophage, and contaminated phage solution (MET P1-103) during analyses. The results show that P1-103 couldn't be used before it is completely cleared from contamination. Moreover, the results also indicated the importance of using fully characterized host in phage studies.

4.13   *In vitro* phage application on feed

Efficacy of phages MET P1-001, P1-137, P1-179, and P1-100 were tested on *Salmonella* contaminated feed (Figure 4.54, Figure 4.53, Figure 4.55, Figure 4.56). These phages selected because they had the higher virulence index at 8 log PFU/mL. Each experiment was done separately, and compared to their controls only.
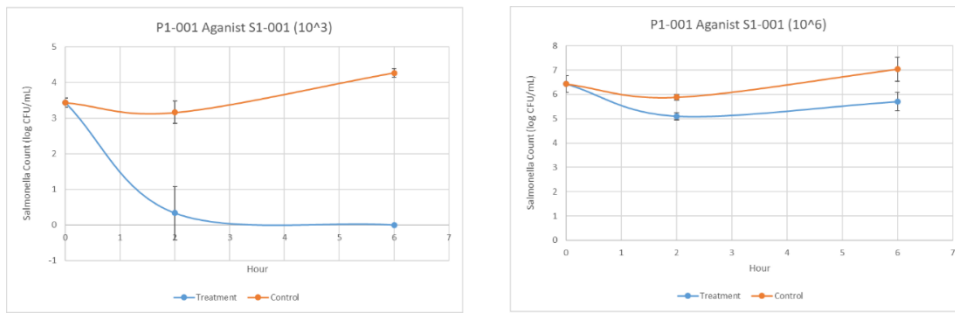
Figure 4.53 *Salmonella* Enteritidis counts on treated and untreated feed samples. Two different initial concentrations; 10^3 (left) and 10^6 (right) were tested.
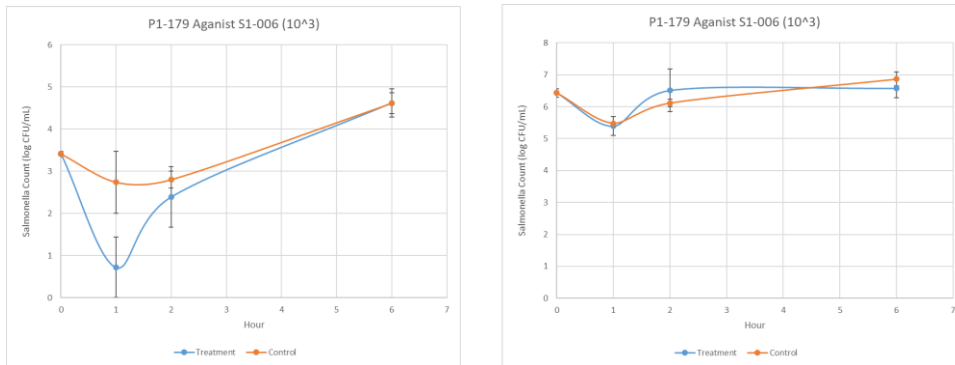
Figure 4.54 *Salmonella* Infantis counts on treated with MET P1-179 and untreated feed samples. Two different initial concentrations; 10^3 (left) and 10^6 (right) were tested.
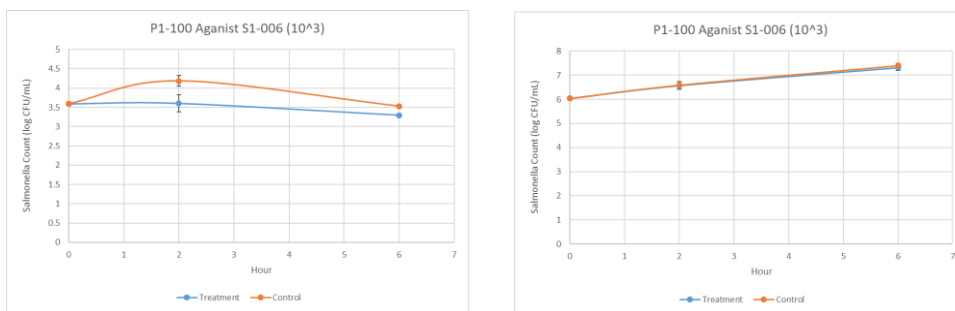
Figure 4.55 *Salmonella* Infantis counts on treated with MET P1-100 and untreated feed samples. Two different initial concentrations; 10^3 (left) and 10^6 (right) were tested.
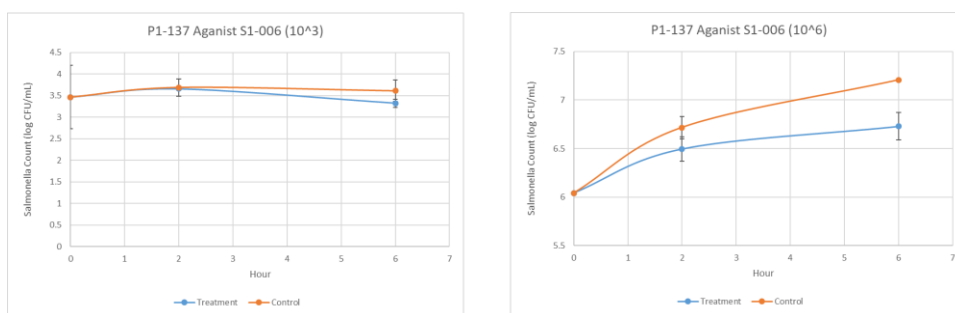
Figure 4.56 *Salmonella* Infantis counts on treated with MET P1-179 and untreated feed samples. Two different initial concentrations; 10^3 (left) and 10^6 (right) were tested.

There was a significant difference between the efficacy of Enteritidis phage and Infantis phages. For Infantis, none of the tested 3 phages exhibited a satisfactory reduction. While significant changes were observed at some data points, they were found inconclusive and unreliable. On the other hand, P1-001 caused huge reductions in Enteritidis populations on feed. At MOI 10^5, P1-001 reduced the Enteritidis populations to undetectable levels after 6 hours of incubation. At MOI 10^2, 1.3 log reduction was observed in Enteritidis population after 6 hours. Both of the reductions were significant ($p<0.05$).

Table 4.13 Phage application results at 2 and 6-hour incubation for different phages

Phage	*Salmonella* initial dose (log CFU/mL)	Incubation time (h)	Treated	Untreated
MET P1-179	3.409771968	2	2.38907563[a]	2.80103[a]
		6	4.61610897[a]	4.60953[a]
	6.43461586	2	6.51436482[a]	6.115224[a]
		6	6.58070951[a]	6.870732[a]
MET P1-137	3.464607252	2	3.65729596[a]	3.68842[a]
		6	3.32179437[a]	3.61066[a]
	6.041392685	2	6.49631774[a]	6.717284[a]
		6	6.73019331[b]	7.206826[a]
MET P1-100	3.59285605	2	3.60373065[b]	4.184691[a]
		6	3.29327745[b]	3.531479[a]
	6.041392685	2	6.56951592[a]	6.590922[a]
		6	7.3104734[a]	7.401113[a]
MET P1-001	3.43461586	2	3.16111[a]	0.33333333[b]
		6	4.267647[a]	0[b]
	6.428666248	2	5.889076[a]	5.10034333[b]
		6	7.040625[a]	5.69968006[b]

These results were in agreement with phenotypic characteristics such as latent period and burst size and adsorption. P1-001 had shorter latent period, higher burst size and better adsorption rates than the rest of tested phages. On the other hand, these results contradicted with planktonic killing assay. In that experiment, P1-100, P1-137, and P1-179 were found to have higher virulence index than P1-001 at 8 log PFU/mL level. The difference between these experiments might be associated with the difference in matrix. Feed is much more complex environment than media, and it might have affected the performance of phages and bacteria.

Limited number of reports are available in the literature concerning the in vitro application of phages in feed. Andreatti Filho et al. (2007) treated *Salmonella* Enteritidis contaminated feed with a monophage at different titers. In that study, two initial Enteritidis concentration (10^3 and 10^6 CFU/mL) were used. Feed were incubated for 6 hours after the application of phage at 8 log PFU/mL. *Salmonella* counts in phage treated feeds were 1.3 log CFU/mL lower than the untreated control for 10^3 initial dose. For, 10^6 initial dose, the reduction after incubation was only 0.4 log CFU/mL, and was not found significant (Andreatti Filho et al., 2007).

In another study, a phage cocktail was applied in vitro to reduce *Salmonella* Enteritidis population in feed (Wójcik et al., 2020). In that study, 10^7 PFU/mL phage cocktail was applied in two ways, spray and immersion, to feed contaminated with 10^3 CFU/mL *Salmonella* Enteritidis. After 6 hours of incubation, *Salmonella* counts of treated and untreated feed were compared. At room temperature, phage cocktail caused 0.7 log reduction, whereas at 37 °C the reduction was increased to 1 log. There was no difference between the application methods. The phage cocktail in that study was consisting of 4 phages (Wójcik et al., 2020). Interestingly, all of the phages were from same genus with our phages (Tequintavirus and Jerseyvirus). In fact, our Enteritidis phages is a member of Jerseyvirus genus as well.

CHAPTER 5

CONCLUSION

Salmonella contamination may occur throughout the food chain. Biocontrol of *Salmonella* from pre-harvest to retail level is essential for food safety. For each step, different actions may be used such as heat treatment, antibiotics, and surface decontaminants. However, each treatment comes with a cost. Misuse and overuse of antibiotics in medicine and veterinary caused a serious "superbug" problem which cannot be treated by first line of antibiotics. Furthermore, *Salmonella* serotypes show variation between regions and products.

Phages offer an alternative food safety method which can be used in different steps of food production steps. Phages have a number benefits compared to traditional biocontrol methods. However, certain requirements must be met before the utilization of phages. These requirements include the genomic and phenotypic features of phages as well as their interaction with target organism.

In this study, 12 *Salmonella* strains and 68 *Salmonella* phages were isolated from different regions in Turkey. *Salmonella* positive samples were higher than the EU average. Serotypes of 9 *Salmonella* isolates were also determined by PFGE. 5 of the isolates were either belonged to Kentucky or Infantis serotypes. Genomic characterization showed that isolates showed serotype based clustering. Antibiotic resistance profiles of the isolates were determined. 66% of the isolates were multi drug resistant. In addition, plasmid mediated fluoroquinolone genes were found in one isolate, which confers resistance against a clinically important antibiotic, ciprofloxacin.

46 Enteritidis, 27 Typhimurium, 11 Infantis, 3 Kentucky, 3 Hadar, 2 Anatum, 2 Telaviv, and 1 Montevideo phage was isolated from poultry and cattle farms as well as wastewater facility in 11-month span. All phages were purified and stored in triplicate. Each phage was tested against 36 hosts from 18 serotype to determine their lysis profile.

Majority of the phages show a board host range (>10 host). In general, Typhimurium and Enteritidis strains were infected by same phages, were as those phages were ineffective against Infantis. Some *Salmonella* strains (i.e. Hadar, Braenderup, Mbandaka, Liverpool) were highly resistant against phages. Phages and hosts were clustered based on the interactions. Based on their host interactions, 5 Enteritidis-Typhimurium, 4 Infantis, and 1 Kentucky phage were selected for further characterization.

Phenotypic characterization of selected phages was done. MET P1-001 (Enteritidis) had the shortest latent period and highest burst size among the phages. Anatum phage had the second best burst size-latent period combination. Infantis phages had lower burst size and longer latent period than other phages. Similar results were observed in adsorption rates. Infantis phages had the worst free phage % after 10-minute adsorption whereas Hadar phage was the best.

Phage genome sizes were determined with PFGE. 19 phages produced bands between 30 kbp to 240 kbp. In some samples, two bands were observed. These bands might be resulted due to contamination of another phage. Morphology of the phages was investigated by TEM. Different measurements and different morphologies were observed in phage lysates. Majority of the phages showed *Siphoviridae* morphology while a number of phages were *Myoviridae* like morphology.

Whole genome sequencing is the current gold standard for characterization of phages. Genomes of 10 phages were sequenced. In 8 samples, multiple phage genomes were present. However, these phages couldn't be differentiated by plaque morphology. All genomes were assembled and annotated. Also taxonomy of genomes was determined in molecular level. In all Enteritidis phages, there were one Chivirus-like and one Jerseyvirus-like genome. In addition, in P1-103 there was a prophage resembling Coliphage P2. Furthermore, in P1-082 there was a jumbophage with 240 kbp genome. In 3 Infantis phages there were a Chi-like virus and a T5 like virus genome. Two samples had monophage genomes. Genome sizes of phages were in agreement with PFGE. None of the phage genomes carried a virulence or antibiotic resistance gene.

Dynamic relationship between the phage and host were investigated with bacterial reduction curve. Enteritidis phages were successfully inhibited bacterial growth for 4 to 6 hours even in low concentrations. Similar effect observed in Infantis phages only at high titers. Virulence index of phages were determined based on their reduction curve. Among Enteritidis phages P1-082 had the highest virulence index at 8 log PFU/mL level whereas 164 had the lowest. On the other hand, P1-137 had the highest virulence index among all tested phages. All phages were found effective against their host.

Several phages were tested against their hosts in feed matrix. 10^3 and 10^6 CFU/ mL *Salmonella* Enteritidis and Infantis were inoculated into separate, sterile feeds, and incubated 6 hours after 8 log PFU/ mL phage application. P1-001 reduced Enteritidis populations significantly at both contamination levels. However, Infantis phages were ineffective. The results might be explained with the poor latent period and burst size combination of Infantis phages.

All in all, our study documented a wide range of phages and their interaction with different *Salmonella* strains. Furthermore, phenotypical and genomic features of a number of phages were documented. Some of those phages have already been utilized in different commercial phage cocktails. In this study, we identify and characterize phages with commercialization potential.

Further characterization of phages is required before commercialization. Their efficacy in different food matrices or food contact surfaces should be tested. In addition, preparation of a cocktail consisting of these phages would be necessary to increase the host range.

REFERENCES

Abdelsattar, A. S., Dawooud, A., Rezk, N., Makky, S., Safwat, A., Richards, P. J., & El-Shibiny, A. (2021). How to Train Your Phage: The Recent Efforts in Phage Training. *Biologics*, *1*(2), 70–88.

Abdelsattar, A. S., Safwat, A., Nofal, R., Elsayed, A., Makky, S., & El-Shibiny, A. (2021). Isolation and Characterization of Bacteriophage ZCSE6 against Salmonella spp.: Phage Application in Milk. *Biologics*, *1*(2), 164–176. https://doi.org/10.3390/biologics1020010

Abedon, S. T., & Yin, J. (2009). Bacteriophage plaques: theory and analysis. In *Bacteriophages* (pp. 161–174). Springer.

Abhisingha, M., Dumnil, J., & Pitaksutheepong, C. (2020). Efficiency of phage cocktail to reduce Salmonella Typhimurium on chicken meat during low temperature storage. *Lwt*, *129*(March), 109580. https://doi.org/10.1016/j.lwt.2020.109580

Abràmoff, M. D., Magalhães, P. J., & Ram, S. J. (2004). Image processing with ImageJ. *Biophotonics International*, *11*(7), 36–42.

Acar, S., Bulut, E., Durul, B., Uner, I., Kur, M., Avsaroglu, M. D., Kirmaci, H. A., Tel, Y. O., Zeyrek, F. Y., & Soyer, Y. (2017). Phenotyping and genetic characterization of Salmonella enterica isolates from Turkey revealing arise of different features specific to geography. *International Journal of Food Microbiology*, *241*, 98–107. https://doi.org/10.1016/j.ijfoodmicro.2016.09.031

Ackermann, H.-W. (2007). Salmonella phages examined in the electron microscope. In *Salmonella* (pp. 213–234). Springer.

Ackermann, H.-W. (2009). Basic phage electron microscopy. In *Bacteriophages* (pp. 113–126). Springer.

Ackermann, H. W. (2011). Bacteriophage taxonomy. *Microbiology Australia*, *32*(2), 90–94.

Adriaenssens, E. M., Sullivan, M. B., Knezevic, P., van Zyl, L. J., Sarkar, B. L., Dutilh, B. E., Alfenas-Zerbini, P., Łobocka, M., Tong, Y., & Brister, J. R. (2020). Taxonomy of prokaryotic viruses: 2018-2019 update from the ICTV Bacterial and Archaeal Viruses Subcommittee. *Archives of Virology*, *165*(5), 1253–1260.

Aiewsakun, P., & Simmonds, P. (2018). The genomic underpinnings of eukaryotic virus taxonomy: Creating a sequence-based framework for family-level virus classification. *Microbiome*, *6*(1), 1–24. https://doi.org/10.1186/s40168-018-0422-7

Akhtar, M., Viazis, S., & Diez-Gonzalez, F. (2014). Isolation, identification and characterization of lytic, wide host range bacteriophages from waste effluents against Salmonella enterica serovars. *Food Control*, *38*(1), 67–74. https://doi.org/10.1016/j.foodcont.2013.09.064

Alcaine, S. D., Warnick, L. D., & Wiedmann, M. (2007). Antimicrobial resistance in nontyphoidal Salmonella. *Journal of Food Protection*, *70*(3), 780–790. https://doi.org/10.4315/0362-028X-70.3.780

Altamirano, F. L. G., Kostoulias, X., Subedi, D., Korneev, D., & Peleg, A. Y. (2022). Articles Phage-antibiotic combination is a superior treatment against Acinetobacter baumannii in a preclinical study. *EBioMedicine*, *80*, 104045. https://doi.org/10.1016/j.ebiom.2022.104045

Andreatti Filho, R. L., Higgins, J. P., Higgins, S. E., Gaona, G., Wolfenden, A. D., Tellez, G., & Hargis, B. M. (2007). Ability of bacteriophages isolated from different sources to reduce Salmonella enterica serovar Enteritidis in vitro and in vivo. *Poultry Science*, *86*(9), 1904–1909. https://doi.org/10.1093/ps/86.9.1904

Antunes, P., Mourão, J., Campos, J., & Peixe, L. (2016). Salmonellosis: The role of poultry meat. In *Clinical Microbiology and Infection* (Vol. 22, Issue 2, pp. 110–121). Elsevier B.V. https://doi.org/10.1016/j.cmi.2015.12.004

Arkali, A., & Çetinkaya, B. (2020). Molecular identification and antibiotic resistance profiling of Salmonella species isolated from chickens in eastern Turkey. *BMC Veterinary Research*, *16*(1), 1–8.

Arnold, B. J., Huang, I., & Hanage, W. P. (2021). Horizontal gene transfer and adaptive evolution in bacteria. *Nature Reviews Microbiology*, 1–13.

ASSESSMENT, J. E.-E. R. O. (2021). *Multi-country outbreak of Salmonella Braenderup ST22, presumed to be linked to imported melons*.

Atterbury, Robert J, Van Bergen, M. A. P., Ortiz, F., Lovell, M. A., Harris, J. A., De Boer, A., Wagenaar, J. A., Allen, V. M., & Barrow, P. A. (2007). Bacteriophage therapy to reduce Salmonella colonization of broiler chickens. *Applied and Environmental Microbiology*, *73*(14), 4543–4549.

Atterbury, Robert Joseph, Gigante, A. M., Lozano, M. de la S. R., Medina, R. D. M., Robinson, G., Alloush, H., Barrow, P. A., & Allen, V. M. (2020). Reduction of Salmonella contamination on the surface of chicken skin using bacteriophage. *Virology Journal*, *17*(1), 1–8.

Aziz, R. K., Edwards, R. A., Taylor, W. W., Low, D. E., McGeer, A., & Kotb, M. (2005). Mosaic prophages with horizontally acquired genes account for the emergence and diversification of the globally disseminated M1T1 clone of Streptococcus pyogenes. *Journal of Bacteriology*, *187*(10), 3311–3318.

Baggesen, D. L., Sørensen, G., Nielsen, E. M., & Wegener, H. C. (2010). Phage typing of Salmonella Typhimurium–is it still a useful tool for surveillance and outbreak investigation? *Eurosurveillance*, *15*(4), 19471.

Bailly-Bechet, M., Vergassola, M., & Rocha, E. (2007). Causes for the intriguing presence of tRNAs in phages. *Genome Research*, *17*(10), 1486–1495. https://doi.org/10.1101/gr.6649807

Bankevich, A., Nurk, S., Antipov, D., Gurevich, A. A., Dvorkin, M., Kulikov, A. S., Lesin, V. M., Nikolenko, S. I., Pham, S., & Prjibelski, A. D. (2012). SPAdes: a

new genome assembly algorithm and its applications to single-cell sequencing. *Journal of Computational Biology*, *19*(5), 455–477.

Bao, H., Zhang, P., Zhang, H., Zhou, Y., Zhang, L., & Wang, R. (2015). Bio-control of Salmonella Enteritidis in foods using bacteriophages. *Viruses*, *7*(8), 4836–4853.

Baquero, F., Alvarez-Ortega, C., & Martinez, J. L. (2009). Ecology and evolution of antibiotic resistance. *Environmental Microbiology Reports*, *1*(6), 469–476.

Bardina, C., Spricigo, D. A., Cortés, P., & Llagostera, M. (2012). Significance of the bacteriophage treatment schedule in reducing Salmonella colonization of poultry. *Applied and Environmental Microbiology*, *78*(18), 6600–6607.

Barroug, S., Chaple, S., & Bourke, P. (2021). Combination of Natural Compounds With Novel Non-thermal Technologies for Poultry Products: A Review. *Frontiers in Nutrition*, *8*.

Bearson, B. L., & Brunelle, B. W. (2015). Fluoroquinolone induction of phage-mediated gene transfer in multidrug-resistant Salmonella. *International Journal of Antimicrobial Agents*, *46*(2), 201–204.

Bertozzi Silva, J., Storms, Z., & Sauvageau, D. (2016). Host receptors for bacteriophage adsorption. *FEMS Microbiology Letters*, *363*(4), fnw002.

Beutin, L., & Martin, A. (2012). Outbreak of Shiga toxin–producing Escherichia coli (STEC) O104: H4 infection in Germany causes a paradigm shift with regard to human pathogenicity of STEC strains. *Journal of Food Protection*, *75*(2), 408–418.

Bjork, K. E., Kopral, C. A., Wagner, B. A., & Dargatz, D. A. (2015). Comparison of mixed effects models of antimicrobial resistance metrics of livestock and poultry Salmonella isolates from a national monitoring system. *Preventive Veterinary Medicine*, *122*(3), 265–272.

Bolger, A. M., Lohse, M., & Usadel, B. (2014). Trimmomatic: a flexible trimmer for Illumina sequence data. *Bioinformatics*, *30*(15), 2114–2120.

Bonilla, N., Rojas, M. I., Cruz, G. N. F., Hung, S. H., Rohwer, F., & Barr, J. J. (2016). Phage on tap-a quick and efficient protocol for the preparation of bacteriophage laboratory stocks. *PeerJ*, *2016*(7). https://doi.org/10.7717/peerj.2261

Borie, C., Albala, I., Sánchez, P., Sánchez, M. L., Ramírez, S., Navarro, C., Morales, M. A., Retamales, J., & Robeson, J. (2008). Bacteriophage treatment reduces Salmonella colonization of infected chickens. *Avian Diseases*, *52*(1), 64–67.

Bortolaia, V., Kaas, R. S., Ruppe, E., Roberts, M. C., Schwarz, S., Cattoir, V., Philippon, A., Allesoe, R. L., Rebelo, A. R., & Florensa, A. F. (2020). ResFinder 4.0 for predictions of phenotypes from genotypes. *Journal of Antimicrobial Chemotherapy*, *75*(12), 3491–3500.

Boudreaux, D. P., & Srinivasan, V. R. (1981). Bacteriophage-induced Sporulation in Bacillus cereus T. *Microbiology*, *126*(2), 459–462.

Brady, A., Felipe-Ruiz, A., Gallego del Sol, F., Marina, A., Quiles-Puchalt, N., & Penadés, J. R. (2021). Molecular Basis of Lysis–Lysogeny Decisions in Gram-Positive Phages. *Annual Review of Microbiology*, *75*, 563–581.

Brown-Jaque, M., Calero-Cáceres, W., & Muniesa, M. (2015). Transfer of antibiotic-resistance genes via phage-related mobile elements. *Plasmid*, *79*, 1–7.

Brüssow, H., Canchaya, C., & Hardt, W.-D. (2004). Phages and the evolution of bacterial pathogens: from genomic rearrangements to lysogenic conversion. *Microbiology and Molecular Biology Reviews*, *68*(3), 560–602.

Bushnell, B., Egan, R., Copeland, A., Foster, B., Clum, A., & Sun, H. (2019). BBMap: a fast, accurate, splice-aware aligner. 2014. *Available at: Sourceforge. Net/Projects/Bbmap*.

Callow, B. R. (1959). A new phage-typing scheme for Salmonella typhi-murium. *Epidemiology & Infection*, *57*(3), 346–359.

Canchaya, C., Proux, C., Fournous, G., Bruttin, A., & Brüssow, H. (2003). Prophage genomics. *Microbiology and Molecular Biology Reviews*, *67*(2), 238–276.

Carroll, L. M., Wiedmann, M., den Bakker, H., Siler, J., Warchocki, S., Kent, D., Lyalina, S., Davis, M., Sischo, W., & Besser, T. (2017). Whole-genome sequencing of drug-resistant Salmonella enterica isolates from dairy cattle and humans in New York and Washington states reveals source and geographic associations. *Applied and Environmental Microbiology*, *83*(12), e00140-17.

Chan, B. K., Abedon, S. T., & Loc-Carrillo, C. (2013). Phage cocktails and the future of phage therapy. *Future Microbiology*, *8*(6), 769–783.

Chan, K., Baker, S., Kim, C. C., Detweiler, C. S., Dougan, G., & Falkow, S. (2003). Genomic comparison of Salmonella enterica serovars and Salmonella bongori by use of an S. enterica serovar Typhimurium DNA microarray. *Journal of Bacteriology*, *185*(2), 553–563.

Chen, Z., Sun, L., Zhang, Z., Fokine, A., Padilla-Sanchez, V., Hanein, D., Jiang, W., Rossmann, M. G., & Rao, V. B. (2017). Cryo-EM structure of the bacteriophage T4 isometric head at 3.3-Å resolution and its relevance to the assembly of icosahedral viruses. *Proceedings of the National Academy of Sciences*, *114*(39), E8184–E8193.

Chevallereau, A., Pons, B. J., van Houte, S., & Westra, E. R. (2022). Interactions between bacterial and phage communities in natural environments. *Nature Reviews Microbiology*, *20*(1), 49–62.

Chibeu, A., Ceyssens, P.-J., Hertveldt, K., Volckaert, G., Cornelis, P., Matthijs, S., & Lavigne, R. (2009). The adsorption of Pseudomonas aeruginosa bacteriophage φKMV is dependent on expression regulation of type IV pili genes. *FEMS Microbiology Letters*, *296*(2), 210–218.

Choi, Y., Shin, H., Lee, J.-H., & Ryu, S. (2013). Identification and characterization of a novel flagellum-dependent Salmonella-infecting bacteriophage, iEPS5. *Applied and Environmental Microbiology*, *79*(16), 4829–4837.

Clavijo, V., Baquero, D., Hernandez, S., Farfan, J. C., Arias, J., Arévalo, A., Donado-Godoy, P., & Vives-Flores, M. (2019). Phage cocktail SalmoFREE® reduces

Salmonella on a commercial broiler farm. *Poultry Science*, *98*(10), 5054–5063.

Clokie, M. R., Kropinski, A. M., & Lavigne, R. (2018). Bacteriophages, Methods and Protocols Volume III. In *Methods in Molecular Biology* (Vol. 1681). http://www.springer.com/series/7651

Cobbold, R. N., Rice, D. H., Davis, M. A., Besser, T. E., & Hancock, D. D. (2006). Long-term persistence of multi–drug-resistant Salmonella enterica serovar Newport in two dairy herds. *Journal of the American Veterinary Medical Association*, *228*(4), 585–591.

Committee, I. C. on T. of V. E. (2020). The new scope of virus taxonomy: partitioning the virosphere into 15 hierarchical ranks. *Nature Microbiology*, *5*(5), 668.

Committee, T. E., Testing, A. S., Changes, N., & Pseudomonas, E. (2015). European Committee on Antimicrobial Susceptibility Testing Breakpoint tables for interpretation of MICs and zone diameters European Committee on Antimicrobial Susceptibility Testing Breakpoint tables for interpretation of MICs and zone diameters. *Http://Www.Eucast.Org/Fileadmin/Src/Media/PDFs/EUCAST_files/Breakpoint_tables/V_5.0_Breakpoint_Table_01.Pdf*, 0–77. http://www.eucast.org/fileadmin/src/media/PDFs/EUCAST_files/Breakpoint_tables/v_5.0_Breakpoint_Table_01.pdf

Cook, R., Brown, N., Redgwell, T., Rihtman, B., Barnes, M., Clokie, M., Stekel, D. J., Hobman, J., Jones, M. A., & Millard, A. (2021). INfrastructure for a PHAge REference Database: Identification of Large-Scale Biases in the Current Collection of Cultured Phage Genomes. *PHAGE*, *2*(4), 214–223.

Cooke, F. J., Wain, J., Fookes, M., Ivens, A., Thomson, N., Brown, D. J., Threlfall, E. J., Gunn, G., Foster, G., & Dougan, G. (2007). Prophage sequences defining hot spots of genome variation in Salmonella enterica serovar Typhimurium can be used to discriminate between field isolates. *Journal of Clinical Microbiology*, *45*(8), 2590–2598.

Crabb, H. K., Allen, J. L., Devlin, J. M., Firestone, S. M., Stevenson, M., Wilks, C. R., & Gilkerson, J. R. (2019). Traditional Salmonella Typhimurium typing tools (phage typing and MLVA) are sufficient to resolve well-defined outbreak events only. *Food Microbiology*, *84*, 103237.

Delesalle, V. A., Tanke, N. T., Vill, A. C., & Krukonis, G. P. (2016). Testing hypotheses for the presence of tRNA genes in mycobacteriophage genomes. *Bacteriophage*, *6*(3), e1219441. https://doi.org/10.1080/21597081.2016.1219441

Diaz-Munoz, S. L. (2017). Viral coinfection is shaped by host ecology and virus–virus interactions across diverse microbial taxa and environments. *Virus Evolution*, *3*(1).

Dibner, J. J., & Richards, J. D. (2005). Antibiotic growth promoters in agriculture: history and mode of action. *Poultry Science*, *84*(4), 634–643.

Dion, M. B., Oechslin, F., & Moineau, S. (2020). Phage diversity, genomics and phylogeny. *Nature Reviews Microbiology*, *18*(3), 125–138. https://doi.org/10.1038/s41579-019-0311-5

Dowah, A. S. A., & Clokie, M. R. J. (2018). Review of the nature, diversity and structure of bacteriophage receptor binding proteins that target Gram-positive bacteria. *Biophysical Reviews*, *10*(2), 535–542.

Drulis-Kawa, Z., Majkowska-Skrobek, G., Maciejewska, B., Delattre, A.-S., & Lavigne, R. (2012). Learning from bacteriophages-advantages and limitations of phage and phage-encoded protein applications. *Current Protein and Peptide Science*, *13*(8), 699–722.

Duc, H. M., Son, H. M., Honjoh, K., & Miyamoto, T. (2018). Isolation and application of bacteriophages to reduce Salmonella contamination in raw chicken meat. *Lwt*, *91*, 353–360.

Durul, B., Acar, S., Bulut, E., Kyere, E. O., & Soyer, Y. (2015). Subtyping of Salmonella food isolates suggests the geographic clustering of serotype Telaviv. *Foodborne Pathogens and Disease*, *12*(12), 958–965.

El-Shibiny, A., & El-Sahhar, S. (2017). Bacteriophages: the possible solution to treat infections caused by pathogenic bacteria. *Canadian Journal of Microbiology*, *63*(11), 865–879.

Esteves, N. C., Porwollik, S., McClelland, M., & Scharf, B. E. (2021). The Multidrug Efflux System AcrABZ-TolC Is Essential for Infection of Salmonella Typhimurium by the Flagellum-Dependent Bacteriophage Chi. *Journal of Virology*, *95*(11), e00394-21.

European Food Safety Authority,, E. C. for D. P. and C. (2021). The European Union One Health 2020 Zoonoses Report. *EFSA Journal*, *19*(12), e06971.

European Food Safety Authority (2021). The European Union one health 2019 zoonoses report. *Efsa Journal*, *19*(2).

Farris, J. S. (1972). Estimating phylogenetic trees from distance matrices. *The American Naturalist*, *106*(951), 645–668.

Ferrari, R. G., Rosario, D. K. A., Cunha-Neto, A., Mano, S. B., Figueiredo, E. E. S., & Conte-Juniora, C. A. (2019). Worldwide epidemiology of Salmonella serovars in animal-based foods: A meta-analysis. *Applied and Environmental Microbiology*, *85*(14), 1–21. https://doi.org/10.1128/AEM.00591-19

Fiorentin, L., Vieira, N. D., & Barioni Jr, W. (2005). Oral treatment with bacteriophages reduces the concentration of Salmonella Enteritidis PT4 in caecal contents of broilers. *Avian Pathology*, *34*(3), 258–263.

Fong, K., LaBossiere, B., Switt, A. I. M., Delaquis, P., Goodridge, L., Levesque, R. C., Danyluk, M. D., & Wang, S. (2017). Characterization of four novel bacteriophages isolated from British Columbia for control of non-typhoidal Salmonella in vitro and on sprouting alfalfa seeds. *Frontiers in Microbiology*, *8*(11), 1–14. https://doi.org/10.3389/fmicb.2017.02193

Fong, K., Tremblay, D. M., Delaquis, P., Goodridge, L., Levesque, R. C., Moineau, S., Suttle, C. A., & Wang, S. (2019). Diversity and host specificity revealed by

biological characterization and whole genome sequencing of bacteriophages infecting Salmonella enterica. *Viruses*, *11*(9), 854. https://doi.org/10.3390/v11090854

Fortier, L.-C., & Sekulovic, O. (2013). Importance of prophages to evolution and virulence of bacterial pathogens. *Virulence*, *4*(5), 354–365.

Fortier, L. C., & Moineau, S. (2009). Phage production and maintenance of stocks, including expected stock lifetimes. *Methods in Molecular Biology (Clifton, N.J.)*, *501*, 203–219. https://doi.org/10.1007/978-1-60327-164-6_19

Gabashvili, E., Osepashvili, M., Koulouris, S., Ujmajuridze, L., Tskhitishvili, Z., & Kotetishvili, M. (2020). Phage transduction is involved in the intergeneric spread of antibiotic resistance-associated blaCTX-M, mel, and tetM Loci in natural populations of some human and animal bacterial pathogens. *Current Microbiology*, *77*(2), 185–193.

Gallet, R., Kannoly, S., & Wang, I.-N. (2011). Effects of bacteriophage traits on plaque formation. *BMC Microbiology*, *11*(1), 1–16.

Gao, R., Naushad, S., Moineau, S., Levesque, R., Goodridge, L., & Ogunremi, D. (2020). Comparative genomic analysis of 142 bacteriophages infecting Salmonella enterica subsp. enterica. *BMC Genomics*, *21*(1), 1–13.

Garcia, J. S., Gast, R. K., Guard, J. Y., Karcher, D. M., & Jones, D. (2022). Tissue Colonization and Egg and Environmental Contamination Associated with the Experimental Infection of Cage-Free Laying Hens with Salmonella Braenderup. *Avian Diseases*, *66*(1), 74–78.

Garneau, J. R., Depardieu, F., Fortier, L.-C., Bikard, D., & Monot, M. (2017). PhageTerm: a tool for fast and accurate determination of phage termini and packaging mechanism using next-generation sequencing data. *Scientific Reports*, *7*(1), 1–10.

Gaul, S. B., Wedel, S., Erdman, M. M., Harris, D. L. H., Harris, I. T., Ferris, K. E., &

Hoffman, L. J. (2007). Identification of Swine Salmonella serotypes using pulsed-field gel electrophoresis of conserved Xba1 fragments. *Iowa State University Animal Industry Report*, *4*(1).

Ge, H., Lin, C., Xu, Y., Hu, M., Xu, Z., Geng, S., & Chen, X. (2022). A phage for the controlling of Salmonella in poultry and reducing biofilms. *Veterinary Microbiology*, 109432.

Genel, K. (2018). *ULUSAL SALMONELLA KONTROL PROGRAMI Gıda ve Kontrol Genel Müdürlüğü-2018*.

Golomidova, A. K., Kulikov, E. E., Prokhorov, N. S., Guerrero-Ferreira, R. C., Knirel, Y. A., Kostryukova, E. S., Tarasyan, K. K., & Letarov, A. V. (2016). Branched lateral tail fiber organization in T5-like bacteriophages DT57C and DT571/2 is revealed by genetic and functional analysis. *Viruses*, *8*(1), 26.

Gossner, C. M., Hello, S. Le, Jong, B. De, Rolfhamre, P., Faensen, D., Weill, F., & Giesecke, J. (2016). *Around the World in 1,475*. *22*(7).

Greer, G. G. (2005). Bacteriophage control of foodborne bacteria. *Journal of Food Protection*, *68*(5), 1102–1111.

Gurevich, A., Saveliev, V., Vyahhi, N., & Tesler, G. (2013). QUAST: quality assessment tool for genome assemblies. *Bioinformatics*, *29*(8), 1072–1075.

Hagens, S., & Loessner, M. J. (2010). Bacteriophage for biocontrol of foodborne pathogens: calculations and considerations. *Current Pharmaceutical Biotechnology*, *11*(1), 58–68.

Haines, M. E. K., Hodges, F. E., Nale, J. Y., Mahony, J., Van Sinderen, D., Kaczorowska, J., Alrashid, B., Akter, M., Brown, N., & Sauvageau, D. (2021). Analysis of selection methods to develop novel phage therapy cocktails against antimicrobial resistant clinical isolates of bacteria. *Frontiers in Microbiology*, *12*, 564.

Haines, M. E. K., Hodges, F. E., Nale, J. Y., Mahony, J., van Sinderen, D.,

Kaczorowska, J., Alrashid, B., Akter, M., Brown, N., Sauvageau, D., Sicheritz-Pontén, T., Thanki, A. M., Millard, A. D., Galyov, E. E., & Clokie, M. R. J. (2021). Analysis of Selection Methods to Develop Novel Phage Therapy Cocktails Against Antimicrobial Resistant Clinical Isolates of Bacteria. *Frontiers in Microbiology*, *12*(March), 1–15. https://doi.org/10.3389/fmicb.2021.613529

Han, S., Byun, K.-H., Mizan, M. F. R., Kang, I., & Ha, S.-D. (2022). Bacteriophage and their lysins: A new era of biocontrol for inactivation of pathogenic bacteria in poultry processing and production—A review. *Food Control*, 108976.

Harada, L. K., Silva, E. C., Campos, W. F., Del Fiol, F. S., Vila, M., Dąbrowska, K., Krylov, V. N., & Balcão, V. M. (2018). Biotechnological applications of bacteriophages: State of the art. In *Microbiological Research* (Vols. 212–213, pp. 38–58). Elsevier GmbH. https://doi.org/10.1016/j.micres.2018.04.007

Harrison, O. L., Rensing, S., Jones, C. K., & Trinetta, V. (2022). Salmonella enterica 4,[5], 12: i:−, an Emerging Threat for the Swine Feed and Pork Production Industry. *Journal of Food Protection*, *85*(4), 660–663.

Hassan, A. Y., Lin, J. T., Ricker, N., & Anany, H. (2021). The age of phage: friend or foe in the new dawn of therapeutic and biocontrol applications? *Pharmaceuticals*, *14*(3), 199.

Havelaar, A. H., Kirk, M. D., Torgerson, P. R., Gibb, H. J., Hald, T., Lake, R. J., Praet, N., Bellinger, D. C., De Silva, N. R., & Gargouri, N. (2015). World Health Organization global estimates and regional comparisons of the burden of foodborne disease in 2010. *PLoS Medicine*, *12*(12), e1001923.

Hendriksen, R. S., Vieira, A. R., Karlsmose, S., Lo Fo Wong, D. M. A., Jensen, A. B., Wegener, H. C., & Aarestrup, F. M. (2011). Global monitoring of Salmonella serovar distribution from the World Health Organization Global Foodborne Infections Network Country Data Bank: results of quality assured laboratories from 2001 to 2007. *Foodborne Pathogens and Disease*, *8*(8), 887–900.

Hendrix, R. W., Ko, C.-C., Jacobs-Sera, D., Hatfull, G. F., Erhardt, M., Hughes, K. T.,

& Casjens, S. R. (2015). Genome sequence of Salmonella phage χ. *Genome Announcements*, *3*(1), e01229-14.

Higgins, J. P., Higgins, S. E., Guenther, K. L., Huff, W., Donoghue, A. M., Donoghue, D. J., & Hargis, B. M. (2005). Use of a specific bacteriophage treatment to reduce Salmonella in poultry products. *Poultry Science*, *84*(7), 1141–1145.

Hoelzer, K., Moreno Switt, A. I., & Wiedmann, M. (2011). Animal contact as a source of human non-typhoidal salmonellosis. *Veterinary Research*, *42*(1), 1–28.

Hu, Y., Gao, G. F., & Zhu, B. (2017). The antibiotic resistome: gene flow in environments, animals and human beings. *Frontiers of Medicine*, *11*(2), 161–168.

Hussein, N. H., AL-Kadmy, I., Taha, B. M., & Hussein, J. D. (2021). Mobilized colistin resistance (mcr) genes from 1 to 10: a comprehensive review. *Molecular Biology Reports*, *48*(3), 2897–2907.

Islam, M. S., Zhou, Y., Liang, L., Nime, I., Liu, K., Yan, T., Wang, X., & Li, J. (2019). Application of a Phage Cocktail for Control of Salmonella in Foods and Reducing Biofilms. *Viruses*, *11*(9), 1–19. https://doi.org/10.3390/v11090841

Jacoby, G. A. (2009). AmpC β-lactamases. *Clinical Microbiology Reviews*, *22*(1), 161–182.

Jones, F. T. (2011). A review of practical Salmonella control measures in animal feed. *Journal of Applied Poultry Research*, *20*(1), 102–113.

Karp, B. E., Tate, H., Plumblee, J. R., Dessai, U., Whichard, J. M., Thacker, E. L., Hale, K. R., Wilson, W., Friedman, C. R., & Griffin, P. M. (2017). National antimicrobial resistance monitoring system: two decades of advancing public health through integrated surveillance of antimicrobial resistance. *Foodborne Pathogens and Disease*, *14*(10), 545–557.

Kim, M.-S., & Bae, J.-W. (2018). Lysogeny is prevalent and widely distributed in the murine gut microbiota. *The ISME Journal*, *12*(4), 1127–1141.

King, A. M. Q., Adams, M. J., Carstens, E. B., & Lefcowits, E. J. (2011). *ICTV— International committee on taxonomy of viruses ninth report of the international committee on taxonomy of viruses*. Academic Press/Elsevier, London.

Kondo, K., Kawano, M., & Sugai, M. (2020). Prophage elements function as reservoir for antibiotic resistance and virulence genes in nosocomial pathogens. *BioRxiv*.

Kosznik-Kwaśnicka, K., Ciemińska, K., Grabski, M., Grabowski, Ł., Górniak, M., Jurczak-Kurek, A., Węgrzyn, G., & Węgrzyn, A. (2020). Characteristics of a series of three bacteriophages infecting Salmonella enterica strains. *International Journal of Molecular Sciences*, *21*(17), 6152.

Kropinski, A. M. (2009). Measurement of the rate of attachment of bacteriophage to cells. In *Bacteriophages* (pp. 151–155). Springer.

Kropinski, A. M. (2018). Practical advice on the one-step growth curve. In *Bacteriophages* (pp. 41–47). Springer.

Kuźmińska-Bajor, M., Śliwka, P., Ugorski, M., Korzeniowski, P., Skaradzińska, A., Kuczkowski, M., Narajaczyk, M., Wieliczko, A., & Kolenda, R. (2021). Genomic and functional characterization of five novel Salmonella-targeting bacteriophages. *Virology Journal*, *18*(1), 1–14. https://doi.org/10.1186/s12985-021-01655-4

Lai, M.-J., Chang, K.-C., Huang, S.-W., Luo, C.-H., Chiou, P.-Y., Wu, C.-C., & Lin, N.-T. (2016). The tail associated protein of Acinetobacter baumannii phage ΦAB6 is the host specificity determinant possessing exopolysaccharide depolymerase activity. *PloS One*, *11*(4), e0153361.

Landers, T. F., Cohen, B., Wittum, T. E., & Larson, E. L. (2012). A review of antibiotic use in food animals: perspective, policy, and potential. *Public Health Reports*, *127*(1), 4–22.

Landers, T. F., Cohen, B., Wittum, T. E., Larson, E. L., Rajan, K., Shi, Z., Ricke, S. C., Borie, C., Albala, I., Sánchez, P., Sánchez, M. L., Ramírez, S., Navarro, C., Morales, M. A., Retamales, J., Robeson, J., Vandenheuvel, D., Meeus, J., Lavigne,

R., … El-Shibiny, A. (2014). Bacteriophage and probiotics both enhance the performance of growing pigs but bacteriophage are more effective. *International Journal of Pharmaceutics*, *472*(1), 64–67.

Lee, C., Kim, H., & Ryu, S. (2022). Bacteriophage and endolysin engineering for biocontrol of food pathogens/pathogens in the food: recent advances and future trends. *Critical Reviews in Food Science and Nutrition*, 1–20.

Lee, J.-H., Shin, H., Kim, H., & Ryu, S. (2011). *Complete genome sequence of Salmonella bacteriophage SPN3US*. Am Soc Microbiol.

Lee, Y.-D., & Park, J.-H. (2015). Characterization and application of phages isolated from sewage for reduction of Escherichia coli O157: H7 in biofilm. *LWT-Food Science and Technology*, *60*(1), 571–577.

Lefort, V., Desper, R., & Gascuel, O. (2015). FastME 2.0: a comprehensive, accurate, and fast distance-based phylogeny inference program. *Molecular Biology and Evolution*, *32*(10), 2798–2800.

Letunic, I., & Bork, P. (2019). Interactive Tree Of Life (iTOL) v4: recent updates and new developments. *Nucleic Acids Research*, *47*(W1), W256–W259.

Li, J., Li, Y., Ding, Y., Huang, C., Zhang, Y., Wang, J., & Wang, X. (2021). Characterization of a novel Siphoviridae Salmonella bacteriophage T156 and its microencapsulation application in food matrix. *Food Research International*, *140*(September 2020), 110004. https://doi.org/10.1016/j.foodres.2020.110004

Li, S., He, Y., Mann, D. A., & Deng, X. (2021). Global spread of Salmonella Enteritidis via centralized sourcing and international trade of poultry breeding stocks. *Nature Communications*, *12*(1), 1–12.

Lin, D., Chen, K., Wai-Chi Chan, E., & Chen, S. (2015). Increasing prevalence of ciprofloxacin-resistant food-borne Salmonella strains harboring multiple PMQR elements but not target gene mutations. *Scientific Reports*, *5*(1), 1–8.

Lingohr, E., Frost, S., & Johnson, R. P. (2009). Determination of bacteriophage genome

size by pulsed-field gel electrophoresis. In *Bacteriophages* (pp. 19–25). Springer.

Liu, B., Zheng, D., Jin, Q., Chen, L., & Yang, J. (2019). VFDB 2019: a comparative pathogenomic platform with an interactive web interface. *Nucleic Acids Research*, *47*(D1), D687–D692.

Maciorowski, K. G., Herrera, P., Kundinger, M. M., & Ricke, S. C. (2006). Animal feed production and contamination by foodborne Salmonella. *Journal Für Verbraucherschutz Und Lebensmittelsicherheit*, *1*(3), 197–209.

Martino, G., Holtappels, D., Vallino, M., Chiapello, M., Turina, M., Lavigne, R., Wagemans, J., & Ciuffo, M. (2021). Molecular Characterization and Taxonomic Assignment of Three Phage Isolates from a Collection Infecting Pseudomonas syringae pv. actinidiae and P. syringae pv. phaseolicola from Northern Italy. *Viruses*, *13*(10), 2083.

Mather, A. E., Reid, S. W. J., Maskell, D. J., Parkhill, J., Fookes, M. C., Harris, S. R., Brown, D. J., Coia, J. E., Mulvey, M. R., & Gilmour, M. W. (2013a). Distinguishable epidemics of multidrug-resistant Salmonella Typhimurium DT104 in different hosts. *Science*, *341*(6153), 1514–1517.

Mather, A. E., Reid, S. W. J., Maskell, D. J., Parkhill, J., Fookes, M. C., Harris, S. R., Brown, D. J., Coia, J. E., Mulvey, M. R., & Gilmour, M. W. (2013b). Distinguishable Epidemics Within Different Hosts of the Multidrug Resistant Zoonotic Pathogen Salmonella Typhimurium DT. *Science*, *341*(6153), 1514–1517.

McDermott, P. F., Zhao, S., & Tate, H. (2018). Antimicrobial resistance in nontyphoidal Salmonella. *Microbiology Spectrum*, *6*(4), 4–6.

McGrath, S., & Sinderen, D. van. (2007). *Bacteriophage: genetics and molecular biology*. Caister Academic Press.

Meier-Kolthoff, J. P., & Göker, M. (2017). VICTOR: genome-based phylogeny and classification of prokaryotic viruses. *Bioinformatics*, *33*(21), 3396–3404.

Meier-Kolthoff, J. P., Hahnke, R. L., Petersen, J., Scheuner, C., Michael, V., Fiebig, A., Rohde, C., Rohde, M., Fartmann, B., & Goodwin, L. A. (2014). Complete genome sequence of DSM 30083T, the type strain (U5/41T) of Escherichia coli, and a proposal for delineating subspecies in microbial taxonomy. *Standards in Genomic Sciences*, *9*(1), 1–19.

Merabishvili, M., Vervaet, C., Pirnay, J.-P., De Vos, D., Verbeken, G., Mast, J., Chanishvili, N., & Vaneechoutte, M. (2013). Stability of Staphylococcus aureus phage ISP after freeze-drying (lyophilization). *PloS One*, *8*(7), e68797.

Milho, C., Silva, M. D., Alves, D., Oliveira, H., Sousa, C., Pastrana, L. M., Azeredo, J., & Sillankorva, S. (2019). Escherichia coli and Salmonella Enteritidis dual-species biofilms: interspecies interactions and antibiofilm efficacy of phages. *Scientific Reports*, *9*(1), 1–15.

Modi, R., Hirvi, Y., Hill, A., & Griffiths, M. W. (2001). Effect of phage on survival of Salmonella enteritidis during manufacture and storage of cheddar cheese made from raw and pasteurized milk. *Journal of Food Protection*, *64*(7), 927–933.

Monteiro, R., Pires, D. P., Costa, A. R., & Azeredo, J. (2019). Phage therapy: going temperate? *Trends in Microbiology*, *27*(4), 368–378.

Moreno Switt, A. I., Orsi, R. H., den Bakker, H. C., Vongkamjan, K., Altier, C., & Wiedmann, M. (2013). Genomic characterization provides new insight into Salmonella phage diversity. *BMC Genomics*, *14*(1). https://doi.org/10.1186/1471-2164-14-481

Moye, Z. D., Woolston, J., & Sulakvelidze, A. (2018). Bacteriophage applications for food production and processing. *Viruses*, *10*(4), 205.

Nair, D. V. T., & Kollanoor Johny, A. (2019). Salmonella in poultry meat production. In *Food Safety in Poultry Meat Production* (pp. 1–24). Springer.

Neoh, H., Tan, X.-E., Sapri, H. F., & Tan, T. L. (2019). Pulsed-field gel electrophoresis (PFGE): A review of the "gold standard" for bacteria typing and current

alternatives. *Infection, Genetics and Evolution*, *74*, 103935.

Nobrega, F. L., Vlot, M., de Jonge, P. A., Dreesens, L. L., Beaumont, H. J. E., Lavigne, R., Dutilh, B. E., & Brouns, S. J. J. (2018). Targeting mechanisms of tailed bacteriophages. *Nature Reviews Microbiology*, *16*(12), 760–773.

Ochman, H., Lawrence, J. G., & Groisman, E. A. (2000). Lateral gene transfer and the nature of bacterial innovation. *Nature*, *405*(6784), 299–304.

OECD. (2016). *Antimicrobial resistance–Policy insights*.

Organization, W. H. (2013). *Integrated surveillance of antimicrobial resistance: guidance from a WHO Advisory Group*.

Organization, W. H. (2017). *WHO guidelines on use of medically important antimicrobials in food-producing animals: web annex A: evidence base*. World Health Organization.

Organization, W. H. (2020). *Central Asian and European surveillance of antimicrobial resistance: annual report 2020*. World Health Organization. Regional Office for Europe.

Pardo-Este, C., Lorca, D., Castro-Severyn, J., Krüger, G., Alvarez-Thon, L., Zepeda, P., Sulbaran-Bracho, Y., Hidalgo, A., Tello, M., & Molina, F. (2021). Genetic Characterization of Salmonella Infantis with Multiple Drug Resistance Profiles Isolated from a Poultry-Farm in Chile. *Microorganisms*, *9*(11), 2370.

Parent, K. N., Khayat, R., Tu, L. H., Suhanovsky, M. M., Cortines, J. R., Teschke, C. M., Johnson, J. E., & Baker, T. S. (2010). P22 coat protein structures reveal a novel mechanism for capsid maturation: stability without auxiliary proteins or chemical crosslinks. *Structure*, *18*(3), 390–401.

Parmar, K., Dafale, N., Pal, R., Tikariha, H., & Purohit, H. (2018). An insight into phage diversity at environmental habitats using comparative metagenomics approach. *Current Microbiology*, *75*(2), 132–141.

Patel, S. J., Wellington, M., Shah, R. M., & Ferreira, M. J. (2020). Antibiotic stewardship in food-producing animals: challenges, progress, and opportunities. *Clinical Therapeutics*, *42*(9), 1649–1658.

Pessoa, J., Rodrigues da Costa, M., Nesbakken, T., & Meemken, D. (2021). Assessment of the Effectiveness of Pre-harvest Meat Safety Interventions to Control Foodborne Pathogens in Broilers: a Systematic Review. *Current Clinical Microbiology Reports*, *8*(2), 21–30.

Peterson, E., & Kaur, P. (2018). Antibiotic resistance mechanisms in bacteria: relationships between resistance determinants of antibiotic producers, environmental bacteria, and clinical pathogens. *Frontiers in Microbiology*, 2928.

Phothaworn, P., Dunne, M., Supokaivanich, R., Ong, C., Lim, J., Taharnklaew, R., Vesaratchavest, M., Khumthong, R., Pringsulaka, O., & Ajawatanawong, P. (2019). Characterization of flagellotropic, Chi-Like salmonella phages isolated from thai poultry farms. *Viruses*, *11*(6), 520.

Phothaworn, P., Supokaivanich, R., Lim, J., Klumpp, J., Imam, M., Kutter, E., Galyov, E. E., Dunne, M., & Korbsrisate, S. (2020). Development of a broad-spectrum Salmonella phage cocktail containing Viunalike and Jerseylike viruses isolated from Thailand. *Food Microbiology*, *92*, 103586.

Pickard, D., Toribio, A. L., Petty, N. K., Van Tonder, A., Yu, L., Goulding, D., Barrell, B., Rance, R., Harris, D., & Wetter, M. (2010). A conserved acetyl esterase domain targets diverse bacteriophages to the Vi capsular receptor of Salmonella enterica serovar Typhi. *Journal of Bacteriology*, *192*(21), 5746–5754.

Pires, D. P., Oliveira, H., Melo, L. D. R., Sillankorva, S., & Azeredo, J. (2016). Bacteriophage-encoded depolymerases: their diversity and biotechnological applications. *Applied Microbiology and Biotechnology*, *100*(5), 2141–2151.

Pires, S. M., Desta, B. N., Mughini-Gras, L., Mmbaga, B. T., Fayemi, O. E., Salvador, E. M., Gobena, T., Majowicz, S. E., Hald, T., & Hoejskov, P. S. (2021). Burden of foodborne diseases: Think global, act local. *Current Opinion in Food Science*, *39*,

152–159.

Pirnay, J.-P., De Vos, D., & Verbeken, G. (2019). Clinical application of bacteriophages in Europe. *Microbiology Australia*, *40*(1), 8–15.

Postollec, F., Mathot, A.-G., Bernard, M., Divanac'h, M.-L., Pavan, S., & Sohier, D. (2012). Tracking spore-forming bacteria in food: from natural biodiversity to selection by processes. *International Journal of Food Microbiology*, *158*(1), 1–8.

Pribul, B. R., Festivo, M. L., Souza, M. M. S. de, & Rodrigues, D. dos P. (2016). Characterization of quinolone resistance in Salmonella spp. isolates from food products and human samples in Brazil. *Brazilian Journal of Microbiology*, *47*, 196–201.

Rahn, K., De Grandis, S. A., Clarke, R. C., McEwen, S. A., Galan, J. E., Ginocchio, C., Curtiss Iii, R., & Gyles, C. L. (1992). Amplification of an invA gene sequence of Salmonella typhimurium by polymerase chain reaction as a specific method of detection of Salmonella. *Molecular and Cellular Probes*, *6*(4), 271–279.

Rajan, K., Shi, Z., & Ricke, S. C. (2017). Current aspects of Salmonella contamination in the US poultry production chain and the potential application of risk strategies in understanding emerging hazards. *Critical Reviews in Microbiology*, *43*(3), 370–392.

Rambaut, A. (n.d.). *FigTree-a graphical viewer of phylogenetic trees and a program for producing publication-ready figures, 2012*.

Ranasinghe, R. M. (2019). *Literature study of virus size, burst size, latent period and genome size across different lytic eukaryotic and prokaryotic virus groups-an overview of traits and possible trade-offs*. The University of Bergen.

Revolledo, L., & Ferreira, A. J. P. (2012). Current perspectives in avian salmonellosis: Vaccines and immune mechanisms of protection. *Journal of Applied Poultry Research*, *21*(2), 418–431.

Rohwer, F., & Edwards, R. (2002). The Phage Proteomic Tree: a genome-based

taxonomy for phage. *Journal of Bacteriology*, *184*(16), 4529–4535.

Roux, S., Hallam, S. J., Woyke, T., & Sullivan, M. B. (2015). Viral dark matter and virus–host interactions resolved from publicly available microbial genomes. *Elife*, *4*, e08490.

Sasikala, D., & Srinivasan, P. (2016). Characterization of potential lytic bacteriophage against Vibrio alginolyticus and its therapeutic implications on biofilm dispersal. *Microbial Pathogenesis*, *101*, 24–35.

Schade, S. Z., Adler, J., & Ris, H. (1967). How bacteriophage χ attacks motile bacteria. *Journal of Virology*, *1*(3), 599–609.

Seemann, T. (2014). Prokka: rapid prokaryotic genome annotation. *Bioinformatics*, *30*(14), 2068–2069.

Shen, A., & Millard, A. (2021). Phage Genome Annotation: Where to Begin and End. *Phage*, *2*(4), 183–193. https://doi.org/10.1089/phage.2021.0015

Singer, R. S., Mayer, A. E., Hanson, T. E., & Isaacson, R. E. (2009). Do microbial interactions and cultivation media decrease the accuracy of Salmonella surveillance systems and outbreak investigations? *Journal of Food Protection*, *72*(4), 707–713.

Siriken, B., Al, G., & Erol, I. (2020). Prevalence and antibiotic resistance of Salmonella Enteritidis and Salmonella Typhimurium in ground beef and meatball samples in Samsun, Turkey. *Microbial Drug Resistance*, *26*(2), 136–144.

Siriken, B., Türk, H., Yildirim, T., Durupinar, B., & Erol, I. (2015). Prevalence and characterization of Salmonella isolated from chicken meat in Turkey. *Journal of Food Science*, *80*(5), M1044–M1050.

SKLAR, I. A. N. B., & JOERGER, R. D. (2001). Attempts to utilize bacteriophage to combat Salmonella Enterica serovar entemtidis infection in chickens. *Journal of Food Safety*, *21*(1), 15–29.

Soucy, S. M., Huang, J., & Gogarten, J. P. (2015). Horizontal gene transfer: building the web of life. *Nature Reviews Genetics*, *16*(8), 472–482.

Steffan, S. M., Shakeri, G., Kehrenberg, C., Peh, E., Rohde, M., Plötz, M., & Kittler, S. (2022). Campylobacter Bacteriophage Cocktail Design Based on an Advanced Selection Scheme. *Antibiotics*, *11*(2), 228.

Storms, Z. J., Teel, M. R., Mercurio, K., & Sauvageau, D. (2020). The Virulence Index: A Metric for Quantitative Analysis of Phage Virulence. *Phage*, *1*(1), 27–36. https://doi.org/10.1089/phage.2019.0001

Storms, Z. J., Teel, M. R., Mercurio, K., Sauvageau, D., & Andrews, S. (2010). FastQC: a quality control tool for high throughput sequence data. *Phage*, *1*(1), 27–36.

Sukumaran, A. T., Nannapaneni, R., Kiess, A., & Sharma, C. S. (2015). Reduction of Salmonella on chicken meat and chicken skin by combined or sequential application of lytic bacteriophage with chemical antimicrobials. *International Journal of Food Microbiology*, *207*, 8–15.

Sukumaran, A. T., Nannapaneni, R., Kiess, A., & Sharma, C. S. (2016). Reduction of Salmonella on chicken breast fillets stored under aerobic or modified atmosphere packaging by the application of lytic bacteriophage preparation SalmoFreshTM. *Poultry Science*, *95*(3), 668–675.

Summers, W. C. (2016). Félix Hubert d'Herelle (1873–1949): History of a scientific mind. *Bacteriophage*, *6*(4), e1270090.

Switt, A. I. M., Sulakvelidze, A., Wiedmann, M., Kropinski, A. M., Wishart, D. S., Poppe, C., & Liang, Y. (2015). Salmonella phages and prophages: genomics, taxonomy, and applied aspects. *Salmonella*, 237–287.

Tassinari, E., Bawn, M., Thilliez, G., Charity, O., Acton, L., Kirkwood, M., Petrovska, L., Dallman, T., Burgess, C. M., & Hall, N. (2020). Whole-genome epidemiology links phage-mediated acquisition of a virulence gene to the clonal expansion of a pandemic Salmonella enterica serovar Typhimurium clone. *Microbial Genomics*,

6(11).

Tenover, F. C. (2006). Mechanisms of antimicrobial resistance in bacteria. *The American Journal of Medicine*, *119*(6), S3–S10.

Trun, N., & Trempy, J. (2009). *Fundamental bacterial genetics*. John Wiley & Sons.

Turner, D., Adriaenssens, E. M., Tolstoy, I., & Kropinski, A. M. (2021). Phage Annotation Guide: Guidelines for Assembly and High-Quality Annotation. *Phage*, *2*(4), 170–182. https://doi.org/10.1089/phage.2021.0013

Turner, D., Kropinski, A. M., & Adriaenssens, E. M. (2021). A roadmap for genome-based phage taxonomy. *Viruses*, *13*(3), 506.

Vandenheuvel, D., Singh, A., Vandersteegen, K., Klumpp, J., Lavigne, R., & Van den Mooter, G. (2013). Feasibility of spray drying bacteriophages into respirable powders to combat pulmonary bacterial infections. *European Journal of Pharmaceutics and Biopharmaceutics*, *84*(3), 578–582.

Vandeplas, S., & Adisseo France SAS, F. (2017). Zoonoses affecting poultry: the case of Salmonella. In *Achieving sustainable production of poultry meat Volume 1* (pp. 39–70). Burleigh Dodds Science Publishing.

Vernhes, E., Renouard, M., Gilquin, B., Cuniasse, P., Durand, D., England, P., Hoos, S., Huet, A., Conway, J. F., & Glukhov, A. (2017). High affinity anchoring of the decoration protein pb10 onto the bacteriophage T5 capsid. *Scientific Reports*, *7*(1), 1–14.

Walker, B. J., Abeel, T., Shea, T., Priest, M., Abouelliel, A., Sakthikumar, S., Cuomo, C. A., Zeng, Q., Wortman, J., & Young, S. K. (2014). Pilon: an integrated tool for comprehensive microbial variant detection and genome assembly improvement. *PloS One*, *9*(11), e112963.

Wang, J., Jiang, Y., Vincent, M., Sun, Y., Yu, H., Wang, J., Bao, Q., Kong, H., & Hu, S. (2005). Complete genome sequence of bacteriophage T5. *Virology*, *332*(1), 45–65.

Wang, X., Kim, Y., Ma, Q., Hong, S. H., Pokusaeva, K., Sturino, J. M., & Wood, T. K. (2010). Cryptic prophages help bacteria cope with adverse environments. *Nature Communications*, *1*(1), 1–9.

Ward, L. R., De Sa, J. D. H., & Rowe, B. (1987). A phage-typing scheme for Salmonella enteritidis. *Epidemiology & Infection*, *99*(2), 291–294.

White, H. E., & Orlova, E. V. (2019). Bacteriophages: their structural organisation and function. *Bacteriophages-Perspectives and Future*.

WHO. (2021). Central Asian and European Surveillance of Antimicrobial Resistance: Annual report 2019. *Central Asian and European Surveillance of Antimicrobial Resistance*. https://www.euro.who.int/en/health-topics/disease-prevention/antimicrobial-resistance/publications/2019/central-asian-and-european-surveillance-of-antimicrobial-resistance.-annual-report-2019

Wick, R. R., Schultz, M. B., Zobel, J., & Holt, K. E. (2015). Bandage: interactive visualization of de novo genome assemblies. *Bioinformatics*, *31*(20), 3350–3352.

Wigley, P. (2014). Salmonella enterica in the chicken: how it has helped our understanding of immunology in a non-biomedical model species. *Frontiers in Immunology*, *5*, 482.

Wójcik, E. A., Stanczyk, M., Wojtasik, A., Kowalska, J. D., Nowakowska, M., Lukasiak, M., Bartnicka, M., Kazimierczak, J., & Dastych, J. (2020). Comprehensive evaluation of the safety and efficacy of BAFASAL® bacteriophage preparation for the reduction of salmonella in the food chain. *Viruses*, *12*(7). https://doi.org/10.3390/v12070742

Wongsuntornpoj, S., Switt, A. I. M., Bergholz, P., Wiedmann, M., & Chaturongakul, S. (2014). Salmonella phages isolated from dairy farms in Thailand show wider host range than a comparable set of phages isolated from US dairy farms. *Veterinary Microbiology*, *172*(1–2), 345–352.

Woolston, J., Parks, A. R., Abuladze, T., Anderson, B., Li, M., Carter, C., Hanna, L. F.,

Heyse, S., Charbonneau, D., & Sulakvelidze, A. (2013). Bacteriophages lytic for Salmonella rapidly reduce Salmonella contamination on glass and stainless steel surfaces. *Bacteriophage*, *3*(3), e25697.

Xia, G., Corrigan, R. M., Winstel, V., Goerke, C., Gründling, A., & Peschel, A. (2011). Wall teichoic acid-dependent adsorption of staphylococcal siphovirus and myovirus. *Journal of Bacteriology*, *193*(15), 4006–4009.

Yan, J., Mao, J., & Xie, J. (2014). Bacteriophage polysaccharide depolymerases and biomedical applications. *BioDrugs*, *28*(3), 265–274.

YAPICIER, Ö. Ş., & SAREYYÜPOĞLU, B. (2022). Prevalence and rapid identification of Salmonella Infantis in broiler production in Turkey. *Ankara Üniversitesi Veteriner Fakültesi Dergisi*, *69*(1), 1–8.

Ye, M., Sun, M., Huang, D., Zhang, Z., Zhang, H., Zhang, S., Hu, F., Jiang, X., & Jiao, W. (2019). A review of bacteriophage therapy for pathogenic bacteria inactivation in the soil environment. *Environment International*, *129*, 488–496.

Yeh, Y., Purushothaman, P., Gupta, N., Ragnone, M., Verma, S. C., & De Mello, A. S. (2017). Bacteriophage application on red meats and poultry: Effects on Salmonella population in final ground products. *Meat Science*, *127*, 30–34.

Yildirim, Z., Sakın, T., & Çoban, F. (2018). Isolation of lytic bacteriophages infecting Salmonella Typhimurium and Salmonella Enteritidis. *Acta Biologica Hungarica*, *69*(3), 350–369.

Yuan, Y., & Gao, M. (2017). Jumbo bacteriophages: an overview. *Frontiers in Microbiology*, *8*, 403.

Zafer, A. T. A., Gökçen, D., Yibar, A., MÜŞTAK, H. K., & ŞAHAN, Ö. (2015). Extended spectrum beta-lactamase activity and multidrug resistance of Salmonella serovars isolated from chicken carcasses from different regions of Turkey. *Ankara Üniversitesi Veteriner Fakültesi Dergisi*, *62*(2), 119–123.

Żbikowska, K., Michalczuk, M., & Dolka, B. (2020). The use of bacteriophages in the

poultry industry. *Animals*, *10*(5), 872.

Zhang, Y., Ding, Y., Li, W., Zhu, W., Wang, J., & Wang, X. (2021). Application of a novel lytic podoviridae phage Pu20 for biological control of drug-resistant Salmonella in liquid eggs. *Pathogens*, *10*(1), 34.

Zinke, M., Schröder, G. F., & Lange, A. (2022). Major tail proteins of bacteriophages of the order Caudovirales. *Journal of Biological Chemistry*, *298*(1), 101472. https://doi.org/10.1016/j.jbc.2021.101472

Zou, W., Lin, W.-J., Foley, S. L., Chen, C.-H., Nayak, R., & Chen, J. J. (2010). Evaluation of pulsed-field gel electrophoresis profiles for identification of Salmonella serotypes. *Journal of Clinical Microbiology*, *48*(9), 3122–3126.

A. Antibiotic resistance results.

ID	Cn	S	Amp	Eft	Fox	Ak	C	Cro	Kf	Amc	Etp	Imp	Pef	N	Te	Sxt	Sf	cip	Phenotypic AMR Profile
MET A2-188	20	15	26	28	25	21	30	38	26	26	37	35	27	25	24	28	17	35	susceptible
MET A2-191	20	9	22	27	24	24	23	35	24	24	40	40	16	6	6	6	6	23	SPefNTeSxtSf
MET A2-194	17	9	20	27	23	24	22	33	22	22	37	34	16	6	6	6	6	24	SPefNTeSxtSf
MET A2-197	19	13	25	26	25	20	28	34	26	26	35	37	26	23	25	30	16	35	S
MET A2-200	10	6	6	28	27	24	28	31	10	10	36	35	6	6	6	25	6	12	CnSAmpKfAmcPefNTeSfCip
MET A2-209	19	15	25	30	28	21	30	35	26	26	40	40	29	24	25	30	17	40	susceptible
MET A2-212	10	6	6	28	29	20	29	32	14	14	35	30	6	6	6	27	6	12	CnSAmpPefNTeSfCip
MET A2-215	19	15	6	30	26	20	6	36	19	19	40	37	12	9	6	26	13	20	AmpCPefNTe
MET A2-218	20	6	17	29	26	21	34	34	19	19	35	40	27	22	29	27	23	30	S
MET A2-221	19	16	6	30	6	24	27	35	6	6	40	31	30	24	25	29	15	37	AmpFoxKfAmc
MET A2-224	17	17	6	20	6	22	25	28	6	6	33	26	27	22	22	25	17	33	AmpFoxKfAmc
MET A2-227	19	6	6	27	6	24	27	32	6	6	30	26	30	23	6	22	6	40	SAmpFoxKfAmcTeSf

Sf: Sulfisoxazole, Sxt: sulfamethoxazole-trimethoprim, Ak: Amikacin, Cn: Gentamicin, K: Kanamycin, S: Streptomycin, Cip: Ciprofloxacin, N: Nalidixic Acid, Amp: Ampicillin, Amc: Amoxicillin-clavulanic acid, T: Tetracycline, Fox: Cefoxitin, Kf: Cephalotin

B. Phage database entries

METUID	PreviousID	Genus	Serotype	Titer (PFU/mL)	VerifiedBy	Source General	Source Specific	Keywords	Month	Exact Date	City	Country
MET P1-001	Feb_AB1-p1	*Salmonella*	Enteritidis, Typhimurium	$4.8*10^{11}$	Mustafa Guzel	Cattle Farm	Cow Manure	True	February	10.02.2020	Adiyaman	Turkey
MET P1-002	Feb_AB1-p1	*Salmonella*	Enteritidis, Typhimurium	$4.8*10^{11}$	Mustafa Guzel	Cattle Farm	Cow Manure	Representative	February	10.02.2020	Adiyaman	Turkey
MET P1-003	Feb_AB1-p1	*Salmonella*	Enteritidis, Typhimurium	$4.8*10^{11}$	Mustafa Guzel	Cattle Farm	Cow Manure	Representative	February	10.02.2020	Adiyaman	Turkey
MET P1-004	Feb_AB1-p2	*Salmonella*	Enteritidis, Typhimurium	$4.5*10^{12}$	Mustafa Guzel	Cattle Farm	Cow Manure	True	February	10.02.2020	Adiyaman	Turkey
MET P1-005	Feb_AB1-p2	*Salmonella*	Enteritidis, Typhimurium	$4.5*10^{12}$	Mustafa Guzel	Cattle Farm	Cow Manure	Representative	February	10.02.2020	Adiyaman	Turkey
MET P1-006	Feb_AB1-p2	*Salmonella*	Enteritidis, Typhimurium	$4.5*10^{12}$	Mustafa Guzel	Cattle Farm	Cow Manure	Representative	February	10.02.2020	Adiyaman	Turkey
MET P1-007	Feb_UB2-p1	*Salmonella*	Enteritidis, Typhimurium	$9.2*10^{10}$	Mustafa Guzel	Cattle Farm	Cow Manure	True	February	10.02.2020	Şanlıurfa	Turkey
MET P1-008	Feb_UB2-p1	*Salmonella*	Enteritidis, Typhimurium	$9.2*10^{10}$	Mustafa Guzel	Cattle Farm	Cow Manure	Representative	February	10.02.2020	Şanlıurfa	Turkey
MET P1-009	Feb_UB2-p1	*Salmonella*	Enteritidis, Typhimurium	$9.2*10^{10}$	Mustafa Guzel	Cattle Farm	Cow Manure	Representative	February	10.02.2020	Şanlıurfa	Turkey
MET P1-010	Feb_UB2-p2	*Salmonella*	Enteritidis, Typhimurium	$7*10^{9}$	Mustafa Guzel	Cattle Farm	Cow Manure	True	February	10.02.2020	Şanlıurfa	Turkey
MET P1-011	Feb_UB2-p2	*Salmonella*	Enteritidis, Typhimurium	$7*10^{9}$	Mustafa Guzel	Cattle Farm	Cow Manure	Representative	February	10.02.2020	Şanlıurfa	Turkey
MET P1-012	Feb_UB2-p2	*Salmonella*	Enteritidis, Typhimurium	$7*10^{9}$	Mustafa Guzel	Cattle Farm	Cow Manure	Representative	February	10.02.2020	Şanlıurfa	Turkey
MET P1-013	Feb_UB3-p1	*Salmonella*	Enteritidis, Typhimurium	$8.9*10^{10}$	Mustafa Guzel	Cattle Farm	Cow Manure	True	February	10.02.2020	Şanlıurfa	Turkey
MET P1-014	Feb_UB3-p1	*Salmonella*	Enteritidis, Typhimurium	$8.9*10^{10}$	Mustafa Guzel	Cattle Farm	Cow Manure	Representative	February	10.02.2020	Şanlıurfa	Turkey
MET P1-015	Feb_UB3-p1	*Salmonella*	Enteritidis, Typhimurium	$8.9*10^{10}$	Mustafa Guzel	Cattle Farm	Cow Manure	Representative	February	10.02.2020	Şanlıurfa	Turkey
MET P1-016	Feb_UB3-p2	*Salmonella*	Enteritidis	$4.7*10^{11}$	Mustafa Guzel	Cattle Farm	Cow Manure	True	February	10.02.2020	Şanlıurfa	Turkey
MET P1-017	Feb_UB3-p2	*Salmonella*	Enteritidis	$4.7*10^{11}$	Mustafa Guzel	Cattle Farm	Cow Manure	Representative	February	10.02.2020	Şanlıurfa	Turkey

Appendix B (continued)

MET P1-018	Feb_UB3-p2	*Salmonella*	Enteritidis	$4.7*10^{11}$	Mustafa Guzel	Cattle Farm	Cow Manure	Representative	February	10.02.2020	Şanlıurfa	Turkey
MET P1-019	Feb_UK2-p1	*Salmonella*	Enteritidis, Typhimurium	$3.3*10^{10}$	Mustafa Guzel	Poultry Farm	Chicken Manure	True	February	10.02.2020	Şanlıurfa	Turkey
MET P1-020	Feb_UK2-p1	*Salmonella*	Enteritidis, Typhimurium	$3.3*10^{10}$	Mustafa Guzel	Poultry Farm	Chicken Manure	Representative	February	10.02.2020	Şanlıurfa	Turkey
MET P1-021	Feb_UK2-p1	*Salmonella*	Enteritidis, Typhimurium	$3.3*10^{10}$	Mustafa Guzel	Poultry Farm	Chicken Manure	Representative	February	10.02.2020	Şanlıurfa	Turkey
MET P1-022	Feb_UK2-p2	*Salmonella*	Enteritidis, Typhimurium	$1.35*10^{12}$	Mustafa Guzel	Poultry Farm	Chicken Manure	True	February	10.02.2020	Şanlıurfa	Turkey
MET P1-023	Feb_UK2-p2	*Salmonella*	Enteritidis, Typhimurium	$1.35*10^{12}$	Mustafa Guzel	Poultry Farm	Chicken Manure	Representative	February	10.02.2020	Şanlıurfa	Turkey
MET P1-024	Feb_UK2-p2	*Salmonella*	Enteritidis, Typhimurium	$1.35*10^{12}$	Mustafa Guzel	Poultry Farm	Chicken Manure	Representative	February	10.02.2020	Şanlıurfa	Turkey
MET P1-025	Feb_UK2-p3	*Salmonella*	Enteritidis	$8.7*10^{11}$	Mustafa Guzel	Poultry Farm	Chicken Manure	True	February	10.02.2020	Şanlıurfa	Turkey
MET P1-026	Feb_UK2-p3	*Salmonella*	Enteritidis	$8.7*10^{11}$	Mustafa Guzel	Poultry Farm	Chicken Manure	Representative	February	10.02.2020	Şanlıurfa	Turkey
MET P1-027	Feb_UK2-p3	*Salmonella*	Enteritidis	$8.7*10^{11}$	Mustafa Guzel	Poultry Farm	Chicken Manure	Representative	February	10.02.2020	Şanlıurfa	Turkey
MET P1-028	Feb_UK2-p4	*Salmonella*	Enteritidis, Typhimurium	$1.7*10^{12}$	Mustafa Guzel	Poultry Farm	Chicken Manure	True	February	10.02.2020	Şanlıurfa	Turkey
MET P1-029	Feb_UK2-p4	*Salmonella*	Enteritidis, Typhimurium	$1.7*10^{12}$	Mustafa Guzel	Poultry Farm	Chicken Manure	Representative	February	10.02.2020	Şanlıurfa	Turkey
MET P1-030	Feb_UK2-p4	*Salmonella*	Enteritidis, Typhimurium	$1.7*10^{12}$	Mustafa Guzel	Poultry Farm	Chicken Manure	Representative	February	10.02.2020	Şanlıurfa	Turkey
MET P1-031	Feb_UK2-p5	*Salmonella*	Enteritidis, Typhimurium	$2.06*10^{12}$	Mustafa Guzel	Poultry Farm	Chicken Manure	True	February	10.02.2020	Şanlıurfa	Turkey
MET P1-032	Feb_UK2-p5	*Salmonella*	Enteritidis, Typhimurium	$2.06*10^{12}$	Mustafa Guzel	Poultry Farm	Chicken Manure	Representative	February	10.02.2020	Şanlıurfa	Turkey
MET P1-033	Feb_UK2-p5	*Salmonella*	Enteritidis, Typhimurium	$2.06*10^{12}$	Mustafa Guzel	Poultry Farm	Chicken Manure	Representative	February	10.02.2020	Şanlıurfa	Turkey
MET P1-034	Feb_AK1-p1	*Salmonella*	Enteritidis, Typhimurium	$9.1*10^{11}$	Mustafa Guzel	Poultry Farm	Chicken Manure	True	February	10.02.2020	Adiyaman	Turkey
MET P1-035	Feb_AK1-p1	*Salmonella*	Enteritidis, Typhimurium	$9.1*10^{11}$	Mustafa Guzel	Poultry Farm	Chicken Manure	Representative	February	10.02.2020	Adiyaman	Turkey
MET P1-036	Feb_AK1-p1	*Salmonella*	Enteritidis, Typhimurium	$9.1*10^{11}$	Mustafa Guzel	Poultry Farm	Chicken Manure	Representative	February	10.02.2020	Adiyaman	Turkey

Appendix B (continued)

MET P1-037	Feb_AK1-p2	*Salmonella*	Enteritidis, Typhimurium	$1.4*10^{12}$	Mustafa Guzel	Poultry Farm	Chicken Manure	True	February	10.02.2020	Adiyaman	Turkey
MET P1-038	Feb_AK1-p2	*Salmonella*	Enteritidis, Typhimurium	$1.4*10^{12}$	Mustafa Guzel	Poultry Farm	Chicken Manure	Representative	February	10.02.2020	Adiyaman	Turkey
MET P1-039	Feb_AK1-p2	*Salmonella*	Enteritidis, Typhimurium	$1.4*10^{12}$	Mustafa Guzel	Poultry Farm	Chicken Manure	Representative	February	10.02.2020	Adiyaman	Turkey
MET P1-040	Feb_AK1-p3	*Salmonella*	Enteritidis, Typhimurium	$2.8*10^{12}$	Mustafa Guzel	Poultry Farm	Chicken Manure	True	February	10.02.2020	Adiyaman	Turkey
MET P1-041	Feb_AK1-p3	*Salmonella*	Enteritidis, Typhimurium	$2.8*10^{12}$	Mustafa Guzel	Poultry Farm	Chicken Manure	Representative	February	10.02.2020	Adiyaman	Turkey
MET P1-042	Feb_AK1-p3	*Salmonella*	Enteritidis, Typhimurium	$2.8*10^{12}$	Mustafa Guzel	Poultry Farm	Chicken Manure	Representative	February	10.02.2020	Adiyaman	Turkey
MET P1-043	Feb_AK2-p1	*Salmonella*	Enteritidis, Typhimurium	$8.2*10^{11}$	Mustafa Guzel	Poultry Farm	Chicken Manure	True	February	10.02.2020	Adiyaman	Turkey
MET P1-044	Feb_AK2-p1	*Salmonella*	Enteritidis, Typhimurium	$8.2*10^{11}$	Mustafa Guzel	Poultry Farm	Chicken Manure	Representative	February	10.02.2020	Adiyaman	Turkey
MET P1-045	Feb_AK2-p1	*Salmonella*	Enteritidis, Typhimurium	$8.2*10^{11}$	Mustafa Guzel	Poultry Farm	Chicken Manure	Representative	February	10.02.2020	Adiyaman	Turkey
MET P1-046	Feb_AK2-p2	*Salmonella*	Enteritidis, Typhimurium	$7.3*10^{9}$	Mustafa Guzel	Poultry Farm	Chicken Manure	True	February	10.02.2020	Adiyaman	Turkey
MET P1-047	Feb_AK2-p2	*Salmonella*	Enteritidis, Typhimurium	$7.3*10^{9}$	Mustafa Guzel	Poultry Farm	Chicken Manure	Representative	February	10.02.2020	Adiyaman	Turkey
MET P1-048	Feb_AK2-p2	*Salmonella*	Enteritidis, Typhimurium	$7.3*10^{9}$	Mustafa Guzel	Poultry Farm	Chicken Manure	Representative	February	10.02.2020	Adiyaman	Turkey
MET P1-049	Aug_AK1p1	*Salmonella*	Enteritidis, Typhimurium	$1.02*10^{11}$	Mustafa Guzel	Poultry Farm	Chicken Manure	True	August	14.08.2020	Adiyaman	Turkey
MET P1-050	Aug_AK1p1	*Salmonella*	Enteritidis, Typhimurium	$1.02*10^{11}$	Mustafa Guzel	Poultry Farm	Chicken Manure	Representative	August	14.08.2020	Adiyaman	Turkey
MET P1-051	Aug_AK1p1	*Salmonella*	Enteritidis, Typhimurium	$1.02*10^{11}$	Mustafa Guzel	Poultry Farm	Chicken Manure	Representative	August	14.08.2020	Adiyaman	Turkey
MET P1-052	Aug_AK2p1	*Salmonella*	Enteritidis, Typhimurium	$6.5*10^{11}$	Mustafa Guzel	Poultry Farm	Chicken Manure	True	August	14.08.2020	Adiyaman	Turkey
MET P1-053	Aug_AK2p1	*Salmonella*	Enteritidis, Typhimurium	$6.5*10^{11}$	Mustafa Guzel	Poultry Farm	Chicken Manure	Representative	August	14.08.2020	Adiyaman	Turkey
MET P1-054	Aug_AK2p1	*Salmonella*	Enteritidis, Typhimurium	$6.5*10^{11}$	Mustafa Guzel	Poultry Farm	Chicken Manure	Representative	August	14.08.2020	Adiyaman	Turkey
MET P1-055	Aug_AK2p2	*Salmonella*	Enteritidis, Typhimurium	$9.6*10^{10}$	Mustafa Guzel	Poultry Farm	Chicken Manure	True	August	14.08.2020	Adiyaman	Turkey

Appendix B (continued)

MET P1-056	Aug_AK2p2	*Salmonella*	Enteritidis, Typhimurium	$9.6*10^{10}$	Mustafa Guzel		Poultry Farm	Chicken Manure	Representative	August	14.08.2020	Adiyaman	Turkey
MET P1-057	Aug_AK2p2	*Salmonella*	Enteritidis, Typhimurium	$9.6*10^{10}$	Mustafa Guzel		Poultry Farm	Chicken Manure	Representative	August	14.08.2020	Adiyaman	Turkey
MET P1-058	Aug_AK3p1	*Salmonella*	Enteritidis, Typhimurium	$2.5*10^{11}$	Mustafa Guzel		Poultry Farm	Chicken Manure	True	August	14.08.2020	Adiyaman	Turkey
MET P1-059	Aug_AK3p1	*Salmonella*	Enteritidis, Typhimurium	$2.5*10^{11}$	Mustafa Guzel		Poultry Farm	Chicken Manure	Representative	August	14.08.2020	Adiyaman	Turkey
MET P1-060	Aug_AK3p1	*Salmonella*	Enteritidis, Typhimurium	$2.5*10^{11}$	Mustafa Guzel		Poultry Farm	Chicken Manure	Representative	August	14.08.2020	Adiyaman	Turkey
MET P1-061	Aug_AK4p1	*Salmonella*	Enteritidis, Typhimurium	$1.69*10^{12}$	Mustafa Guzel		Poultry Farm	Chicken Manure	True	August	14.08.2020	Adiyaman	Turkey
MET P1-062	Aug_AK4p1	*Salmonella*	Enteritidis, Typhimurium	$1.69*10^{12}$	Mustafa Guzel		Poultry Farm	Chicken Manure	Representative	August	14.08.2020	Adiyaman	Turkey
MET P1-063	Aug_AK4p1	*Salmonella*	Enteritidis, Typhimurium	$1.69*10^{12}$	Mustafa Guzel		Poultry Farm	Chicken Manure	Representative	August	14.08.2020	Adiyaman	Turkey
MET P1-064	Aug_AK4p2	*Salmonella*	Enteritidis, Typhimurium	$2.64*10^{11}$	Mustafa Guzel		Poultry Farm	Chicken Manure	True	August	14.08.2020	Adiyaman	Turkey
MET P1-065	Aug_AK4p2	*Salmonella*	Enteritidis, Typhimurium	$2.64*10^{11}$	Mustafa Guzel		Poultry Farm	Chicken Manure	Representative	August	14.08.2020	Adiyaman	Turkey
MET P1-066	Aug_AK4p2	*Salmonella*	Enteritidis, Typhimurium	$2.64*10^{11}$	Mustafa Guzel		Poultry Farm	Chicken Manure	Representative	August	14.08.2020	Adiyaman	Turkey
MET P1-067	Aug_AK5p1	*Salmonella*	Enteritidis, Typhimurium	$2.4*10^{11}$	Mustafa Guzel		Poultry Farm	Chicken Manure	True	August	14.08.2020	Adiyaman	Turkey
MET P1-068	Aug_AK5p1	*Salmonella*	Enteritidis, Typhimurium	$2.4*10^{11}$	Mustafa Guzel		Poultry Farm	Chicken Manure	Representative	August	14.08.2020	Adiyaman	Turkey
MET P1-069	Aug_AK5p1	*Salmonella*	Enteritidis, Typhimurium	$2.4*10^{11}$	Mustafa Guzel		Poultry Farm	Chicken Manure	Representative	August	14.08.2020	Adiyaman	Turkey
MET P1-070	Aug_AK5p2	*Salmonella*	Enteritidis, Typhimurium	$1.06*10^{11}$	Mustafa Guzel		Poultry Farm	Chicken Manure	True	August	14.08.2020	Adiyaman	Turkey
MET P1-071	Aug_AK5p2	*Salmonella*	Enteritidis, Typhimurium	$1.06*10^{11}$	Mustafa Guzel		Poultry Farm	Chicken Manure	Representative	August	14.08.2020	Adiyaman	Turkey
MET P1-072	Aug_AK5p2	*Salmonella*	Enteritidis, Typhimurium	$1.06*10^{11}$	Mustafa Guzel		Poultry Farm	Chicken Manure	Representative	August	14.08.2020	Adiyaman	Turkey
MET P1-073	Aug_BK3p1	*Salmonella*	Enteritidis, Typhimurium	$1.8*10^{12}$	Mustafa Guzel		Poultry Farm	Chicken Manure	True	August	14.08.2020	Bolu	Turkey
MET P1-074	Aug_BK3p1	*Salmonella*	Enteritidis, Typhimurium	$1.8*10^{12}$	Mustafa Guzel		Poultry Farm	Chicken Manure	Representative	August	14.08.2020	Bolu	Turkey

MET P1-075	Aug_BK3p1	*Salmonella*	Enteritidis, Typhimurium	$1.8*10^{12}$	Mustafa Guzel	Poultry Farm	Chicken Manure	Representative	August	14.08.2020	Bolu	Turkey
MET P1-076	Aug_BK4p1	*Salmonella*	Enteritidis, Typhimurium	$7.7*10^{11}$	Mustafa Guzel	Poultry Farm	Chicken Manure	True	August	14.08.2020	Bolu	Turkey
MET P1-077	Aug_BK4p1	*Salmonella*	Enteritidis, Typhimurium	$7.7*10^{11}$	Mustafa Guzel	Poultry Farm	Chicken Manure	Representative	August	14.08.2020	Bolu	Turkey
MET P1-078	Aug_BK4p1	*Salmonella*	Enteritidis, Typhimurium	$7.7*10^{11}$	Mustafa Guzel	Poultry Farm	Chicken Manure	Representative	August	14.08.2020	Bolu	Turkey
MET P1-079	Aug_BK4p2	*Salmonella*	Enteritidis, Typhimurium	$1.25*10^{12}$	Mustafa Guzel	Poultry Farm	Chicken Manure	True	August	14.08.2020	Bolu	Turkey
MET P1-080	Aug_BK4p2	*Salmonella*	Enteritidis, Typhimurium	$1.25*10^{12}$	Mustafa Guzel	Poultry Farm	Chicken Manure	Representative	August	14.08.2020	Bolu	Turkey
MET P1-081	Aug_BK4p2	*Salmonella*	Enteritidis, Typhimurium	$1.25*10^{12}$	Mustafa Guzel	Poultry Farm	Chicken Manure	Representative	August	14.08.2020	Bolu	Turkey
MET P1-082	Aug_BK5p1	*Salmonella*	Enteritidis, Typhimurium	$7.6*10^{11}$	Mustafa Guzel	Poultry Farm	Chicken Manure	True	August	14.08.2020	Bolu	Turkey
MET P1-083	Aug_BK5p1	*Salmonella*	Enteritidis, Typhimurium	$7.6*10^{11}$	Mustafa Guzel	Poultry Farm	Chicken Manure	Representative	August	14.08.2020	Bolu	Turkey
MET P1-084	Aug_BK5p1	*Salmonella*	Enteritidis, Typhimurium	$7.6*10^{11}$	Mustafa Guzel	Poultry Farm	Chicken Manure	Representative	August	14.08.2020	Bolu	Turkey
MET P1-085	Aug_MW1p163	*Salmonella*	Hadar	$5.63*10^{10}$	Mustafa Guzel	Wastewater Facility	Wastewater	True	August	17.08.2020	Ankara	Turkey
MET P1-086	Aug_MW1p163	*Salmonella*	Hadar	$5.63*10^{10}$	Mustafa Guzel	Wastewater Facility	Wastewater	Representative	August	17.08.2020	Ankara	Turkey
MET P1-087	Aug_MW1p163	*Salmonella*	Hadar	$5.63*10^{10}$	Mustafa Guzel	Wastewater Facility	Wastewater	Representative	August	17.08.2020	Ankara	Turkey
MET P1-088	Sep_MW1p163	*Salmonella*	Hadar	$1.5*10^{10}$	Mustafa Guzel	Wastewater Facility	Wastewater	True	October	01.10.2020	Ankara	Turkey
MET P1-089	Sep_MW1p163	*Salmonella*	Hadar	$1.5*10^{10}$	Mustafa Guzel	Wastewater Facility	Wastewater	Representative	October	01.10.2020	Ankara	Turkey
MET P1-090	Sep_MW1p163	*Salmonella*	Hadar	$1.5*10^{10}$	Mustafa Guzel	Wastewater Facility	Wastewater	Representative	October	01.10.2020	Ankara	Turkey
MET P1-091	Oct_AB3p1	*Salmonella*	Infantis	$1.7*10^{8}$	Mustafa Guzel	Cattle Farm	Cow Manure	True	October	08.10.2020	Adiyaman	Turkey
MET P1-092	Oct_AB3p1	*Salmonella*	Infantis	$1.7*10^{8}$	Mustafa Guzel	Cattle Farm	Cow Manure	Representative	October	08.10.2020	Adiyaman	Turkey

Appendix B (continued)

MET P1-093	Oct_AB3p1	*Salmonella*	Infantis	$1.7*10^8$	Mustafa Guzel	Cattle Farm	Cow Manure	Representative	October	08.10.2020	Adiyaman	Turkey
MET P1-094	Oct_AK2p1	*Salmonella*	Infantis	$3.9*10^9$	Mustafa Guzel	Poultry Farm	Chicken Manure	True	October	08.10.2020	Adiyaman	Turkey
MET P1-095	Oct_AK2p1	*Salmonella*	Infantis	$3.9*10^9$	Mustafa Guzel	Poultry Farm	Chicken Manure	Representative	October	08.10.2020	Adiyaman	Turkey
MET P1-096	Oct_AK2p1	*Salmonella*	Infantis	$3.9*10^9$	Mustafa Guzel	Poultry Farm	Chicken Manure	Representative	October	08.10.2020	Adiyaman	Turkey
MET P1-097	Sep_UK2p1	*Salmonella*	Infantis	$5.1*10^{10}$	Mustafa Guzel	Poultry Farm	Chicken Manure	True	September	23.09.2020	Şanlıurfa	Turkey
MET P1-098	Sep_UK2p2	*Salmonella*	Infantis	$5.1*10^{10}$	Mustafa Guzel	Poultry Farm	Chicken Manure	Representative	September	23.09.2020	Şanlıurfa	Turkey
MET P1-099	Sep_UK2p3	*Salmonella*	Infantis	$5.1*10^{10}$	Mustafa Guzel	Poultry Farm	Chicken Manure	Representative	September	23.09.2020	Şanlıurfa	Turkey
MET P1-100	Aug_MW1p2	*Salmonella*	Infantis	$8.5*10^{10}$	Mustafa Guzel	Wastewater Facility	Wastewater	True	August	17.08.2020	Ankara	Turkey
MET P1-101	Aug_MW1p2	*Salmonella*	Infantis	$8.5*10^{10}$	Mustafa Guzel	Wastewater Facility	Wastewater	Representative	August	17.08.2020	Ankara	Turkey
MET P1-102	Aug_MW1p2	*Salmonella*	Infantis	$8.5*10^{10}$	Mustafa Guzel	Wastewater Facility	Wastewater	Representative	August	17.08.2020	Ankara	Turkey
MET P1-103	Oct_AB2p1	*Salmonella*	Enteritidis	$9.2*10^{10}$	Mustafa Guzel	Cattle Farm	Cow Manure	True	October	08.10.2020	Adiyaman	Turkey
MET P1-104	Oct_AB2p1	*Salmonella*	Enteritidis	$9.2*10^{10}$	Mustafa Guzel	Cattle Farm	Cow Manure	Representative	October	08.10.2020	Adiyaman	Turkey
MET P1-105	Oct_AB2p1	*Salmonella*	Enteritidis	$9.2*10^{10}$	Mustafa Guzel	Cattle Farm	Cow Manure	Representative	October	08.10.2020	Adiyaman	Turkey
MET P1-107	Oct_AB1p1	*Salmonella*	Enteritidis	$1.97*10^{12}$	Mustafa Guzel	Cattle Farm	Cow Manure	True	October	08.10.2020	Adiyaman	Turkey
MET P1-108	Oct_AB1p1	*Salmonella*	Enteritidis	$1.97*10^{12}$	Mustafa Guzel	Cattle Farm	Cow Manure	Representative	October	08.10.2020	Adiyaman	Turkey
MET P1-109	Oct_AB1p1	*Salmonella*	Enteritidis	$1.97*10^{12}$	Mustafa Guzel	Cattle Farm	Cow Manure	Representative	October	08.10.2020	Adiyaman	Turkey
MET P1-110	Sep_UK4p1	*Salmonella*	Infantis	$3.3*10^{10}$	Mustafa Guzel	Poultry Farm	Chicken Manure	True	September	23.09.2020	Şanlıurfa	Turkey
MET P1-111	Sep_UK4p1	*Salmonella*	Infantis	$3.3*10^{10}$	Mustafa Guzel	Poultry Farm	Chicken Manure	Representative	September	23.09.2020	Şanlıurfa	Turkey
MET P1-112	Sep_UK4p1	*Salmonella*	Infantis	$3.3*10^{10}$	Mustafa Guzel	Poultry Farm	Chicken Manure	Representative	September	23.09.2020	Şanlıurfa	Turkey

Appendix B (continued)

MET P1-113	Sep_UK1p1	*Salmonella*	Enteritidis	$3.21*10^{12}$	Mustafa Guzel	Poultry Farm	Chicken Manure	True	September	23.09.2020	Şanlıurfa	Turkey
MET P1-114	Sep_UK1p1	*Salmonella*	Enteritidis	$3.21*10^{12}$	Mustafa Guzel	Poultry Farm	Chicken Manure	Representative	September	23.09.2020	Şanlıurfa	Turkey
MET P1-115	Sep_UK1p1	*Salmonella*	Enteritidis	$3.21*10^{12}$	Mustafa Guzel	Poultry Farm	Chicken Manure	Representative	September	23.09.2020	Şanlıurfa	Turkey
MET P1-116	Aug_MW5p1	*Salmonella*	Infantis	$9.5*10^{9}$	Mustafa Guzel	Wastewater Facility	Wastewater	True	October	01.10.2020	Ankara	Turkey
MET P1-117	Aug_MW5p1	*Salmonella*	Infantis	$9.5*10^{9}$	Mustafa Guzel	Wastewater Facility	Wastewater	Representative	October	01.10.2020	Ankara	Turkey
MET P1-118	Aug_MW5p1	*Salmonella*	Infantis	$9.5*10^{9}$	Mustafa Guzel	Wastewater Facility	Wastewater	Representative	October	01.10.2020	Ankara	Turkey
MET P1-119	Oct_AB2p2	*Salmonella*	Infantis	$4.73*10^{10}$	Mustafa Guzel	Cattle Farm	Cow Manure	True	October	08.10.2020	Adiyaman	Turkey
MET P1-120	Oct_AB2p2	*Salmonella*	Infantis	$4.73*10^{10}$	Mustafa Guzel	Cattle Farm	Cow Manure	Representative	October	08.10.2020	Adiyaman	Turkey
MET P1-121	Oct_AB2p2	*Salmonella*	Infantis	$4.73*10^{10}$	Mustafa Guzel	Cattle Farm	Cow Manure	Representative	October	08.10.2020	Adiyaman	Turkey
MET P1-122	Oct_AB3p1	*Salmonella*	Enteritidis	$1.18*10^{12}$	Mustafa Guzel	Cattle Farm	Cow Manure	True	October	08.10.2020	Adiyaman	Turkey
MET P1-123	Oct_AB3p1	*Salmonella*	Enteritidis	$1.18*10^{12}$	Mustafa Guzel	Cattle Farm	Cow Manure	Representative	October	08.10.2020	Adiyaman	Turkey
MET P1-124	Oct_AB3p1	*Salmonella*	Enteritidis	$1.18*10^{12}$	Mustafa Guzel	Cattle Farm	Cow Manure	Representative	October	08.10.2020	Adiyaman	Turkey
MET P1-125	Oct_MW1p007	*Salmonella*	Kentucky	$9.6*10^{10}$	Mustafa Guzel	Wastewater Facility	Wastewater	True	October	01.10.2020	Ankara	Turkey
MET P1-126	Oct_MW1p007	*Salmonella*	Kentucky	$9.6*10^{10}$	Mustafa Guzel	Wastewater Facility	Wastewater	Representative	October	01.10.2020	Ankara	Turkey
MET P1-127	Oct_MW1p007	*Salmonella*	Kentucky	$9.6*10^{10}$	Mustafa Guzel	Wastewater Facility	Wastewater	Representative	October	01.10.2020	Ankara	Turkey
MET P1-128	Oct_MW1p248	*Salmonella*	Anatum	$2.8*10^{7}$	Mustafa Guzel	Wastewater Facility	Wastewater	True	October	01.10.2020	Ankara	Turkey
MET P1-129	Oct_MW1p248	*Salmonella*	Anatum	$2.8*10^{7}$	Mustafa Guzel	Wastewater Facility	Wastewater	Representative	October	01.10.2020	Ankara	Turkey
MET P1-130	Oct_MW1p248	*Salmonella*	Anatum	$2.8*10^{7}$	Mustafa Guzel	Wastewater Facility	Wastewater	Representative	October	01.10.2020	Ankara	Turkey
MET P1-131	Nov_MW1p001	*Salmonella*	Enteritidis	$1.57*10^{10}$	Mustafa Guzel	Wastewater Facility	Wastewater	True	October	11.11.2020	Ankara	Turkey

156

Appendix B (continued)

MET P1-132	Nov_MW1p001	*Salmonella*	Enteritidis	$1.57*10^{10}$	Mustafa Guzel	Wastewater Facility	Wastewater	Representative	October	11.11.2020	Ankara	Turkey
MET P1-133	Nov_MW1p001	*Salmonella*	Enteritidis	$1.57*10^{10}$	Mustafa Guzel	Wastewater Facility	Wastewater	Representative	October	11.11.2020	Ankara	Turkey
MET P1-134	Nov_MW1p006	*Salmonella*	Infantis	ND	Mustafa Guzel	Wastewater Facility	Wastewater	True	October	11.11.2020	Ankara	Turkey
MET P1-135	Nov_MW1p006	*Salmonella*	Infantis	ND	Mustafa Guzel	Wastewater Facility	Wastewater	Representative	October	11.11.2020	Ankara	Turkey
MET P1-136	Nov_MW1p006	*Salmonella*	Infantis	ND	Mustafa Guzel	Wastewater Facility	Wastewater	Representative	October	11.11.2020	Ankara	Turkey
MET P1-137	Nov_MW1p007	*Salmonella*	Kentucky	$7.84*10^{11}$	Mustafa Guzel	Wastewater Facility	Wastewater	True	October	11.11.2020	Ankara	Turkey
MET P1-138	Nov_MW1p007	*Salmonella*	Kentucky	$7.84*10^{11}$	Mustafa Guzel	Wastewater Facility	Wastewater	Representative	October	11.11.2020	Ankara	Turkey
MET P1-139	Nov_MW1p007	*Salmonella*	Kentucky	$7.84*10^{11}$	Mustafa Guzel	Wastewater Facility	Wastewater	Representative	October	11.11.2020	Ankara	Turkey
MET P1-140	Nov_MW1p063	*Salmonella*	Telaviv	$1.94*10^{11}$	Mustafa Guzel	Wastewater Facility	Wastewater	True	October	11.11.2020	Ankara	Turkey
MET P1-141	Nov_MW1p063	*Salmonella*	Telaviv	$1.94*10^{11}$	Mustafa Guzel	Wastewater Facility	Wastewater	Representative	October	11.11.2020	Ankara	Turkey
MET P1-142	Nov_MW1p063	*Salmonella*	Telaviv	$1.94*10^{11}$	Mustafa Guzel	Wastewater Facility	Wastewater	Representative	October	11.11.2020	Ankara	Turkey
MET P1-143	Nov_UB1p1	*Salmonella*	Enteritidis	$1.39*10^{12}$	Mustafa Guzel	Cattle Farm	Cow Manure	True	November	19.11.2020	Şanlıurfa	Turkey
MET P1-144	Nov_UB1p1	*Salmonella*	Enteritidis	$1.39*10^{12}$	Mustafa Guzel	Cattle Farm	Cow Manure	Representative	November	19.11.2020	Şanlıurfa	Turkey
MET P1-145	Nov_UB1p1	*Salmonella*	Enteritidis	$1.39*10^{12}$	Mustafa Guzel	Cattle Farm	Cow Manure	Representative	November	19.11.2020	Şanlıurfa	Turkey
MET P1-146	Nov_UB2p1	*Salmonella*	Enteritidis	$9*10^{11}$	Mustafa Guzel	Cattle Farm	Cow Manure	True	November	19.11.2020	Şanlıurfa	Turkey
MET P1-147	Nov_UB2p1	*Salmonella*	Enteritidis	$9*10^{11}$	Mustafa Guzel	Cattle Farm	Cow Manure	Representative	November	19.11.2020	Şanlıurfa	Turkey
MET P1-148	Nov_UB2p1	*Salmonella*	Enteritidis	$9*10^{11}$	Mustafa Guzel	Cattle Farm	Cow Manure	Representative	November	19.11.2020	Şanlıurfa	Turkey
MET P1-149	Nov_UB3p1	*Salmonella*	Enteritidis	$1.4*10^{11}$	Mustafa Guzel	Cattle Farm	Cow Manure	True	November	19.11.2020	Şanlıurfa	Turkey
MET P1-150	Nov_UB3p1	*Salmonella*	Enteritidis	$1.4*10^{11}$	Mustafa Guzel	Cattle Farm	Cow Manure	Representative	November	19.11.2020	Şanlıurfa	Turkey

Appendix B (continued)

MET P1-151	Nov_UB3p1	*Salmonella*	Enteritidis	$1.4*10^{11}$	Mustafa Guzel	Cattle Farm	Cow Manure	Representative	November	19.11.2020	Şanlıurfa	Turkey
MET P1-152	Nov_UK1p1	*Salmonella*	Enteritidis	$1.03*10^{11}$	Mustafa Guzel	Poultry Farm	Chicken Manure	True	November	19.11.2020	Şanlıurfa	Turkey
MET P1-153	Nov_UK1p1	*Salmonella*	Enteritidis	$1.03*10^{11}$	Mustafa Guzel	Poultry Farm	Chicken Manure	Representative	November	19.11.2020	Şanlıurfa	Turkey
MET P1-154	Nov_UK1p1	*Salmonella*	Enteritidis	$1.03*10^{11}$	Mustafa Guzel	Poultry Farm	Chicken Manure	Representative	November	19.11.2020	Şanlıurfa	Turkey
MET P1-155	Nov_UK2p1	*Salmonella*	Enteritidis	$1.44*10^{11}$	Mustafa Guzel	Poultry Farm	Chicken Manure	True	November	19.11.2020	Şanlıurfa	Turkey
MET P1-156	Nov_UK2p1	*Salmonella*	Enteritidis	$1.44*10^{11}$	Mustafa Guzel	Poultry Farm	Chicken Manure	Representative	November	19.11.2020	Şanlıurfa	Turkey
MET P1-157	Nov_UK2p1	*Salmonella*	Enteritidis	$1.44*10^{11}$	Mustafa Guzel	Poultry Farm	Chicken Manure	Representative	November	19.11.2020	Şanlıurfa	Turkey
MET P1-158	Nov_AB1p1	*Salmonella*	Enteritidis	$5.72*10^{12}$	Mustafa Guzel	Cattle Farm	Cow Manure	True	November	19.11.2020	Adiyaman	Turkey
MET P1-159	Nov_AB1p1	*Salmonella*	Enteritidis	$5.72*10^{12}$	Mustafa Guzel	Cattle Farm	Cow Manure	Representative	November	19.11.2020	Adiyaman	Turkey
MET P1-160	Nov_AB1p1	*Salmonella*	Enteritidis	$5.72*10^{12}$	Mustafa Guzel	Cattle Farm	Cow Manure	Representative	November	19.11.2020	Adiyaman	Turkey
MET P1-161	Nov_AB2p1	*Salmonella*	Enteritidis	$9.8*10^{11}$	Mustafa Guzel	Cattle Farm	Cow Manure	True	November	19.11.2020	Adiyaman	Turkey
MET P1-162	Nov_AB2p1	*Salmonella*	Enteritidis	$9.8*10^{11}$	Mustafa Guzel	Cattle Farm	Cow Manure	Representative	November	19.11.2020	Adiyaman	Turkey
MET P1-163	Nov_AB2p1	*Salmonella*	Enteritidis	$9.8*10^{11}$	Mustafa Guzel	Cattle Farm	Cow Manure	Representative	November	19.11.2020	Adiyaman	Turkey
MET P1-164	Nov_AB3p1	*Salmonella*	Enteritidis	$1.11*10^{12}$	Mustafa Guzel	Cattle Farm	Cow Manure	True	November	19.11.2020	Adiyaman	Turkey
MET P1-165	Nov_AB3p1	*Salmonella*	Enteritidis	$1.11*10^{12}$	Mustafa Guzel	Cattle Farm	Cow Manure	Representative	November	19.11.2020	Adiyaman	Turkey
MET P1-166	Nov_AB3p1	*Salmonella*	Enteritidis	$1.11*10^{12}$	Mustafa Guzel	Cattle Farm	Cow Manure	Representative	November	19.11.2020	Adiyaman	Turkey
MET P1-167	Nov_AK1p1	*Salmonella*	Enteritidis	$>10^{13}$	Mustafa Guzel	Poultry Farm	Chicken Manure	True	November	19.11.2020	Adiyaman	Turkey
MET P1-168	Nov_AK1p1	*Salmonella*	Enteritidis	$>10^{13}$	Mustafa Guzel	Poultry Farm	Chicken Manure	Representative	November	19.11.2020	Adiyaman	Turkey
MET P1-169	Nov_AK1p1	*Salmonella*	Enteritidis	$>10^{13}$	Mustafa Guzel	Poultry Farm	Chicken Manure	Representative	November	19.11.2020	Adiyaman	Turkey

Appendix B (continued)

MET P1-170	Nov_AK2p1	*Salmonella*	Enteritidis	$>10^{13}$	Mustafa Guzel	Poultry Farm	Chicken Manure	True	November	19.11.2020	Adiyaman	Turkey
MET P1-171	Nov_AK2p1	*Salmonella*	Enteritidis	$>10^{13}$	Mustafa Guzel	Poultry Farm	Chicken Manure	Representative	November	19.11.2020	Adiyaman	Turkey
MET P1-172	Nov_AK2p1	*Salmonella*	Enteritidis	$>10^{13}$	Mustafa Guzel	Poultry Farm	Chicken Manure	Representative	November	19.11.2020	Adiyaman	Turkey
MET P1-173	Nov_AK1p006	*Salmonella*	Infantis	$8.3*10^{10}$	Mustafa Guzel	Poultry Farm	Chicken Manure	True	November	19.11.2020	Adiyaman	Turkey
MET P1-174	Nov_AK1p006	*Salmonella*	Infantis	$8.3*10^{10}$	Mustafa Guzel	Poultry Farm	Chicken Manure	Representative	November	19.11.2020	Adiyaman	Turkey
MET P1-175	Nov_AK1p006	*Salmonella*	Infantis	$8.3*10^{10}$	Mustafa Guzel	Poultry Farm	Chicken Manure	Representative	November	19.11.2020	Adiyaman	Turkey
MET P1-176	Nov_AK2p006	*Salmonella*	Infantis	$1.25*10^{10}$	Mustafa Guzel	Poultry Farm	Chicken Manure	True	November	19.11.2020	Adiyaman	Turkey
MET P1-177	Nov_AK2p006	*Salmonella*	Infantis	$1.25*10^{10}$	Mustafa Guzel	Poultry Farm	Chicken Manure	Representative	November	19.11.2020	Adiyaman	Turkey
MET P1-178	Nov_AK2p006	*Salmonella*	Infantis	$1.25*10^{10}$	Mustafa Guzel	Poultry Farm	Chicken Manure	Representative	November	19.11.2020	Adiyaman	Turkey
MET P1-179	Dec_MWp006	*Salmonella*	Infantis	ND	Mustafa Guzel	Wastewater Facility	Wastewater	True	December	09.12.2020	Ankara	Turkey
MET P1-180	Dec_MWp006	*Salmonella*	Infantis	ND	Mustafa Guzel	Wastewater Facility	Wastewater	Representative	December	09.12.2020	Ankara	Turkey
MET P1-181	Dec_MWp006	*Salmonella*	Infantis	ND	Mustafa Guzel	Wastewater Facility	Wastewater	Representative	December	09.12.2020	Ankara	Turkey
MET P1-182	Dec_MWp001	*Salmonella*	Enteritidis	$2.69*10^{12}$	Mustafa Guzel	Wastewater Facility	Wastewater	True	December	09.12.2020	Ankara	Turkey
MET P1-183	Dec_MWp001	*Salmonella*	Enteritidis	$2.69*10^{12}$	Mustafa Guzel	Wastewater Facility	Wastewater	Representative	December	09.12.2020	Ankara	Turkey
MET P1-184	Dec_MWp001	*Salmonella*	Enteritidis	$2.69*10^{12}$	Mustafa Guzel	Wastewater Facility	Wastewater	Representative	December	09.12.2020	Ankara	Turkey
MET P1-185	Dec_MWp002	*Salmonella*	Typhimurium	$1*10^9$	Mustafa Guzel	Wastewater Facility	Wastewater	True	December	09.12.2020	Ankara	Turkey
MET P1-186	Dec_MWp002	*Salmonella*	Typhimurium	$1*10^9$	Mustafa Guzel	Wastewater Facility	Wastewater	Representative	December	09.12.2020	Ankara	Turkey
MET P1-187	Dec_MWp002	*Salmonella*	Typhimurium	$1*10^9$	Mustafa Guzel	Wastewater Facility	Wastewater	Representative	December	09.12.2020	Ankara	Turkey
MET P1-188	Dec_MWp007	*Salmonella*	Kentucky	$4*10^9$	Mustafa Guzel	Wastewater Facility	Wastewater	True	December	09.12.2020	Ankara	Turkey

Appendix B (continued)

MET P1-189	Dec_MWp007	*Salmonella*	Kentucky	$4*10^9$	Mustafa Guzel	Wastewater Facility	Wastewater	Representative	December	09.12.2020	Ankara	Turkey
MET P1-190	Dec_MWp007	*Salmonella*	Kentucky	$4*10^9$	Mustafa Guzel	Wastewater Facility	Wastewater	Representative	December	09.12.2020	Ankara	Turkey
MET P1-191	Dec_MWp063	*Salmonella*	Telaviv	$3.72*10^{11}$	Mustafa Guzel	Wastewater Facility	Wastewater	True	December	09.12.2020	Ankara	Turkey
MET P1-192	Dec_MWp063	*Salmonella*	Telaviv	$3.72*10^{11}$	Mustafa Guzel	Wastewater Facility	Wastewater	Representative	December	09.12.2020	Ankara	Turkey
MET P1-193	Dec_MWp063	*Salmonella*	Telaviv	$3.72*10^{11}$	Mustafa Guzel	Wastewater Facility	Wastewater	Representative	December	09.12.2020	Ankara	Turkey
MET P1-194	Dec_MWp163	*Salmonella*	Hadar	$8.2*10^{11}$	Mustafa Guzel	Wastewater Facility	Wastewater	True	December	09.12.2020	Ankara	Turkey
MET P1-195	Dec_MWp163	*Salmonella*	Hadar	$8.2*10^{11}$	Mustafa Guzel	Wastewater Facility	Wastewater	Representative	December	09.12.2020	Ankara	Turkey
MET P1-196	Dec_MWp163	*Salmonella*	Hadar	$8.2*10^{11}$	Mustafa Guzel	Wastewater Facility	Wastewater	Representative	December	09.12.2020	Ankara	Turkey
MET P1-197	Dec_MWp248	*Salmonella*	Anatum	$1.4*10^{11}$	Mustafa Guzel	Wastewater Facility	Wastewater	True	December	09.12.2020	Ankara	Turkey
MET P1-198	Dec_MWp248	*Salmonella*	Anatum	$1.4*10^{11}$	Mustafa Guzel	Wastewater Facility	Wastewater	Representative	December	09.12.2020	Ankara	Turkey
MET P1-199	Dec_MWp248	*Salmonella*	Anatum	$1.4*10^{11}$	Mustafa Guzel	Wastewater Facility	Wastewater	Representative	December	09.12.2020	Ankara	Turkey
MET P1-200	Dec_MWp015	*Salmonella*	Montevideo	ND	Mustafa Guzel	Wastewater Facility	Wastewater	True	December	09.12.2020	Ankara	Turkey
MET P1-201	Dec_MWp015	*Salmonella*	Montevideo	ND	Mustafa Guzel	Wastewater Facility	Wastewater	Representative	December	09.12.2020	Ankara	Turkey
MET P1-202	Dec_MWp015	*Salmonella*	Montevideo	ND	Mustafa Guzel	Wastewater Facility	Wastewater	Representative	December	09.12.2020	Ankara	Turkey
MET P1-203	Nov_UB1p002	*Salmonella*	Typhimurium	$1*10^9$	Mustafa Guzel	Cattle Farm	Cow Manure	True	November	19.11.2020	Şanlıurfa	Turkey
MET P1-204	Nov_UB1p002	*Salmonella*	Typhimurium	$1*10^9$	Mustafa Guzel	Cattle Farm	Cow Manure	Representative	November	19.11.2020	Şanlıurfa	Turkey
MET P1-205	Nov_UB1p002	*Salmonella*	Typhimurium	$1*10^9$	Mustafa Guzel	Cattle Farm	Cow Manure	Representative	November	19.11.2020	Şanlıurfa	Turkey

C. Titers of the phages after purification step

METUID	Serotype	Titer (PFU/mL)
MET P1-010	Enteritidis	7.00E+09
MET P1-046	Enteritidis	7.30E+09
MET P1-131	Enteritidis	1.57E+10
MET P1-019	Enteritidis	3.30E+10
MET P1-013	Enteritidis	8.90E+10
MET P1-103	Enteritidis	9.20E+10
MET P1-007	Enteritidis	9.20E+10
MET P1-055	Enteritidis	9.60E+10
MET P1-049	Enteritidis	1.02E+11
MET P1-152	Enteritidis	1.03E+11
MET P1-070	Enteritidis	1.06E+11
MET P1-149	Enteritidis	1.40E+11
MET P1-155	Enteritidis	1.44E+11
MET P1-067	Enteritidis	2.40E+11
MET P1-058	Enteritidis	2.50E+11
MET P1-064	Enteritidis	2.64E+11
MET P1-016	Enteritidis	4.70E+11
MET P1-001	Enteritidis	4.80E+11
MET P1-052	Enteritidis	6.50E+11
MET P1-082	Enteritidis	7.60E+11
MET P1-076	Enteritidis	7.70E+11
MET P1-043	Enteritidis	8.20E+11
MET P1-025	Enteritidis	8.70E+11
MET P1-146	Enteritidis	9.00E+11
MET P1-034	Enteritidis	9.10E+11
MET P1-161	Enteritidis	9.80E+11
MET P1-164	Enteritidis	1.11E+12
MET P1-122	Enteritidis	1.18E+12
MET P1-079	Enteritidis	1.25E+12
MET P1-022	Enteritidis	1.35E+12
MET P1-143	Enteritidis	1.39E+12
MET P1-037	Enteritidis	1.40E+12
MET P1-061	Enteritidis	1.69E+12
MET P1-028	Enteritidis	1.70E+12
MET P1-073	Enteritidis	1.80E+12
MET P1-107	Enteritidis	1.97E+12

Appendix C (continued)

MET P1-031	Enteritidis	2.06E+12
MET P1-182	Enteritidis	2.69E+12
MET P1-040	Enteritidis	2.80E+12
MET P1-113	Enteritidis	3.21E+12
MET P1-004	Enteritidis	4.50E+12
MET P1-158	Enteritidis	5.72E+12
MET P1-167	Enteritidis	1.00E+13
MET P1-170	Enteritidis	1.00E+13
MET P1-128	Anatum	2.80E+07
MET P1-197	Anatum	1.40E+11
MET P1-085	Hadar	5.63E+10
MET P1-088	Hadar	1.50E+10
MET P1-194	Hadar	8.20E+11
MET P1-091	Infantis	1.70E+08
MET P1-094	Infantis	3.90E+09
MET P1-097	Infantis	5.10E+10
MET P1-100	Infantis	8.50E+10
MET P1-110	Infantis	3.30E+10
MET P1-116	Infantis	9.50E+09
MET P1-119	Infantis	4.73E+10
MET P1-134	Infantis	ND
MET P1-173	Infantis	8.30E+10
MET P1-176	Infantis	1.25E+10
MET P1-179	Infantis	ND
MET P1-125	Kentucky	9.60E+10
MET P1-137	Kentucky	7.84E+11
MET P1-188	Kentucky	4.00E+09
MET P1-200	Montevideo	ND
MET P1-140	Telaviv	1.94E+11
MET P1-191	Telaviv	3.72E+11
MET P1-185	Typhimurium	1.00E+09
MET P1-203	Typhimurium	1.00E+09

D. Host range analysis

Serotype	Isolate Source	METUID	p001	p004	p007	p010	p013	p016	p019	p022	p025	p028	p031	p034	p037	p040	p043	p046	p049
Enteritidis	FOOD	MET S1-742	+	+	+	+	+	+	+	+	+	+	+	+	+	+	+	+	+
Enteritidis	HUMAN	MET S1-217	-	-	-	-	-	-	-	-	-	-	-	-	-	-	-	-	T+
Enteritidis	HUMAN	MET S1-221	+	+	+	+	+	+	+	+	+	+	+	+	+	+	+	+	T+
Enteritidis	FOOD	MET S1-411	+	+	+	+	+	+	+	+	+	+	+	+	+	+	+	+	+
Enteritidis	SLUDGE	MET A2-012	+	+	+	+	+	+	+	+	+	+	+	+	+	+	+	T+	+
Typhimurium	HUMAN	MET S1-223	+	+	+	+	+	+	+	+	+	-	+	+	+	+	+	-	+
Typhimurium	HUMAN	MET S1-185	T+	P	P	-	T+	T+	T+	T+	-	-	-	-	-	-	-	-	-
Typhimurium	ANIMAL	MET S1-663	T+	T+	T+	T+	+	+	+	+	T+	+	+	+	T+	T+	T+	T+	+
Typhimurium	SLUDGE	MET A2-003	T+	T+	T+	T+	T+	T+	T+	T+	T+	T+	T+	T+	T+	T+	T+	T+	+
Typhimurim	DT104	MET A2-088	+	+	+	+	+	+	+	+	+	+	+	+	+	+	+	+	+
Typhimurium	ANIMAL	MET S1-657	+	+	T+	T+	+	+	+	T+	T+	+	+	+	+	+	T+	T+	T+
Infantis	FOOD	MET S1-050	-	-	-	-	-	-	-	-	-	-	-	-	-	-	-	-	-
Infantis	Thailand	MET S1-807	-	-	-	-	-	-	-	-	-	T+	-	-	-	-	-	-	-
Infantis	SLUDGE	MET S1-857	T+	T+	T+	T+	T+	T+	T+	T+	-	-	-	-	-	-	-	-	-
Kentucky	HUMAN	MET S1-240	-	-	-	-	-	-	-	-	-	-	-	-	-	-	-	-	-
Kentucky	ANIMAL	MET S1-542	T+	-	-	-	-	-	-	-	-	-	-	-	-	-	-	-	-
Kentucky	SLUDGE	MET A2-072	-	-	-	-	-	-	-	-	-	-	-	-	-	-	-	-	-
Montevideo	FOOD	MET S1-065	-	-	-	-	-	-	-	-	-	-	-	-	-	-	-	-	-
Montevideo	ANIMAL	MET S1-170	T+	-	-	-	-	-	-	-	-	-	-	-	-	-	-	-	-
Montevideo	ANIMAL	MET S1-172	-	-	-	-	-	-	-	-	-	-	-	-	-	-	-	-	-
Anatum	Food	MET S1-548	T+	-	-	-	-	-	-	-	-	-	-	-	-	-	-	-	-

Anatum	Food	MET S1-579	T+	-	T+	-	-	-	T+	-	-	T+	-	-	-	-	-	-	-
Hadar	Food	MET S1-163	-	-	-	-	-	-	-	-	-	-	-	-	-	-	-	-	-
Telaviv	Food	MET S1-074	+	-	-	-	-	-	-	-	-	T+	-	-	-	-	-	-	-
Telaviv	Food	MET S1-530	-	-	-	-	-	-	-	-	-	-	-	-	-	-	-	-	-
Thompson	NA	MET S1-008	-	-	-	-	-	-	-	-	-	-	-	-	-	-	-	-	-
Senftenberg	Food	MET S1-010	+	-	-	-	-	-	+	-	-	-	-	-	-	-	-	-	-
Othmarschen	Food	MET S1-087	-	-	-	-	-	-	-	-	-	-	-	-	-	-	-	-	-
Newport	Animal	MET S1-166	-	-	-	-	-	-	-	-	-	-	-	-	-	-	T+	T+	-
Braenderup	NI	MET S1-713	-	-	-	-	-	-	-	-	-	-	-	-	-	-	-	-	-
Mbandaka	Sludge	MET S1-864	-	-	-	-	-	-	-	-	-	-	-	-	-	-	-	-	-
Liverpool	Food	MET A2-099	-	-	-	-	-	-	T+	T+	-	-	-	-	-	-	-	-	-
Virchow	Food	MET S1-003	+	+	+	+	+	+	T+	T+	+	+	+	+	+	+	+	+	+
Agona	Food	MET S1-011	-	-	-	-	-	-	-	-	-	T+	-	-	-	-	-	-	-
Typhi	Human	MET S1-220	-	-	-	-	-	-	-	-	-	-	-	-	-	-	-	-	-
Paratyphi B	Human	MET S1-184	+	+	+	+	+	+	+	+	T+	T+	T+	T+	T+	T+	T+	T+	+

+: complete clearing

T+: Turbid zone

P: Individual phages

-: No interaction

Appendix D (continued)

Serotype	Isolate Source	METUID	p052	p055	p058	p061	p064	p067	p070	p073	p076	p079	p082	p085	p088	p091	p094	p097	p100
Enteritidis	FOOD	MET S1-742	+	+	+	+	+	+	+	+	+	+	+	+	+	T+	T+	-	T+
Enteritidis	HUMAN	MET S1-217	T+	T+	T+	T+	T+	T+	T+	+	+	+	+	+	+	T+	T+	+	+
Enteritidis	HUMAN	MET S1-221	T+	T+	T+	T+	T+	T+	T+	+	+	+	+	+	+	T+	T+	-	-
Enteritidis	FOOD	MET S1-411	+	+	+	+	+	+	+	+	+	+	+	+	+	T+	T+	-	-
Enteritidis	SLUDGE	MET A2-012	+	+	+	+	+	+	+	+	+	+	+	+	+	-	-	-	-
Typhimurium	HUMAN	MET S1-223	+	T+	T+	T+	T+	+	+	+	+	+	+	T+	+	T+	T+	-	-
Typhimurium	HUMAN	MET S1-185	-	T+	-	-	-	-	-	-	-	-	T+	T+	T+	T+	T+	-	-
Typhimurium	ANIMAL	MET S1-663	+	+	+	T+	T+	T+	T+	+	+	+	+	+	+	T+	T+	-	-
Typhimurium	SLUDGE	MET A2-003	+	+	T+	T+	T+	T+	T+	+	+	+	+	+	+	T+	T+	-	-
Typhimurim	DT104	MET A2-088	+	+	+	+	+	+	+	+	+	+	+	T+	T+	T+	T+	-	+
Typhimurium	ANIMAL	MET S1-657	T+	T+	T+	T+	T+	T+	T+	+	+	+	+	+	+	T+	T+	-	-
Infantis	FOOD	MET S1-050	-	T+	-	-	-	-	-	-	-	-	-	T+	-	+	+	+	+
Infantis	Thailand	MET S1-807	-	-	-	-	-	-	-	-	-	-	-	-	-	+	+	T+	+
Infantis	SLUDGE	MET S1-857	-	-	-	-	-	-	-	-	-	-	-	-	-	+	+	T+	+
Kentucky	HUMAN	MET S1-240	-	-	-	-	-	-	-	-	-	-	-	-	T+	+	+	+	+
Kentucky	ANIMAL	MET S1-542	-	T+	-	-	-	-	-	-	-	-	T+	-	-	+	+	+	+
Kentucky	SLUDGE	MET A2-072	-	-	-	-	-	-	-	-	-	-	T+	-	T+	+	+	+	T+
Montevideo	FOOD	MET S1-065	-	-	-	-	-	-	-	-	-	-	-	-	T+	T+	T+	T+	+
Montevideo	ANIMAL	MET S1-170	-	-	-	-	-	-	-	-	-	-	-	-	-	T+	T+	-	T+
Montevideo	ANIMAL	MET S1-172	-	-	-	-	-	-	-	-	-	-	-	-	-	-	-	T+	T+
Anatum	Food	MET S1-548	-	T+	-	-	-	-	-	-	-	-	T+	-	-	+	+	T+	+
Anatum	Food	MET S1-579	-	-	-	-	-	-	-	-	-	-	-	+	+	-	P	T+	-
Hadar	Food	MET S1-163	-	-	-	-	-	-	-	-	-	-	-	+	+	-	-	-	-

Appendix D (continued)

Telaviv	Food	MET S1-074	-	T+	-	-	-	-	-	-	-	-	-	T+	T+	+	T+	+	+
Telaviv	Food	MET S1-530	-	-	-	-	-	-	-	-	-	-	-	-	T+	+	+	T+	T+
Thompson	NA	MET S1-008	T+	-	-	-	-	-	-	-	-	-	T+	+	T+	T+	T+	T+	+
Senftenberg	Food	MET S1-010	-	T+	-	-	T+	-	-	-	-	-	+	T+	T+	-	-	-	-
Othmarschen	Food	MET S1-087	-	-	-	-	-	-	-	-	-	-	+	-	T+	T+	+	T+	+
Newport	Animal	MET S1-166	-	-	-	-	-	-	-	-	-	-	+	+	+	T+	+	-	-
Braenderup	NI	MET S1-713	-	-	-	-	-	-	-	-	-	-	-	-	T+	T+	+	+	+
Mbandaka	Sludge	MET S1-864	-	-	-	-	-	-	-	-	-	-	-	-	-	-	-	-	-
Liverpool	Food	MET A2-099	-	-	-	-	-	-	-	-	-	-	-	-	-	-	-	-	-
Virchow	Food	MET S1-003	+	+	+	+	+	+	+	+	+	+	+	+	+	-	-	-	T+
Agona	Food	MET S1-011	T+	T+	-	-	-	-	-	-	-	+	+	+	+	+	+	+	+
Typhi	Human	MET S1-220	-	-	-	-	-	-	-	-	-	-	-	-	-	-	+	+	+
Paratyphi B	Human	MET S1-184	+	T+	T+	T+	T+	T+	T+	T+	T+	T+	T+	T+	T+	T+	T+	T+	+

+: complete clearing

T+: Turbid zone

P: Individual phages

-: No interaction

Appendix D (continued)

Serotype	Isolate Source	METUID	p103	p107	p110	p113	p116	p119	p122	p125	p128	p131	p134	p137	p140	p143	p146	p149	p152
Enteritidis	FOOD	MET S1-742	+	+	+	+	T+	+	+	+	+	+	P	T+	T+	+	+	+	+
Enteritidis	HUMAN	MET S1-217	P	-	+	+	+	+	-	+	-	-	+	+	+	-	-	-	-
Enteritidis	HUMAN	MET S1-221	T+	T+	T+	T+	-	-	+	T+	T+	T+	T+	T+	T+	T+	T+	T+	T+
Enteritidis	FOOD	MET S1-411	+	+	-	T+	T+	-	+	-	+	+		T+	T+	T+	+	T+	+
Enteritidis	SLUDGE	MET A2-012	+	+	-	+	-	-	+	-	-	+	-	-	+	T+	+	T+	T+
Typhimurium	HUMAN	MET S1-223	T+	T+	-	T+	-	-	T+	+	-	T+	T+	-	-	T+	T+	T+	T+
Typhimurium	HUMAN	MET S1-185	+	T+	T+	T+	-	-	+	T+	T+	T+	T+	-	T+	T+	+	T+	T+
Typhimurium	ANIMAL	MET S1-663	+	T+	-	+	-	-	T+	T+	-	T+	-	-	-	T+	T+	+	T+
Typhimurium	SLUDGE	MET A2-003	+	T+	T+	T+	-	-	+	-	-	T+	-	-	-	T+	T+	T+	T+
Typhimurim	DT104	MET A2-088	+	+	-	-	+	-	+	T+	T+	+	T+	+	-	-	-	+	T+
Typhimurium	ANIMAL	MET S1-657	T+	T+	-	T+	-	-	T+	T+	-	T+	-	-	-	T+	T+	T+	T+
Infantis	FOOD	MET S1-050	T+	T+	T+	-	+	+	+	+	T+	T+	T+	T+	-	-	-	-	-
Infantis	Thailand	MET S1-807	P	T+	P	T+	+	+	T+	T+	-	T+	-	-	T+	-	-	-	-
Infantis	SLUDGE	MET S1-857	-	-	T+	+	+	-	-	-	+	T+	-	T+	T+	T+	-	T+	-
Kentucky	HUMAN	MET S1-240	-	T+	-	-	+	+	T+	T+	-	-	+	+	+	-	-	-	-
Kentucky	ANIMAL	MET S1-542	+	+	-	-	+	+	T+	+	-	+	+	+	+	+	T+	T+	T+
Kentucky	SLUDGE	MET A2-072	-	-	-	-	T+	T+	-	T+	-	T+	+	+	-	-	-	-	-
Montevideo	FOOD	MET S1-065	T+	-	-	-	T+	T+	T+	-	-	-	-	-	-	-	-	-	-
Montevideo	ANIMAL	MET S1-170	T+	-	-	-	T+	T+	T+	-	-	-	-	-	-	-	T+	-	-
Montevideo	ANIMAL	MET S1-172	-	-	-	-	T+	T+	-	T+	T+	T+	T+	T+	T+	T+	T+	-	-
Anatum	Food	MET S1-548	+	-	T+	+	+	+	+	T+	-	T+	T+	T+	T+	T+	T+	-	-
Anatum	Food	MET S1-579	-	-	-	-	-	-	-	+	T+	T+	-	-	-	-	-	T+	-
Hadar	Food	MET S1-163	-	-	-	-	-	-	-	+	-	+	T+	T+	-	-	-	-	-

Telaviv	Food	MET S1-074	+	T+	T+	+	+	+	+	T+	T+	T+	T+	T+	+	-	T+	-	-
Telaviv	Food	MET S1-530	T+	T+	P	T+	T+	T+	T+	+	T+	-	T+	T+	T+	-	T+	-	-
Thompson	NA	MET S1-008	T+	-	+	T+	+	+	-	-	T+	-	T+	-	-	-	-	-	T+
Senftenberg	Food	MET S1-010	-	T+	-	-	-	-	-	T+	-	T+	-	-	-	-	+	+	-
Othmarschen	Food	MET S1-087	T+	T+	T+	-	+	+	T+	T+	T+	T+	-	-	-	-	T+	-	-
Newport	Animal	MET S1-166	-	-	-	-	-	-	-	+	T+	T+	T+	T+	-	-	T+	-	-
Braenderup	NI	MET S1-713	-	-	-	-	+	+	-	T+	-	-	-	-	T+	-	-	-	-
Mbandaka	Sludge	MET S1-864	-	-	-	-	-	-	-	-	-	-	-	-	T+	-	-	-	-
Liverpool	Food	MET A2-099	-	-	-	-	-	-	-	-	-	-	-	-	+	-	-	-	-
Virchow	Food	MET S1-003	+	+	T+	T+	T+	-	-	T+	+	T+	+	-	+	+	T+	T+	
Agona	Food	MET S1-011	+	T+	T+	T+	T+	T+	T+	T+	-	-	-	-	T+	T+	-	-	-
Typhi	Human	MET S1-220	-	-	-	-	+	+	P	+	-	-	T+	T+	-	-	T+	-	-
Paratyphi B	Human	MET S1-184	+	+	-	-	T+	+	T+	T+	T+	T+	-	T+	-	T+	+	+	+

+: complete clearing

T+: Turbid zone

P: Individual phages

-: No interaction

Appendix D (continued)

Serotype	Isolate Source	METUID	p155	p158	p161	p164	p167	p170	p173	p176	p179	p182	p185	p188	p191	p194	p197	p200	p203
Enteritidis	FOOD	MET S1-742	+	+	+	+	+	+	+	+	+	+	+	+	+	+	T+	T+	T+
Enteritidis	HUMAN	MET S1-217	-	-	-	-	-	-	-	+	+	-	-	T+	-	+	+	+	-
Enteritidis	HUMAN	MET S1-221	T+	T+	T+	T+	T+	T+	-	-	T+	T+	-	-	T+	+	T+	T+	T+
Enteritidis	FOOD	MET S1-411	+	+	+	+	T+	T+	-	-	+	-	T+	-	T+	+	T+	T+	T+
Enteritidis	SLUDGE	MET A2-012	T+	T+	T+	T+	T+	T+	-	-	P	+	-	-	-	+	T+	-	-
Typhimurium	HUMAN	MET S1-223	T+	T+	T+	T+	T+	T+	-	T+	T+	T+	-	-	T+	T+	+	-	T+
Typhimurium	HUMAN	MET S1-185	-	T+	+	+	+	T+	T+	+	+	T+	+	-	T+	T+	-	T+	T+
Typhimurium	ANIMAL	MET S1-663	T+	+	T+	+	+	+	-	-	-	T+	-	-	T+	+	-	-	T+
Typhimurium	SLUDGE	MET A2-003	T+	T+	T+	T+	T+	T+	-	-	T+	T+	-	-	T+	+	+	-	+
Typhimurium	DT104	MET A2-088	+	+	+	+	+	+	-	-	T+	T+	T+	-	T+	-	T+	-	T+
Typhimurium	ANIMAL	MET S1-657	+	+	+	+	T+	T+	-	T+	T+	T+	-	-	T+	T+	-	T+	-
Infantis	FOOD	MET S1-050	-	-	+	+	+	-	-	T+	-	-	-	-	-	-	T+	T+	-
Infantis	Thailand	MET S1-807	-	-	-	-	-	-	-	-	-	-	-	-	-	-	T+	T+	-
Infantis	SLUDGE	MET S1-857	-	-	-	-	-	-	T+	T+	T+	-	T+	T+	T+	-	T+	T+	-
Kentucky	HUMAN	MET S1-240	-	-	-	-	-	-	-	-	-	-	P	+	-	-	-	+	T+
Kentucky	ANIMAL	MET S1-542	T+	T+	T+	T+	T+	T+	-	-	T+	T+	+	+	+	+	+	-	-
Kentucky	SLUDGE	MET A2-072	-	-	-	-	-	-	-	-	T+	T+	+	-	-	-	T+	T+	-
Montevideo	FOOD	MET S1-065	-	-	T+	T+	-	-	-	-	T+	-	-	-	-	-	-	T+	-
Montevideo	ANIMAL	MET S1-170	-	-	T+	T+	-	-	-	-	T+	-	-	-	T+	-	-	-	T+
Montevideo	ANIMAL	MET S1-172	-	-	T+	T+	-	-	-	T+	T+	T+	-	-	-	-	T+	-	T+
Anatum	Food	MET S1-548	-	-	T+	-	T+	-	T+	T+	T+	-	T+	T+	+	-	-	T+	-
Anatum	Food	MET S1-579	-	-	-	T+	T+	T+	-	-	-	-	-	-	-	+	-	T+	-
Hadar	Food	MET S1-163	-	-	-	-	-	-	-	-	+	-	-	-	-	+	+	-	-

Telaviv	Food	MET S1-074	T+	-	+	+	T+	-	T+	+	+	-	-	-	+	-	-	T+	T+
Telaviv	Food	MET S1-530	-	-	-	T+	T+	T+	P	P	-	-	-	-	T+	T+	T+	T+	-
Thompson	NA	MET S1-008	T+	T+	-	-	-	-	-	-	-	-	-	-	-	-	-	T+	T+
Senftenberg	Food	MET S1-010	T+	-	-	-	-	+	-	-	-	-	-	-	-	+	+	-	-
Othmarschen	Food	MET S1-087	-	-	-	-	-	-	-	-	T+	-	-	-	+	-	T+	-	-
Newport	Animal	MET S1-166	-	-	-	-	-	-	-	-	+	-	-	T+	-	+	+	T+	-
Braenderup	NI	MET S1-713	-	-	-	-	-	-	-	-	-	-	-	-	-	-	-	-	-
Mbandaka	Sludge	MET S1-864	-	-	-	-	-	-	T+	T+	-	-	-	-	-	-	-	-	-
Liverpool	Food	MET A2-099	-	-	-	-	-	-	-	-	-	-	-	T+	-	T+	T+	-	-
Virchow	Food	MET S1-003	T+	T+	T+	T+	T+	T+	-	-	T+	T+	T+	-	T+	T+	+	+	-
Agona	Food	MET S1-011	T+	-	-	-	-	-	-	T+	-	T+	-	T+	T+	-	-	-	-
Typhi	Human	MET S1-220	-	-	T+	T+	-	-	-	T+	T+	-	P	T+	-	T+	-	-	-
Paratyphi B	Human	MET S1-184	+	+	+	+	+	+	T+	T+	T+	T+	-	-	T+	+	T+	-	T+

+: complete clearing

T+: Turbid zone

P: Individual phages

-: No interaction

E. PhageTerm reports

putative_phage PhageTerm Analysis

COS (5')

PhageTerm Method

Ends	Left (red)	Right (green)	Permuted	Orientation	Class	Type
Non Red.	6635	6646	No	NA	COS (5')	Lambda

Sequence cohesive: GCTCTGCGCACC

Strand	Location	T	pvalue	T (Start. Pos. Cov. / Whole Cov.)
	6635	0.44	9.23e-58	strand (+)
	58795	0.06	1.00e+00	
+	1	0.06	1.99e-01	6635
	58524	0.06	1.00e+00	
	58520	0.05	1.00e+00	
	6646	0.56	4.08e-164	strand (-)
	79	0.07	1.00e+00	
-	415	0.07	1.00e+00	6646
	417	0.07	1.00e+00	
	161	0.07	1.00e+00	

Li's Method

Packaging	Termini	Forward	Reverse	Orientation
COS	Fixed	Obvious Termini	Obvious Termini	Reverse

Sequence cohesive: GCTCTGCGCACC

PhageTerm report of Group 1 (59k) phages. These phages had obvious termini, and reoriented automatically

my_phage PhageTerm Analysis

UNKNOWN

?

PhageTerm Method

Ends	Left (red)	Right (green)	Permuted	Orientation	Class	Type
Redundant	Random	Random	Yes		-	-

Strand	Location	T	pvalue	T (Start. Pos. Cov. / Whole Cov.)
	29195	0.18	1.00e+00	
	11440	0.16	1.00e+00	
+	40709	0.16	1.00e+00	
	37813	0.16	1.00e+00	
	7825	0.15	1.00e+00	
	12437	0.18	1.00e+00	
	15455	0.18	1.00e+00	
-	34379	0.17	1.00e+00	
	8015	0.16	1.00e+00	
	29041	0.15	1.00e+00	

Li's Method

Packaging	Termini	Forward	Reverse	Orientation
OTHER	Absence	No Obvious Termini	No Obvious Termini	Reverse

PhageTerm report of Group 2 (43k) phages. These phages couldn't be identified by the program, and reoriented manually

putative_phage PhageTerm Analysis

DTR (long)

- - - - - - - - WARNING: Coverage (14) is under the limit of the software, Please consider results carrefuly. - - - - - - - -

PhageTerm Method

Ends	Left (red)	Right (green)	Permuted	Orientation	Class	Type
Redundant	90116	99877	No	NA	DTR (long)	T5

Direct Terminal Repeats: 9762 bp

Strand	Location	T	pvalue	T (Start. Pos. Cov. / Whole Cov.)
	90116	0.52	1.03e-11	strand (+)
	20680	0.20	1.00e+00	
+	2362	0.14	1.00e+00	90116
	68979	0.14	1.00e+00	
	20946	0.14	1.00e+00	
	99877	0.41	7.03e-08	strand (-)
	99406	0.22	5.69e-02	
-	106782	0.17	1.00e+00	99877
	37783	0.16	1.00e+00	
	20956	0.14	1.00e+00	

Li's Method

Packaging	Termini	Forward	Reverse	Orientation
PAC	Fixed	Obvious Termini	Multiple-Pref. Term.	Forward

PhageTerm report of Group 3 (112k) phages. These phages had Direct Terminal Repeats, and reoriented automatically

putative_phage PhageTerm Analysis

PhageTerm Method

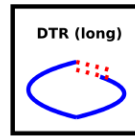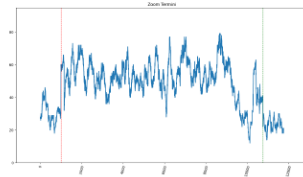| Ends	Left (red)	Right (green)	Permuted	Orientation	Class	Type
Redundant	16606	27295	No	NA	DTR (long)	T5

Direct Terminal Repeats: 10690 bp

Strand	Location	T	pvalue
	16606	0.40	4.73e-32
	3789	0.10	1.00e+00
+	425	0.07	1.00e+00
	111799	0.07	1.00e+00
	71682	0.07	1.08e-04
	27295	0.38	3.07e-25
	97142	0.10	1.00e+00
-	3804	0.10	6.08e-02
	97140	0.09	1.00e+00
	3784	0.08	2.56e-03

T (Start. Pos. Cov. / Whole Cov.)

Li's Method

Packaging	Termini	Forward	Reverse	Orientation
COS	Fixed	Obvious Termini	Obvious Termini	Reverse

Direct Terminal Repeats: 10690 bp

PhageTerm report of Group 4 (122k) phages. These phages had Direct Terminal Repeats, and reoriented automatically

putative_phage PhageTerm Analysis

UNKNOWN

?

PhageTerm Method

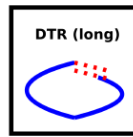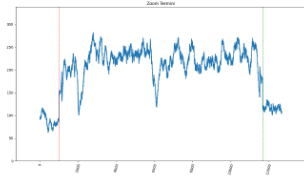| Ends	Left (red)	Right (green)	Permuted	Orientation	Class	Type
Redundant	Random	Random	Yes		-	-

Strand	Location	T	pvalue	T (Start. Pos. Cov. / Whole Cov.)
	11062	0.12	1.00e+00	
	26890	0.10	1.00e+00	
+	29988	0.10	1.00e+00	
	4196	0.10	1.00e+00	
	6145	0.10	1.00e+00	
	17276	0.20	1.00e+00	
	13148	0.10	1.00e+00	
-	15693	0.10	1.00e+00	
	7755	0.10	1.00e+00	
	23212	0.10	1.00e+00	

Li's Method

Packaging	Termini	Forward	Reverse	Orientation
OTHER	Fixed	Multiple-Pref. Term.	Multiple-Pref. Term.	Forward

PhageTerm report of Group 5 (31k) phage. This phage couldn't be identified by the program, and reoriented manually

F. Phage annotations

Phage Annotation of Group 1 Phages (59k)

Gene		Close Relative (Chi)	Caudovirales Database
locus_tag	length _bp	product	product
JKDLMKBC_ 00001	288	HTH DNA binding protein	hypothetical protein
JKDLMKBC_ 00002	2586	DNA primase	hypothetical protein
JKDLMKBC_ 00003	282	hypothetical protein	hypothetical protein
JKDLMKBC_ 00004	405	hypothetical protein	hypothetical protein
JKDLMKBC_ 00005	330	hypothetical protein	hypothetical protein
JKDLMKBC_ 00006	1338	exonuclease	hypothetical protein
JKDLMKBC_ 00007	597	Gp2.5-like ssDNA binding protein and ssDNA annealing protein	hypothetical protein
JKDLMKBC_ 00008	2040	DNA polymerase	hypothetical protein
JKDLMKBC_ 00009	528	HNH endonuclease	hypothetical protein
JKDLMKBC_ 00010	288	endonuclease	hypothetical protein
JKDLMKBC_ 00011	1476	DNA helicase	hypothetical protein
JKDLMKBC_ 00012	570	terminase small subunit	hypothetical protein
JKDLMKBC_ 00013	2076	terminase large subunit	hypothetical protein
JKDLMKBC_ 00014	255	head-tail adaptor Ad1	hypothetical protein
JKDLMKBC_ 00015	1680	portal protein	Portal protein B
JKDLMKBC_ 00016	1317	head maturation protease	hypothetical protein
JKDLMKBC_ 00017	396	head decoration	hypothetical protein
JKDLMKBC_ 00018	1065	major head protein	Major capsid protein
JKDLMKBC_ 00019	294	hypothetical protein	hypothetical protein
JKDLMKBC_ 00020	366	hypothetical protein	hypothetical protein
JKDLMKBC_ 00021	627	tail completion or Neck1 protein	hypothetical protein

Appendix F (continued)

JKDLMKBC_0002 2	504	tail terminator	hypothetical protein
JKDLMKBC_0002 3	114 0	major tail protein with Ig-like domain protein	hypothetical protein
JKDLMKBC_0002 4	462	tail protein	hypothetical protein
JKDLMKBC_0002 5	429 6	tail length tape measure protein	hypothetical protein
JKDLMKBC_0002 6	168 9	tail assembly protein	hypothetical protein
JKDLMKBC_0002 7	819	tail assembly protein	hypothetical protein
JKDLMKBC_0002 8	231	tail assembly chaperone	hypothetical protein
JKDLMKBC_0002 9	240	tail assembly chaperone	hypothetical protein
JKDLMKBC_0003 0	390 0	tail protein	hypothetical protein
JKDLMKBC_0003 1	741	tail fiber protein	hypothetical protein
JKDLMKBC_0003 2	100 8	hypothetical protein	hypothetical protein
JKDLMKBC_0003 3	963	hypothetical protein	hypothetical protein
JKDLMKBC_0003 4	102 0	hypothetical protein	hypothetical protein
JKDLMKBC_0003 5	122 7	hypothetical protein	hypothetical protein
JKDLMKBC_0003 6	213 0	hypothetical protein	hypothetical protein
JKDLMKBC_0003 7	339	Rz-like spanin	hypothetical protein
JKDLMKBC_0003 8	714	endolysin	hypothetical protein
JKDLMKBC_0003 9	255	Rz-like spanin	hypothetical protein
JKDLMKBC_0004 0	462	nucleoside 2-deoxyribosyltransferase	hypothetical protein
JKDLMKBC_0004 1	285	hypothetical protein	hypothetical protein
JKDLMKBC_0004 2	705	hypothetical protein	hypothetical protein
JKDLMKBC_0004 3	264	hypothetical protein	hypothetical protein
JKDLMKBC_0004 4	453	hypothetical protein	hypothetical protein
JKDLMKBC_0004 5	312	hypothetical protein	hypothetical protein
JKDLMKBC_0004 6	282	hypothetical protein	hypothetical protein

Appendix F (continued)

JKDLMKBC_0004 7	513	thymidylate synthase complementing protein	hypothetical protein
JKDLMKBC_0004 8	255	hypothetical protein	hypothetical protein
JKDLMKBC_0004 9	216	hypothetical protein	hypothetical protein
JKDLMKBC_0005 0	195	hypothetical protein	hypothetical protein
JKDLMKBC_0005 1	534	hypothetical protein	hypothetical protein
JKDLMKBC_0005 2	687	DNA methyltransferase	hypothetical protein
JKDLMKBC_0005 3	110 1	hypothetical protein	hypothetical protein
JKDLMKBC_0005 4	606	hypothetical protein	hypothetical protein
JKDLMKBC_0005 5	741	hypothetical protein	hypothetical protein
JKDLMKBC_0005 6	276	hypothetical protein	hypothetical protein
JKDLMKBC_0005 7	234	hypothetical protein	hypothetical protein
JKDLMKBC_0005 8	107 4	exonuclease recombination-associated	hypothetical protein
JKDLMKBC_0005 9	363	hypothetical protein	hypothetical protein
JKDLMKBC_0006 0	336	hypothetical protein	hypothetical protein
JKDLMKBC_0006 1	441	hypothetical protein	hypothetical protein
JKDLMKBC_0006 2	372	hypothetical protein	hypothetical protein
JKDLMKBC_0006 3	525	HNH endonuclease	hypothetical protein
JKDLMKBC_0006 4	258	hypothetical protein	hypothetical protein
JKDLMKBC_0006 5	540	hypothetical protein	hypothetical protein
JKDLMKBC_0006 6	483	hypothetical protein	hypothetical protein
JKDLMKBC_0006 7	549	hypothetical protein	hypothetical protein
JKDLMKBC_0006 8	222	hypothetical protein	hypothetical protein
JKDLMKBC_0006 9	459	hypothetical protein	hypothetical protein
JKDLMKBC_0007 0	222	hypothetical protein	hypothetical protein
JKDLMKBC_0007 1	129	hypothetical protein	hypothetical protein

Appendix F (continued)

JKDLMKBC_00072	273	hypothetical protein	hypothetical protein

Phage Annotation of Group 3 Phages (112k)

Gene		Close Relative (se8)	Caudovirales Database
locus_tag	length_bp	product	product
APGFIDEJ_00001	195	hypothetical protein	product
APGFIDEJ_00002	162	hypothetical protein	hypothetical protein
APGFIDEJ_00003	345	hypothetical protein	hypothetical protein
APGFIDEJ_00004	126	hypothetical protein	hypothetical protein
APGFIDEJ_00005	213	hypothetical protein	hypothetical protein
APGFIDEJ_00006	147	hypothetical protein	hypothetical protein
APGFIDEJ_00007	231	hypothetical protein	hypothetical protein
APGFIDEJ_00008	996	hypothetical protein	hypothetical protein
APGFIDEJ_00009	204	hypothetical protein	hypothetical protein
APGFIDEJ_00010	252	hypothetical protein	hypothetical protein
APGFIDEJ_00011	408	A2 protein	hypothetical protein
APGFIDEJ_00012	198	membrane protein	hypothetical protein
APGFIDEJ_00013	1665	DNA transfer protein	Protein A2
APGFIDEJ_00014	258	hypothetical protein	hypothetical protein
APGFIDEJ_00015	393	hypothetical protein	Protein A1
APGFIDEJ_00016	735	deoxynucleoside-5'-monophosphatase	hypothetical protein
APGFIDEJ_00017	192	membrane protein	hypothetical protein
APGFIDEJ_00018	138	membrane protein	5'-deoxynucleotidase
APGFIDEJ_00019	108	tail fiber protein	hypothetical protein
APGFIDEJ_00020	156	hypothetical protein	hypothetical protein
APGFIDEJ_00021	129	hypothetical protein	hypothetical protein

APGFIDEJ_00022	267	receptor-blocking protein	hypothetical protein
APGFIDEJ_00023	1758	receptor-blocking protein	hypothetical protein
APGFIDEJ_00024	483	terminase small subunit	hypothetical protein
APGFIDEJ_00025	1317	terminase large subunit	hypothetical protein
APGFIDEJ_00026	438	hypothetical protein	hypothetical protein
APGFIDEJ_00027	1212	portal protein	putative terminase, small subunit
APGFIDEJ_00028	495	Hoc-like head decoration	Terminase, large subunit
APGFIDEJ_00029	633	putative prohead protease	Nicking endonuclease
APGFIDEJ_00030	1377	capsid family protein	Portal protein
APGFIDEJ_00031	513	head-tail adaptor	Decoration protein
APGFIDEJ_00032	768	tail completion protein	Prohead protease
APGFIDEJ_00033	486	tail terminator	Major capsid protein
APGFIDEJ_00034	1398	tail fibers protein	hypothetical protein
APGFIDEJ_00035	897	tail fibers protein	Tail completion protein
APGFIDEJ_00036	405	Tail assembly chaperone	Tail tube terminator protein
APGFIDEJ_00037	369	tail assembly chaperone	Tail tube protein
APGFIDEJ_00038	3681	tape measure protein	Minor tail protein
APGFIDEJ_00039	615	distal tail protein	hypothetical protein
APGFIDEJ_00040	2850	tail length tape-measure protein	hypothetical protein
APGFIDEJ_00041	2085	straight fibre tail protein	putative tape measure protein
APGFIDEJ_00042	423	collar tail protein for L-shaped tail fibre attachment	Distal tail protein
APGFIDEJ_00043	2940	tail fiber protein	putative baseplate hub protein
APGFIDEJ_00044	264	hypothetical protein	putative central straight fiber
APGFIDEJ_00045	447	deoxyUTPpyrophosphatase	L-shaped tail fiber protein p132
APGFIDEJ_00046	876	flap endonuclease	hypothetical protein

Appendix F (continued)

APGFIDEJ_00047	483	D14 protein	hypothetical protein
APGFIDEJ_00048	1839	recombination-related exonuclease	Deoxyuridine 5'-triphosphate nucleotidohydrolase
APGFIDEJ_00049	978	SbcD-like subunit of palindrome specific endonuclease	Flap endonuclease
APGFIDEJ_00050	774	D11 protein	Protein D14
APGFIDEJ_00051	285	hypothetical protein	putative exonuclease subunit 2
APGFIDEJ_00052	1353	putative ATP-dependent helicase	putative exonuclease subunit 1
APGFIDEJ_00053	498	hypothetical protein	putative ssDNA-binding protein
APGFIDEJ_00054	2568	DNA polymerase I	hypothetical protein
APGFIDEJ_00055	891	putative DNA replication primase	putative helicase D10
APGFIDEJ_00056	1524	DnaB-like replicative helicase	DNA polymerase
APGFIDEJ_00057	768	endonuclease	hypothetical protein
APGFIDEJ_00058	780	DNA ligase	hypothetical protein
APGFIDEJ_00059	972	DNA ligase	Putative transcription factor D5
APGFIDEJ_00060	309	transcriptional regulator	hypothetical protein
APGFIDEJ_00061	297	hypothetical protein	DNA ligase
APGFIDEJ_00062	411	DNA binding protein	hypothetical protein
APGFIDEJ_00063	237	transcriptional regulator	hypothetical protein
APGFIDEJ_00064	705	D2 protein	hypothetical protein
APGFIDEJ_00065	234	hypothetical protein	hypothetical protein
APGFIDEJ_00066	519	HNH endonuclease	hypothetical protein
APGFIDEJ_00067	2787	putative replication origin binding protein	hypothetical protein
APGFIDEJ_00068	393	hypothetical protein	Putative replication origin binding protein
APGFIDEJ_00069	429	hypothetical protein	hypothetical protein
APGFIDEJ_00070	507	Sir2 (NAD-dependent deacetylase)	hypothetical protein
APGFIDEJ_00071	168	hypothetical protein	hypothetical protein

Appendix F (continued)

APGFIDEJ_00072	825	SIR2 family protein	hypothetical protein
APGFIDEJ_00073	222	hypothetical protein	hypothetical protein
APGFIDEJ_00074	204	hypothetical protein	hypothetical protein
APGFIDEJ_00075	282	hypothetical protein	hypothetical protein
APGFIDEJ_00076	1875	anaerobic ribonucleoside-triphosphate reductase	hypothetical protein
APGFIDEJ_00077	753	phosphate starvation inducible protein	Anaerobic ribonucleoside-triphosphate reductase
APGFIDEJ_00078	222	tail length tape measure protein	hypothetical protein
APGFIDEJ_00079	2436	aerobic ribonucleoside diphosphate reductase, large subunit	hypothetical protein
APGFIDEJ_00080	1146	putative aerobic ribonucleoside diphosphate reductase, small subunit	Ribonucleoside-diphosphate reductase large subunit
APGFIDEJ_00081	534	putative dihydrofolate reductase	hypothetical protein
APGFIDEJ_00082	840	thymidylate synthase	Dihydrofolate reductase
APGFIDEJ_00083	204	hypothetical protein	putative thymidylate synthase
APGFIDEJ_00084	282	hypothetical protein	hypothetical protein
APGFIDEJ_00085	477	ribonuclease H	hypothetical protein
APGFIDEJ_00086	285	hypothetical protein	hypothetical protein
APGFIDEJ_00087	450	swarming motility protein	hypothetical protein
APGFIDEJ_00088	516	hypothetical protein	hypothetical protein
APGFIDEJ_00089	216	baseplate wedge subunit	hypothetical protein
APGFIDEJ_00090	237	hypothetical protein	hypothetical protein
APGFIDEJ_00091	702	metallopeptidase	hypothetical protein
APGFIDEJ_00092	183	hypothetical protein	hypothetical protein
APGFIDEJ_00093	639	tail fibers protein	hypothetical protein
APGFIDEJ_00094	318	hypothetical protein	hypothetical protein
APGFIDEJ_00095	450	cell wall hydrolase	hypothetical protein

Appendix F (continued)

APGFIDEJ_00096	171	hypothetical protein	hypothetical protein
APGFIDEJ_00097	444	recombination-related exonuclease	hypothetical protein
APGFIDEJ_00098	75	tRNA-Arg(tct)	hypothetical protein
APGFIDEJ_00099	948	putative transmembrane protein	tRNA-Arg(tct)
APGFIDEJ_00100	417	hypothetical protein	hypothetical protein
APGFIDEJ_00101	987	hypothetical protein	hypothetical protein
APGFIDEJ_00102	519	DNA primase	hypothetical protein
APGFIDEJ_00103	89	tRNA-Ser(gct)	hypothetical protein
APGFIDEJ_00104	189	hypothetical protein	tRNA-Ser(gct)
APGFIDEJ_00105	186	antitermination protein Q	hypothetical protein
APGFIDEJ_00106	339	hypothetical protein	hypothetical protein
APGFIDEJ_00107	77	tRNA-Leu(taa)	hypothetical protein
APGFIDEJ_00108	168	hypothetical protein	tRNA-Leu(taa)
APGFIDEJ_00109	207	hypothetical protein	hypothetical protein
APGFIDEJ_00110	270	hypothetical protein	hypothetical protein
APGFIDEJ_00111	88	tRNA-Tyr(gta)	hypothetical protein
APGFIDEJ_00112	75	tRNA-Glu(ttc)	tRNA-Tyr(gta)
APGFIDEJ_00113	77	tRNA-Trp(cca)	tRNA-Glu(ttc)
APGFIDEJ_00114	75	tRNA-Phe(gaa)	tRNA-Trp(cca)
APGFIDEJ_00115	273	hypothetical protein	tRNA-Phe(gaa)
APGFIDEJ_00116	76	tRNA-Cys(gca)	hypothetical protein
APGFIDEJ_00117	83	tRNA-Asn(gtt)	tRNA-Cys(gca)
APGFIDEJ_00118	186	hypothetical protein	tRNA-Asn(gtt)
APGFIDEJ_00119	77	tRNA-Asp(gtc)	hypothetical protein
APGFIDEJ_00120	348	hypothetical protein	tRNA-Asp(gtc)

Appendix F (continued)

APGFIDEJ_00121	159	hypothetical protein	hypothetical protein
APGFIDEJ_00122	78	tRNA-Pro(tgg)	hypothetical protein
APGFIDEJ_00123	78	tRNA-Met(cat)	tRNA-Pro(tgg)
APGFIDEJ_00124	168	hypothetical protein	tRNA-Met(cat)
APGFIDEJ_00125	79	tRNA-Lys(ttt)	hypothetical protein
APGFIDEJ_00126	318	hypothetical protein	tRNA-Lys(ttt)
APGFIDEJ_00127	74	tRNA-Val(tac)	hypothetical protein
APGFIDEJ_00128	74	tRNA-Ala(tgc)	tRNA-Val(tac)
APGFIDEJ_00129	77	tRNA-Leu(tag)	tRNA-Ala(tgc)
APGFIDEJ_00130	90	tRNA-Ser(tga)	tRNA-Leu(tag)
APGFIDEJ_00131	174	hypothetical protein	tRNA-Ser(tga)
APGFIDEJ_00132	77	tRNA-His(gtg)	hypothetical protein
APGFIDEJ_00133	195	hypothetical protein	tRNA-His(gtg)
APGFIDEJ_00134	76	tRNA-Gln(ctg)	hypothetical protein
APGFIDEJ_00135	76	tRNA-Gln(ttg)	tRNA-Gln(ctg)
APGFIDEJ_00136	75	tRNA-Gly(tcc)	tRNA-Gln(ttg)
APGFIDEJ_00137	222	hypothetical protein	tRNA-Gly(tcc)
APGFIDEJ_00138	165	hypothetical protein	hypothetical protein
APGFIDEJ_00139	75	tRNA-Thr(tgt)	hypothetical protein
APGFIDEJ_00140	291	hypothetical protein	tRNA-Thr(tgt)
APGFIDEJ_00141	77	tRNA-Ile(gat)	hypothetical protein
APGFIDEJ_00142	76	tRNA-Met(cat)	tRNA-Ile(gat)
APGFIDEJ_00143	108	hypothetical protein	tRNA-Met(cat)
APGFIDEJ_00144	348	hypothetical protein	hypothetical protein
APGFIDEJ_00145	282	hypothetical protein	hypothetical protein

Appendix F (continued)

APGFIDEJ_00146	300	hypothetical protein	hypothetical protein
APGFIDEJ_00147	396	hypothetical protein	hypothetical protein
APGFIDEJ_00148	297	hypothetical protein	hypothetical protein
APGFIDEJ_00149	285	hypothetical protein	hypothetical protein
APGFIDEJ_00150	345	hypothetical protein	hypothetical protein
APGFIDEJ_00151	699	hypothetical protein	hypothetical protein
APGFIDEJ_00152	450	Rz-like spanin	hypothetical protein
APGFIDEJ_00153	753	deoxynucleoside-5'-monophosphate kinase	hypothetical protein
APGFIDEJ_00154	576	Clp protease	Deoxynucleoside-5'-monophosphate kinase
APGFIDEJ_00155	657	putative holin	hypothetical protein
APGFIDEJ_00156	414	lysozyme	Holin
APGFIDEJ_00157	417	hypothetical protein	L-alanyl-D-glutamate peptidase
APGFIDEJ_00158	432	hypothetical protein	hypothetical protein
APGFIDEJ_00159	291	thioredoxin	hypothetical protein
APGFIDEJ_00160	246	major head protein	hypothetical protein
APGFIDEJ_00161	864	putative serine/threonine protein phosphatase	hypothetical protein
APGFIDEJ_00162	291	hypothetical protein	Serine/threonine-protein phosphatase
APGFIDEJ_00163	591	putative serine/threonine protein phosphatase	hypothetical protein
APGFIDEJ_00164	432	D11 protein	hypothetical protein
APGFIDEJ_00165	252	hypothetical protein	hypothetical protein
APGFIDEJ_00166	282	tail sheath monomer	hypothetical protein
APGFIDEJ_00167	246	hypothetical protein	hypothetical protein
APGFIDEJ_00168	327	hypothetical protein	hypothetical protein
APGFIDEJ_00169	147	hypothetical protein	hypothetical protein

Appendix F (continued)

APGFIDEJ_00170	201	hypothetical protein	hypothetical protein
APGFIDEJ_00171	462	hypothetical protein	hypothetical protein
APGFIDEJ_00172	372	capsid and scaffold protein	hypothetical protein
APGFIDEJ_00173	204	hypothetical protein	hypothetical protein
APGFIDEJ_00174	447	hypothetical protein	hypothetical protein
APGFIDEJ_00175	291	hypothetical protein	hypothetical protein
APGFIDEJ_00176	234	hypothetical protein	hypothetical protein
APGFIDEJ_00177	186	hypothetical protein	hypothetical protein
APGFIDEJ_00178	597	hypothetical protein	hypothetical protein
APGFIDEJ_00179	732	hypothetical protein	hypothetical protein
APGFIDEJ_00180	357	endonuclease	hypothetical protein
APGFIDEJ_00181	195	hypothetical protein	hypothetical protein
APGFIDEJ_00182	162	hypothetical protein	hypothetical protein
APGFIDEJ_00183	345	hypothetical protein	hypothetical protein
APGFIDEJ_00184	126	hypothetical protein	hypothetical protein
APGFIDEJ_00185	213	hypothetical protein	hypothetical protein
APGFIDEJ_00186	147	hypothetical protein	hypothetical protein
APGFIDEJ_00187	231	hypothetical protein	hypothetical protein
APGFIDEJ_00188	996	hypothetical protein	hypothetical protein
APGFIDEJ_00189	204	hypothetical protein	hypothetical protein
APGFIDEJ_00190	252	hypothetical protein	hypothetical protein
APGFIDEJ_00191	408	A2 protein	hypothetical protein
APGFIDEJ_00192	198	membrane protein	Protein A2
APGFIDEJ_00193	1665	DNA transfer protein	hypothetical protein
APGFIDEJ_00194	258	hypothetical protein	Protein A1

Appendix F (continued)

APGFIDEJ_00195	393	hypothetical protein	hypothetical protein
APGFIDEJ_00196	735	deoxynucleoside-5'-monophosphatase	hypothetical protein

Phage Annotation of Group 4 Phages P1-137 (122k)

Gene		Close Relative (bux)	Caudovirales Database
locus_tag	length_bp	product	product
BFPMOJOJ_00001	735	deoxynucleoside-5'-monophosphatase	5'-deoxynucleotidase
BFPMOJOJ_00002	393	hypothetical protein	hypothetical protein
BFPMOJOJ_00003	279	hypothetical protein	hypothetical protein
BFPMOJOJ_00004	1665	A1 protein	Protein A1
BFPMOJOJ_00005	228	membrane protein	Protein A2
BFPMOJOJ_00006	417	putative A2 protein	hypothetical protein
BFPMOJOJ_00007	252	hypothetical protein	hypothetical protein
BFPMOJOJ_00008	1002	hypothetical protein	hypothetical protein
BFPMOJOJ_00009	522	hypothetical protein	hypothetical protein
BFPMOJOJ_00010	228	hypothetical protein	hypothetical protein
BFPMOJOJ_00011	150	putative membrane protein	hypothetical protein
BFPMOJOJ_00012	213	hypothetical protein	hypothetical protein
BFPMOJOJ_00013	108	hypothetical protein	hypothetical protein
BFPMOJOJ_00014	345	hypothetical protein	hypothetical protein
BFPMOJOJ_00015	141	hypothetical protein	hypothetical protein
BFPMOJOJ_00016	240	hypothetical protein	hypothetical protein
BFPMOJOJ_00017	882	hypothetical protein	hypothetical protein
BFPMOJOJ_00018	351	hypothetical protein	hypothetical protein
BFPMOJOJ_00019	606	hypothetical protein	hypothetical protein

Appendix F (continued)

BFPMOJO J_00020	186	putative membrane protein	hypothetical protein
BFPMOJO J_00021	234	putative membrane protein	hypothetical protein
BFPMOJO J_00022	519	hypothetical protein	hypothetical protein
BFPMOJO J_00023	198	hypothetical protein	hypothetical protein
BFPMOJO J_00024	384	capsid and scaffold protein	hypothetical protein
BFPMOJO J_00025	468	hypothetical protein	hypothetical protein
BFPMOJO J_00026	201	putative membrane protein	hypothetical protein
BFPMOJO J_00027	333	hypothetical protein	hypothetical protein
BFPMOJO J_00028	246	putative membrane protein	hypothetical protein
BFPMOJO J_00029	282	putative membrane protein	hypothetical protein
BFPMOJO J_00030	159	hypothetical protein	hypothetical protein
BFPMOJO J_00031	261	putative protein 2C	hypothetical protein
BFPMOJO J_00032	432	hypothetical protein	hypothetical protein
BFPMOJO J_00033	468	HNH endonuclease	hypothetical protein
BFPMOJO J_00034	279	phosphoesterase	hypothetical protein
BFPMOJO J_00035	171	phosphoesterase	Serine/threonine-protein phosphatase
BFPMOJO J_00036	369	hypothetical protein	hypothetical protein
BFPMOJO J_00037	864	putative serine/threonine protein phosphatase 2	hypothetical protein
BFPMOJO J_00038	291	putative thioredoxin	L-alanyl-D-glutamate peptidase
BFPMOJO J_00039	411	hypothetical protein	Holin
BFPMOJO J_00040	417	putative membrane protein	hypothetical protein
BFPMOJO J_00041	414	lysozyme	Deoxynucleoside-5'-monophosphate kinase
BFPMOJO J_00042	657	putative holin	hypothetical protein
BFPMOJO J_00043	600	ATP-dependent Clp protease	hypothetical protein
BFPMOJO J_00044	753	deoxynucleoside-5'-monophosphate kinase	hypothetical protein

Appendix F (continued)

BFPMOJO J_00045	450	i-spanin	hypothetical protein
BFPMOJO J_00046	699	hypothetical protein	hypothetical protein
BFPMOJO J_00047	348	putative membrane protein	hypothetical protein
BFPMOJO J_00048	285	putative membrane protein	hypothetical protein
BFPMOJO J_00049	297	hypothetical protein	hypothetical protein
BFPMOJO J_00050	420	hypothetical protein	hypothetical protein
BFPMOJO J_00051	300	hypothetical protein	hypothetical protein
BFPMOJO J_00052	279	hypothetical protein	hypothetical protein
BFPMOJO J_00053	396	hypothetical protein	hypothetical protein
BFPMOJO J_00054	186	hypothetical protein	tRNA-Met(cat)
BFPMOJO J_00055	300	hypothetical protein	tRNA-Ile(gat)
BFPMOJO J_00056	369	glycyl radical cofactor	hypothetical protein
BFPMOJO J_00057	76	tRNA-Met(cat)	hypothetical protein
BFPMOJO J_00058	76	tRNA-Ile(gat)	tRNA-Thr(tgt)
BFPMOJO J_00059	201	hypothetical protein	hypothetical protein
BFPMOJO J_00060	294	hypothetical protein	hypothetical protein
BFPMOJO J_00061	75	tRNA-Thr(tgt)	tRNA-Gln(ttg)
BFPMOJO J_00062	165	hypothetical protein	tRNA-Gln(ctg)
BFPMOJO J_00063	180	hypothetical protein	hypothetical protein
BFPMOJO J_00064	78	tRNA-Gln(ttg)	tRNA-Arg(acg)
BFPMOJO J_00065	76	tRNA-Gln(ctg)	tRNA-His(gtg)
BFPMOJO J_00066	201	hypothetical protein	tRNA-Ser(tga)
BFPMOJO J_00067	75	tRNA-Arg(acg)	hypothetical protein
BFPMOJO J_00068	77	tRNA-His(gtg)	tRNA-Leu(tag)
BFPMOJO J_00069	90	tRNA-Ser(tga)	hypothetical protein

Appendix F (continued)

BFPMOJO J_00070	177	hypothetical protein	tRNA-Ala(tgc)
BFPMOJO J_00071	81	tRNA-Leu(tag)	tRNA-Ala(tgc)
BFPMOJO J_00072	219	hypothetical protein	hypothetical protein
BFPMOJO J_00073	76	tRNA-Ala(tgc)	tRNA-Val(tac)
BFPMOJO J_00074	79	tRNA-Ala(tgc)	tRNA-Lys(ttt)
BFPMOJO J_00075	354	hypothetical protein	tRNA-Pro(tgg)
BFPMOJO J_00076	74	tRNA-Val(tac)	hypothetical protein
BFPMOJO J_00077	78	tRNA-Lys(ttt)	tRNA-Lys(ctt)
BFPMOJO J_00078	76	tRNA-Pro(tgg)	tRNA-Asp(gtc)
BFPMOJO J_00079	198	Rz-like spanin	hypothetical protein
BFPMOJO J_00080	369	HNH endonuclease	tRNA-Asn(gtt)
BFPMOJO J_00081	77	tRNA-Lys(ctt)	tRNA-Cys(gca)
BFPMOJO J_00082	75	tRNA-Asp(gtc)	hypothetical protein
BFPMOJO J_00083	186	hypothetical protein	hypothetical protein
BFPMOJO J_00084	83	tRNA-Asn(gtt)	tRNA-Phe(gaa)
BFPMOJO J_00085	76	tRNA-Cys(gca)	tRNA-Tyr(gta)
BFPMOJO J_00086	189	hypothetical protein	hypothetical protein
BFPMOJO J_00087	273	hypothetical protein	hypothetical protein
BFPMOJO J_00088	75	tRNA-Phe(gaa)	hypothetical protein
BFPMOJO J_00089	81	tRNA-Tyr(gta)	tRNA-Leu(taa)
BFPMOJO J_00090	276	hypothetical protein	tRNA-Met(cat)
BFPMOJO J_00091	207	hypothetical protein	tRNA-Ser(gct)
BFPMOJO J_00092	123	hypothetical protein	hypothetical protein
BFPMOJO J_00093	86	tRNA-Leu(taa)	hypothetical protein
BFPMOJO J_00094	78	tRNA-Met(cat)	hypothetical protein

Appendix F (continued)

BFPMOJO J_00095	94	tRNA-Ser(gct)	hypothetical protein
BFPMOJO J_00096	519	DNA primase	hypothetical protein
BFPMOJO J_00097	297	hypothetical protein	hypothetical protein
BFPMOJO J_00098	678	PnuC-like ribosyl nicotinamide transporter	tRNA-Arg(tct)
BFPMOJO J_00099	1056	putative nicotinamide-nucleotide adenylyltransferase	hypothetical protein
BFPMOJO J_00100	945	putative SPFH domain-containing protein/band 7 family protein	tRNA-SeC(tca)
BFPMOJO J_00101	201	hypothetical protein	hypothetical protein
BFPMOJO J_00102	75	tRNA-Arg(tct)	hypothetical protein
BFPMOJO J_00103	510	hypothetical protein	hypothetical protein
BFPMOJO J_00104	74	tRNA-SeC(tca)	hypothetical protein
BFPMOJO J_00105	483	homing endonuclease	hypothetical protein
BFPMOJO J_00106	444	YqeY protein domain-containing protein	hypothetical protein
BFPMOJO J_00107	171	hypothetical protein	hypothetical protein
BFPMOJO J_00108	450	cell wall hydrolase	hypothetical protein
BFPMOJO J_00109	318	hypothetical protein	hypothetical protein
BFPMOJO J_00110	639	tail fiber protein	hypothetical protein
BFPMOJO J_00111	183	hypothetical protein	hypothetical protein
BFPMOJO J_00112	702	putative metallopeptidase	hypothetical protein
BFPMOJO J_00113	213	metallopeptidase	hypothetical protein
BFPMOJO J_00114	261	hypothetical protein	hypothetical protein
BFPMOJO J_00115	216	tail length tape-measure protein	hypothetical protein
BFPMOJO J_00116	516	hypothetical protein	hypothetical protein
BFPMOJO J_00117	279	hypothetical protein	hypothetical protein
BFPMOJO J_00118	513	homing endonuclease	Thymidylate synthase
BFPMOJO J_00119	477	ribonuclease H	Dihydrofolate reductase

Appendix F (continued)

BFPMOJO J_00120	270	hypothetical protein	hypothetical protein
BFPMOJO J_00121	255	hypothetical protein	hypothetical protein
BFPMOJO J_00122	309	membrane protein	Ribonucleoside-diphosphate reductase large subunit
BFPMOJO J_00123	855	thymidylate synthase	hypothetical protein
BFPMOJO J_00124	531	dihydrofolate reductase	hypothetical protein
BFPMOJO J_00125	1146	ribonucleotide-diphosphate reductase class Ia (aerobic) beta subunit	Anaerobic ribonucleoside-triphosphate reductase
BFPMOJO J_00126	516	homing endonuclease	hypothetical protein
BFPMOJO J_00127	2334	ribonucleoside diphosphate reductase 1 alpha chain	hypothetical protein
BFPMOJO J_00128	243	tail length tape measure protein	hypothetical protein
BFPMOJO J_00129	753	phosphate starvation-inducible protein	hypothetical protein
BFPMOJO J_00130	1875	anaerobic NTP reductase large subunit	hypothetical protein
BFPMOJO J_00131	219	hypothetical protein	hypothetical protein
BFPMOJO J_00132	843	putative Sir2-like protein	hypothetical protein
BFPMOJO J_00133	216	hypothetical protein	Putative replication origin binding protein
BFPMOJO J_00134	186	hypothetical protein	hypothetical protein
BFPMOJO J_00135	516	Sir2 (NAD-dependent deacetylase)	hypothetical protein
BFPMOJO J_00136	429	hypothetical protein	hypothetical protein
BFPMOJO J_00137	396	hypothetical protein	hypothetical protein
BFPMOJO J_00138	2790	replication origin binding protein	hypothetical protein
BFPMOJO J_00139	255	hypothetical protein	hypothetical protein
BFPMOJO J_00140	705	D2 protein	DNA ligase
BFPMOJO J_00141	237	transcriptional regulator	hypothetical protein
BFPMOJO J_00142	411	putative D3 protein	Putative transcription factor D5
BFPMOJO J_00143	297	hypothetical protein	hypothetical protein
BFPMOJO J_00144	309	transcriptional regulator protein	hypothetical protein

Appendix F (continued)

BFPMOJO J_00145	201	hypothetical protein	DNA polymerase
BFPMOJO J_00146	975	NAD-dependent DNA ligase subunit A	putative helicase D10
BFPMOJO J_00147	780	NAD-dependent DNA ligase subunit B	hypothetical protein
BFPMOJO J_00148	768	D5 protein	hypothetical protein
BFPMOJO J_00149	1524	putative DNA helicase	putative ssDNA-binding protein
BFPMOJO J_00150	891	DNA replication primase	putative exonuclease subunit 1
BFPMOJO J_00151	2568	DNA polymerase I	putative exonuclease subunit 2
BFPMOJO J_00152	498	hypothetical protein	Protein D14
BFPMOJO J_00153	1347	helicase	Flap endonuclease
BFPMOJO J_00154	531	homing endonuclease	Deoxyuridine 5'-triphosphate nucleotidohydrolase
BFPMOJO J_00155	363	hypothetical protein	hypothetical protein
BFPMOJO J_00156	774	ssDNA-binding protein	hypothetical protein
BFPMOJO J_00157	978	recombinase	L-shaped tail fiber protein p132
BFPMOJO J_00158	1839	exonuclease	putative central straight fiber
BFPMOJO J_00159	483	D14 protein	putative baseplate hub protein
BFPMOJO J_00160	876	flap endonuclease	Distal tail protein
BFPMOJO J_00161	447	putative deoxyUTP pyrophosphatase	putative tape measure protein
BFPMOJO J_00162	267	hypothetical protein	hypothetical protein
BFPMOJO J_00163	2973	tail fiber protein	hypothetical protein
BFPMOJO J_00164	423	tail protein	Minor tail protein
BFPMOJO J_00165	2058	putative tail protein	Tail tube protein
BFPMOJO J_00166	2850	tail length tape-measure protein	Tail tube terminator protein
BFPMOJO J_00167	615	distal tail protein	Tail completion protein
BFPMOJO J_00168	3708	putative pore-forming tail tip protein	hypothetical protein
BFPMOJO J_00169	369	putative tape measure chaperone	Major capsid protein

BFPMOJO J_00170	405	putative tape measure chaperone	Prohead protease
BFPMOJO J_00171	900	putative minor tail protein	Decoration protein
BFPMOJO J_00172	1410	major tail protein	Portal protein
BFPMOJO J_00173	486	tail tube terminator protein	Nicking endonuclease
BFPMOJO J_00174	768	tail completion protein	Terminase, large subunit
BFPMOJO J_00175	513	head completion protein	putative terminase, small subunit
BFPMOJO J_00176	1377	capsid protein	Receptor-binding protein
BFPMOJO J_00177	633	putative prohead protease	hypothetical protein
BFPMOJO J_00178	483	putative tail protein	hypothetical protein
BFPMOJO J_00179	1218	portal (connector) protein	hypothetical protein
BFPMOJO J_00180	438	putative nicking site-specific endonuclease	hypothetical protein
BFPMOJO J_00181	1317	terminase large subunit	5'-deoxynucleotidase
BFPMOJO J_00182	483	putative terminase small subunit	hypothetical protein
BFPMOJO J_00183	1782	receptor-binding tail protein	hypothetical protein
BFPMOJO J_00184	267	receptor-blocking protein	Protein A1
BFPMOJO J_00185	315	hypothetical protein	Protein A2
BFPMOJO J_00186	105	hypothetical protein	hypothetical protein
BFPMOJO J_00187	246	membrane protein	hypothetical protein
BFPMOJO J_00188	735	deoxynucleoside-5'-monophosphatase	hypothetical protein
BFPMOJO J_00189	393	hypothetical protein	hypothetical protein
BFPMOJO J_00190	279	hypothetical protein	hypothetical protein
BFPMOJO J_00191	1665	A1 protein	hypothetical protein
BFPMOJO J_00192	228	membrane protein	hypothetical protein
BFPMOJO J_00193	417	putative A2 protein	hypothetical protein
BFPMOJO J_00194	252	hypothetical protein	hypothetical protein

Appendix F (continued)

BFPMOJO J_00195	1002	hypothetical protein	hypothetical protein
BFPMOJO J_00196	522	hypothetical protein	
BFPMOJO J_00197	228	hypothetical protein	
BFPMOJO J_00198	150	putative membrane protein	
BFPMOJO J_00199	213	hypothetical protein	
BFPMOJO J_00200	108	hypothetical protein	
BFPMOJO J_00201	345	hypothetical protein	
BFPMOJO J_00202	141	hypothetical protein	
BFPMOJO J_00203	240	hypothetical protein	

Phage Annotation of Group 4 Phages P1-179 (122k)

Gene		Close Relative (bux)	Caudovirales Database
locus_tag	length_bp	product	product
CIIAGBDK _00001	540	HNH endonuclease	hypothetical protein
CIIAGBDK _00002	240	hypothetical protein	hypothetical protein
CIIAGBDK _00003	198	hypothetical protein	hypothetical protein
CIIAGBDK _00004	345	hypothetical protein	hypothetical protein
CIIAGBDK _00005	213	hypothetical protein	hypothetical protein
CIIAGBDK _00006	150	hypothetical protein	hypothetical protein
CIIAGBDK _00007	231	hypothetical protein	hypothetical protein
CIIAGBDK _00008	495	hypothetical protein	hypothetical protein
CIIAGBDK _00009	1011	hypothetical protein	hypothetical protein
CIIAGBDK _00010	204	hypothetical protein	hypothetical protein
CIIAGBDK _00011	252	hypothetical protein	hypothetical protein
CIIAGBDK _00012	408	DNA-binding protein	Protein A2
CIIAGBDK _00013	198	membrane protein	hypothetical protein
CIIAGBDK _00014	1671	DNA transfer protein	Protein A1
CIIAGBDK _00015	258	hypothetical protein	hypothetical protein
CIIAGBDK _00016	393	hypothetical protein	hypothetical protein
CIIAGBDK _00017	735	deoxynucleoside-5'-monophosphatase	5'-deoxynucleotidase
CIIAGBDK _00018	384	deoxynucleoside-5'-monophosphatase	hypothetical protein
CIIAGBDK _00019	537	HNH homing endonuclease	hypothetical protein
CIIAGBDK _00020	246	membrane protein	hypothetical protein
CIIAGBDK _00021	195	hypothetical protein	hypothetical protein
CIIAGBDK _00022	108	hypothetical protein	hypothetical protein
CIIAGBDK _00023	129	hypothetical protein	hypothetical protein
CIIAGBDK _00024	267	receptor-blocking protein	Receptor-binding protein

Appendix F (continued)

CIIAGBDK _00025	1758	receptor-binding tail protein	putative terminase, small subunit
CIIAGBDK _00026	483	terminase small subunit	Terminase, large subunit
CIIAGBDK _00027	1317	terminase large subunit	Nicking endonuclease
CIIAGBDK _00028	438	hypothetical protein	Portal protein
CIIAGBDK _00029	1218	portal protein	Decoration protein
CIIAGBDK _00030	492	tail fibers protein	Prohead protease
CIIAGBDK _00031	633	prohead protease	Major capsid protein
CIIAGBDK _00032	1377	major capsid protein	hypothetical protein
CIIAGBDK _00033	513	head-tail adaptor	Tail completion protein
CIIAGBDK _00034	768	tail completion or Neck1 protein	Tail tube terminator protein
CIIAGBDK _00035	486	tail terminator	Tail tube protein
CIIAGBDK _00036	1407	major tail protein	Minor tail protein
CIIAGBDK _00037	903	minor tail protein	hypothetical protein
CIIAGBDK _00038	405	Tail assembly chaperone	hypothetical protein
CIIAGBDK _00039	369	tail assembly chaperone	putative tape measure protein
CIIAGBDK _00040	3681	pore forming tail tip protein	Distal tail protein
CIIAGBDK _00041	615	distal tail protein	putative baseplate hub protein
CIIAGBDK _00042	2850	tail protein	putative central straight fiber
CIIAGBDK _00043	2058	tail protein	L-shaped tail fiber protein p132
CIIAGBDK _00044	423	tail protein	hypothetical protein
CIIAGBDK _00045	2802	tail tip protein	hypothetical protein
CIIAGBDK _00046	258	hypothetical protein	Deoxyuridine 5'-triphosphate nucleotidohydrolase
CIIAGBDK _00047	447	deoxyUTP pyrophosphatase	Flap endonuclease
CIIAGBDK _00048	876	flap endonuclease	Protein D14
CIIAGBDK _00049	483	RusA-like Holliday junction resolvase	putative exonuclease subunit 2

Appendix F (continued)

CIIAGBDK_00050	1839	recombination or repair nuclease	putative exonuclease subunit 1
CIIAGBDK_00051	978	recombinase	hypothetical protein
CIIAGBDK_00052	363	HNH endonuclease	putative ssDNA-binding protein
CIIAGBDK_00053	774	single strand DNA binding protein	putative helicase D10
CIIAGBDK_00054	285	hypothetical protein	hypothetical protein
CIIAGBDK_00055	1353	DNA helicase	DNA polymerase
CIIAGBDK_00056	498	hypothetical protein	hypothetical protein
CIIAGBDK_00057	2568	DNA polymerase I	hypothetical protein
CIIAGBDK_00058	891	DNA primase	hypothetical protein
CIIAGBDK_00059	534	HNH homing endonuclease	Putative transcription factor D5
CIIAGBDK_00060	1524	DnaB-like replicative helicase	hypothetical protein
CIIAGBDK_00061	768	endonuclease	DNA ligase
CIIAGBDK_00062	780	DNA ligase subunit	hypothetical protein
CIIAGBDK_00063	972	NAD-dependent DNA ligase subunit A	hypothetical protein
CIIAGBDK_00064	273	hypothetical protein	hypothetical protein
CIIAGBDK_00065	309	transcriptional regulator	hypothetical protein
CIIAGBDK_00066	297	hypothetical protein	hypothetical protein
CIIAGBDK_00067	411	DNA binding protein	Putative replication origin binding protein
CIIAGBDK_00068	252	transcriptional regulator	hypothetical protein
CIIAGBDK_00069	705	helicase	hypothetical protein
CIIAGBDK_00070	234	hypothetical protein	hypothetical protein
CIIAGBDK_00071	2790	replication origin binding protein	hypothetical protein
CIIAGBDK_00072	321	hypothetical protein	hypothetical protein
CIIAGBDK_00073	429	hypothetical protein	hypothetical protein
CIIAGBDK_00074	513	Sir2 (NAD-dependent deacetylase)	hypothetical protein

Appendix F (continued)

CIIAGBDK_00075	816	Sir2 (NAD-dependent deacetylase)	Anaerobic ribonucleoside-triphosphate reductase
CIIAGBDK_00076	222	hypothetical protein	hypothetical protein
CIIAGBDK_00077	204	hypothetical protein	hypothetical protein
CIIAGBDK_00078	282	hypothetical protein	Ribonucleoside-diphosphate reductase large subunit
CIIAGBDK_00079	1875	ribonucleotide reductase of class III (anaerobic), large subunit	hypothetical protein
CIIAGBDK_00080	753	phosphate starvation-inducible protein	Dihydrofolate reductase
CIIAGBDK_00081	198	tail length tape measure protein	putative thymidylate synthase
CIIAGBDK_00082	2436	ribonucleoside-diphosphate reductase, alpha subunit	hypothetical protein
CIIAGBDK_00083	1146	ribonucleotide reductase of class Ia (aerobic), beta subunit	hypothetical protein
CIIAGBDK_00084	534	dihydrofolate reductase	hypothetical protein
CIIAGBDK_00085	840	thymidylate synthase	hypothetical protein
CIIAGBDK_00086	282	hypothetical protein	hypothetical protein
CIIAGBDK_00087	477	ribonuclease H	hypothetical protein
CIIAGBDK_00088	285	hypothetical protein	hypothetical protein
CIIAGBDK_00089	450	hypothetical protein	hypothetical protein
CIIAGBDK_00090	516	hypothetical protein	hypothetical protein
CIIAGBDK_00091	216	hypothetical protein	hypothetical protein
CIIAGBDK_00092	237	hypothetical protein	hypothetical protein
CIIAGBDK_00093	702	metallopeptidase	hypothetical protein
CIIAGBDK_00094	183	hypothetical protein	hypothetical protein
CIIAGBDK_00095	639	tail fiber protein	hypothetical protein
CIIAGBDK_00096	318	hypothetical protein	tRNA-Arg(tct)
CIIAGBDK_00097	450	cell wall hydrolase	hypothetical protein
CIIAGBDK_00098	171	hypothetical protein	hypothetical protein
CIIAGBDK_00099	444	tRNA amidotransferase	hypothetical protein

Appendix F (continued)

CIIAGBDK _00100	75	tRNA-Arg(tct)	hypothetical protein
CIIAGBDK _00101	948	lipoprotein	hypothetical protein
CIIAGBDK _00102	1056	Bifunctional NAD biosynthesis protein NadR	tRNA-Ser(gct)
CIIAGBDK _00103	678	Nicotinamide riboside transporter PnuC	tRNA-Met(cat)
CIIAGBDK _00104	102	hypothetical protein	hypothetical protein
CIIAGBDK _00105	519	DNA primase	hypothetical protein
CIIAGBDK _00106	94	tRNA-Ser(gct)	hypothetical protein
CIIAGBDK _00107	78	tRNA-Met(cat)	tRNA-Leu(taa)
CIIAGBDK _00108	189	hypothetical protein	hypothetical protein
CIIAGBDK _00109	186	anti-termination protein Q-like protein	hypothetical protein
CIIAGBDK _00110	339	hypothetical protein	hypothetical protein
CIIAGBDK _00111	77	tRNA-Leu(taa)	tRNA-Tyr(gta)
CIIAGBDK _00112	123	hypothetical protein	tRNA-Glu(ttc)
CIIAGBDK _00113	273	hypothetical protein	tRNA-Trp(cca)
CIIAGBDK _00114	276	hypothetical protein	tRNA-Phe(gaa)
CIIAGBDK _00115	91	tRNA-Tyr(gta)	hypothetical protein
CIIAGBDK _00116	77	tRNA-Glu(ttc)	hypothetical protein
CIIAGBDK _00117	77	tRNA-Trp(cca)	tRNA-Cys(gca)
CIIAGBDK _00118	75	tRNA-Phe(gaa)	tRNA-Asn(gtt)
CIIAGBDK _00119	273	hypothetical protein	hypothetical protein
CIIAGBDK _00120	273	hypothetical protein	tRNA-Asp(gtc)
CIIAGBDK _00121	75	tRNA-Cys(gca)	tRNA-Lys(ctt)
CIIAGBDK _00122	78	tRNA-Asn(gtt)	tRNA-Gly(gcc)
CIIAGBDK _00123	189	hypothetical protein	tRNA-Pro(tgg)
CIIAGBDK _00124	75	tRNA-Asp(gtc)	tRNA-Met(cat)

Appendix F (continued)

CIIAGBDK _00125	77	tRNA-Lys(ctt)	hypothetical protein
CIIAGBDK _00126	74	tRNA-Gly(gcc)	tRNA-Lys(ttt)
CIIAGBDK _00127	76	tRNA-Pro(tgg)	hypothetical protein
CIIAGBDK _00128	78	tRNA-Met(cat)	tRNA-Val(tac)
CIIAGBDK _00129	168	hypothetical protein	hypothetical protein
CIIAGBDK _00130	79	tRNA-Lys(ttt)	tRNA-Ala(tgc)
CIIAGBDK _00131	318	hypothetical protein	tRNA-Leu(tag)
CIIAGBDK _00132	74	tRNA-Val(tac)	tRNA-Ser(tga)
CIIAGBDK _00133	354	hypothetical protein	hypothetical protein
CIIAGBDK _00134	75	tRNA-Ala(tgc)	tRNA-His(gtg)
CIIAGBDK _00135	77	tRNA-Leu(tag)	hypothetical protein
CIIAGBDK _00136	90	tRNA-Ser(tga)	tRNA-Gln(ctg)
CIIAGBDK _00137	183	hypothetical protein	tRNA-Gln(ttg)
CIIAGBDK _00138	77	tRNA-His(gtg)	hypothetical protein
CIIAGBDK _00139	195	hypothetical protein	hypothetical protein
CIIAGBDK _00140	76	tRNA-Gln(ctg)	tRNA-Thr(tgt)
CIIAGBDK _00141	76	tRNA-Gln(ttg)	hypothetical protein
CIIAGBDK _00142	252	hypothetical protein	tRNA-Ile(gat)
CIIAGBDK _00143	165	hypothetical protein	tRNA-Met(cat)
CIIAGBDK _00144	75	tRNA-Thr(tgt)	hypothetical protein
CIIAGBDK _00145	291	hypothetical protein	hypothetical protein
CIIAGBDK _00146	77	tRNA-Ile(gat)	hypothetical protein
CIIAGBDK _00147	76	tRNA-Met(cat)	hypothetical protein
CIIAGBDK _00148	195	hypothetical protein	hypothetical protein
CIIAGBDK _00149	369	acetyltransferase-like protein	hypothetical protein

Appendix F (continued)

CIIAGBDK_00150	315	hypothetical protein	hypothetical protein
CIIAGBDK_00151	348	hypothetical protein	hypothetical protein
CIIAGBDK_00152	282	hypothetical protein	hypothetical protein
CIIAGBDK_00153	303	hypothetical protein	hypothetical protein
CIIAGBDK_00154	639	hypothetical protein	hypothetical protein
CIIAGBDK_00155	303	hypothetical protein	hypothetical protein
CIIAGBDK_00156	420	hypothetical protein	hypothetical protein
CIIAGBDK_00157	297	hypothetical protein	hypothetical protein
CIIAGBDK_00158	285	hypothetical protein	Deoxynucleoside-5'-monophosphate kinase
CIIAGBDK_00159	345	hypothetical protein	hypothetical protein
CIIAGBDK_00160	699	hypothetical protein	Holin
CIIAGBDK_00161	498	HNH homing endonuclease	L-alanyl-D-glutamate peptidase
CIIAGBDK_00162	444	Rz-like spanin	hypothetical protein
CIIAGBDK_00163	753	deoxynucleoside monophosphate kinase	hypothetical protein
CIIAGBDK_00164	600	ATP-dependent Clp protease proteolytic subunit	hypothetical protein
CIIAGBDK_00165	657	holin	hypothetical protein
CIIAGBDK_00166	414	endolysin	Serine/threonine-protein phosphatase
CIIAGBDK_00167	417	hypothetical protein	hypothetical protein
CIIAGBDK_00168	432	hypothetical protein	hypothetical protein
CIIAGBDK_00169	291	thioredoxin	hypothetical protein
CIIAGBDK_00170	246	major head protein	hypothetical protein
CIIAGBDK_00171	864	serine/threonine protein phosphatase	hypothetical protein
CIIAGBDK_00172	291	hypothetical protein	hypothetical protein
CIIAGBDK_00173	591	phosphoesterase	hypothetical protein
CIIAGBDK_00174	432	hypothetical protein	hypothetical protein

Appendix F (continued)

CIIAGBDK _00175	279	hypothetical protein	hypothetical protein
CIIAGBDK _00176	537	HNH homing endonuclease	hypothetical protein
CIIAGBDK _00177	282	hypothetical protein	hypothetical protein
CIIAGBDK _00178	243	hypothetical protein	hypothetical protein
CIIAGBDK _00179	327	hypothetical protein	hypothetical protein
CIIAGBDK _00180	147	hypothetical protein	hypothetical protein
CIIAGBDK _00181	201	hypothetical protein	hypothetical protein
CIIAGBDK _00182	462	hypothetical protein	hypothetical protein
CIIAGBDK _00183	372	hypothetical protein	hypothetical protein
CIIAGBDK _00184	204	hypothetical protein	hypothetical protein
CIIAGBDK _00185	447	hypothetical protein	hypothetical protein
CIIAGBDK _00186	291	hypothetical protein	hypothetical protein
CIIAGBDK _00187	234	hypothetical protein	hypothetical protein
CIIAGBDK _00188	186	hypothetical protein	hypothetical protein
CIIAGBDK _00189	600	hypothetical protein	hypothetical protein
CIIAGBDK _00190	348	hypothetical protein	hypothetical protein
CIIAGBDK _00191	714	hypothetical protein	hypothetical protein
CIIAGBDK _00192	330	hypothetical protein	hypothetical protein
CIIAGBDK _00193	540	HNH endonuclease	hypothetical protein
CIIAGBDK _00194	240	hypothetical protein	hypothetical protein
CIIAGBDK _00195	198	hypothetical protein	hypothetical protein
CIIAGBDK _00196	345	hypothetical protein	hypothetical protein
CIIAGBDK _00197	213	hypothetical protein	Protein A2
CIIAGBDK _00198	150	hypothetical protein	hypothetical protein
CIIAGBDK _00199	231	hypothetical protein	Protein A1

Appendix F (continued)

CIIAGBDK _00200	495	hypothetical protein	hypothetical protein
CIIAGBDK _00201	1011	hypothetical protein	hypothetical protein
CIIAGBDK _00202	204	hypothetical protein	5'-deoxynucleotidase
CIIAGBDK _00203	252	hypothetical protein	
CIIAGBDK _00204	408	DNA-binding protein	
CIIAGBDK _00205	198	membrane protein	
CIIAGBDK _00206	1671	DNA transfer protein	
CIIAGBDK _00207	258	hypothetical protein	
CIIAGBDK _00208	393	hypothetical protein	
CIIAGBDK _00209	735	deoxynucleoside-5'- monophosphatase	

Phage Annotation of Group 5 Phages (31k)

Gene		Close Relative (p2)
locus_tag	length_bp	product
KLEPLIDL_00001	663	integrase
KLEPLIDL_00002	219	transcriptional regulator
KLEPLIDL_00003	1164	tail protein
KLEPLIDL_00004	480	tail protein
KLEPLIDL_00005	2448	tail length tape measure protein
KLEPLIDL_00006	276	tail protein
KLEPLIDL_00007	519	head closure
KLEPLIDL_00008	1191	Putative prophage major tail sheath protein
KLEPLIDL_00009	594	DNA-invertase hin
KLEPLIDL_00010	441	tail fiber assembly protein
KLEPLIDL_00011	603	Prophage tail fiber assembly protein TfaE
KLEPLIDL_00012	1338	tail protein
KLEPLIDL_00013	612	tail protein
KLEPLIDL_00014	909	baseplate protein
KLEPLIDL_00015	348	baseplate wedge subunit
KLEPLIDL_00016	636	baseplate assembly protein
KLEPLIDL_00017	453	tail completion or Neck1 protein

204

Appendix F (continued)

KLEPLIDL_00018	468	tail terminator
KLEPLIDL_00019	159	Rz-like spanin
KLEPLIDL_00020	426	Rz-like spanin
KLEPLIDL_00021	426	endolysin
KLEPLIDL_00022	498	hypothetical protein
KLEPLIDL_00023	282	holin
KLEPLIDL_00024	204	tail protein
KLEPLIDL_00025	510	head-tail adaptor Ad1
KLEPLIDL_00026	744	terminase small subunit
KLEPLIDL_00027	1074	major head protein
KLEPLIDL_00028	855	head scaffolding protein
KLEPLIDL_00029	1773	terminase large subunit
KLEPLIDL_00030	1035	portal protein
KLEPLIDL_00031	942	hypothetical protein
KLEPLIDL_00032	600	hypothetical protein
KLEPLIDL_00033	486	metallo-protease
KLEPLIDL_00034	114	hypothetical protein
KLEPLIDL_00035	2277	nicking at origin of replication
KLEPLIDL_00036	276	replication initiation protein
KLEPLIDL_00037	225	DksA-like zinc-finger protein
KLEPLIDL_00038	300	replication initiation protein
KLEPLIDL_00039	225	hypothetical protein
KLEPLIDL_00040	501	hypothetical protein
KLEPLIDL_00041	273	Cox-like excisionase and repressor
KLEPLIDL_00042	294	transcriptional regulator

Phage Annotation of Group 5 Phages (240k)

Gene		Close Relative (SPN33US)	Caudovirales Database
locus_tag	length_bp		product
LIONMAAH_00001	492	product	hypothetical protein
LIONMAAH_00002	76	peptidase HslV family protein	tRNA-Trp(cca)
LIONMAAH_00003	243	tRNA-Trp(cca)	hypothetical protein
LIONMAAH_00004	76	hypothetical protein	tRNA-Asn(gtt)
LIONMAAH_00005	822	tRNA-Asn(gtt)	hypothetical protein
LIONMAAH_00006	948	hypothetical protein	hypothetical protein
LIONMAAH_00007	417	hypothetical protein	hypothetical protein
LIONMAAH_00008	390	hypothetical protein	hypothetical protein
LIONMAAH_00009	813	hypothetical protein	hypothetical protein
LIONMAAH_00010	321	hypothetical protein	hypothetical protein
LIONMAAH_00011	564	hypothetical protein	hypothetical protein
LIONMAAH_00012	309	hypothetical protein	hypothetical protein
LIONMAAH_00013	408	hypothetical protein	hypothetical protein
LIONMAAH_00014	510	hypothetical protein	hypothetical protein
LIONMAAH_00015	489	hypothetical protein	hypothetical protein
LIONMAAH_00016	432	hypothetical protein	hypothetical protein
LIONMAAH_00017	600	hypothetical protein	hypothetical protein
LIONMAAH_00018	411	hypothetical protein	hypothetical protein
LIONMAAH_00019	2127	DNA polymerase	hypothetical protein
LIONMAAH_00020	201	hypothetical protein	hypothetical protein
LIONMAAH_00021	1068	hypothetical protein	hypothetical protein
LIONMAAH_00022	1854	hypothetical protein	hypothetical protein
LIONMAAH_00023	1425	hypothetical protein	hypothetical protein
LIONMAAH_00024	582	putative DNA-directed RNA polymerase beta subunit 1	hypothetical protein
LIONMAAH_00025	387	hypothetical protein	hypothetical protein
LIONMAAH_00026	675	hypothetical protein	hypothetical protein
LIONMAAH_00027	1149	hypothetical protein	hypothetical protein
LIONMAAH_00028	837	putative nuclease SbcCD D subunit	hypothetical protein
LIONMAAH_00029	651	hypothetical protein	hypothetical protein
LIONMAAH_00030	1635	hypothetical protein	hypothetical protein
LIONMAAH_00031	1701	hypothetical protein	hypothetical protein
LIONMAAH_00032	1365	hypothetical protein	hypothetical protein
LIONMAAH_00033	324	hypothetical protein	hypothetical protein
LIONMAAH_00034	2238	hypothetical protein	hypothetical protein
LIONMAAH_00035	2106	putative DNA-directed RNA polymerase beta subunit 2	hypothetical protein

Appendix F (continued)

LIONMAAH_00036	1464	putative DNA-directed RNA polymerase beta' subunit	hypothetical protein
LIONMAAH_00037	384	DNA helicase	hypothetical protein
LIONMAAH_00038	621	hypothetical protein	hypothetical protein
LIONMAAH_00039	1971	hypothetical protein	hypothetical protein
LIONMAAH_00040	372	hypothetical protein	hypothetical protein
LIONMAAH_00041	858	hypothetical protein	hypothetical protein
LIONMAAH_00042	1296	hypothetical protein	hypothetical protein
LIONMAAH_00043	501	putative DNA-directed RNA polymerase beta subunit 3	hypothetical protein
LIONMAAH_00044	1785	hypothetical protein	hypothetical protein
LIONMAAH_00045	1353	DNA polymerase	hypothetical protein
LIONMAAH_00046	444	putative virion structural protein 1	hypothetical protein
LIONMAAH_00047	1734	hypothetical protein	hypothetical protein
LIONMAAH_00048	2961	hypothetical protein	hypothetical protein
LIONMAAH_00049	1260	putative virion structural protein 2	hypothetical protein
LIONMAAH_00050	1119	putative virion structural protein 3	hypothetical protein
LIONMAAH_00051	933	putative virion structural protein 4	hypothetical protein
LIONMAAH_00052	558	putative virion structural protein 5	hypothetical protein
LIONMAAH_00053	1278	hypothetical protein	hypothetical protein
LIONMAAH_00054	1260	internal head protein	hypothetical protein
LIONMAAH_00055	756	internal head protein	hypothetical protein
LIONMAAH_00056	546	hypothetical protein	hypothetical protein
LIONMAAH_00057	372	hypothetical protein	hypothetical protein
LIONMAAH_00058	528	hypothetical protein	hypothetical protein
LIONMAAH_00059	300	putative dihydrofolate reductase	hypothetical protein
LIONMAAH_00060	1503	hypothetical protein	hypothetical protein
LIONMAAH_00061	1356	hypothetical protein	hypothetical protein
LIONMAAH_00062	540	putative virion structural protein 6	hypothetical protein
LIONMAAH_00063	1314	hypothetical protein	hypothetical protein
LIONMAAH_00064	798	putative virion structural protein 7	hypothetical protein
LIONMAAH_00065	144	hypothetical protein	hypothetical protein
LIONMAAH_00066	183	hypothetical protein	hypothetical protein

Appendix F (continued)

LIONMAAH_00067	189	hypothetical protein	hypothetical protein
LIONMAAH_00068	417	hypothetical protein	hypothetical protein
LIONMAAH_00069	861	hypothetical protein	hypothetical protein
LIONMAAH_00070	147	hypothetical protein	hypothetical protein
LIONMAAH_00071	147	hypothetical protein	hypothetical protein
LIONMAAH_00072	1563	hypothetical protein	hypothetical protein
LIONMAAH_00073	525	putative helicase	hypothetical protein
LIONMAAH_00074	2301	hypothetical protein	hypothetical protein
LIONMAAH_00075	699	putative major capsid protein	hypothetical protein
LIONMAAH_00076	1005	hypothetical protein	hypothetical protein
LIONMAAH_00077	1575	hypothetical protein	hypothetical protein
LIONMAAH_00078	1677	polymerase	hypothetical protein
LIONMAAH_00079	267	hypothetical protein	hypothetical protein
LIONMAAH_00080	303	hypothetical protein	hypothetical protein
LIONMAAH_00081	2745	hypothetical protein	hypothetical protein
LIONMAAH_00082	2184	putative virion structural protein 8	hypothetical protein
LIONMAAH_00083	528	putative virion structural protein 9	hypothetical protein
LIONMAAH_00084	888	virion structural protein	hypothetical protein
LIONMAAH_00085	651	putative virion structural protein 10	hypothetical protein
LIONMAAH_00086	573	RuvC-like Holliday junction resolvase	hypothetical protein
LIONMAAH_00087	639	hypothetical protein	hypothetical protein
LIONMAAH_00088	483	hypothetical protein	hypothetical protein
LIONMAAH_00089	477	putative acetyltransferase	hypothetical protein
LIONMAAH_00090	387	hypothetical protein	hypothetical protein
LIONMAAH_00091	618	hypothetical protein	hypothetical protein
LIONMAAH_00092	600	hypothetical protein	hypothetical protein
LIONMAAH_00093	273	DprA-like DNA recombination-mediator protein	hypothetical protein
LIONMAAH_00094	1134	hypothetical protein	hypothetical protein
LIONMAAH_00095	465	internal head protein	hypothetical protein
LIONMAAH_00096	609	putative GNAT family acetyltransferase	hypothetical protein
LIONMAAH_00097	372	hypothetical protein	hypothetical protein
LIONMAAH_00098	597	hypothetical protein	hypothetical protein
LIONMAAH_00099	759	hypothetical protein	hypothetical protein
LIONMAAH_00100	624	hypothetical protein	hypothetical protein

Appendix F (continued)

LIONMAAH_00101	366	putative thymidylate kinase	hypothetical protein
LIONMAAH_00102	387	putative transcriptional regulator	hypothetical protein
LIONMAAH_00103	657	hypothetical protein	hypothetical protein
LIONMAAH_00104	999	hypothetical protein	hypothetical protein
LIONMAAH_00105	795	putative GCN5-related N-acetyltransferase	Methyltransferase Dmt
LIONMAAH_00106	804	putative DNA adenine methylase	hypothetical protein
LIONMAAH_00107	813	hypothetical protein	hypothetical protein
LIONMAAH_00108	279	hypothetical protein	hypothetical protein
LIONMAAH_00109	483	hypothetical protein	hypothetical protein
LIONMAAH_00110	351	hypothetical protein	hypothetical protein
LIONMAAH_00111	315	hypothetical protein	hypothetical protein
LIONMAAH_00112	306	hypothetical protein	hypothetical protein
LIONMAAH_00113	453	hypothetical protein	hypothetical protein
LIONMAAH_00114	471	hypothetical protein	hypothetical protein
LIONMAAH_00115	699	hypothetical protein	hypothetical protein
LIONMAAH_00116	210	hypothetical protein	hypothetical protein
LIONMAAH_00117	1761	hypothetical protein	hypothetical protein
LIONMAAH_00118	486	hypothetical protein	hypothetical protein
LIONMAAH_00119	333	head maturation protease	hypothetical protein
LIONMAAH_00120	1008	hypothetical protein	hypothetical protein
LIONMAAH_00121	405	hypothetical protein	hypothetical protein
LIONMAAH_00122	393	hypothetical protein	hypothetical protein
LIONMAAH_00123	402	hypothetical protein	hypothetical protein
LIONMAAH_00124	213	hypothetical protein	hypothetical protein
LIONMAAH_00125	534	hypothetical protein	hypothetical protein
LIONMAAH_00126	474	virion structural protein	hypothetical protein
LIONMAAH_00127	3018	tail fiber protein	hypothetical protein
LIONMAAH_00128	333	tail-associated protein	hypothetical protein
LIONMAAH_00129	285	hypothetical protein	hypothetical protein
LIONMAAH_00130	507	hypothetical protein	hypothetical protein
LIONMAAH_00131	321	hypothetical protein	hypothetical protein
LIONMAAH_00132	384	hypothetical protein	hypothetical protein
LIONMAAH_00133	426	hypothetical protein	hypothetical protein
LIONMAAH_00134	402	hypothetical protein	hypothetical protein
LIONMAAH_00135	372	hypothetical protein	hypothetical protein
LIONMAAH_00136	441	hypothetical protein	hypothetical protein
LIONMAAH_00137	447	hypothetical protein	hypothetical protein

Appendix F (continued)

LIONMAAH_00138	219	hypothetical protein	hypothetical protein
LIONMAAH_00139	387	hypothetical protein	hypothetical protein
LIONMAAH_00140	798	hypothetical protein	hypothetical protein
LIONMAAH_00141	813	putative virion structural protein 11	hypothetical protein
LIONMAAH_00142	846	virion structural protein	hypothetical protein
LIONMAAH_00143	912	putative virion structural protein 11	hypothetical protein
LIONMAAH_00144	840	virion structural protein	hypothetical protein
LIONMAAH_00145	888	virion structural protein	hypothetical protein
LIONMAAH_00146	828	putative virion structural protein 11	hypothetical protein
LIONMAAH_00147	1413	virion structural protein	hypothetical protein
LIONMAAH_00148	999	putative virion structural protein 12	hypothetical protein
LIONMAAH_00149	924	putative virion structural protein 13	hypothetical protein
LIONMAAH_00150	1497	putative virion structural protein 14	hypothetical protein
LIONMAAH_00151	987	putative virion structural protein 15	hypothetical protein
LIONMAAH_00152	900	putative virion structural protein 18	hypothetical protein
LIONMAAH_00153	1443	putative virion structural protein 16	hypothetical protein
LIONMAAH_00154	999	putative virion structural protein 17	hypothetical protein
LIONMAAH_00155	903	putative virion structural protein 18	hypothetical protein
LIONMAAH_00156	1320	putative virion structural protein 19	hypothetical protein
LIONMAAH_00157	2178	virion structural protein	hypothetical protein
LIONMAAH_00158	618	hypothetical protein	hypothetical protein
LIONMAAH_00159	93	endolysin	hypothetical protein
LIONMAAH_00160	642	hypothetical protein	hypothetical protein
LIONMAAH_00161	516	tail assembly chaperone	hypothetical protein
LIONMAAH_00162	492	endolysin	hypothetical protein
LIONMAAH_00163	528	hypothetical protein	hypothetical protein
LIONMAAH_00164	672	hypothetical protein	hypothetical protein
LIONMAAH_00165	567	hypothetical protein	hypothetical protein
LIONMAAH_00166	1329	hypothetical protein	hypothetical protein

Appendix F (continued)

|			
LIONMAAH_00167	915	putative radical SAM superfamily protein 1	hypothetical protein
LIONMAAH_00168	888	putative radical SAM superfamily protein 2	hypothetical protein
LIONMAAH_00169	1203	hypothetical protein	hypothetical protein
LIONMAAH_00170	5184	putative virion structural protein 20	hypothetical protein
LIONMAAH_00171	4131	hypothetical protein	hypothetical protein
LIONMAAH_00172	3714	virion structural protein	hypothetical protein
LIONMAAH_00173	705	virion structural protein	hypothetical protein
LIONMAAH_00174	210	hypothetical protein	hypothetical protein
LIONMAAH_00175	933	hypothetical protein	hypothetical protein
LIONMAAH_00176	318	putative structural protein	hypothetical protein
LIONMAAH_00177	1239	hypothetical protein	hypothetical protein
LIONMAAH_00178	582	hypothetical protein	hypothetical protein
LIONMAAH_00179	564	hypothetical protein	hypothetical protein
LIONMAAH_00180	528	hypothetical protein	hypothetical protein
LIONMAAH_00181	588	hypothetical protein	hypothetical protein
LIONMAAH_00182	402	hypothetical protein	hypothetical protein
LIONMAAH_00183	492	hypothetical protein	hypothetical protein
LIONMAAH_00184	411	hypothetical protein	hypothetical protein
LIONMAAH_00185	384	hypothetical protein	hypothetical protein
LIONMAAH_00186	501	hypothetical protein	hypothetical protein
LIONMAAH_00187	627	hypothetical protein	hypothetical protein
LIONMAAH_00188	2511	hypothetical protein	hypothetical protein
LIONMAAH_00189	105	putative SMC domain-containing protein	hypothetical protein
LIONMAAH_00190	204	hypothetical protein	hypothetical protein
LIONMAAH_00191	489	hypothetical protein	hypothetical protein
LIONMAAH_00192	210	acetyltransferase	hypothetical protein
LIONMAAH_00193	519	hypothetical protein	hypothetical protein
LIONMAAH_00194	423	hypothetical protein	hypothetical protein
LIONMAAH_00195	249	hypothetical protein	hypothetical protein
LIONMAAH_00196	501	hypothetical protein	hypothetical protein
LIONMAAH_00197	723	phosphatase	hypothetical protein
LIONMAAH_00198	303	putative endolysin	hypothetical protein
LIONMAAH_00199	1134	hypothetical protein	hypothetical protein
LIONMAAH_00200	624	hypothetical protein	hypothetical protein
LIONMAAH_00201	1380	hypothetical protein	hypothetical protein

Appendix F (continued)

|			
LIONMAAH_00202	510	putative virion structural protein 21	hypothetical protein
LIONMAAH_00203	480	hypothetical protein	hypothetical protein
LIONMAAH_00204	720	hypothetical protein	hypothetical protein
LIONMAAH_00205	1515	putative endodeoxyribonuclease	hypothetical protein
LIONMAAH_00206	741	putative ribonuclease H	hypothetical protein
LIONMAAH_00207	735	hypothetical protein	hypothetical protein
LIONMAAH_00208	378	hypothetical protein	hypothetical protein
LIONMAAH_00209	408	hypothetical protein	hypothetical protein
LIONMAAH_00210	540	hypothetical protein	hypothetical protein
LIONMAAH_00211	543	hypothetical protein	hypothetical protein
LIONMAAH_00212	756	hypothetical protein	hypothetical protein
LIONMAAH_00213	300	hypothetical protein	hypothetical protein
LIONMAAH_00214	1494	hypothetical protein	hypothetical protein
LIONMAAH_00215	276	UvsX-like recombinase	hypothetical protein
LIONMAAH_00216	669	hypothetical protein	hypothetical protein
LIONMAAH_00217	729	putative virion structural protein 22	hypothetical protein
LIONMAAH_00218	471	hypothetical protein	hypothetical protein
LIONMAAH_00219	531	hypothetical protein	hypothetical protein
LIONMAAH_00220	879	hypothetical protein	hypothetical protein
LIONMAAH_00221	1275	hypothetical protein	hypothetical protein
LIONMAAH_00222	852	hypothetical protein	hypothetical protein
LIONMAAH_00223	660	hypothetical protein	hypothetical protein
LIONMAAH_00224	363	hypothetical protein	hypothetical protein
LIONMAAH_00225	423	hypothetical protein	hypothetical protein
LIONMAAH_00226	564	hypothetical protein	hypothetical protein
LIONMAAH_00227	1044	hypothetical protein	Thymidylate synthase
LIONMAAH_00228	537	thymidylate synthase	hypothetical protein
LIONMAAH_00229	252	hypothetical protein	hypothetical protein
LIONMAAH_00230	765	hypothetical protein	hypothetical protein
LIONMAAH_00231	480	hypothetical protein	hypothetical protein
LIONMAAH_00232	189	hypothetical protein	hypothetical protein
LIONMAAH_00233	942	hypothetical protein	hypothetical protein
LIONMAAH_00234	423	mazG nucleotide pyrophosphohydrolase	hypothetical protein
LIONMAAH_00235	540	hypothetical protein	hypothetical protein
LIONMAAH_00236	2115	virion structural protein	hypothetical protein
LIONMAAH_00237	7122	hypothetical protein	hypothetical protein
LIONMAAH_00238	1206	putative tail fibre protein	hypothetical protein

Appendix F (continued)

|			
LIONMAAH_00239	4206	putative DNA-directed RNA polymerase beta subunit 4	hypothetical protein
LIONMAAH_00240	294	putative DNA-directed RNA polymerase beta subunit 5	hypothetical protein
LIONMAAH_00241	1476	hypothetical protein	hypothetical protein
LIONMAAH_00242	402	hypothetical protein	hypothetical protein
LIONMAAH_00243	804	virion structural protein	hypothetical protein
LIONMAAH_00244	630	putative virion structural protein 23	hypothetical protein
LIONMAAH_00245	300	hypothetical protein	hypothetical protein
LIONMAAH_00246	549	hypothetical protein	hypothetical protein
LIONMAAH_00247	399	unknown function	hypothetical protein
LIONMAAH_00248	390	hypothetical protein	hypothetical protein
LIONMAAH_00249	672	hypothetical protein	hypothetical protein
LIONMAAH_00250	489	putative HD domain protein	hypothetical protein
LIONMAAH_00251	204	hypothetical protein	hypothetical protein
LIONMAAH_00252	543	hypothetical protein	hypothetical protein
LIONMAAH_00253	876	hypothetical protein	hypothetical protein
LIONMAAH_00254	2046	putative virion structural protein 24	hypothetical protein
LIONMAAH_00255	906	putative tail sheath protein	hypothetical protein
LIONMAAH_00256	2514	hypothetical protein	hypothetical protein
LIONMAAH_00257	1644	putative virion structural protein 25	hypothetical protein
LIONMAAH_00258	2112	putative virion structural protein 26	hypothetical protein
LIONMAAH_00259	240	putative terminase large subunit	hypothetical protein
LIONMAAH_00260	1377	hypothetical protein	hypothetical protein
LIONMAAH_00261	1134	hypothetical protein	hypothetical protein
LIONMAAH_00262	510	hypothetical protein	hypothetical protein

G. Phylogenomic distance tree
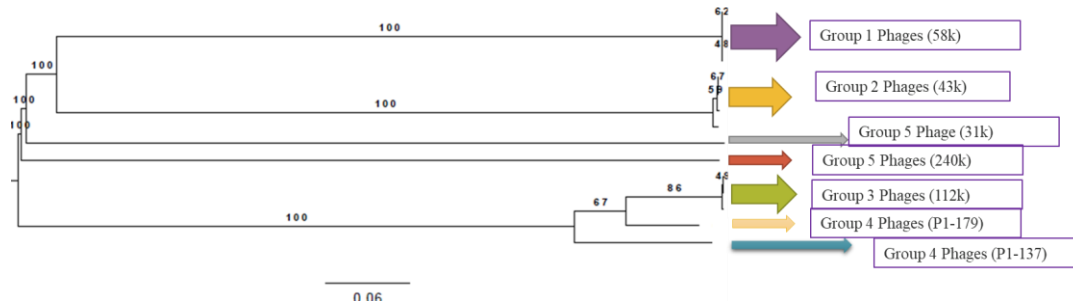
Dendogram showing the phylogenetic relationship between the phages. Numbers on branches indicate the bootstrap values. Tree was drawn with VICTOR.
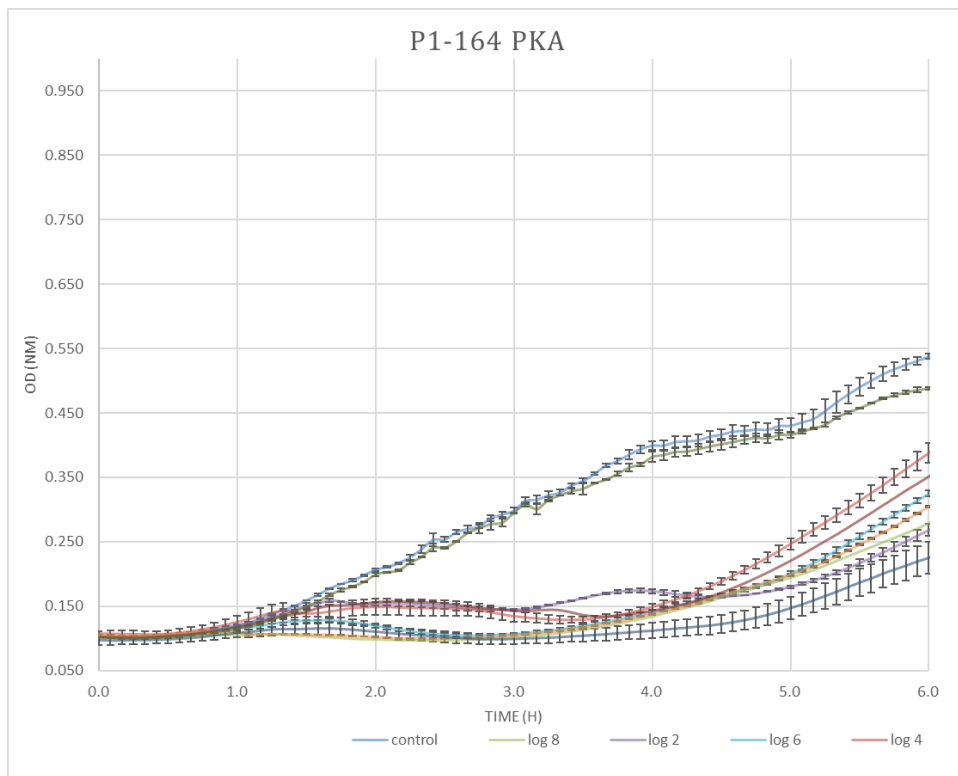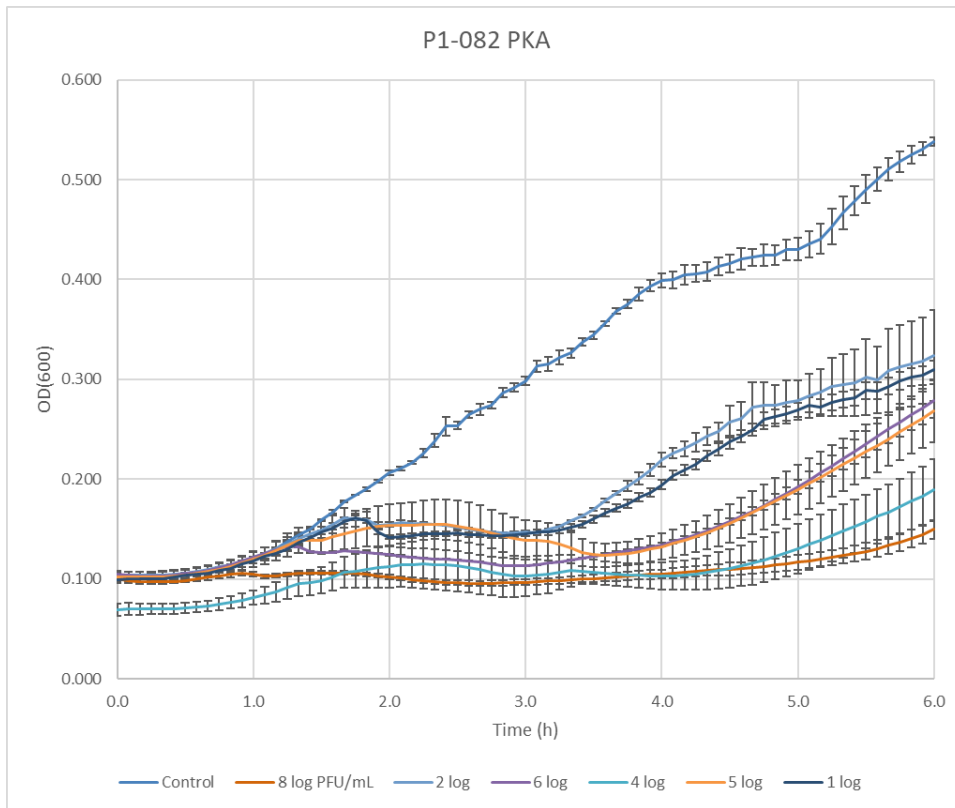
H. Bacterial reduction curves
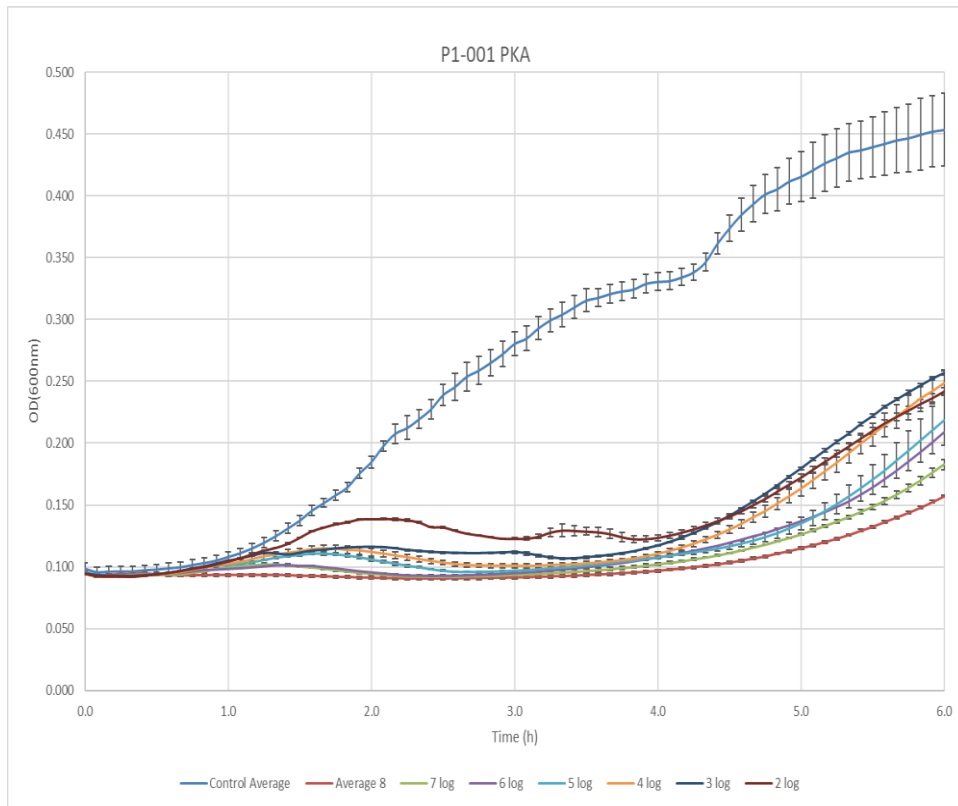
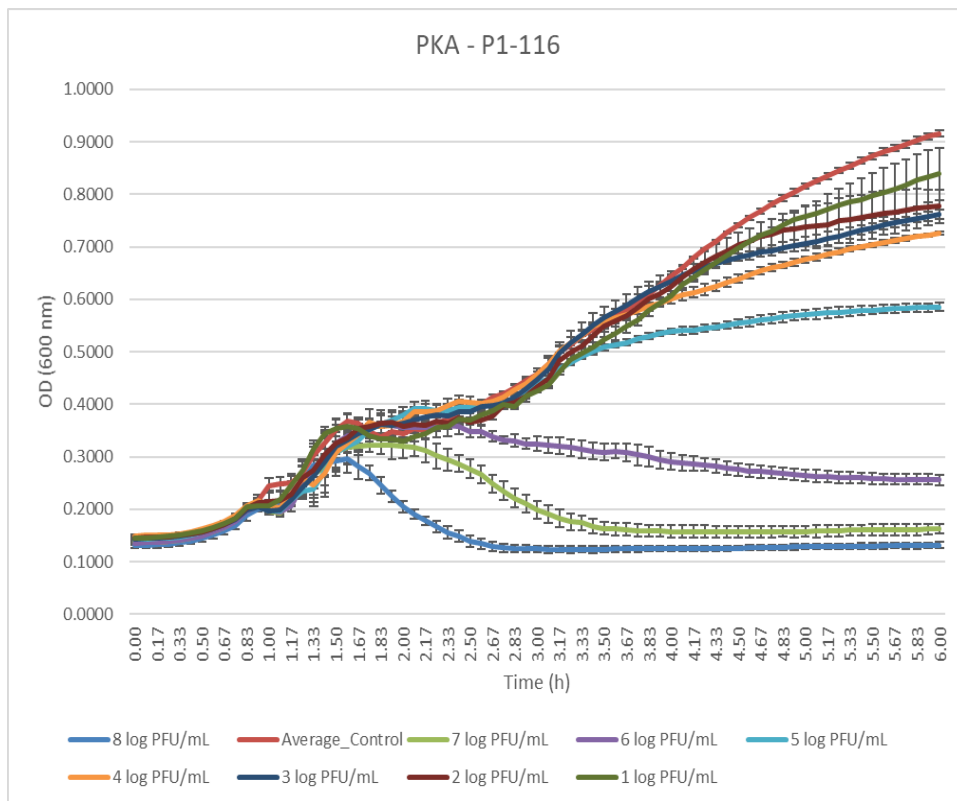Bacterial Reduction curve of MET P1-001 against Enteritidis
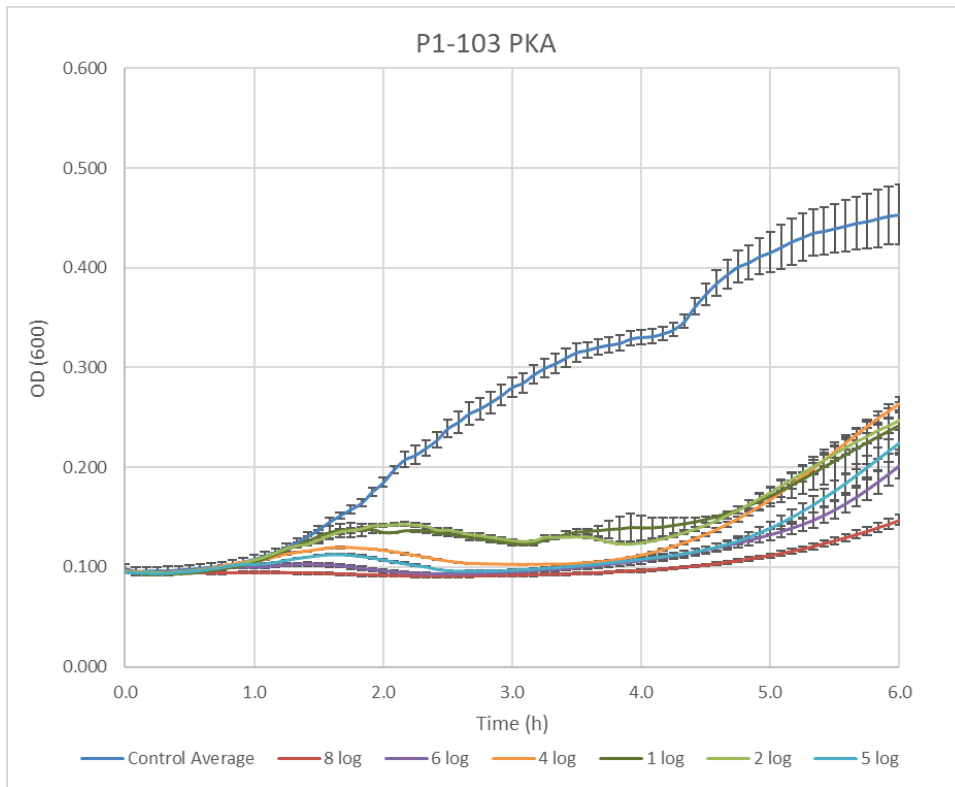
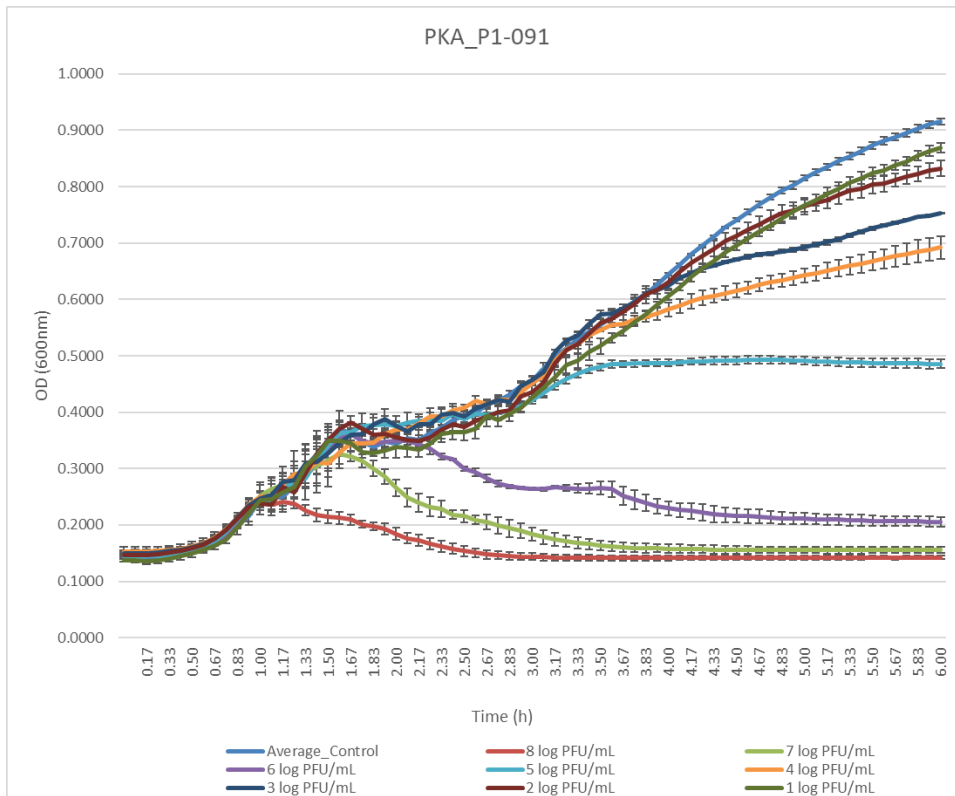Bacterial Reduction curve of MET P1-103 against Enteritidis

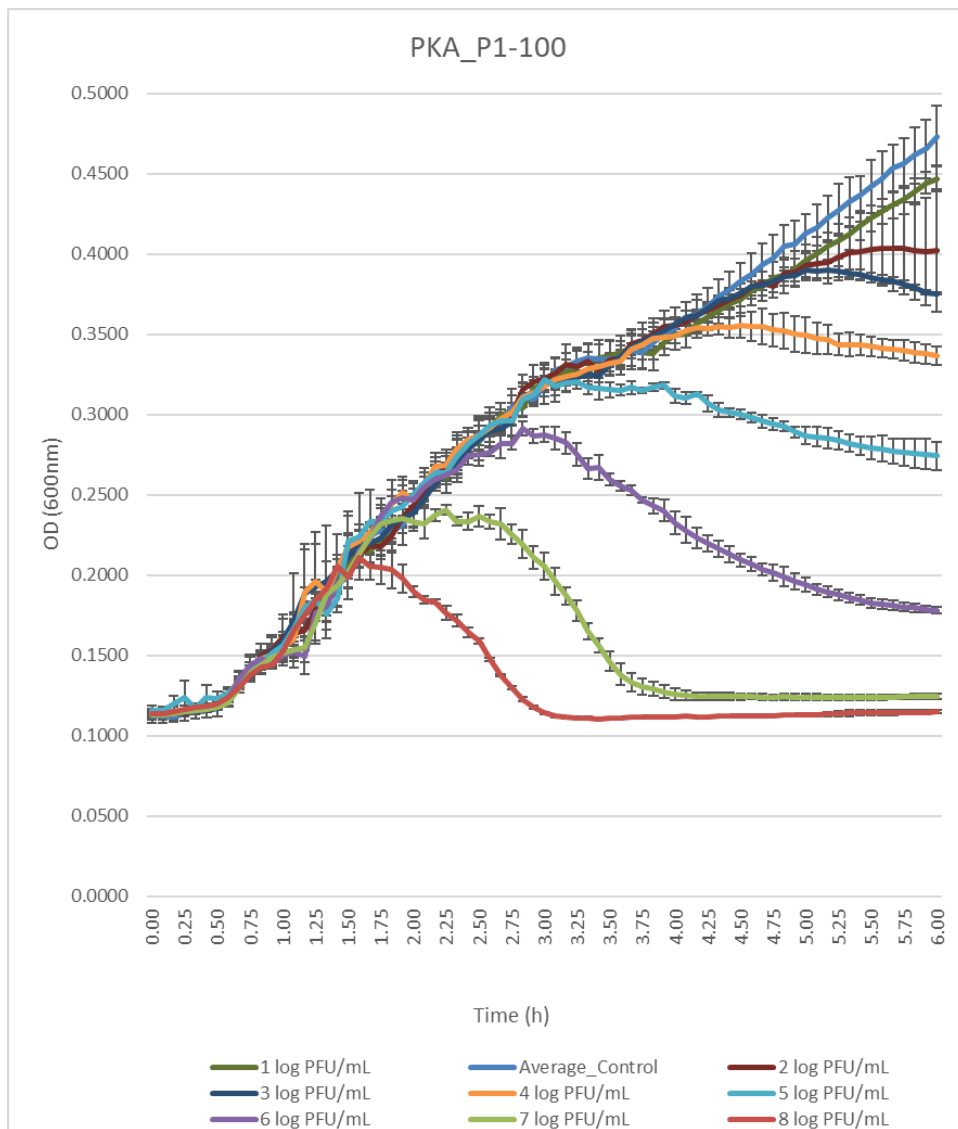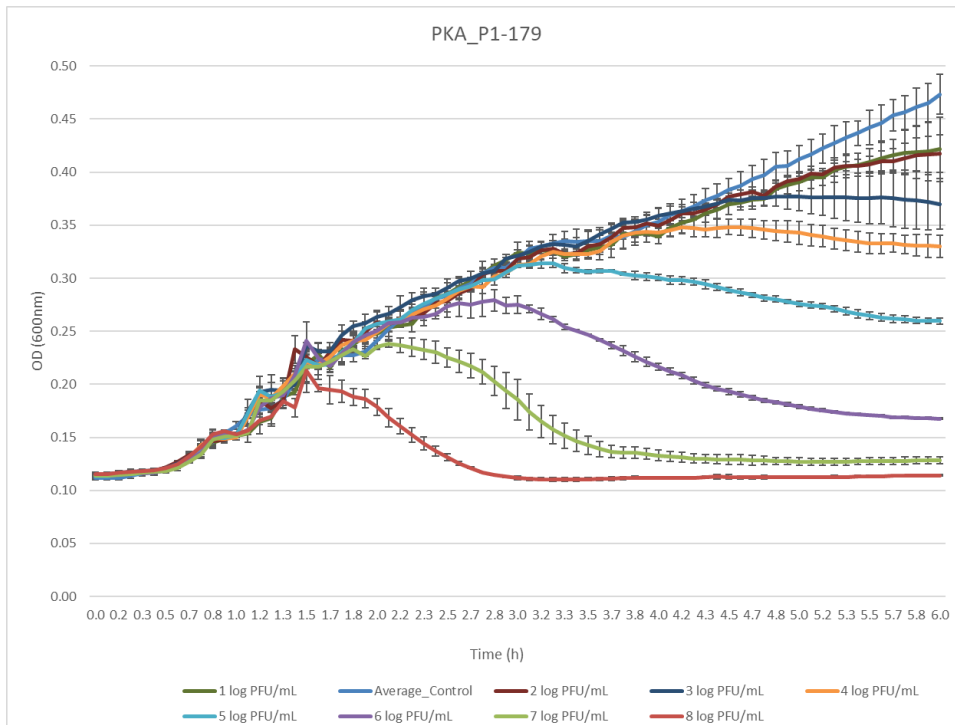Bacterial Reduction curve of MET P1-164 against Enteritidis

Bacterial Reduction curve of MET P1-082 against Enteritidis

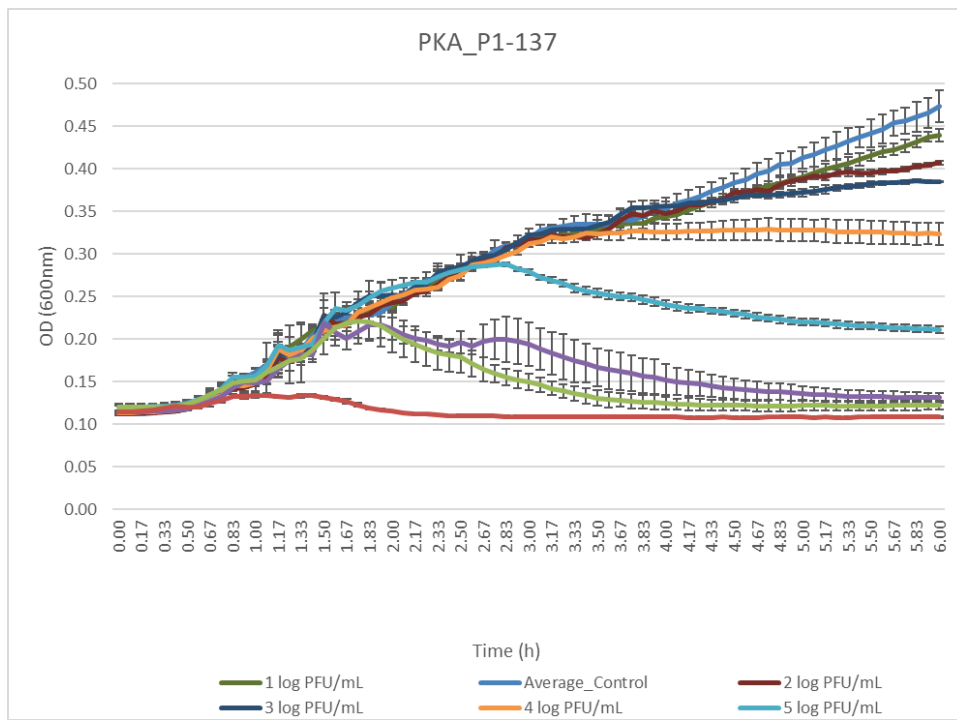Bacterial Reduction curve of MET P1-116 against Infantis

Bacterial Reduction curve of MET P1-091 against Infantis
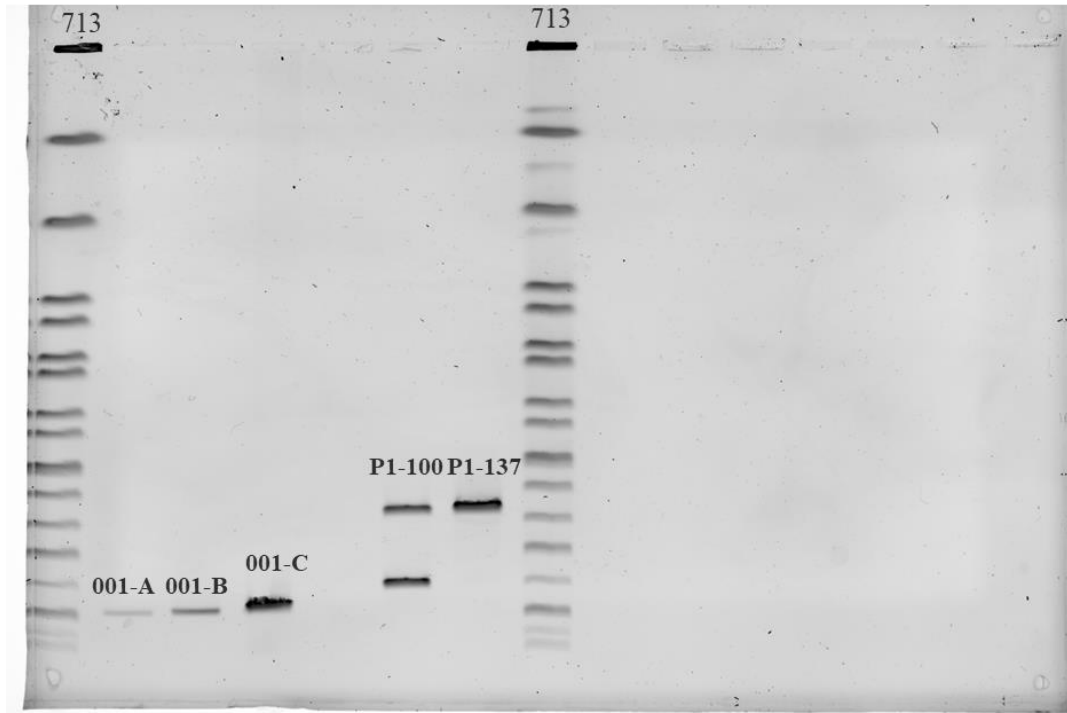
Bacterial Reduction curve of MET P1-100 against Infantis
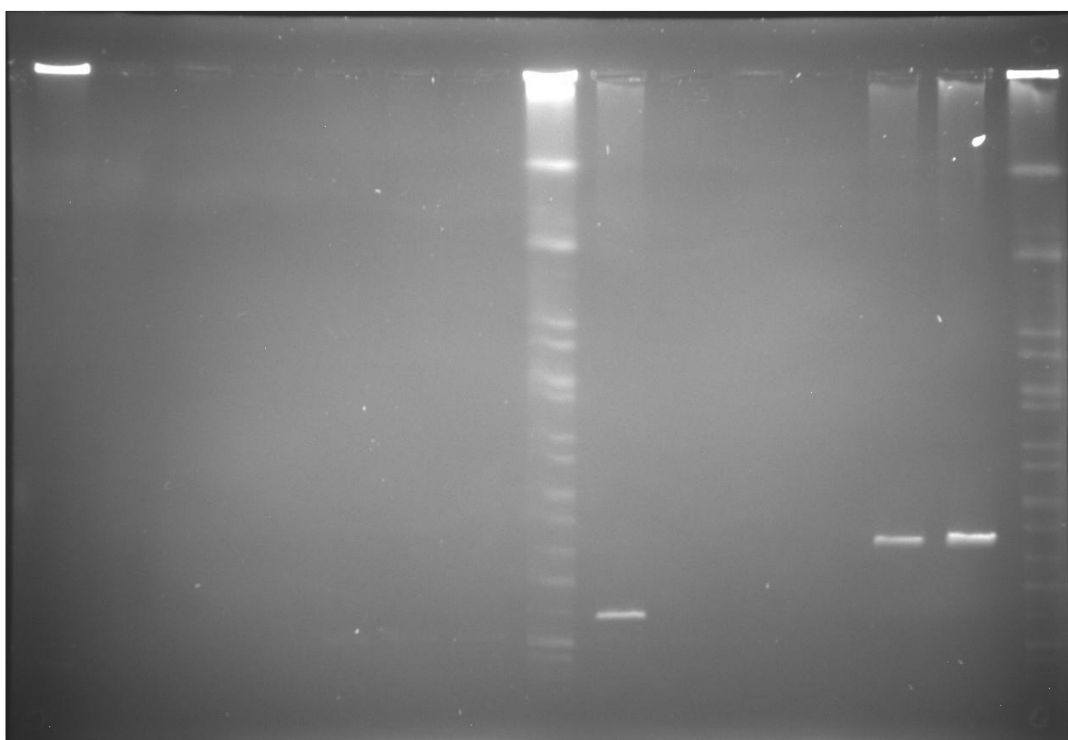
Bacterial Reduction curve of MET P1-179 against Infantis

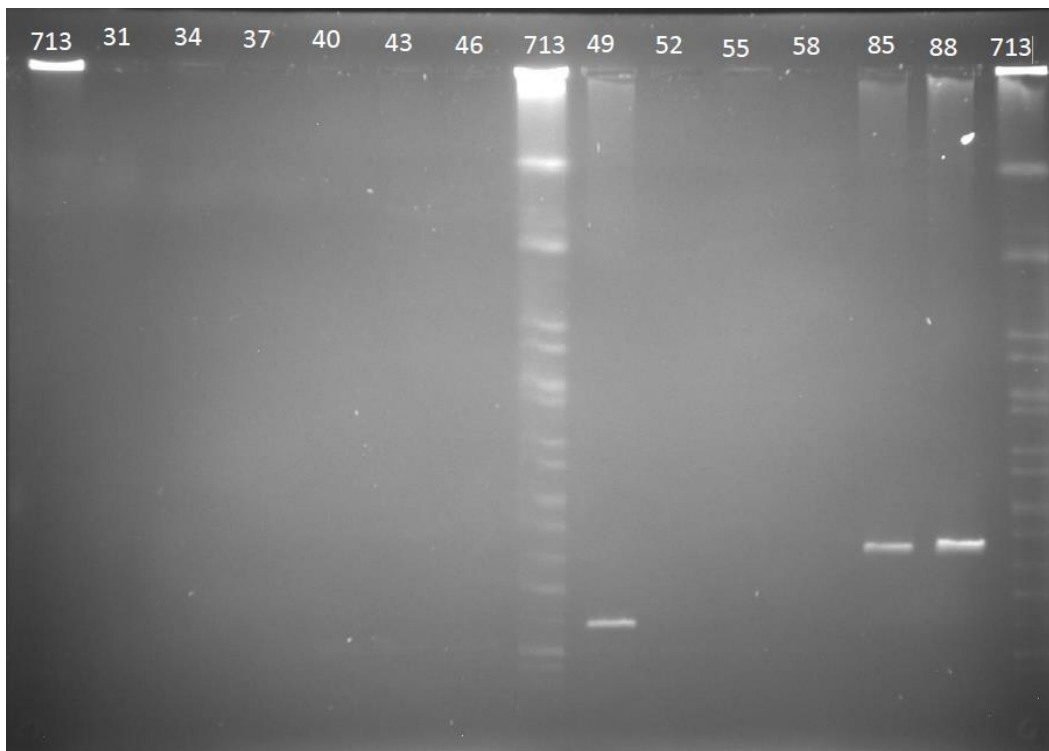Bacterial Reduction curve of MET P1-137 against Infantis
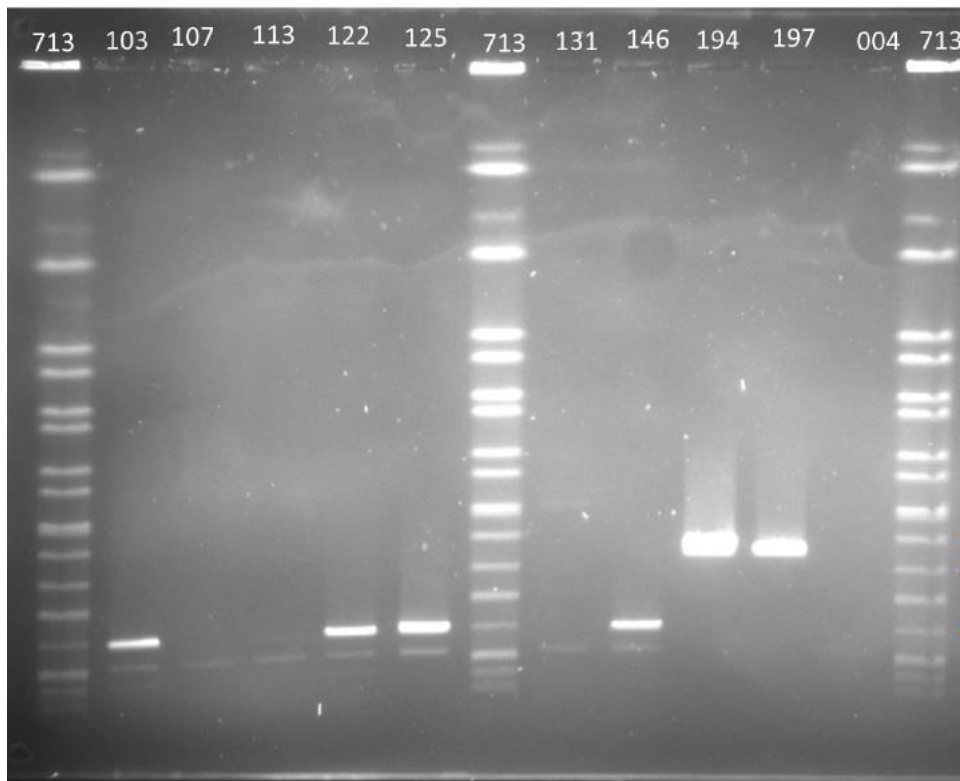
İ. PFGE gel pictures

PFGE gel picture of phages. From left to right: MET S1-713 (ref), MET P1-001-A, MET P1-001-B, MET P1-001-C, MET P1-100, MET P1-137, MET S1-713 (ref)
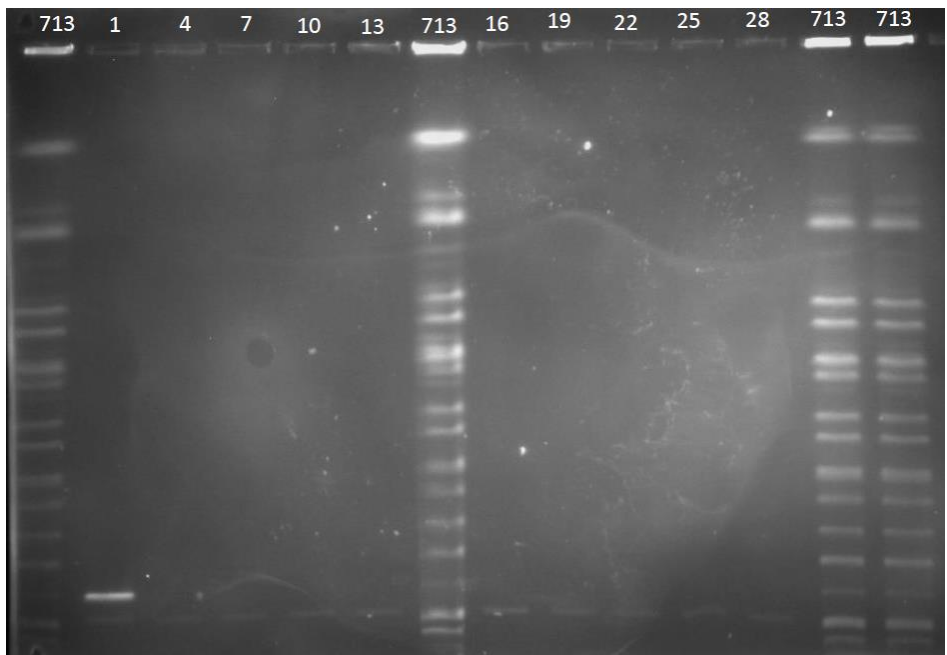
PFGE gel picture of phages. From left to right: MET S1-713 (ref), MET P1-049, MET P1-001-B, MET P1-001-C, MET P1-100, MET P1-137, MET S1-713 (ref)

PFGE gel picture of phages.   From left to right: MET S1-713 (ref), MET P1-031, MET P1-034, MET P1-037, MET P1-040, MET P1-043, MET P1-046, MET S1-713 (ref), MET P1-049, MET P1-052, MET P1-055, MET P1-58, MET P1-085, MET P1-088, MET S1-713 (ref)

PFGE gel picture of phages. From left to right: MET S1-713 (ref), MET P1-103, MET P1-107, MET P1-113, MET P1-122, MET P1-125, MET S1-713 (ref), MET P1-131, MET P1-146, MET P1-194, MET P1-197, MET P1-004, MET S1-713 (ref)

PFGE gel picture of phages.   From left to right: MET S1-713 (ref), MET P1-001, MET P1-004, MET P1-007, MET P1-010, MET P1-013, MET S1-713 (ref), MET P1-016, MET P1-019, MET P1-022, MET P1-025, MET P1-028, MET S1-713 (ref), MET S1-713 (ref)

J. Chemicals and materials used in this study

Chemicals	Producers
American Bacteriological Agar	Condalab (Madrid, Spain)
Luria Bertani (LB) Broth	Condalab (Madrid, Spain)
Buffered Peptone Water	Merck (Darmstadt, Germany)
Xylose-Lysin-Desoxycholat (XLD) Agar	Merck (Darmstadt, Germany)
Rappaport-Vassiliadis *Salmonella* Enrichment Broth	Merck (Darmstadt, Germany)
Brain Heart Infusion Broth	Merck (Darmstadt, Germany)
Gelatin from bovine skin	Merck (Darmstadt, Germany)
Sodium chloride	Merck (Darmstadt, Germany)
Magnesium sulfate hexahydrate ($MgSO_4*6H_2O$)	Merck (Darmstadt, Germany)
Ethylenediaminetetraacetic acid	Merck (Darmstadt, Germany)
TRIS hydrochloride	Merck (Darmstadt, Germany)
SeaKem Gold Agarose	Lonza (USA)
Boric Acid	Merck (Darmstadt, Germany)
Proteinase K	Roche
Xba1	Roche
H buffer	Roche
DirectLoad PCR 100 bp Low Ladder	Sigma-Aldrich (St. Lois, MO, USA)
0.45 µm and 0.22 µm poresize syringe filters	ISOLAB
Ammonium acetate	Merck (Darmstadt, Germany)
Phosphotungstic Acid	Merck (Darmstadt, Germany)

Mustafa GÜZEL

Research Assistant

Department of Food Engineering

Hitit University

19030, Çorum, TURKEY

+90(364)227-4533

mustafaguzel@hitit.edu.tr

musguzel@gmail.com

GENERAL INFORMATION

Academic Experience

Degree Received	Institution	Date
Ph.D. Food Engineering	Middle East Technical University	2022
	Thesis Title: An Alternative Way for Reduction of	
	Pathogens in Poultry Farms:	
	Bacteriophages Against Antimicrobials	
M.S. Food Engineering	Texas A&M University	2015
	Thesis Title: Quantitative Microbial Risk	
	Assessment for *Listeria monocytogenes* in	

	Fresh-cut Cantaloupe and Fresh-cut Romaine Lettuce		
B.S. Food Engineering	Ankara University		2008

Professional Experience

Position	Department	Institution	Dates
Teaching Assistant	Food Engineering	Hitit University	2015-

Membership in Professional Societies

2015 – 2017 Institute of Food Technologists (IFT)

2018 -   Turkish Society of Microbiology

Awards and Fellowships

Ministry of National Education, Selection and Placement of Candidates Sent Abroad for Postgraduate Education. Master's education, 2011-2015

Visiting Scholar, University of Illinois, Department of Food Science, Genomic Characterization of *Salmonella* Isolates from Poultry in Querétaro, 2015-2018, 01/02/2019-30/04/2019

Short Term Scientific Mission Grant, COST Action 16110, Aarhus University, Department of Environmental Science, Research, 20/01/2020 - 07/02/2020

Congress Attendance Grant, FEMS 2022, Belgrade, 30/06/2022 – 03/07/2022

Publications

Research articles

1. Zervas, A., Aggerbeck, M. R., Allaga, H., **Güzel, M.,** Hendriks, M., Jonuškienė, I., ... & Hendriksen, N. B. (2020). Identification and Characterization of 33 *Bacillus cereus sensu* lato Isolates from Agricultural Fields from Eleven Widely Distributed Countries by Whole Genome Sequencing. Microorganisms, 8(12), 2028.

2. **Guzel, M.,** Avsaroglu, M. D., & Soyer, Y. (2020). Determination of colistin resistance in *Escherichia coli* isolates from foods in Turkey, 2011-2015. Food and Health, 6(3), 160-169.

3. **Guzel, M.,** Moreira, R. G., Omac, B., & Castell-Perez, M. E. (2017). Quantifying the effectiveness of washing treatments on the microbial quality of fresh-cut romaine lettuce and cantaloupe. LWT-Food Science and Technology, 86, 270-276.

Book Chapters

1. **Guzel M.**, Guzel N., Tuksoy S., Rusu A.V., Trif M. (2022, in press). Methodologies for the Development of Cereals and Pseudocereals for Improved Quality and Nutritional Value. In Developing sustainable and health promoting cereals and pseudocereals: Conventional and molecular breeding. Elsevier, Editor Mariann Rakszegi

2. Güzel N., **Güzel M**, Bahçeci K., S. (2020). Trends in Non-alcoholic Beverages, Chapter:(Nonalcoholic Beer) Academic Press, Editor:Charis M. Galanakis,1,402, ISBN:9780128169384,

3. **Guzel, M.**, & Soyer, Y. (2017). Microbial Control of Milk and Milk Products. In Microbial Control and Food Preservation (pp. 255-280). Springer, New York, NY.

4. Kara, G. N., **Guzel, M.**, & Kabak, B. (2017). Novel Approaches to Identify and Characterize Microorganisms in Food Industry. In Modern Tools and Techniques to Understand Microbes (pp. 25-43). Springer, Cham.

Presentations

1. Modeling Growth of Listeria innocua on Fresh-cut Cantaloupe under Different Storage Temperatures. (IFT 2015, Poster Presentation)
2. Modeling Growth of Listeria innocua on Fresh-cut Romaine Lettuce Stored at Different Temperatures (IFT 2015, Poster Presentation)
3. Quantitative Microbial Risk Assessment for Listeria monocytogenes on Fresh-cut Cantaloupe (IFT 2015, Poster Presentation)
4. Quantitative Microbial Risk Assessment for Listeria monocytogenes on Fresh-cut Romaine Lettuce (IFT 2015, Poster Presentation)
5. Determination of colistin resistance in Escherichia coli isolates from foods in Turkey, 2011-2015 (3. International Congress on Food Technology, 2018, Poster Presentation)
6. Colistin Resistance is Emerging in Foodborne Pathogens in Turkey (FEMS 2020, Poster Presentation)
7. Rheological and Functional Properties of Fortified Gluten-free Sorghum Sourdough Bread (Euro-Aliment 10. International Symposium, 2021, Oral Presentation)
8. Genomic Characterization of Cephalosporin, Quinolone and Macrolide Resistance in *Salmonella enterica*. (World Microbe Forum, 2021, Poster Presentation).
9. Characterization of 5 Broad-range *Salmonella* Bacteriophages, (FEMS 2022, Poster Presentation)